

© 2007 The Authors
Journal compilation © 2007 Blackwell Publishing Ltd



**SYNTHESIS AND STRUCTURAL
CHARACTERIZATION OF QUADRUPLEX
FORMING OLIGONUCLEOTIDES AND
STUDIES ON SOLID PHASE SYNTHESIS
OF NUCLEOSIDE AND NUCLEOTIDES
ANALOGUES**

Stefano D'Errico

Dottorando:	Stefano D'Errico
Relatore:	Prof. Gennaro Piccialli
Coordinatore:	Prof. Giovanni Sannia

Ai Miei Cari

INDEX

SHORT ABSTRACT	1
LONG ABSTRACT	2

Chapter 1

Synthesis of Tetra-End-Linked oligonucleotides forming DNA G-quadruplexes: structure characterization and stability	10
1.1. Topological classification of G-Quadruplex DNA structures	11
1.2. G-quadruplex: molecular recognition	16
1.3 Quadruplexes in telomeres or quadruplexes everywhere?	18
1.4 Applications of quadruplexes: bio- and nano-technologies	21
1.5 The aim of the work	23
1.6 Synthesis and Purification of TEL-ODNs type 1, 2, 3 and 4.	26
1.7 CD and CD Thermal Analysis	27
1.8 Native Gel Electrophoresis.	29
1.9 ¹ H NMR Studies on L- and S-TEL-ODNs	30
1.10 Molecular Modelling	31
1.11 Conclusions	32
1.12 Experimental	33
1.12.1 Reagents and Equipment.	33
1.12.2 Syntheses of linkers 8a-b.	33
1.12.3 Syntheses and Purifications of TEL-ODNs L1-2 and S1-2	34
1.12.4 Syntheses and purifications of TEL-ODNs 3 and 4	34
1.12.5 Preparation of Quadruple Helices (Annealing).	35
1.12.6 Native gel electrophoresis.	35
1.12.7 CD Experiments.	35
1.12.8 ¹ H NMR Experiments.	36
1.12.9 Molecular Modelling	36
References	37

Chapter 2

Synthesis of combinatorial libraries of nucleosides, specifically inosine analogues	40
2.1. Nucleoside analogues	42
2.2. Nucleoside analogue uptake	43
2.3. Nucleoside analogue activation	44
2.4. Mechanism of action of nucleoside analogues	44
2.5. Mitochondrial toxicity of nucleoside analogues	46
2.6. Nucleotide analogues	46
2.7. Solid-phase synthesis of nucleoside analogues	47
2.8. The aim of the work	48
2.9. Chemistry	48
2.10. Conclusions	51
2.11 Experimental Session	52
2.11.1 General Methods	52
2.11.2 General Procedures	52
2.11.3 Synthesis of N-1-alkylated-inosine library	53

2.11.4 Synthesis of N-1-alkylated-2',3'-secoinosine derivative library	55
References	57

Chapter 3

Synthesis of N-4-alkyl and ribose-modified AICAR analogues

on solid support	58
3.1 Chemical synthesis of AICAR and its derivatives	59
3.2 The aim of the work	61
3.3 Biological results.....	64
3.4 Conclusions	64
3.5. Experimental.....	65
3.5.1. General.....	65
3.5.2 Synthesis.....	65
3.5.3. General procedure for the scaffold synthesis	66
3.5.4 Synthesized scaffolds.....	67
References	73

Chapter 4

Solid phase synthesis of cADPR analogs

4.1. Enzymatic and chemo-enzymatic synthesis	77
4.2. Chemical synthesis.....	78
4.3. Synthetic strategy	79
4.4. Structural cADPR analogues for SAR elucidation	83
4.5. Cellular effect and metabolic stability of cADPR derivatives.....	85
4.6. The aim of the work	89
4.7. Experimental Session	92
4.7.1. General.....	92
4.7.2. Synthesis.....	92
4.7.3 Synthesized scaffolds.....	95
References	98
Appendix.....	100

SHORT ABSTRACT

Nucleosides and their phosphorylated counterparts (nucleotides) may be considered two of the most important metabolites of the cell. Nucleotides are found primarily as the monomeric units comprising the major nucleic acids of the cell, RNA and DNA. However, they also are required for numerous other important functions within the cell. These functions include:

1. serving as energy stores for future use in phosphate transfer reactions. These reactions are predominantly carried out by ATP;
2. forming a portion of several important coenzymes such as NAD^+ , NADP^+ and coenzyme A;
3. serving as mediators of numerous important cellular processes such as second messengers in signal transduction events;
4. controlling numerous enzymatic reactions through allosteric effects on enzyme activity;
5. serving as activated intermediates in numerous biosynthetic reactions.

During my PhD I focused my attention on:

- 1 chemistry of nucleic acids, in particular synthesis and characterization of a new kind of monomolecular G-quadruplex;
- 2 solid phase synthesis of new base/sugar modified nucleosides;
- 3 solid phase synthesis of new derivatives of cIDPR (cyclic-inosine-diphospho-ribose)

Interest in the field on the chemistry of G-quadruplex has intensified in recent years because G-quadruplex structures have roles in crucial biological processes and can be targeted for therapeutic intervention. G-quadruplexes might also have applications in areas ranging from supramolecular chemistry and nanotechnology to medicinal chemistry. Special attention has been devoted to structural investigation (NMR, CD, UV) on the complexes formed by synthesized oligonucleotides. Recently, medicinal chemistry research emphasizes the need of nucleosides and nucleotides analogues in high number and diversity, to be used as building blocks in the synthesis of new oligonucleotides (ON) generations. Many nucleoside and nucleotide synthetic analogues have been the cornerstone of antiviral therapy over the past 30 years, and many others exhibit anti-proliferative, antibiotic and antifungal properties. The rapid development of drug resistance and high toxicity that characterize the use of these agents, suggest the novel nucleoside drug discovery for critical medical needs. The availability of high-throughput screening capabilities together with the solid phase combinatorial synthesis of small organic molecule libraries offers a unique opportunity to accelerate the discovery in these fields. My research focused on solid phase synthesis of a collection of modified nucleosides and on solid phase synthesis of new derivatives of cIDPR, a mimic of natural metabolite cADPR (cyclic-adenosine-diphospho-ribose). Ca^{2+} mobilization is crucial for a wide variety of cell functions and cADPR is a potent Ca^{2+} mobilizing messenger. Because of its natural instability chemists synthesized new stable mimics in effort to understand the mechanism of cADPR-mediated Ca^{2+} signaling pathways and to obtain lead structures for the development of drugs. With a solid phase approach I synthesized and characterized new cIDPR derivatives that will be tested as potential pharmacological tools and the stability of which, under physiological conditions, will be proved.

LONG ABSTRACT

L'interesse per gli oligonucleotidi sintetici deriva dai grandi successi ottenuti in campo biomedico per il loro utilizzo come agenti antivirali e antitumorali. Oligodeossiribonucleotidi (ODN) di piccole dimensioni (15-17 basi) ed opportuna sequenza possono risultare degli efficaci inibitori o, più in generale, regolatori dell'espressione genica, interferendo con elevata selettività con le normali funzioni degli acidi nucleici o di specifiche proteine [1-3].

Gli ODN deputati per queste funzioni possono essere catalogati in base al tipo di bersaglio e al loro meccanismo di azione. Possono funzionare da "aptameri", cioè riconoscere in maniera assolutamente selettiva una proteina o agire come molecole "antisense" o "antigene" i cui target sono, rispettivamente, uno specifico mRNA e un tratto di DNA a doppia elica. Nel quadro delle nuove terapie geniche la strategia antisense, nata ad Harvard nel 1978 ad opera del gruppo di F. Zamecnik [4] ottenne i primi successi terapeutici nell'utilizzo di oligonucleotidi antisense come farmaci nei confronti di malattie virali. La prima applicazione di queste molecole nell'ambito delle strategie antisense, ha riguardato la formazione di una doppia elica ibrida tra l'oligonucleotide sintetico ed un tratto specifico di m-RNA: in questo modo si impedisce il funzionamento del ribosoma che non riconosce la doppia elica [5-7].

L'applicazione nel caso delle malattie virali riguardava quindi l'impiego di ODN sintetici diretti contro geni esogeni. Solo successivamente si è cominciato ad utilizzare gli ODN antisense nei confronti di malattie dovute a superespressione di geni endogeni, normali o mutati per cause patologiche o per azione di fattori mutageni estrinseci. Attualmente sono stati ammessi all'utilizzo terapeutico soltanto pochi farmaci antivirali di questa classe. Tuttavia un numero elevato di oligonucleotidi modificati è sottoposto a sperimentazione clinica con la speranza di poterne dimostrare l'attività antitumorale già provata in vitro.

Altri tipi di strategie sono basate sulla sintesi e l'introduzione nell'organismo di brevi tratti di DNA a doppia elica identici ad un sito di DNA e quindi capaci di operare come inibitori delle proteine coinvolte nella regolazione o nell'espressione e sintesi o di sequestrare i fattori di trascrizione [8]. In tutti i casi descritti il risultato finale è quello di inibire l'espressione di una proteina. L'impiego farmacologico di ODNs sintetici e loro modifiche è tuttavia limitato da fattori legati alla stabilità, possibilità di somministrazione e biodisponibilità all'interno dell'organismo. Infatti questi composti sono rapidamente degradati dalle esonucleasi e dalle endonucleasi cellulari e, data la natura di polielettroliti idrofilici e l'assenza di specifici meccanismi di trasporto, hanno difficoltà a permeare le membrane cellulari. Negli ultimi anni si è tentato di renderli più idrofobici e più resistenti all'idrolisi enzimatica mediante modifiche chimiche [9].

Più di recente rispetto alla strategia antisense è stata sviluppata la strategia antigenica che si basa sulla formazione di triple eliche fra tratti di DNA a doppia elica e singoli filamenti di oligodeossinucleotidi sintetici (ODNs) progettati in maniera specifica [10-15]. Infatti l'osservazione che tratti purinici-pirimidinici nei plasmidi possono formare strutture a tripla elica intramolecolari, chiamate H-DNA, ha mostrato che la formazione di triple eliche può giocare un ruolo importante nei processi cellulari. La formazione di una tripla elica può intervenire nella regolazione dell'espressione di un gene in almeno due modi: 1) impedendo alle proteine che normalmente regolano l'espressione genica di legarsi al sito di regolazione del DNA

prossimale a quello di trascrizione, 2) bloccando il sito stesso di trascrizione, impedendo l'avanzamento lungo il gene stesso della RNA-polimerasi.

Una tripla elica sul DNA si forma quando un terzo filamento (spesso chiamato TFO, acronimo di Triplex Forming Oligonucleotide) si introduce nel solco maggiore della doppia elica creando dei legami idrogeno di tipo Hoogsteen con le purine delle coppie di basi Watson-Crick. La specificità dell'interazione deriva dal riconoscimento specifico della coppia di basi adenina-timina da parte di una timina del terzo filamento o dal riconoscimento della coppia di basi guanina-citosina da parte di una citosina protonata del terzo filamento.

La strategia antigenica è così basata sul riconoscimento altamente specifico di un tratto di DNA da parte del TFO; quest'ultimo deve legarsi al DNA, in condizioni fisiologiche, in maniera sufficientemente stabile per poterne modulare l'espressione genica. Di conseguenza studi sulla formazione di strutture a tripla elica in condizioni fisiologiche sono divenuti di estremo interesse.

Una limitazione significativa per l'applicazione della formazione delle triple eliche è dovuta alla necessità che la doppia elica bersaglio possieda un blocco omopurinico sufficientemente lungo (15-17 basi) in genere piuttosto raro e biologicamente poco rilevante. Per aumentare il numero di potenziali tratti bersaglio nel DNA naturale, molti gruppi di ricerca hanno progettato e sintetizzato oligonucleotidi modificati in grado di legarsi più stabilmente di un TFO esclusivamente omopirimidinico. Vari approcci si stanno quindi sperimentando. Ad esempio l'introduzione di una giunzione che inverta la polarità del secondo tratto del TFO: in questo modo esso sarà in grado di riconoscere sequenze omopirimidiniche più brevi presenti su filamenti alternati della doppia elica bersaglio [16-22]. Un'altra possibilità è quella di modificare l'oligonucleotide trasformandolo in una catena ibrida recante alle estremità 3' e/o 5' degli oligosaccaridi [23], o in 3' un tratto di PNA. Queste modifiche rendono termodinamicamente più stabili le triplex formate con il TFO "chimerico" che risultano anche più resistenti rispetto agli attacchi idrolitici delle nucleasi [24, 25]. Questo campo di ricerca sembra essere più promettente rispetto all'uso dei PNA puri, in genere troppo poco solubili. Anche l'introduzione di macrocicli o di composti a sandwich contenenti cationi di metalli pesanti comporta una stabilizzazione di doppie e triple eliche; ma l'interesse principale per questi ODN o ON modificati è legato all'attività citotossica e antitumorale esplicita da questi composti [26-28].

Un altro campo di grandissimo interesse si è infine aperto con l'individuazione delle lunghe sequenze telomeriche a singolo filamento presenti all'estremità 3' di tutti i DNA eucariotici. Queste strutture sono molto ricche in guanina, base che favorisce l'organizzazione di strutture a quadrupla elica. L'importanza e l'attualità degli studi in questo campo deriva dal fatto che sequenze telomeriche del gene, ricche di deossiguanosine, possono formare complessi a quadrupla elica [29]. Queste strutture potrebbero giocare un ruolo importante nella regolazione dell'attività telomerasica. In particolare la telomerasi è una ribonucleoproteina composta da una subunità catalitica con attività di trascrittasi inversa (hTERT) e una componente a RNA che funge da template per la sintesi delle sequenze telomeriche (hTR). L'espressione ubiquitaria della telomerasi nelle cellule tumorali e la sua ridotta attività nelle cellule normali ha suggerito l'ipotesi del coinvolgimento di questo enzima nel processo di carcinogenesi [30, 31]. Infatti, l'elevata attività di questo enzima blocca i fenomeni di senescenza e morte nelle cellule tumorali. È stato ipotizzato che le sequenze telomeriche del gene, strutturandosi in quadrupla elica (quadruplex) riescono a regolare l'attività della telomerasi [32, 33]. Da questa ipotesi nasce l'idea di regolare l'attività telomerasica mediante ODNs capaci di formare strutture

quadruplex. Il crescente interesse verso tali strutture è inoltre legato alla scoperta dell'attività inibitoria che alcuni ODNs sintetici, in grado di formare quadruplex, mostrano nei confronti di alcune importanti proteine quali la trombina e l'integrasi dell'HIV-1 [34, 35], quest'ultima responsabile dell'integrazione del DNA virale in quello della cellula ospite. Le strutture a quadrupla elica sono caratterizzate dalla formazione di quartetti di guanine connesse da legami idrogeno di tipo Hoogsteen. Questi complessi possono essere classificati in base al numero dei filamenti oligonucleotidici che li compongono (uno, due, quattro) e in base all'orientamento degli ODNs formanti il complesso (parallelo o antiparallelo). Benché la maggior parte delle strutture G-quadruplex con attività biologica siano di tipo antiparallelo, recenti studi hanno evidenziato interessanti attività anche per quadruplex parallele. Infatti quadruplex parallele interagiscono selettivamente con alcune proteine [36-39], inoltre, è stata osservata per alcuni di questi complessi, una attività anti HIV [40-43] ed anche attività di aptamero verso l'ematoporfirina. Quadruplex parallele si formano quasi esclusivamente in complessi tetramolecolari. Sfortunatamente, in vivo, la formazione intermolecolare di complessi quadruplex è molto lenta e necessita di alte concentrazioni di ODNs, non facilmente raggiungibili in condizioni fisiologiche. Gli sfavorevoli parametri cinetici e termodinamici sono quindi un ostacolo alla potenziale utilizzazione farmacologica di questo tipo di complessi

Recentemente, nel gruppo presso cui ho svolto la mia attività di ricerca, è stata messa a punto la sintesi e la caratterizzazione strutturale (NMR; CD, UV) di un nuovo tipo di quadruplex parallela monomolecolare formata da oligonucleotidi legati a "grappolo". In particolare, la struttura oligonucleotidica a grappolo prevede che i quattro filamenti, formanti il complesso quadruplex, siano legati reciprocamente per le estremità 3' attraverso una molecola tetraramificata simmetricamente. Questa nuova tipologia di quadruplex dovrebbe essere caratterizzata da una maggiore stabilità e da una veloce cinetica di strutturazione rispetto ai corrispondenti complessi tetramolecolari. Nostri preliminari risultati sulla sintesi e sulla stabilità di questo nuovo tipo di quadruplex confermano le ipotesi fatte. La sintesi della molecola "linker" tetraramificata (catene dialchilfosfato) avviene su supporto polimerico insolubile. Ogni ramificazione contiene una funzione alcolica terminale a cui è possibile legare la catena oligonucleotidica. Modulando opportunamente i gruppi protettori delle funzioni alcoliche della struttura ramificante e la tipologia di accrescimento della catena oligonucleotidica, è stato possibile ottenere ODNs a grappolo formanti strutture quadruplex con orientamento dei filamenti predefiniti (paralleli, antiparalleli o con orientazione mista).

Il mio progetto di ricerca, in tale ambito, ha previsto l'ottimizzazione della lunghezza del linker tetraramificato ai fini sia di una maggiore stabilizzazione della struttura quadruplex, sia per poter selezionare quadruplex antiparallele da strutture sintetizzate a filamenti a polarità inversa. È noto che la polarità dei filamenti in una quadruplex riveste fondamentale importanza nelle interazioni con proteine o altre molecole. La strategia degli ON-grappolo trascende da tutte queste limitazioni e consentirebbe di preparare quadruplex antiparallele, purché si utilizzino linker di opportuna lunghezza. L'eccessiva lunghezza del linker tetraramificato, infatti, sembra compromettere la formazione della quadruplex antiparallela, favorendo la formazione della struttura parallela per ripiegamento dei "loop" alchilici, come dimostrato dai dati ottenuti da calcoli di meccanica molecolare condotti in tale ambito e da studi NMR. La lunghezza del linker sembra giocare anche un ruolo di cruciale importanza sulla riproducibilità e la velocità dei meccanismi di "melting" e "refolding" delle strutture quadruplex-grappolo.

È stato anche valutato il diverso effetto stabilizzante dovuto alla presenza di cationi sodio e potassio. I dati ricavati dalla spettroscopia NMR, inseriti in software di calcolo (Cyana e Dyana) consentiranno di proporre valide strutture per i complessi studiati.

Sintesi di collezioni nucleosidiche in fase solida

I nucleosidi sono fondamentali in molte vie metaboliche e di particolare interesse risultano i loro meccanismi di riconoscimento associati ad un ampio spettro d'azione. I nucleosidi modificati sono alla base di una serie di terapie farmacologiche. Essi, mantenendo inalterate le proprietà metaboliche dei composti naturali di partenza, sono in grado di penetrare all'interno della cellula e di sottostare ai normali processi metabolici, inibendo in maniera reversibile o irreversibile gli enzimi target, così da bloccarne le normali funzioni. La caratteristica sostanziale di questa classe di molecole è la sostituzione di uno o più atomi, o gruppi funzionali, rispetto ai metaboliti naturali che sono i costituenti essenziali di DNA ed RNA. Essi sono in grado di interagire con un terzo delle classi di proteine del genoma umano, incluso polimerasi, chinasi, reduttasi, recettori di membrana e proteine strutturali. Tra questi composti i nucleosidi modificati svolgono un ruolo importantissimo; basti pensare che la maggior parte dei farmaci approvati per il trattamento di infezioni virali sono analoghi nucleosidici.

Nel corso degli ultimi anni, la sintesi degli analoghi nucleosidici ha interessato un numero sempre crescente di studiosi. È utile suddividere queste specie in tre grandi categorie a seconda delle caratteristiche strutturali che li differenziano rispetto ai corrispondenti composti naturali:

- Nucleosidi contenenti la base eterociclica modificata;
- Nucleosidi contenenti l'unità di zucchero, ribosio o 2'-deossiribosio, modificata;
- Nucleosidi altamente modificati nella struttura.

L'approccio sintetico convenzionale per la sintesi di molecole biologicamente attive fa uso delle cosiddette metodiche classiche della sintesi organica, da sempre utilizzate nella ricerca di nuovi farmaci e di molecole d'interesse biologico in generale. Tali strategie prevedono essenzialmente tre fasi:

- Sintesi chimica attraverso reazioni tradizionali (sintesi in soluzione);
- Purificazione e caratterizzazione strutturale;
- Determinazione delle proprietà biologiche del target in esame, usando saggi biologici convenzionali.

Recentemente, invece, la ricerca nel campo della scoperta di nuovi agenti terapeutici, si è rivolta alla preparazione di "librerie chimiche" come potenziali fonti di candidati per lo sviluppo di nuovi farmaci. Le librerie chimiche costituiscono vere e proprie collezioni di molecole strutturalmente correlate che possono essere ottenute sinteticamente o biosinteticamente ed essere successivamente sottoposte a test di attività biologica.

In via del tutto generale, librerie di composti si possono ottenere sia in soluzione che in fase solida. In soluzione esistono due approcci fondamentali: è possibile sintetizzare delle miscele di vari composti di complessità variabile oppure realizzare una sintesi parallela che produce un numero molto minore di composti, ma presenta

vantaggi nella caratterizzazione strutturale e nella determinazione delle proprietà biologiche della singola molecola.

La sintesi di composti in fase solida, invece, (solid phase organic synthesis – SPOS) presenta numerosi vantaggi rispetto a quella in soluzione. Ad esempio le procedure di reazione risultano notevolmente semplificate in quanto complessi processi di purificazione ed isolamento dei prodotti sono sostituiti da semplice filtrazione con solventi; si può usare un largo eccesso di reagente per condurre le reazioni a completezza ed il supporto può essere rigenerato dopo l'uso. Inoltre le metodiche sintetiche in fase solida, in linea di principio, sono suscettibili di automazione. Solitamente, il supporto solido è costituito da una resina polistirenica funzionalizzata opportunamente in modo da consentire l'ancoraggio di un linker o direttamente del substrato.

La disponibilità di strategie sintetiche basate su una chimica semplice ed efficiente, quale la chimica combinatoriale e sull'utilizzo di materiali di partenza poco costosi e facilmente reperibili costituisce un obiettivo molto ambito per la sintesi di mimetici di composti naturali. La ricerca attuale nel campo dei nucleosidi ad attività antivirale, ma anche antitumorale, antifungina, etc. è indirizzata verso la scoperta di nuovi analoghi caratterizzati da un ampio spettro di attività biologiche e da un'elevata specificità d'azione al fine di minimizzare gli effetti collaterali di queste molecole.

Per rispondere all'esigenza di avere, in tempi brevi, un elevato numero di analoghi nucleosidici da saggiare nelle loro eventuali proprietà farmacologiche, il mio progetto di ricerca ha previsto la messa a punto di una strategia di sintesi in fase solida per l'ottenimento di una collezione di analoghi ciclici e aciclici (2',3'-seco-) dell'inosina e dei corrispondenti AICAR derivati, differenziati per la lunghezza della catena alchilica lineare in posizione N-1 della base ipoxantina o in N-4 del residuo 5-amminoimidazolo-4-carbossiammide rispettivamente.

In letteratura sono riportati diversi esempi di strategie combinatoriali in fase solida per la preparazione di collezioni di nucleosidi e piccoli oligonucleotidi analoghi. In ogni caso, qualunque sia l'approccio seguito, un requisito fondamentale è la scelta di una molecola "linker" appropriata che funga da ponte tra il nucleoside e il supporto solido. Esso deve essere sufficientemente stabile alle condizioni di reazione usate durante la sintesi, ma allo stesso tempo abbastanza labile nelle condizioni di rimozione dal supporto solido senza inficiare l'integrità dei prodotti d'interesse.

La strategia seguita per la sintesi combinatoriale in fase solida di derivati N-1-alchilati dell'inosina è basata su studi, condotti in precedenza dal gruppo di ricerca presso cui ho svolto il mio lavoro di tesi, sulla reattività dell' N-1-dinitrofenil-2'-deossi-inosina nei confronti di nucleofili all'azoto, al fine di ottenere inosine N-1 sostituite e AICAR derivati [22].

Per estendere queste reazioni alla strategia combinatoriale in fase solida, è stato usato un supporto solido polistirenico, disponibile commercialmente, a cui è legato covalentemente il gruppo MMTCI (monometossi-tritil-cloruro). Questo tipo di supporto, già utilizzato efficientemente, come riportato in letteratura [44], per legare nucleosidi o zuccheri, ha la peculiarità di essere stabile in condizioni alcaline, e viceversa molto labile in condizioni acide. A tale supporto è stato ancorato l'ossigeno 5' del ribosio della 2',3'-O-isopropiliden-N-1-(2,4-dinitrofenil)-inosina, con formazione del corrispondente legame etero 5'-O-tritilico.

Succesivamente è stata saggiata la reattività al carbonio C-2 dell'anello purinico nei confronti di diversi nucleofili amminici al fine di costruire una prima collezione di inosine modificate in N-1. Inoltre, la nota reattività di tali substrati nei confronti delle

basi acquose [45] ha permesso di ottenere in resa e purezza molto elevata anche i corrispondenti N-4-alchil AICAR derivati.

Passo successivo è stato quello di studiare la reattività dell'anello ribosidico modificando le posizioni 2' e 3' sia per quanto concerne i derivati in N-1 dell'inosina che in N4 dei corrispondenti AICAR derivati. Ciò ha previsto l'aggancio diretto alla resina del nucleoside N-1-(2,4-dinitrofenil)-inosina non protetto alle funzioni ossidriliche 2' e 3', vista l'instabilità del legame 5'-O-etereo alle condizioni di rimozione dell'isopropilidene.

La condensazione tra il nucleoside e il supporto solido è risultata selettiva a carico delle funzioni alcoliche primarie, in accordo con quanto riportato in letteratura. Dopo alchilazione della posizione N-1 dell'inosina, seguendo la strategia prima descritta, è stata presa in esame la reazione di scissione del legame C-C 2'-3' da parte di agenti ossidanti al fine di ottenere 2',3'-seco-N1-alchil-inosine e 2',3'-seco-N4-alchil-AICAR derivati. Tali composti, in virtù dell'analogia strutturale con composti a riconosciuta attività antivirale, quali il ganciclovir, il penciclovir ed altri, potrebbero costituire target molecolari estremamente interessanti nell'ambito della chemioterapia antivirale.

L'azione del periodato di sodio (NaIO_4) o del piombotetracetato [$\text{Pb}(\text{OAc})_4$] sui nucleosidi deprotetti è ben conosciuta [46]. La dialdeide risultante non è stata isolata, ma ridotta direttamente con sodio boroidruro (NaBH_4) ed i prodotti di interesse sono stati ottenuti in buona resa.

Lo studio ha riguardato quindi la sintesi di nuovi nucleosidi analoghi quali potenziali agenti terapeutici ed ha condotto all'ottenimento di derivati che verranno poi sottoposti a saggi biologici per poterne testare l'attività terapeutica.

Sintesi in fase solida di nuovi derivati del “ADP-ribosio ciclico” (cADPR)

La sintesi in fase solida di nuove collezioni nucleosidiche da noi messa a punto ci ha spinto a mettere le basi per la costruzione in fase solida di nuovi derivati del cADPR.

Il cADPR, un metabolita secondario sintetizzato a partire dal NAADP, esplica una funzione fondamentale nella regolazione del Ca^{2+} , pertanto risulta di grande interesse disporre di un numero maggiore di informazioni circa i meccanismi attraverso i quali quest'azione viene regolata. Purtroppo lo studio del ruolo fisiologico del cADPR è fortemente limitato dal ruolo transiente di tale molecola [47]. Poiché lo ione calcio è coinvolto nella regolazione di diverse funzioni cellulari, come la contrazione dei muscoli, la secrezione dei neurotrasmettitori, di ormoni ed enzimi responsabili della fertilizzazione degli ovociti, nonché nell'attivazione e proliferazione dei linfociti, la cascata dei segnali modulata dal cADPR diventa un interessante target farmacologico.

L'interesse verso il cADPR trova riscontro: 1) nelle sue importanti implicazioni metaboliche, 2) nella esatta definizione dei suoi meccanismi di azione, 3) nel definire le proteine coinvolte nel suo metabolismo, 4) nel disegno di nuovi analoghi strutturali con attività agonista o antagonista. Il cADPR è caratterizzato da un legame N-1-glicosidico fortemente labile, suscettibile a rapida idrolisi sia enzimatica che non, con formazione del prodotto di idrolisi ADP-ribosio, già in soluzione acquosa neutra.

Da qui la necessità di sintetizzare nuovi derivati più stabili del cADPR al fine di chiarire il suo meccanismo di azione all'interno delle cellule, di creare dei modelli di studio per comprendere la relazione struttura-attività e di avere un pool di analoghi di cui testare la potenziale attività farmacologica.

In letteratura sono riportati diversi esempi di analoghi stabili del cADPR, in alcuni casi anche più attivi dell'analogo naturale stesso.

Uno dei primi è stato l' N-1-aristeromicina-adenina-difosforibosio ciclico [48] in cui l'ossigeno del ribosio in N-1 è sostituito da un gruppo metilenico. Questo composto risulta essere resistente sia all'idrolisi chimica, sia a quella enzimatica dal momento che non c'è più il legame N-1glicosidico presente nel cADPR. Alcune modifiche strutturali sull'adenina forniscono derivati più potenti del cADPR, è il caso del 3-deaza-cADPR avente un'attività 70 volte superiore [49]. Ulteriori modifiche strutturali includono il legame pirofosfato: il cATPR è, non solo più stabile, ma anche più attivo nell'indurre il rilascio di Ca^{2+} (20 volte maggiore) rispetto alla controparte cADPR [50].

Ulteriori studi struttura-attività, eseguiti utilizzando derivati opportunamente modificati al ribosio in posizione N-1 e alla funzione amminica in C-6 dell'adenina, indicano che questi non sono punti critici nell'attività del cADPR. Pertanto il cIDPR e diversi suoi analoghi sono stati sintetizzati. Essi mostrano possedere un'aumentata stabilità rispetto al cADPR e sembrano conservarne l'attività in alcuni sistemi cellulari, come le cellule-T, in cui sono stati saggiati [51].

Poiché la sintesi chimica in soluzione limita la possibilità di ottenere molti analoghi in tempi brevi, mi sono occupato di mettere a punto una metodica di sintesi in fase solida, per la costruzione di nuovi derivati del cIDPR utilizzando sempre un supporto polistirenico ad alta funzionalizzazione legante gruppi monometossitritilcloruro (MMTCI). Lo schema sintetico ha previsto cinque reazioni in fase solida tutte in alte rese.

La reazione finale della sintesi ha previsto la formazione di un legame pirofosfato (P-O-P) fra due fosfomonoesteri (uno presente sul 5'-OH del ribosio e l'altro presente sull'OH terminale del pendaglio alchilico legato all'N1 della base eterociclica) e ciò ha reso necessario l'utilizzo di un linker spaziatore che fosse in grado di bloccare le funzioni 2' e 3' del ribosio fungendo quindi da ponte fra il nucleoside e il supporto solido, lasciando così libera di reagire la funzione 5'-OH della porzione zuccherina. L'innovativa metodica qui proposta per la sintesi in fase solida di derivati del cIDPR permette di ottenere in buona resa un maggior numero di analoghi e in tempi più brevi grazie all'eliminazione dei processi intermedi di purificazione.

Riferimenti Bibliografici

- [1] Opalinska, J. B. et al; *Nature reviews* **2002**, 1, 503.
- [2] Uhlman, E., Peyman, A. *Chem.Rev.* **1990**, 90, 543.
- [3] Wagner, R.W. *Nature* **1994**, 372, 333.
- [4] Zamecnik, P. C., Stephenson, M.L. *Proc Natl Acad Sci USA* **1978**, 75, 280.
- [5] Giovannangeli, C., Hélène, C. *Antisense Nucleic Acid Drug Dev.* **1997**, 7, 413.
- [6] Le Doan, T., Perrouault, L., Praseuth, D., Habhoud, N., Decout, J. L., Thuong, N. T., Hélène, C. *Nucleic Acids Res* **1987**, 15, 7749.
- [7] Miller, P. S., Cohen, J. S. (ed) *Oligodeoxynucleotides: antisense inhibitors of gene expression* CRC Press, Boca Rator, FL **1989**, p. 79.
- [8] Famulok, M., Mayer, G., Blind, M. *Acc. Chem. Res.* **2000**, 33, 591.
- [9] "Oligonucleotides as therapeutic agents", Ciba Foundation Symp., J. Wiley, New York, **1997**.
- [10] Thuong, N. T., Hélène, C. *Angew. Chem. Int. Ed. Engl.* **1993**, 32, 666.
- [11] Gowers, D. M, Fox, K.R. *Nucleic Acids Res* **1999**, 27, 1569.
- [12] Praseuth, D., Guieysse, A.L., and Hélène, C. *Biochim. Biophys. Acta* **1999**, 1489, 181-206.
- [13] *Triple Helix Forming Oligonucleotides* Malvy, C.; Harel-Bellam, A.; Pritchard, L.L. Eds., Kluwer Acad. Pub., Norwell, MA, USA, **1999**.

- [14] Faria, M., Wood, C.D., Perrouault, L., Nelson, J.S., Winter, A., White, M. H. R., Hélène, C., and Giovannangeli, C. *Proc. Natl. Acad. Sci. USA* **97** **2000**, 3862-3867.
- [15] Barre, F.X., Ait-Si-ali, S., Giovannangeli, C., Luis, R., Robin, P., Pritchard, L.L., Hélène, C., and Harel-Bellen, A., *Proc. Natl. Acad. Sci. USA* **97** **2000** 3084-3088.
- [16] Horne D. A., and Dervan, P.B. *J. Am. Chem. Soc.* **1990**, *112*, 2435-2437.
- [17] Ono, A., Chen, C. N., and Kan, L. *Biochemistry* **1991**, *30*, 9914-9921.
- [18] Froehler, B. C., Terhorst, T., Shaw, J. P., and McCurdy, S. N. *Biochemistry* **1992**, *31*, 1603-1609.
- [19] Zhou, B. W., Marchand, C., Asseline, U., Thuong, N. T., Sun, J. S., Garestier, T., and Hélène, C. *Bioconjugate Chem.* **1995**, *6*, 516-523.
- [20] De Napoli, L., Messere, A., Montesarchio, D., Piccialli, G., Varra, M., *Nucleosides and Nucleotides* **1997**, *16*, 183-191.
- [21] De Napoli, L., Messere, A., Montesarchio, D., Piccialli, G., Varra, M., *J. Chem. Soc. Perkin Trans. I* **1997**, 2079-2082.
- [22] Giancola, C., Buono, A., Barone, G., De Napoli, L., Montesarchio, D., Palomba, D., Piccialli, G., *J. Thermal Anal. Cal.* **1999**, *56*, 1177-1184.
- [23] "Carbohydrate Modifications in Antisense Research", Sanghvi, Y. S. Ed., ACS Symp. Ser., Washington, USA, **1994**.
- [24] Uhlmann, E., et al. *Angew. Chem. Int. Ed. Engl.* **1998**, *37*, 2796.
- [25] Capasso, D., De Napoli, L., Di Fabio, G., Messere, A., Montesarchio, D., Pedone, C., Piccialli, G., Saviano, M., *Tetrahedron* **2001**, *57*, 9481.
- [26] Farrel, N. *Transition Metal Complexes as Drugs and Chemotherapeutic Agents*, Kluwert Academic Publishers, Dordrecht, **1989**.
- [27] Ihara, T., Nakayama, M., Murata, M., Nakano, K., Maeda, M. *Chem. Commun.* **1997**, 1609.
- [28] Bucci, E., De Napoli, L., Di Fabio, G., Messere, A., Montesarchio, D., Romanelli, A., Piccialli, G., Varra, M. *Tetrahedron* **1999**, *55*, 14435.
- [29] Neilde, S., Parkinson, J. *Nature reviews* **2002**, *1*, 384.
- [30] Thomas, D. W. *Journal of Pathology* **1999**, *187*, 100.
- [31] Zaklan, V. A. *J. Mol. Biol.* **1995**, *219*, 201.
- [32] Han, H., Fedoroff, O., Rangan, A., Izbicka, E., Von Hoff, D. D., Hurley L. *International Symposium on Drug Regulation of Gene Expression* **1999**.
- [33] Mergny, J.L., Heléné, C. *Nature Medicine* **1998**, *4*, 1366.
- [34] Jing N., et al. *DNA Cell Biol.* **2001**, 20,499.
- [35] Smirnov, I. et al. *Biochemistry* **2000**, *37*, 1462.
- [36] Lin, Y. et al. *J. Biol Chem.* **2001**, *50*, 47671.
- [37] Arimondo, P. et al *Nucleic Acids Res.* **2000**, *28*, 4832.
- [38] LaPorte, L. et al. *Biochemistry* **1998**, *37*, 1327.
- [39] Giraldo, R. et al. *Proc natl Acad Sci USA* **1994**, *91*, 7658.
- [40] Agatsuma, T.; et al. "Recent Developments in Antiviral Research" **2001**, *1*, 45-57.
- [41] Koizumi, M.; et al. *Med Chem. Lett.*, **2000**, *10*, 2213.
- [42] Wyatt, J.R. et al., *Proc. Natl. Acad. Sci. USA*, **1994**, *91*, 1356.
- [43] Okazawa, A. et al *Biorg. Med Chem. Lett.* **2000**, *10*, 2653.
- [44] Ding, Y.; Habib, Q.; Shaw, S. Z.; Li, D. Y.; Abt, J. W.; Hong, Z.; An, H. *J. Comb. Chem.* **2003**, *5*, 851–859.
- [45] Fujii, T.; Saito, T.; Risata, H.; Shinbo, K. *Chem. Pharm. Bull.* **1990**, *38*, 3326–3330.
- [46] a) Kumar, A.; Walker, R. T. *Tetrahedron* **1990**, *46*, 3101–3110, b) Criegee, R. *Oxidation in Organic Chemistry*; Wiberg, K. B., Ed.; Academic: New York, NY, **1965**.
- [47] Hutchinson, E.J.; Taylor, B.F. *J. Chem. Soc. Comm.* **1997**, *19*, 1859-1860.
- [48] Shuto, S.; Fukuoka, M. *J. Am. Chem. Soc.* **2001**, *123*, 8750-8759.
- [49] Wang, L.; Aarhus, R. *Biochem. Biophys. Acta* **1999**, *1472*, 555-564.
- [50] Aarhus, R.; Gee, K. *J. Biol. Chem.* **1995**, *270*, 7745-7749.
- [51] Gu, X.; Yang, Z. *J. Med. Chem*, **2004**, *47*, 5674-5682.

Chapter 1

Synthesis of Tetra-End-Linked oligonucleotides forming DNA G-quadruplexes: structure characterization and stability

Introduction

In 1990 Guschlbauer, Chantot and Thiele published the review article “Four-Stranded Nucleic Acid Structures 25 Years Later: From Guanosine Gels to Telomere DNA”¹, in which they highlighted the emerging importance of the G-quartet, a hydrogen-bonded ionophore² first identified in 1962.

Interest in this area has intensified in recent years because G-quadruplex structures have roles in crucial biological processes and can be targeted for therapeutic intervention³ G-quadruplexes might also have applications in areas ranging from supramolecular chemistry and nanotechnology to medicinal chemistry⁴

Quadruplexes can be formed with one, two or four G-rich strands (**Figure 1.1**). Tetramolecular quadruplexes generally adopt a well-defined structure, in which all guanines are in the anti-glycosidic conformation and all strands are parallel, and might be useful for biotechnology applications. J.-L. Mergny (Paris, France) described the stability and kinetics of tetramolecular quadruplexes. He reported that tetramolecular quadruplexes with stacked G-quartets are extremely stable and that quadruplex ligands can act as molecular chaperones to increase the normally slow rate of tetramolecular quadruplex association, so that they form in minutes rather than days⁵

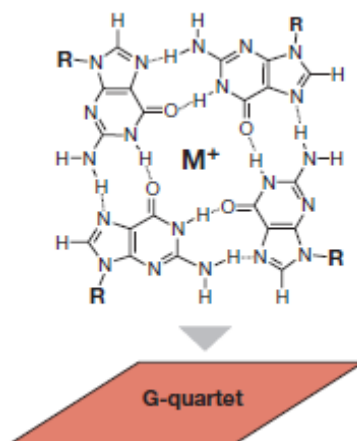


Figure 1.1 G-quartet

Intramolecular G-quadruplexes formed by a single DNA strand have attracted much interest because they might form in telomeres, oncogene promoter sequences and other biologically relevant regions of the genome. In contrast to tetramolecular quadruplexes, intramolecular structures form quickly and are more complex, showing great conformational diversity, such as folding topologies, loop conformations and capping structures. Different sequences adopt distinct topologies, but a given sequence can also fold into various different conformations, which can coexist. One of the best illustrations of this complexity are human telomere sequences, in which variants of the minimal four G-tract core sequence of the human telomere,

5'-(GGGTTA)3GGG, have been synthesized and studied by high-resolution nuclear magnetic resonance (NMR) or crystallography. Although the structure in Na⁺ solution was reported more than a decade ago⁶, the 'potassium structure' has been the subject of intense investigation, largely because the high intracellular concentration of K⁺ ions suggests that it should be the more biologically relevant form. The crystal structure of the human telomeric G-quadruplex in the presence of K⁺ was reported five years ago⁷ and is a parallel-stranded monomer, which is different from the Na⁺ solution structure that contains antiparallel strands. Recently, several groups reported the folding patterns and molecular structures of intramolecular telomeric G-quadruplexes in K⁺ solution⁸.

1.1. Topological classification of G-Quadruplex DNA structures

Numerous reviews have appeared recently discussing the structural characterization and polymorphism of G-quadruplex DNA⁹. It is now well established that certain DNA and RNA sequences, possessing a preponderance of guanosine residues, can form unusual structures. These structures exhibit unusual mobility under gel electrophoresis conditions, protection of the guanosine N7 from methylation with dimethyl sulfate, a characteristic CD spectrum, a signature cation-dependent stability to thermal denaturation, and distinctive imino resonances in the ¹H-NMR spectrum. Early observations related to these structures came from the behaviour of guanosine nucleotides, which form gels in a cation-dependent manner. Fibre diffraction studies of the gels formed by guanosine-3'-monophosphate and poly(G) established the fundamental building block of these unusual structures, the G-tetrad, also called the G-quartet (**Figure 1.1**). The G-tetrad consists of a planar arrangement of four guanine bases associated through a cyclic array of Hoogsteen hydrogen bonds in which each guanine base both accepts and donates two hydrogen bonds. The resulting square planar array is unique due to the "hole" that is created in the center. The G-tetrads form four-stranded helical structures by stacking interactions. In the case of the poly(G), the average distance separating the stacked G-tetrads is 3.4 Å. The tetrads are not stacked linearly, but adopt a right-handed helix. When one or more tetrads are stacked in this way, a cylindrical central cavity is produced. This cavity, lined with the guanine O-6 carbonyl oxygens, forms a specific binding site for metal ions. As deduced from the ability of particular metal ions to induce gel formation in guanosine nucleotides, the binding of metal ions follows the order Sr²⁺>K⁺>>Rb⁺~Ba²⁺>NH₄⁺>Ca²⁺>Na⁺>Mg²⁺ ~Cs⁺>Li⁺⁹. This contrasts sharply with duplex DNA, in which there is only a slight preference in metal ion binding in the series Cs⁺>K⁺>Li⁺>Na⁺.

A wide array of topologies and strand stoichiometries are compatible with the stacking of G-tetrads in helical structures. Hardin¹⁰, expanding on the naming convention suggested by Cech¹¹, has proposed the class name G-DNA for this large class of structures; however, current usage appears to have settled on the class name G-quadruplex DNA. The structure formed from poly(G) consists of four strands, each contributing one G-residue to each G-tetrad. In this arrangement, the four strands are parallel, and there is a four-fold symmetry associated with the structure. This type of intermolecular, parallel-stranded structure has been referred to as G-quadruplex, G-tetraplex, or simply G4-DNA. In accord with the naming convention of Sen and Gilbert¹², these four-stranded, parallel structures are referred to as G4-DNA (**Figure 1.2**).

Alternatively, G-quadruplex DNA may form from two separate DNA strands, each of which contributes two guanosine residues to each G-tetrad. These bimolecular G-quadruplex DNA structures have been referred to as hairpin dimers. This class of structures are referred to as G'2-DNA. There are a number of strand topologies that might be involved in the formation of G'2-DNA, but to date only four of these have been observed or proposed. As Bolton has noted, there are two distinct forms of G'2-DNA in which the loops formed by each of the two DNA strands are on opposite faces of the G-tetrad core¹³. In the edge form (**Figure 1.2**), the loops connect adjacent DNA strands. A distinct crossover form is characterized by loops that connect strands that are diagonally related. A G'2-DNA topology in which the loops connecting DNA strands lie on the same face of the G-tetrad stack has been proposed by Sen and Gilbert (*syn*-edge G'2-DNA, figure 3.2)¹⁴. An alternative topology for a bimolecular G-quadruplex DNA structure is a "dog-eared" structure. This topology requires that the DNA loops run diagonally across the faces of the G-quadruplex that are perpendicular to the G-tetrads. Although this topology has not yet been observed in G'2-DNA, a recently reported intramolecular G-quadruplex DNA has such a dog-eared" loop¹⁵. In addition to the G'2-DNA topologies mentioned above, there are a variety of hypothetical topologies involving alternate strand distribution (i.e. three guanines in each G-tetrad from one strand and the fourth guanine from a second strand) or orientation (i.e. three parallel strands and one antiparallel strand, this latter recently observed in human telomere structure forming an intramolecular 3+1 G-quadruplex scaffold in K⁺). It is likely that future research may uncover examples of these alternative topologies. Just as in the case of the bimolecular G-quadruplex DNA structures, there are multiple topologies that are possible in the formation of a unimolecular, or G4'-DNA. The chair form of G4'-DNA is characterized by loops connecting only adjacent strands¹⁶. This form is similar to the unimolecular form of G'2-DNA proposed by Sundquist and Klug. The basket form has one loop that crosses the G-tetrad face diagonally. A strikingly different folding topology is that reported by Wang and Patel¹⁵ for the Na⁺-stabilized NMR structure of the *Tetrahymena* telomeric repeat d(T₂G₄)₄. This sequence adopts a fold in which adjacent strands are connected by an edge loop on one face of the G-tetrad stack, a second, central lateral loop, and a terminal "dog-eared" loop running diagonally across one of the perpendicular faces of the G-tetrad stack. There are a multitude of alternative G4'-DNA fold topologies involving combinations of crossover, edge, and dog-eared loops; only time will tell if these topologies are energetically accessible to certain natural or engineered DNA sequences.

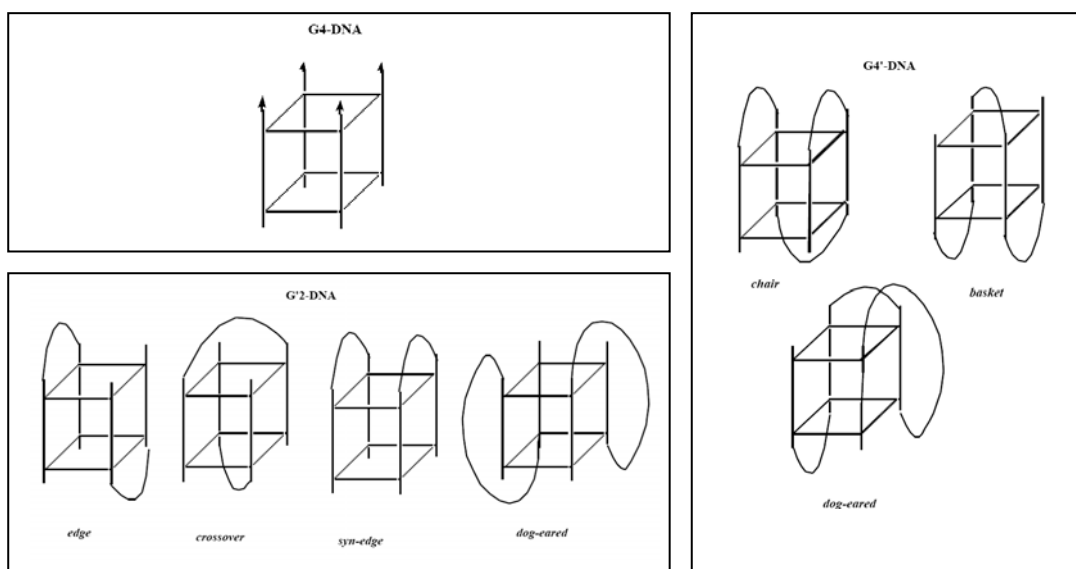


Figure 1.2: Different topological forms of termolecular (G4-DNA), bimolecular (G'2-DNA), and unimolecular (G4'-DNA) G-quadruplex structures.

Related to the overall fold topology demonstrated by G'2-DNA and G4'-DNA are the glycosidic angles of the guanosine nucleotides forming the G-tetrads. In order for adjacent guanines in antiparallel strands to form the hydrogen bonds necessary for G-tetrad formation, one of these guanines must adopt a *syn* glycosidic conformation. Thus, for each topology listed above, there are alternative strand orientations that would result in distinct distributions of glycosidic conformations in the G-tetrads. For example, G'2-DNA having the edge topology can in principle adopt either a symmetrical form, in which the 5'-ends of the two strands are diagonally arranged about a common face, or an unsymmetrical form in which these two ends do not share any common faces. The symmetrical form requires that each G-tetrad have alternating *syn-anti-syn-anti* glycosidic conformations, whereas the unsymmetrical form requires *syn-syn-anti-anti* glycosidic conformations (**Figure 1.3**).

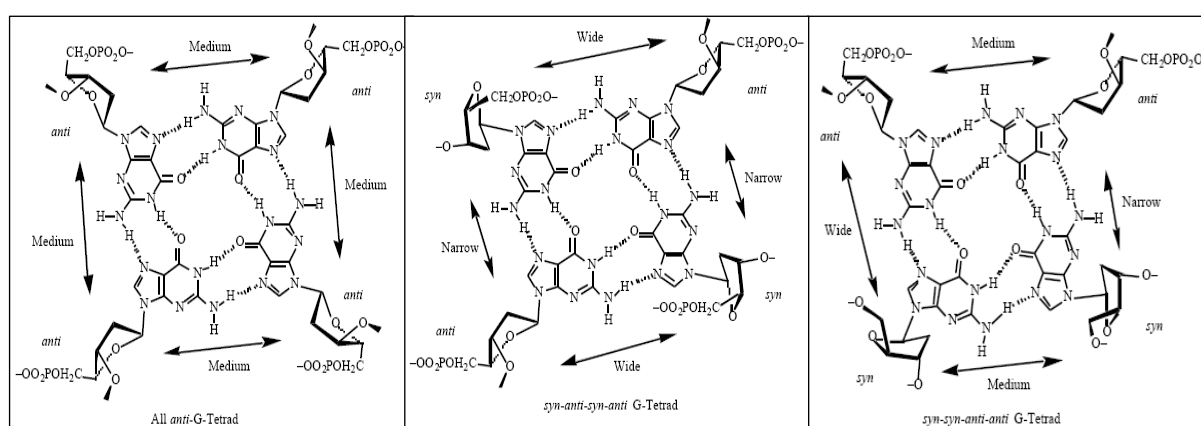


Figure 1.3 G-Quadruplex DNA groove widths

Experimentally, the symmetrical edge form is observed in the X-ray structure of $[d(G4T4G4)]_2$ ¹⁷. One consequence of this variation in glycosidic conformations, is the

distinct nature of the grooves. The parallel G4-DNA G-tetrads, in which all G's adopt the *anti* glycosidic conformation, affords four widths of identical medium width. In cases where a guanosine in the *syn* conformation donates hydrogen bonds to a neighboring guanosine in the *anti* conformation, the groove formed between the two is extremely narrow, with a phosphate to phosphate distance as small as 7-9 Å¹⁸. In contrast, when the hydrogen bonding polarity between adjacent *syn*- and *anti*-guanosines is reversed, a very wide groove is formed. An intermediate width groove results when adjacent guanosines adopt the same glycosidic conformation (**Figure 1.3**). For example, in the structure of the symmetrical G'2-DNA having the edge topology, the G-tetrads are formed from guanosines of alternating *anti-syn-anti-syn* conformation, with each *syn*-guanosine donating hydrogen bonds to an adjacent *anti*-guanosine, and accepting hydrogen bonds from the other adjacent guanosine. This results in a rectangular G-tetrad core with grooves of alternating wide-narrow-wide-narrow widths. The crossover G'2-DNA has guanosines that adopt the *syn-syn-anti-anti* conformations, which results in G-tetrads that adopt a parallelogram arrangement and the formation of alternative wide, medium, narrow, medium width grooves between strands. Individual DNA strands in G-quadruplex structures is also a source of structural diversity, manifest by altered groove geometry. Both *syn-anti-syn-anti* and *syn-syn-anti-anti* G-tetrads typically stack upon each other such that consecutive G's in each DNA strand adopt an alternating 5'-3' *syn-anti* relationship. However, in G4'-DNA structures containing an odd number of stacked G-tetrads, unique *syn-syn* G-G steps are observed. Through a combination of the altered base-edges and twist geometry associated with these *syn-syn* G-dinucleotide steps, the narrow grooves of these particular G4'-DNA structures provide a unique target for ligand design^[26-31]. The ability of DNA minor groove ligands to distinguish the variable groove width engendered by sequence has been reported. The specific array of alternating groove widths in G-quadruplex DNA structures should provide a means of selectively targeting specific topological and conformational forms of G-quadruplex DNA. For example, ligands which are able to span two or more G-quadruplex grooves may be able to distinguish one form from another based upon the specific groove dimensions and their specific orientation.

As has been observed for the association of individual guanosine nucleotides, G-quadruplex structures are stabilized by specific metal ion interactions¹⁹. The central cavity formed by stacked G-tetrads serves as a host to a variety of cations²⁰. The metal cation preference for G4-DNA follows the trend $K^+ > Ca^{2+} > Na^+ > Mg^{2+} > Li^+$ and $K^+ > Rb^+ > Cs^+$, in accord with the trend observed for guanosine nucleotide gel formation. In the case of K^+ , the stacked G-tetrads in G-quadruplex DNA provide a bipyramidal antiprismatic coordination geometry (**Figure 1.4a**), with each of eight carbonyl oxygens interacting equally with the cation.

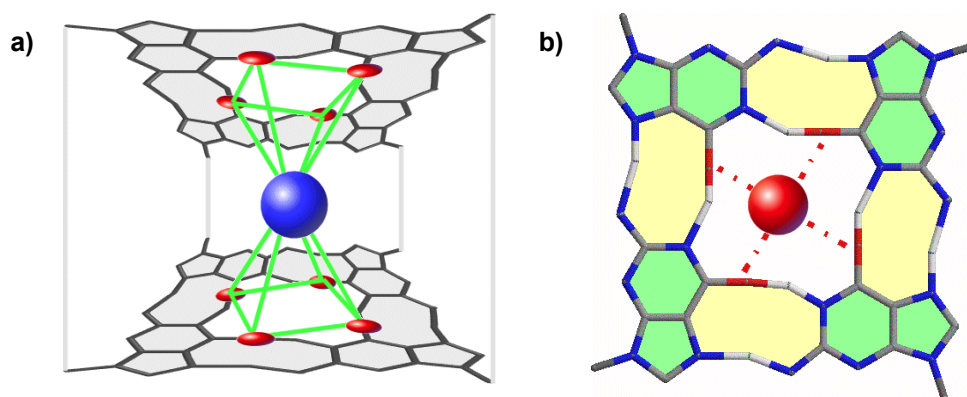


Figure 1.4: Metal ion coordination geometry. a) K⁺; b) Na⁺.

In the crystal structure of [d(G4T4G4)]₂, a region of weak electron density was found between planes of stacked G-tetrads and this was assigned to bound K⁺²¹. In the high resolution crystal structure of [d(TG4T)]₄, two G4-DNA structures stack coaxially upon each other, forming an extended cylindrical central cavity. Sodium ions are located between G-tetrad planes in the center of this cavity (**Figure 1.4b**), but stack out of phase with the G-tetrad repeats, so as to bind in the terminal G-tetrad planes. The selectivity of G-quadruplex DNA for K⁺ versus Na⁺ ion has been studied by Feigon and co-workers using ¹H-NMR and the G'-DNA formed by d(G₃T4G₃), as a model system²². In this system, the G'-DNA binds two K⁺ or Na⁺ ions, corresponding to one metal ion sandwiched between each pair of G-tetrads. Using competition NMR experiments, Feigon and co-workers determined that there is only a modest difference in free energy of 1.7 kcal/mole, favoring the binding of K⁺ versus Na⁺ ions^[37]. They suggest that this modest free energy difference is a result of the contributions of the relative free energies of hydration, which favors K⁺ binding. The effect of various cations on the kinetics of G-quadruplex DNA formation and the conformational polymorphism of G-quadruplex DNA has also been studied. Although original observations by Sen and Gilbert²³ indicated that K⁺ prevented the formation of G4-DNA from DNA oligonucleotides containing multiple runs of G's, this appears to be a kinetic, rather than thermodynamic phenomenon. G-quadruplex DNA structures can be trapped in metastable states in the presence of K⁺ ions, which stabilize and inhibit the interconversion of G-quadruplex DNA structures. Thomas²⁴, Bolton, and Hardin²⁵ have shown that the specific complexation of K⁺ by G-quadruplex DNA leads to a preference for the formation of G4-DNA structures under high K⁺ concentrations. Low K⁺ concentrations, or higher Na⁺/K⁺ ratios, favour G4'-DNA structures. Whether a linear or a folded structure is formed is dependent on the exact sequence and number of repeats per strand, cations have a strong influence on their relative stabilities. It has been found that potassium ions preferably stabilize linear, four-stranded parallel quadruplexes whereas sodium ions stabilize folded forms. Cations have profound effects on loop geometry in G4'-DNA structures. DNA oligonucleotides, with four runs of -GG- separated by two to four bases, can form chair G4'-DNA structures, but only in the presence of K⁺. When the -GG- runs are separated by four residues, a basket G4'-DNA structure can form in either Na⁺ or Na⁺/K⁺. Sequences with runs of three or four G's separated by two to four bases can form basket G4'-DNA structures in the absence of K⁺. The presence of a purine in the loop can block both K⁺ binding and formation of the chair G4'-DNA structure. Modelling indicates that the requirement for K⁺ ion for chair formation is due to the

ability of this ion to interact with the terminal G-tetrad and residues in the adjacent loop. In addition to these cation-induced changes in G-quadruplex DNA topology, there is evidence for K^+ -ion facilitated formation of G-quadruplex DNA structures from duplex DNA precursor¹. Increasing K^+ causes an increased cooperativity of G4-DNA thermal dissociation, despite the increased stabilization of G4-DNA at these higher K^+ concentrations. Structural transitions of G-quadruplex DNA, induced by changes in univalent cation concentrations (i.e. K^+ and Na^+), may play an important role in DNA replication, organization, and function. The transient changes in K^+ concentration during the cell cycle may drive structural transitions in G-rich DNA. Low basal K^+ concentrations (ca. 110 mM²⁶) are thought to stabilize the G4'-DNA structures that may form from single-stranded G-rich sequences at the ends of the telomeres. As the cell cycle proceeds, K^+ concentrations increase (ca. 130mM²⁷) and this temporal elevation in K^+ concentration initially favours the formation of G'2-DNA structures, which may facilitate the alignment of chromosomal pairing in preparation for homologous recombination events. Further elevation in K^+ concentration subsequently promotes the formation of G4-DNA structures that may be involved in the process of meiotic (or mitotic) telomere association. An alternative view is that altered K^+/Na^+ ratios in cancer cells may result in altered G-quadruplex DNA structure and function. A number of reports have documented altered K^+/Na^+ ratios in tumour cells, although the magnitude and trend of change appear to be tumour type specific²⁸. These cancer cell-specific K^+/Na^+ ratios may effect conformational changes in G-quadruplex structures, resulting in altered transcription of particular genes and altered telomere function and maintenance.

1.2. G-quadruplex: molecular recognition

The wide array of G-quadruplex topologies, groove widths, loop conformations, and alternative DNA base-associations observed to date is probably just a small sampling of the structural diversity exemplified by G-quadruplex DNA. The unique features of G-quadruplex DNA: the association of up to four separate DNA strands, the hydrophobic stacking of large, planar hydrogen bonded DNA base quartets, and the specific interactions with metal ions, provide the basis for building up these diverse structures. Once formed, the G-tetrads of G-quadruplex DNA, can provide an "assembly floor" for the creation of unusual DNA base associations. The potential existence of G-quadruplex DNA *in vivo* opens up new vistas for the targeting of DNA sequences by molecular recognition of these structurally diverse DNA motifs. The structural uniqueness of the G-quadruplex can only aid in the realization of this ultimate goal in DNA sequence recognition. As shown in **Figure 1.5** and **Table 1.1**, there are different ways in which molecules can interact with G-quadruplexes: by face recognition, edge recognition, loop recognition, or by simultaneous binding to the surface of the G-quartet and an adjacent loop or groove.

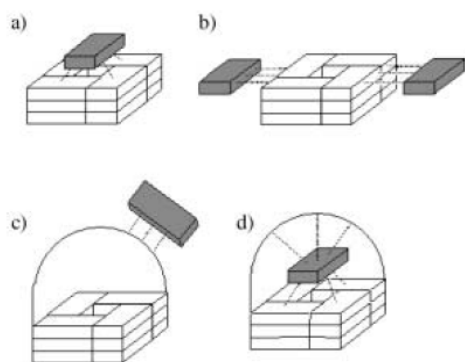


Figure 1.5: Schematic representation showing some of the ways that other molecules recognize a bimolecular G-quadruplex.

Table 1.1: Molecular recognition of G-quadruplexes

a) face recognition through stacking:
<ul style="list-style-type: none"> nucleobase triads and tetrads aromatic molecules/telomerase inhibitors
b) edge recognition through hydrogen bonding:
<ul style="list-style-type: none"> hydrogen bonding of other nucleobases protein recognition: edge interaction with amino acids water-nucleobase interactions
c) loop recognition through hydrogen bonding and electrostatic interactions:
<ul style="list-style-type: none"> protein interactions: electrostatic phosphate -ammonium interactions small molecules and water
d) groove recognition through hydrogen bonding and electrostatic interactions
<ul style="list-style-type: none"> water interactions with the hydration spine side-chain interactions with stacked aromatic molecules

Within the context of nucleic acids, there are two major ways for adjacent nucleobases to recognize a G-quartet: either by stacking on its surface or by hydrogen bonding to an exposed edge. Molecular recognition of the G-Quartet Edges Hydrogen-bond donor (N2-H and C8-H) and acceptor (N3) atoms on the exposed edges of the G-quartet are also molecular recognition sites. These sites, which are located along the floor of a groove running the length of the G-quadruplex, can bind water, ions, amino acid side chains, and other nucleobases. Furthermore, neighboring loops in bimolecular and unimolecular G-quadruplexes are also molecular recognition sites, particularly for proteins and small molecules.

Molecular recognition of G-quadruplexes by proteins

DNA and RNA oligonucleotides called aptamers have been selected by in vitro selection to bind molecular targets²⁹. These targets are often proteins. One well-known aptamer is the thrombin binding aptamer (TBA), a DNA 15 mer that inhibits clotting. Crystallographic³⁰ and NMR³¹ spectroscopic studies have shown that TBA forms a unimolecular G-quadruplex with two G-quartets and three loops. The structure and biological activity of TBA are K⁺-dependent. NMR spectroscopic, calorimetric, and ESI-MS studies have shown, however, that TBA is even more stable with divalent Pb²⁺, Sr²⁺, and Ba²⁺ ions³². Related DNA aptamers are inhibitors of human HIV integrase with IC₅₀ values in the nm region³³ and adopt a unimolecular G-quadruplex similar to TBA³⁴. An intermolecular G-quadruplex aptamer that bound the V3 loop of HIV reverse transcriptase was formed by a 17-mer phosphorothioate oligonucleotide³⁵. Like many G-quadruplexes, this phosphorothioate aptamer was extremely stable and had a dissociation half-life of 60 days. Many other protein-binding aptamers have been proposed to form G-quadruplexes as part of their bioactive structure³⁶. Although many proteins, including aptamers, oncogenic factors³⁷, antibodies, and telomeric proteins, all bind G-quadruplexes, there are few molecular details known about quadruplex-protein interactions. The crystal structure of TBA bound to thrombin showed some ion pairs between the phosphate groups in the loops of the aptamer and Lys and Arg side chains³⁸. A crystal structure of the telomeric protein of *Oxytricha nova* complexed to d[G4T4G4]4 is particularly

valuable. As in the DNA solution structures, the bimolecular quadruplex in this complex has diagonal loops. Most of the DNA–protein contacts take place with these loops, rather than with the quadruplex core. However, the major DNA–protein interactions include: 1) electrostatic interactions, wherein the surface formed by three symmetry-related proteins provides a deep, electropositive cavity to hold the folded DNA; 2) van der Waals interactions, such as where the aromatic rings of Tyr142 and Phe141 pack against the G-4 sugar; 3) water mediated hydrogen bonds, wherein one of the T4 loops forms an extensive network of water-mediated hydrogen bonds with the protein; 4) nucleobase–peptide packing interactions, wherein the T6 residue of the other loop contacts the protein using both van der Waals and H-bond interactions. This T6 nucleobase packs between a Leu side chain and the polarized Asp437–Gly438 peptide bond, while simultaneously hydrogen bonding with atoms of the protein side chain and main chain. In both cases where crystal structures are available, for the *Oxytricha* and for the thrombin systems, there are few direct interactions between the protein and the G-quadruplex core. Instead, the G-quadruplex seems to function as a scaffold on which loops are displayed for molecular recognition. Certainly, the crystal structure of the unimolecular G-quadruplex formed from the human telomeric sequence d(TTAGGG) suggests that the extended loops provide ideal protein-binding sites. In time, as more structural information becomes available, we should learn if a preference to bind loops is general for G-quadruplex protein interactions.

1.3 Quadruplexes in telomeres or quadruplexes everywhere?

Potential quadruplex-forming sequences are also widespread throughout the genome, especially in gene promoters (**Figure 1.6**). These structures are expected to be different from telomeric quadruplexes—not least because they will be in the context of doublestranded DNA —although by no means less complicated. In contrast to the uniform repeating G-rich sequence in telomeres, the G-rich sequences of gene promoters are often composed of more than four G-tracts with each G-tract containing unequal numbers of guanines and separated by various numbers of bases. Therefore, each sequence is able to form many possible quadruplex structures by using different combinations of G-tracts or guanines within a tract.

An interesting feature of the promoter quadruplexes is the occurrence of stable structures with single-nucleotide doublechain-reversal loops³⁹. Such single-nucleotide double-chain-reversal loops have previously been found in the c-myc promoter G-quadruplexes⁴⁰. Phan reported a new quadruplex fold formed in a wild-type sequence of the c-kit promoter. This scaffold is extremely unusual in that an isolated guanine is involved in G-tetrad core formation, despite the presence of four guanine tracts⁴¹. Notably, this structure also contains single-nucleotide-sized loops.

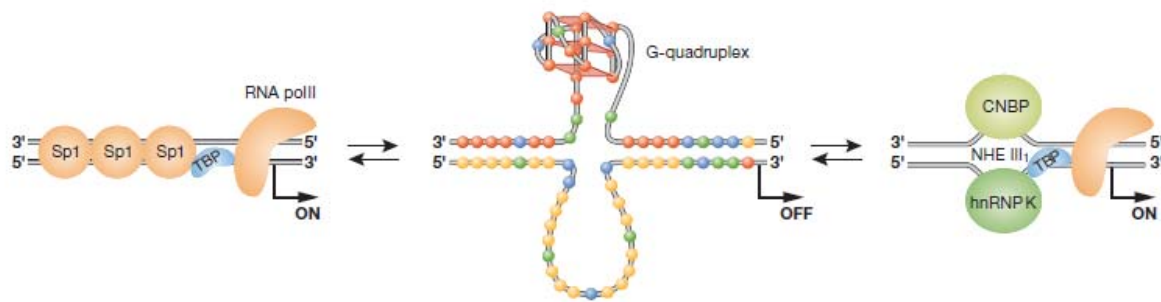


Figure 1.6 Quadruplex in a gene promoter.

For many years, the question facing biologists in the quadruplex field was whether quadruplex structures really exist *in vivo*. There is now overwhelming evidence that they do⁴² and the field has moved forward to focus on understanding the biological functions of various quadruplexes. D. Rhodes (Cambridge, UK) and H. Lipps (Witten, Germany) provided an overview of their work studying telomere regulation in the ciliate *Stylonychia*, in which quadruplex formation in telomeres can be directly observed *in vivo* using specific antibodies. By staining with the antibody throughout the cell cycle, they showed that telomeric quadruplex structures are resolved during replication. Their recent research also indicates that this quadruplex unfolding is mediated by telomerase, which is recruited to telomeres by phosphorylated telomere end binding protein β (TEBP- β). It will be interesting to see what these elegant studies can teach us about the biology of mammalian telomeres. N. Maizels (Seattle, WA, USA) described non-telomeric sequences that have a high potential for quadruplex formation, with particular emphasis on immunoglobulin heavy-chain switch regions. She made the important point that, for quadruplex formation to occur within the context of double-stranded DNA, duplex unwinding must occur. Therefore, quadruplex formation is most likely to be seen during processes such as transcription, replication or recombination, when the DNA duplex is actively denatured. Maizels discussed several proteins that bind to quadruplex-containing structures, including nucleolin, MutS- α , heterogeneous nuclear ribonucleoproteins (hnRNPs) and RecQ family helicases, such as BLM (Bloom syndrome) helicase. Recent whole-genome analyses by several groups have revealed that potential quadruplex-forming sequences are surprisingly common. For example, it is estimated that there might be more than 370,000 potential quadruplex-forming sequences in the human genome⁴³. However, one should emphasize that these sequences remain putative, and that many sequences found in the human genome might well never adopt a quadruplex structure for several reasons. Certainly, with the possible exception of the *c-myc* promoter (**Figure 1.6**⁴⁴), the biological functions of these putative quadruplexes are uncertain at present.

The intramolecular telomeric G-quadruplex has been considered to be an attractive target for anticancer drug design ever since quadruplex ligands were found to inhibit telomerase, an enzyme that is activated in most cancer cells but not in most non-cancerous cells. In addition to the slow erosion of telomeres caused by blocking telomerase, it has recently become apparent that quadruplex ligands can induce rapid apoptosis owing to displacement of telomere-binding proteins. Many quadruplex-specific ligands have been identified and the crystal structures that are available, together with NMR data, provide a consistent view of how many ligands bind. Terminal stacking at the end of the quadruplex is the most frequently encountered method, whereas groove binding is indicated for a few molecules. E. Lewis (Flagstaff, AZ, USA) found two methods of interaction for a cationic porphyrin,

one of them suggestive of an intercalation between two G-quartets. D. Wilson (Atlanta, GA, USA) indicated that some quadruplex ligands might also recognize the grooves of a quadruplex, and used surface plasmon resonance to study the affinity and specificity of such molecules. For some ligands—for example, TMPyP4 (5,10,15,20-tetra(*N*-methyl-4-pyridyl)porphine chloride)—the preference for quadruplexes over duplexes was found to be quite low. All attendees agreed that structural information on ligand binding is an area that requires further investigation. In **Figure 1.7** some possible roles of quadruplex formation *in vivo* and therapeutic strategies based on quadruplex formation are presented. Antiparallel quadruplexes are shown for simplicity, but actual structures might vary. **(A)** Quadruplex formation in the single-stranded regions of telomeres. Ligands that stabilize the quadruplex might lead to cellular senescence by preventing telomere extension mediated by telomerase (TEL), and might also induce rapid apoptosis by displacing telomere-binding proteins, for example, protection of telomeres 1 (POT1). **(B)** Quadruplex formation in the context of duplex DNA is now suspected for many gene promoter regions, especially oncogene promoters. The quadruplex structure is a transcriptional repressor for some oncogenes, for example, *c-myc*, and quadruplex-stabilizing ligands might act to block transcription. **(C)** Quadruplexes can also form in RNA and might hinder translation. **(D)** Ribosomal genes (rDNA), which are located in the nucleolus of the cell, contain a high concentration of potential quadruplex-forming sequences. These rDNA quadruplexes seem to be the target of CX-3543, a quadruplex-binding small molecule that is now in clinical trials as an anticancer agent (quarfloux; Cylene Pharmaceuticals, San Diego, CA, USA). CX-3543 localizes to nucleoli and prevents nucleolin protein (NCL) from binding to rDNA quadruplexes, leading to inhibition of ribosome biogenesis. **(E)** AS1411 (Antisoma, London, UK) is a quadruplex-forming oligonucleotide that is now being tested in human clinical trials. This molecule also targets nucleolin protein and seems to bind to the cell surface form of the protein, which is present at high levels in cancer cells, leading to internalization of the complex. AS1411 can affect the molecular interactions and transport of nucleolin, thereby inhibiting many cancer cell survival pathways.

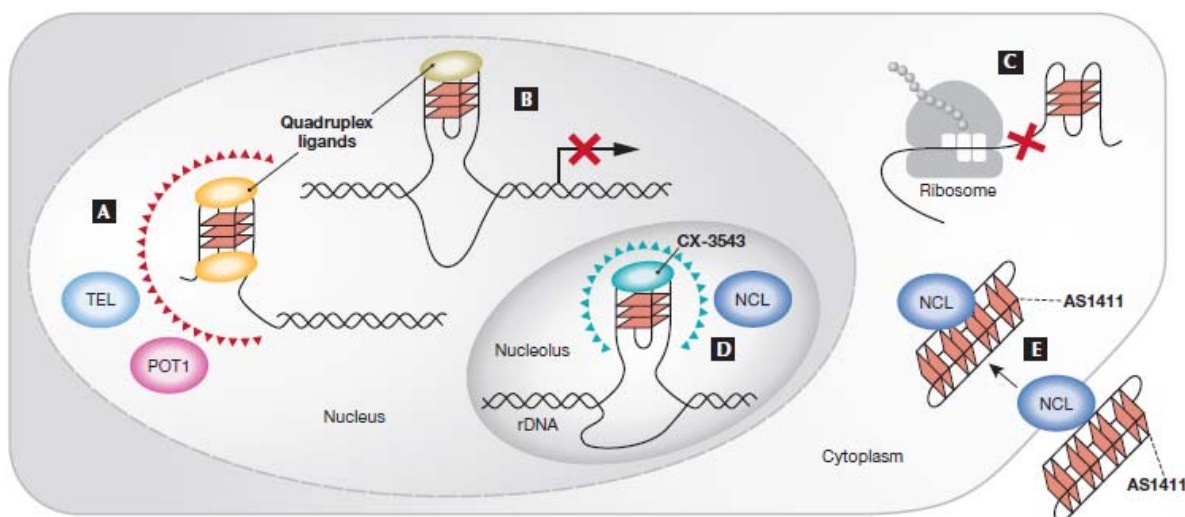


Figure 1.7 Quadruplexes in biology and as therapeutic agents or targets.

1.4 Applications of quadruplexes: bio- and nano-technologies

Quadruplexes show also promise as components for nanowires, ion channels, and building blocks for directing the assembly of nanoscale components into sophisticated structures.

Fiber diffraction studies on crystalline GMP and poly-(guanylic acid) had shown that these compounds self-assemble into rods of stacked G-quartets⁴⁵. In the mid-1990s, the research groups of both Henderson and Sheardy further established that G-rich DNA formed nanometer assemblies⁴⁶. They showed by using gel electrophoresis that d(G4T2G4), in the presence of K⁺ and Mg²⁺ ions formed high molecular weight assemblies that were well resolved from the smaller G-quadruplex [d(G4T2G4)]₄. The polymers were extraordinarily stable; heating at 80°C or dissolving in 8 M urea did not denature them. Marsh and Henderson coined the term “G-wires” to describe the continuous, parallel-stranded DNA superstructures formed when the 5'-end of one DNA-duplex with G-G pairs associates with the 3'-end of a similar duplex⁴⁷. Marsh and Henderson proposed that G-wires could be useful in nanotechnology, nano-electronics and biosensor development.

G-quadruplexes can organize themselves to build transmembrane ion channels. NMR studies have shown that base pairs in DNA G-quadruplexes open slowly and G-quadruplex dissociation is often quite slow, taking days or weeks. These results suggest that ions move without disruption of the G-quartet, thus making the G quadruplex analogous to an ion channel.

While DNA aptamers have potential as therapeutics and diagnostics, they also have applications in bioanalytical chemistry. Small molecules and proteins can be separated by using G-quadruplex DNA as stationary phases in chromatography or electrophoresis. DNA aptamers featuring an intramolecular G-quadruplex served as the stationary phase for the separation of the isomeric dipeptides Trp–Arg and Arg–Trp⁴⁸. DNA G-quadruplex aptamers labeled with fluorescent dyes have also served as a prototype for biosensors⁴⁹. In particular, FRET has been used to study the secondary structure of G-rich DNA oligonucleotides⁵⁰. FRET is a distance-dependent method for detecting conformational changes over distances of 10–100Å. FRET has also been used to monitor the formation of molecular “nanomotors” from single-stranded DNA⁵¹.

DNA is prone to structural polymorphism, potentially expanding the repertoire of nanostructures that may be formed with this nucleic acid. Among these unusual DNA structures, G-quadruplexes are of special interest because they have well defined conformations, are relatively stable under physiological conditions, are highly polymorphic, and are likely to form higher order structures. A motion can result from a reversible equilibrium between two conformational states. Several types of movements have been described with DNA machines: rotation⁵² and “scissorslike” opening and closing⁵³. The transition between these two states may be induced by a change in experimental conditions or by the addition of a “DNA fuel” that provides the energy source for this change. A change in buffer composition or temperature may lead to a transition in the chirality of a double helix, which in turn may induce a movement. Although other dynamic chemical devices that undergo analogous structural modifications have recently been proposed⁵⁴, they are not nucleic acid-based and use a totally different chemical stimulus as a propellant. The system presented by Mergny et al⁵¹ has a large stroke amplitude, may easily be followed by fluorescence, and is DNA encoded. The principle of operation is illustrated in **Figure**.

1.8 and corresponds to a simple two-step cycle, with two structurally defined endpoints.

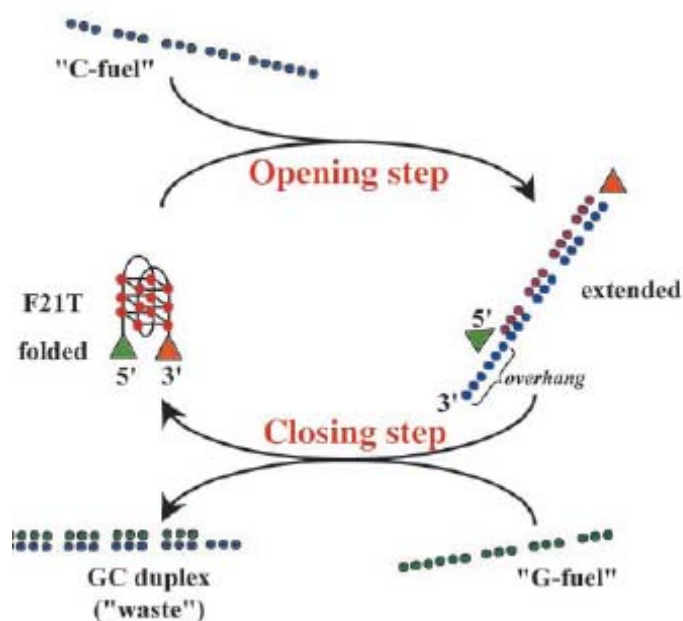


Figure 1.8 Switching between an intramolecular quadruplex (left) and a duplex (right).

An intramolecular quadruplex is formed by the folding of a 21-base oligonucleotide (F21T) that contains four blocks of three guanines mimicking the vertebrate telomeric motif. The schematic topology proposed here corresponds to the Na^+ solution structure. The fluorescent group and the quencher group are depicted by green and orange triangles, respectively. The C-fuel strand is complementary to the F21T sequence, with six extra bases allowing duplex nucleation with the G-fuel strand.

When C-fuel opens F21T, a duplex takes place and fluorescence signal is detected; in the closing step a G-fuel is added and quadruplex refolds; no fluorescence is detected because fluorophore and quencher are now close to each other.

By alternatively adding stoichiometric amounts of the C-fuel and G-fuel strands, F21T may be opened and closed repeatedly.

This system could be used to approach alternatively or separate chemically reactive groups, or to obtain precise control of movements on the nanometer scale.

1.5 The aim of the work

G-quadruplexes (G4s) are unique structures formed by Hoogsteen-type base pairing between four guanines and involving chelation of a metal ion. G4s can be formed by intramolecular folding of guanine-rich sequences or by intermolecular association of two or four sequences leading to the formation of dimeric or tetrameric complexes.

The biological importance of these structures is three-fold: 1) the occurrence of short G-rich sequences able to fold into G-quadruplex structures at the ends of telomeric DNA in eukaryotic chromosomes; 2) the high prevalence of G-rich sequences in a large number of eukaryotic and prokaryotic genomes, and the increasing number of G-quadruplexes arising from these sequences; 3) their presence in the scaffold of several aptamers that have the ability to selectively bind to biologically relevant proteins and small molecules.^{61,62,63,}

G-quadruplexes have the ability to form an array of conformations differing in structural features such as the molecularity, the relative orientation of the strands involved in the structure, the size of the loops connecting the strands, and the glycosidic conformation of guanosine residues (*syn* or *anti*). The structural variability of G-quadruplexes further increases considering their capacity to accommodate A-, T-, and C-tetrads,^{67,} as well as tetrads formed by modified residues.'

Finally, the topology and the chemical nature of the loops contribute to the structural variability of G-quadruplexes. Several studies have been devoted to the effects of the loops on G-quadruplex stability and structure.^{71,72,73,74} Nucleotidic loops can lead to polymorphic G-quadruplex species whose structure depends on the length and base composition of the loops as well as the cation species present in solution. We recently reported the synthesis of a new G-quadruplex forming oligodeoxynucleotide in which the 3'-ends of four ODN strands were linked together by a non-nucleotidic tetra-end-linker (TEL). This ODN analog, also called tetra-end-linked oligonucleotide (TEL-ODN) was able to form a parallel G-quadruplex provided with high thermal stability. These initial studies have been extended to other TEL-ODNs in which four d(TGGGGT) fragments were tethered to the TEL with different orientations (**1-4**, **Figure 1.9**). The results indicated that all the synthesized TEL-ODNs **1-4** formed monomolecular parallel G-quadruplex structures. Analogs **1** and **2** containing all 3'-linked or 5'-linked ODN tracts, respectively, formed very stable parallel G-quadruplexes (**Figure 1.9**, **I** and **II**, respectively) whereas analogs **3** and **4**, containing mixed 3'- or 5'-linked ODN tracts, formed relatively less stable parallel G-quadruplexes (**Figure 1**, **III** and **IV**, respectively). Spectroscopic data and molecular modelling simulations of **3** and **4** suggested that these analogs could adopt the parallel-stranded arrangement shown by **III** and **IV** because of the considerable size of the TEL, which is big enough to fold around the G-quadruplex scaffold.

In this report we have extended our previous studies to investigate the influence of the TEL size on the molecularity, topology, and stability of the G-quadruplex complexes resulting from TEL-ODNs. For this study we have synthesized, by using the reported solid phase procedure, a new set of four TEL-d(TGGGGT)₄ ODNs (**S1** to **S4**, **Figure 1.9**) in which the four ODN tracts are linked to one of the four branches of the new *Short*-TEL (S-TEL). The TEL-ODNs **S1-4** have been studied in comparison to the corresponding **L1-4** TEL-ODNs bearing the *Long*-TEL⁷⁶ (L-TEL).

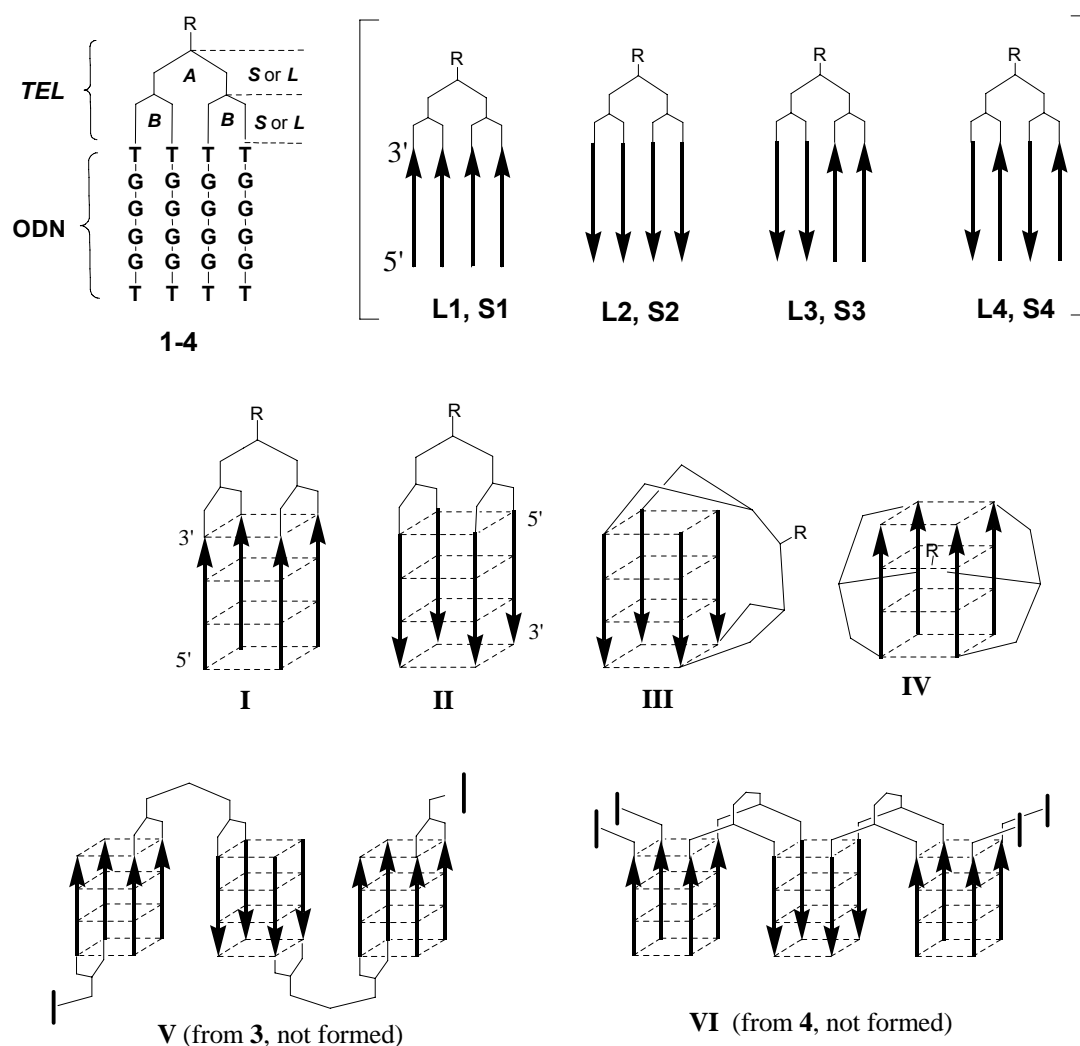
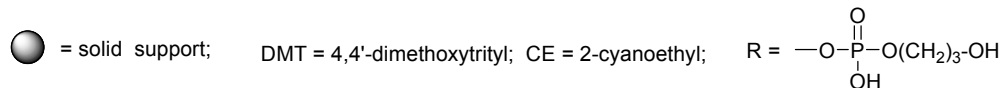
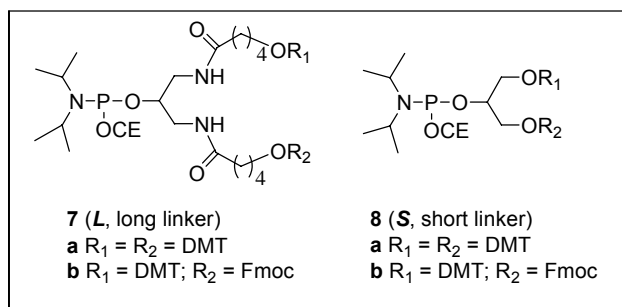
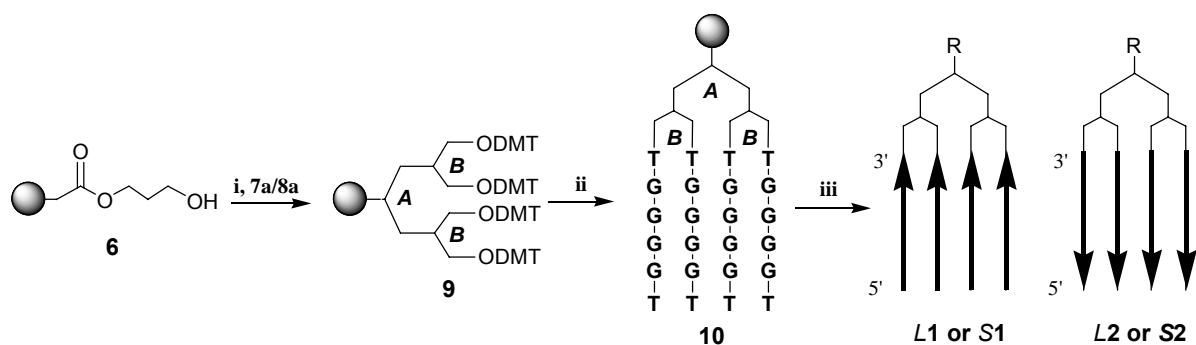


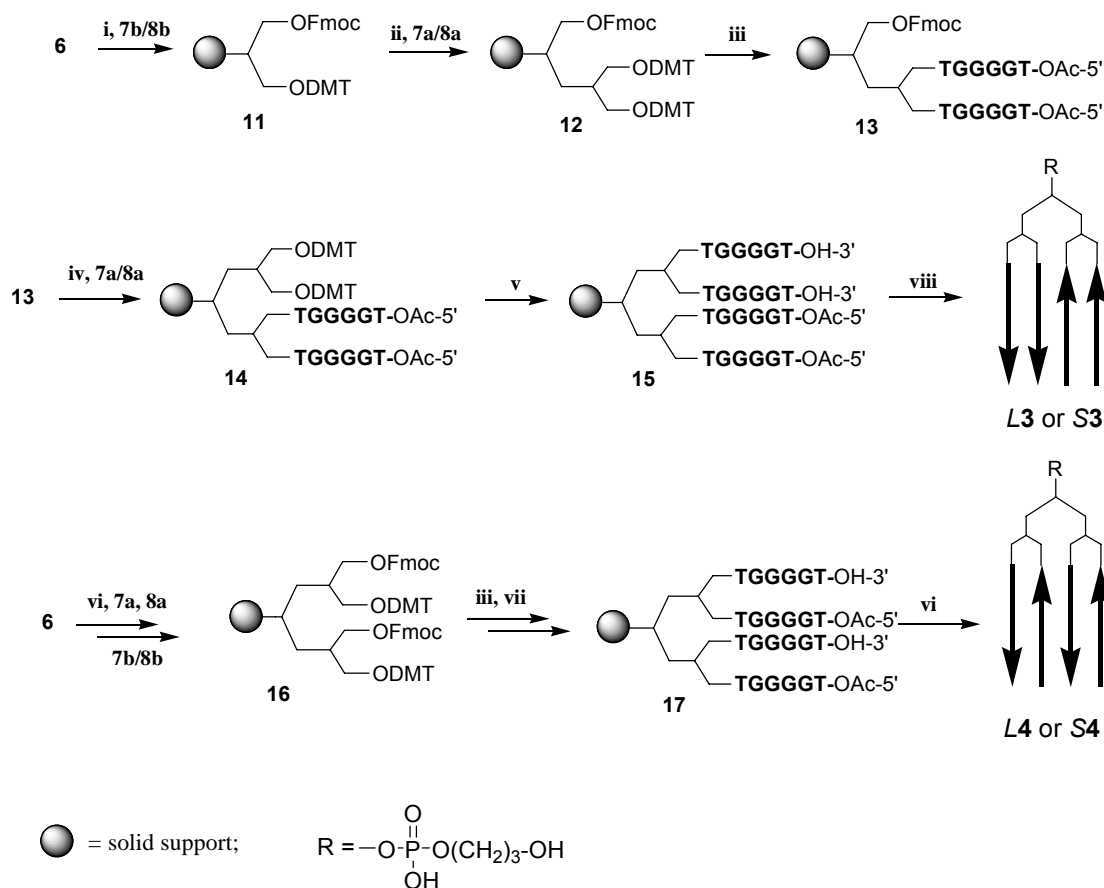
Figure 1.9 TEL-ODNs

The S-TEL linker, like its progenitor, can be regarded as a single primary di-branched linker (**A** in **9**, **Scheme 1.1**) connected to two secondary di-branched linkers (**B** in **9**, **Scheme 1.1**). The shortening of the TEL linker has been achieved by embodying in **A** and **B** the *ad hoc* functionalized glycerol moieties whose synthetic phosphoramidite precursors **8a** and **8b** are shown in **Scheme 1.1**. Conversely, by using the long linker (**7a** or **7b**) in **A** e **B**, the *L*-TEL could be achieved. In the solid phase synthesis the primary linker **A** allows the attachment of the ODN to the polymeric support, and the linkers **B** bear the 3'- or 5'-ends of the ODN tracts. The first synthetic pathway (**Scheme 1.1**) resulted in the synthesis of TEL-ODNs **1** and **2** in which the four ODN strands are parallel oriented and linked to the four TEL arms by their 3'-ends or 5'-ends, respectively.



Scheme 1.1 Synthetic procedure for TEL-ODNs **L1-2** and **S1-2** i: for **L1-2** two coupling cycles with **7a**; for **S1-2** two coupling cycles with **8a**; ii: for TEL-ODNs **1** synthesis using 3'-phosphoramidite building blocks; for TEL-ODNs **2** synthesis using 5'-phosphoramidite building blocks iii: detachment from solid support and deprotection with conc. NH_4OH (7 h, 55°C).

The second synthetic pathway (**Scheme 1.2**) lead to the synthesis of TEL-ODNs **3** and **4** each containing antiparallel oriented strands. Circular dichroism (CD), CD melting, ^1H NMR spectroscopy, molecular modelling and electrophoresis experiments have been employed to explore the propensity of synthesized TEL-ODNs to fold into G-quadruplexes and to investigate their structures and stabilities.



Scheme 1.2 Synthetic procedure for TEL-ODNs **L3-4** and **S3-4**. i: for **L3** coupling with linker **7b**; for **S3** coupling with linker **8b**; ii: DMT removal and coupling with linker **7a** or **8a** respectively for **L3** or **S3**; iii: DMT removal and ODN synthesis with 3'-phosphoramidites; iv: Fmoc removal and coupling with appropriate linker **7a** or **8a**; v: DMT removal and ODN synthesis with 5'-phosphoramidites; vi: for **L4** a coupling cycle with **7a** and then **7b**; for **S4** a coupling cycle with **8a** and then **8b**; vii: Fmoc removal and ODN synthesis with 5'-phosphoramidites; viii: detachment from solid support and deprotection with conc. NH_4OH (7 h, $55^\circ C$).

1.6 Synthesis and Purification of TEL-ODNs type 1, 2, 3 and 4.

For the synthesis of TEL-ODNs **1**, **2**, **3** and **4** we used a hydroxy-functionalized solid support **6** and the reactive bifunctional linkers **7** and **8**. In the first approach (**Scheme 1.1**) support **6**, by way of two coupling cycles with **7a** or **8a** performed on an automatic DNA synthesizer, yielded supports **9** bearing a symmetrical *L*- or *S*-TEL having the four primary alcohols protected by DMT groups. Supports **9** were then used to synthesize either **L1**, **S1** and **L2**, **S2** in which the four ODN strands are attached to the TEL via the 3' or 5'-end. The reaction of 3' or 5'-phosphoramidite nucleotide building blocks with **9** furnished the polymer bound TEL-ODNs **10**. The treatment of **10** with concentrated NH_4OH furnished **L1**, **S1** and **L2**, **S2**.

For the preparation of *L*-3 and *S*-3 we adopted a synthetic strategy (**Scheme 1.2**) based on the use of the linkers **7b** and **8b** in which the two alcoholic functions are orthogonally protected with Fmoc and DMT groups. Support **6**, by reaction with the phosphoramidite linker **7b** (or **8b**) yielded supports **11** that, after DMT deprotection and successive reaction with **7a** (or **8a**), furnished the tri-functionalized support **12**. Six coupling cycles with 5'-phosphoramidite nucleotides and a final capping step of

the 5'-OH ends, gave **13**. Removal of the Fmoc protecting group and coupling with **7a** (or **8a**) yielded the support **14** on which the second ODN domain was assembled using 3'-phosphoramidite nucleotides to obtain polymer bound TEL-ODNs **15**.

The synthetic pathway used to obtain TEL-ODNs *L-4* and *S-4* (**Scheme 1.2**), involved the reaction of **6** with **7a** (or **8a**) and subsequently with **7b** (or **8b**) to obtain the supports **16**. Removal of DMT protecting groups, followed by ODN synthesis with 5'-phosphoramidite nucleotides allowed the assembly of the first pair of ODN chains. After Fmoc deprotection, the remaining ODN pair having opposite polarity was then assembled using 3'-phosphoramidite nucleotides thus obtaining **17**. Detachment from the solid support and complete deprotection of type **3** and **4** TEL-ODNs were achieved by treating the supports **15** and **17**, respectively, with concentrated NH_4OH as described for **1** and **2**. Purification and analysis of crude products **1**, **2**, **3** and **4** were carried out using HPLC. The ^1H NMR and MALDI-MS data confirmed the purity of the products. Purified samples of **1**, **2**, **3** and **4** were dissolved in Na^+ and K^+ buffers and annealed to form G-quadruplexes.

1.7 CD and CD Thermal Analysis

In order to compare the propensity of each synthesized TEL-ODN to form a G-quadruplex structure, we carried out CD studies. CD spectra are used to assess the nature of G-quadruplex folding, though there is some debate about the CD signature of antiparallel and parallel G-quadruplexes. The vast majority of published reports are consistent with the observation that antiparallel G-quadruplexes display a maximum near 295 nm in the presence of sodium or potassium ions, while parallel G-quadruplexes exhibit a maximum around 265 nm.^{78,79} However researchers must take into account that a growing number of exceptions to this rule is coming out.^{81,82} The *L1-4* and *S1-4* samples, annealed at the concentration of 1.0×10^{-5} M, were analyzed by CD in 80 mM and 40 mM Na^+ (data not reported) and K^+ buffers at 25 °C. The CD spectra of all the samples, with the notably exceptions of *L4* and *S4*, exhibited very similar CD profiles regardless the nature of the cation and the medium ionic strength. In **Figure 1.10** are reported the CD spectra in 80 mM Na^+ buffer, characterized by a maximum centred around 264 nm and a minimum centred around 244 nm, which were in agreement with the presence in solution of parallel stranded G-quadruplexes. In the case of *L4* and *S4* the CD profiles showed two maxima centred at 264 nm (the higher) and 289 nm (the lower) thus indicating that a small amount of antiparallel G-quadruplex species could coexist in Na^+ buffer.

These data suggest that all the TEL-ODNs **1** and **2**, no matter what the TEL size is, fold into parallel G-quadruplexes (types **I** and **II**, respectively, in **Figure 1.9**) when annealed in Na^+ or K^+ buffers, indicating that the shortening of the TEL does not hinder the formation of parallel G-quadruplex structures. For TEL-ODNs **3** and **4**, both embodying antiparallel ODN strands, the CD spectra disclosed the formation of parallel G-quadruplexes even in the presence of the S-TEL. Furthermore, it is to be noted that the replacement of the *L*-TEL with the *S*-TEL did not modify the intensity ratio between the two CD maxima observed in the CD spectra of *L4* and *S4* in Na^+ buffer at 25 °C. As anticipated in our previous report²² the CD spectra recorded for ODNs type **3** and **4** are coherent with the formation of type **III** and **IV** monomolecular parallel G-quadruplexes.

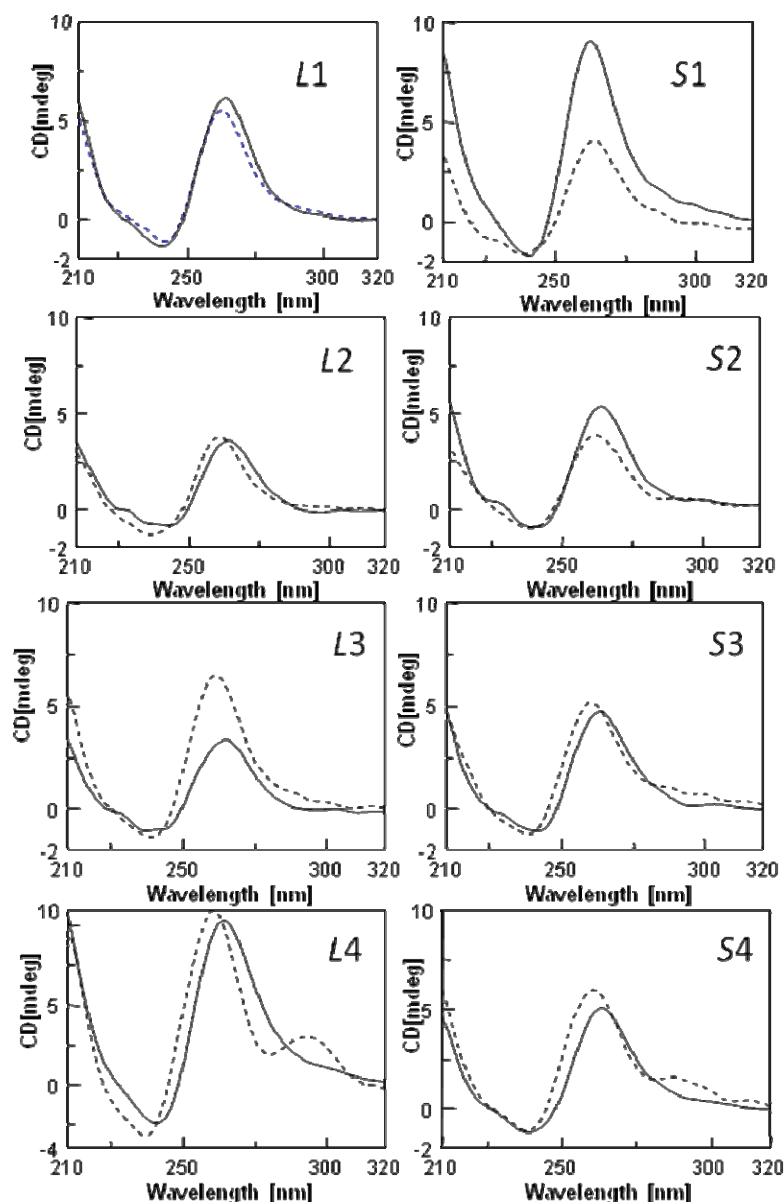


Figure 1.10 CD profiles of *L1-4* (left column) and *S1-4* (right column) in 40mM Na⁺ buffer (dotted line) and in 40mM K⁺ buffer (solid line) at 25°.

To evaluate the influence of TEL size on the stability of the resulting TEL-quadruplexes, CD thermal denaturation experiments were performed in 80 mM and 40 mM Na⁺ and K⁺ buffers. The CD value (mdeg) at 264 nm was monitored in the range 25-90 °C at a heating rate of 0.5 °C/min. Since within the temperature range examined low or irrelevant mdeg variation were observed in 80 mM Na⁺ and K⁺ buffers, the here reported data are referred to the melting data recorded in 40 mM Na⁺ buffer (**Figure 1.11**). Sigmoidal profiles could be observed only for *L1* and *L3* from which the relative T_m values were calculated (62 and 64 °C, respectively). For *L2* and *L4* a well defined and derivatizable sigmoidal profile was not observed. It is to be noted that the melting curves of *L1-4* display a significant decrease of the mdeg value since from the beginning of the melting run. This behaviour, especially for *L2* and *L4*, as well as to induce a not negligible error in the determination of the T_m values, could suggest the co-existence of several kinds of structures that melt at low temperature. An analogous behaviour was observed in the melting curves of *S1-4*. In

particular, **S2** and **S4** showed a marked multiphasic profile which prevented the T_m determination of the resulting G4s. However the melting profiles of **S1** and **S2** indicated that their fusions were not complete even at 90 °C suggesting that **S1** and **S2** folded into G4s more stable than those originated from the corresponding *L*-TEL analogs in the same buffer condition.

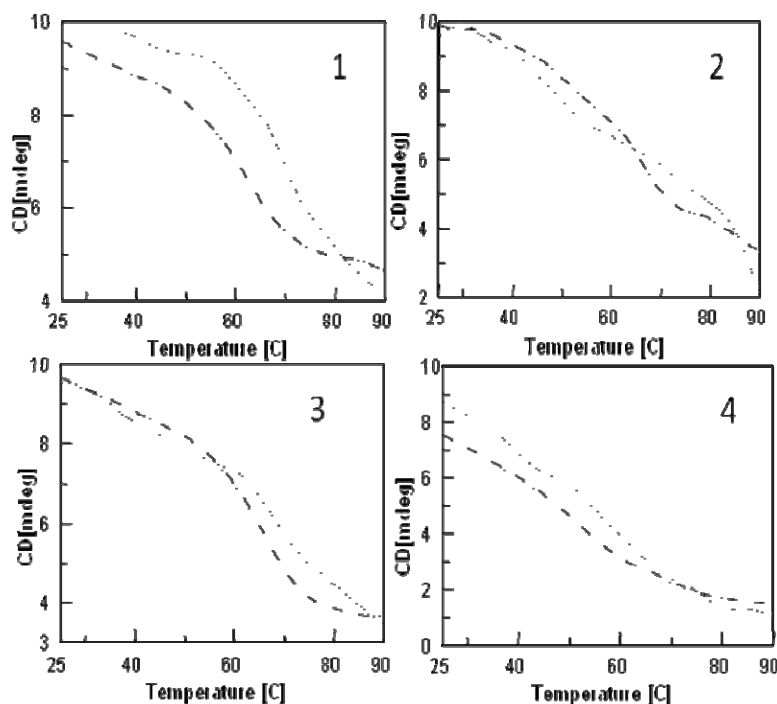


Figure 1.11 CD at 264 nm melting profiles (25-90 °C, 0.5 °C/min) of **L1-4** (dotted line) and **S1-4** (solid line) in 40mM Na⁺ buffer.

1.8 Native Gel Electrophoresis.

We carried out non-denaturing PAGE experiments to investigate the electrophoretic behaviour of the **L1-4** (**Figure 1.12A**) and **S1-4** samples (**Figure 1.12B**), both annealed in 80 mM Na⁺ buffer.

We observed that **L1-4**, annealed at 400 μM TEL-ODN concentration, showed prevalently a defined band with a mobility comparable to that of the tetramolecular (TG₄T)₄. These bands, which we hypothesize corresponding to the intramolecular G-quadruplexes (I, II, III and IV, **Figure 1.9**), were not present in all **S1-4**, for which a marked slow smear was observable (**Figure 1.12B**). Similar migration profiles were observed in 80 mM K⁺ buffer (data not shown). PAGE experiments performed in 40 mM of Na⁺ gave substantially the same results. A different annealing condition was examined for the **S1-4** TEL-ODNs to investigate the effect of TEL-ODN concentration on the smear. In the PAGE reported in Figure 4B the lanes **a** and **b** contain **S1-4** annealed at 400 μM and 10μM TEL-ODN concentrations respectively. We observed that the 10μM TEL-ODN diluted annealing condition leads to a reduction of the smear which could be attributed to the formation of amorphous aggregates that dissociate during the PAGE run. This hypothesis is corroborated by the CD melting data that show in the case of **S1-4** analogues a multi-phasic profile that could be attributed to the melting of the aggregates as above described.

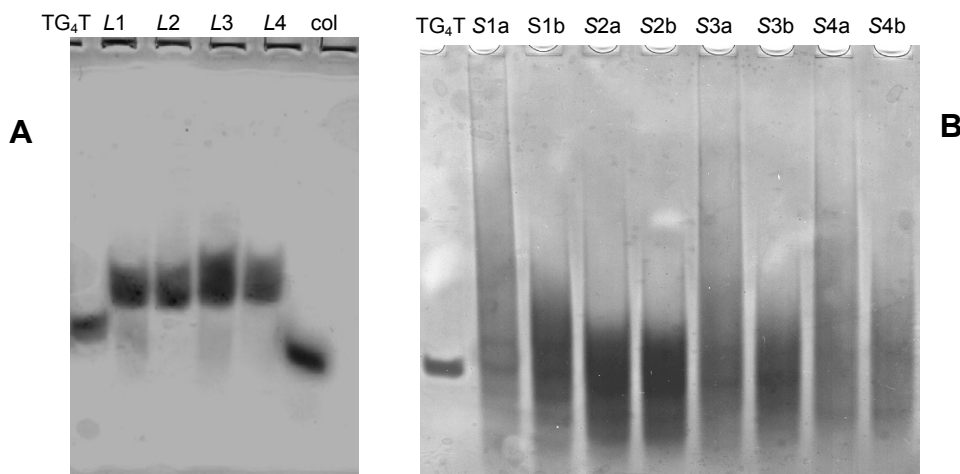


Figure 1.12 Non denaturing 20% PAGE (pH 7.0). **L1-4** (PAGE **A**) annealed at 400 μ M TEL-ODN concentration in 80 mM Na^+ buffer. **S1-4** (PAGE **B**) annealed at 400 μ M TEL-ODN concentration (lanes **S1a-S4a**) and annealed at 10 μ M TEL-ODN concentration (lanes **S1b-S4b**) in 80 mM Na^+ buffer.

1.9 ^1H NMR Studies on L- and S-TEL-ODNs

^1H NMR studies at 25, 45, 65 and 85 $^\circ\text{C}$ on L- and S- TEL-ODN samples **1**, **2**, **3**, and **4** were performed at 0.5 mM quadruplex concentration in $\text{H}_2\text{O}/\text{D}_2\text{O}$ (9:1, v/v) in 10 mM KH_2PO_4 , 0.2 mM EDTA and 70 mM KCl, pH 7.0. All spectra recorded at 25 $^\circ\text{C}$ show the presence of broad signals in the range 10.9-11.8 ppm attributable to exchange of protected imino protons involved in Hoogsteen N(1)/O(6) hydrogen bonds of G-quartets.^{78,83} In all cases, an increase in the temperature resulted in the sharpening of all imino proton signals. This phenomenon could be tentatively explained by the presence in solution of amorphous aggregates of monomolecular G-quadruplexes, which melt at temperatures above 25 $^\circ\text{C}$. In the case of **L1-3** and **S1**, the aggregates are almost completely melted at 45 $^\circ\text{C}$. In fact at this temperature four well resolved signals are detected in the imino proton region. No further sharpening of imino proton signals was observed at 65 and 85 $^\circ\text{C}$ (**Figure 1.13**).

The ^1H NMR spectrum of **S2** and **S3** show broader imino proton signals at 25 $^\circ\text{C}$ than those observed for **L1-3** and **S1** that progressively sharpen when the temperature is increased from 25 to 65 $^\circ\text{C}$. For **S3**, the imino proton signals are significantly attenuated at 85 $^\circ\text{C}$ with a complete loss of the signal at 11.6 ppm at this temperature. These data suggest that **S3** folds into a less stable G-quadruplex compared to those formed by **L1-3** and **S1** and that more stable and/or extended aggregates may be present in solution. The imino proton regions for **L4** and **S4** are almost superimposable at 25 $^\circ\text{C}$. Very broad, overlapped signals are observed at 25 $^\circ\text{C}$ that progressively sharpen as the temperature is increased to 85 $^\circ\text{C}$. At this temperature four G-tetrad signals are still clearly visible for **S4**, while the signal at 11.6 ppm is almost completely undetectable for **L4**. The NMR data indicate that all L and S TEL-ODN analogs fold into a G-quadruplex structure when annealed in K^+ buffer. Furthermore, the data suggest that all analogs fold into very similar parallel G-quadruplex structures, presumably monomolecular, at 65 and 85 $^\circ\text{C}$ since at these temperatures all the imino proton signals occur at about the same chemical shift. TEL-ODN **S2-4** seem to favour the formation of more extended/stable aggregates.

The ^1H NMR spectra in Na^+ buffer (data not shown) suggested the formation of G-quadruplex structures with lower thermal stability as well as the presence in solution of aggregates at lower temperatures for each of the S TEL-ODN analogs (**Figure 1.13**).

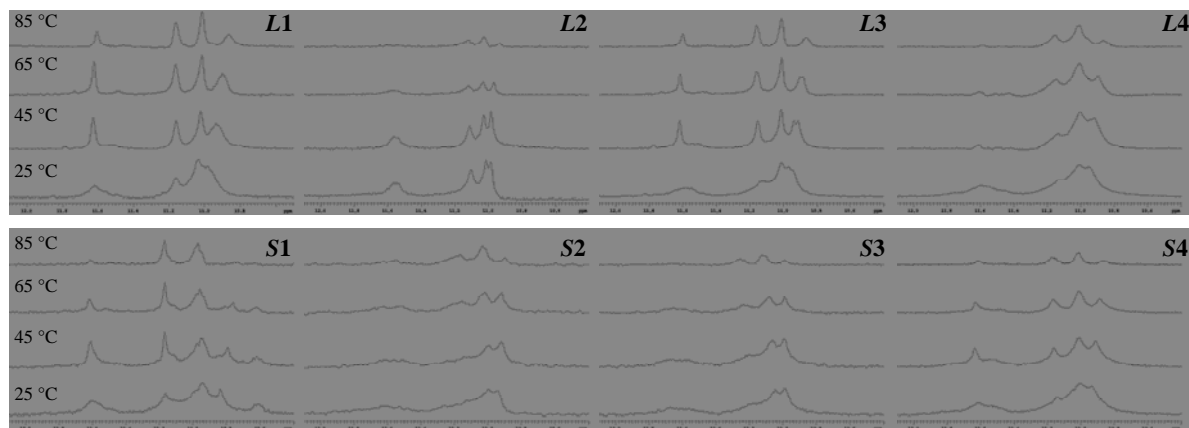


Figure 1.13. Imino proton region of 500-MHz ^1H -NMR spectra of **L1-4** and **S1-4** in 80 mM K^+ buffer.

1.10 Molecular Modelling

Molecular modeling was employed to investigate the propensity of TEL-ODNs assembled with the short TEL (**S1-4**) to adopt parallel G-quadruplex structures. The energy minimized structures obtained are shown in Figure 6. Inspection of the minimized structure of **S1** and **S2** reveals that, despite its shorter length, the S-TEL is still able to connect the four 3' and 5' strands ends, respectively, without causing any distortion in the overall G-quadruplex structure. Specifically, the integrity of G-tetrad stacking and Hoogsten hydrogen bonding interactions are maintained after energy minimization.

In the case of **S3** and, to a greater extent, **S4**, the models clearly show that the linkers are too short to span the distance between the linked 5' and 3' ends of the strands assembled in a parallel G-quadruplex structure, requiring the involvement of the four thymidines directly linked to the TEL to function as an extended linker. Although the overall integrity of the G-tetrads core is maintained after energy minimization for **S3** and **S4**, a detailed analysis of the nature of the H-bonding within the G-tetrads reveals some important differences. Specifically, while optimum distances and angles between H-bond donor and acceptor atoms are observed in the case of **S3**, significant deviations are observed for **S4** resulting in less stable hydrogen bonding between the G residues of each tetrad so that only two or three hydrogen bonds in each G-tetrad are retained in the minimized G-quadruplex structure (**Figure 1.14**).

The molecular modelling studies appear to be consistent with the experimental CD and NMR data revealing that the G4s formed by **L1-4** are more stable than the corresponding originated by **S1-4**. On the base of molecular modelling data the relative stability of S-TEL-d(TGGGGT)₄ G4s follows the order **S1**≈**S2**≥**S3**>**S4**.

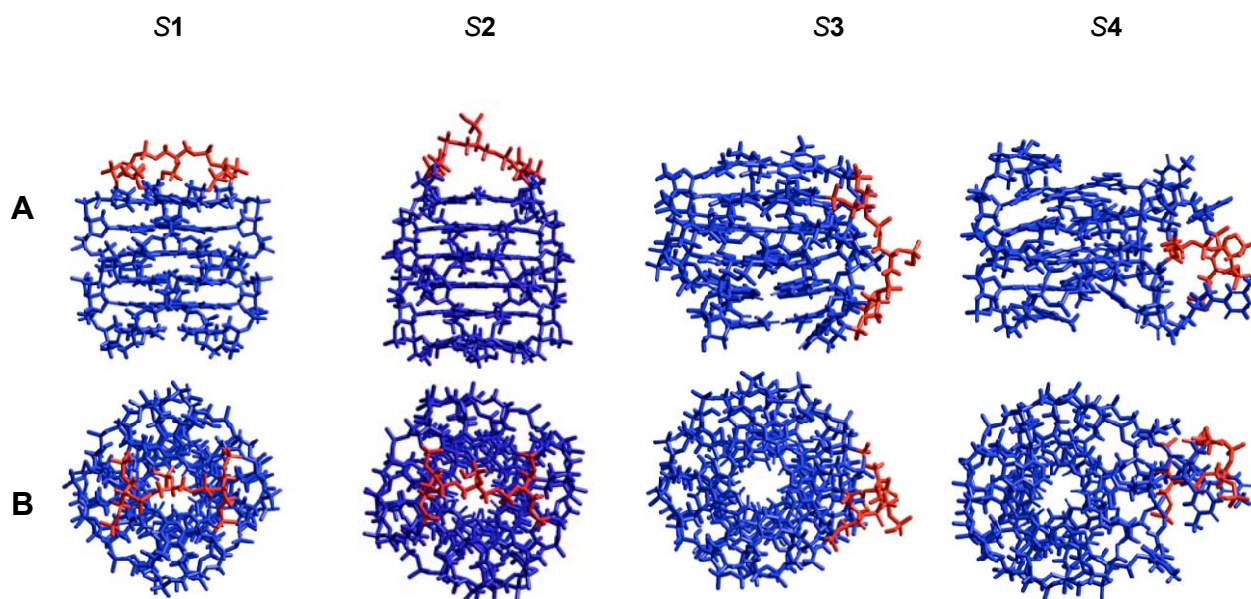


Figure 1.14 Molecular modelling data related to the relative stability of S-TEL-d(TGGGGT)₄.

1.11 Conclusions

In this paper we have investigated the G-quadruplex structures formed by several TEL-d(TGGGGT)₄ analogs which differ both for the relative orientation of the four ODN strands attached to the non-nucleotidic TEL, as well as for the TEL size. The molecularity, topology and stability of the resulting TEL-G-quadruplexes have been investigated using a combination of methods. CD spectra indicate that all TEL-ODN analogs, independently from the TEL size and the structural orientation of the ODN strands, formed parallel TEL-G-quadruplexes. Molecular modelling results point out the ability of the S-TEL to fold around the G4 scaffold, thus allowing the formation of monomolecular G-quadruplexes such as **I-IV** depicted in **Figure 1**. ¹H NMR studies confirmed the folding into parallel G4s for all the here reported TEL-ODN species. Furthermore, the non-denaturing PAGE experiments of **S1-4** showed significant smearing with no single well defined G4 band. We attributed the significant smearing observed in PAGE experiments to the formation of amorphous aggregates made of single G-quadruplex scaffolds, which melt at low temperature and are not detectable by the MS technique. This hypothesis was also corroborated by the ¹H NMR analyses at increasing temperature. The role of the TEL size seems to be crucial in the formation of these aggregates since they were observed almost exclusively for the S-TEL ODNs.

We do not believe that the observed aggregates belong to polymeric species like **V** and **VI** (**Figure 1.9**) on the basis of the following considerations: i) no polymeric species have been detected in the MALDI mass spectra; ii) no defined bands attributable to dimeric or polymeric species have been detected in the PAGE experiments; iii) the thermal stability of type **V** and **VI** polymeric species would have

had to be as stable, or even more stable, than the corresponding monomolecular analogs.

In conclusion we have characterized a small set of parallel TEL-G-quadruplexes whose parallel topology was independent of the nature of the cation species in solution and of the TEL size. Furthermore, the parallel orientation of the G-quadruplex structures leads to a predictable TEL loop arrangement on either the 5'-face, the 3'-face or on one side of the G-quadruplex scaffold. These findings, together with the ability to affect the stability of the TEL-G-quadruplexes through modification of the TEL, indicate that the TEL-ODNs are useful models to study ligand-quadruplex interactions. Furthermore, we believe that TEL-G-quadruplexes with suitable sequences could be used as new kind of aptamers, decoys and molecular probes.

1.12 Experimental

1.12.1 Reagents and Equipment.

Chemicals and solvents were purchased from Fluka-Sigma-Aldrich. Reagents and phosphoramidites for DNA syntheses were purchased from Glen Research. ODN syntheses were performed on a PerSeptive Biosystems Expedite. HPLC analyses and purifications were performed with a JASCO PU2089 pump system equipped with an UV detector model 2075 Plus using a Merck Hibar (5 μ m, 250-10) column. Linkers **7a-b** were purchased from Glen Research. Tentagel carboxy resin, used as starting material for preparation of solid support **6**, was purchased from Novabiochem. Preparation of **6** was carried out in a short column (10 cm length, 1 cm i.d.) equipped with a sintered glass filter, a stopcock and a cap as previously described.²² The ODNs were assembled by a PerSeptive Biosystems Expedite DNA synthesizer using phosphoramidite chemistry. UV spectra were collected using a Jasco V-530 spectrophotometer. CD spectra and thermal denaturation experiments were collected with a Jasco J-715 spectropolarimeter equipped with a JASCO ETC-505T temperature controller unit. NMR spectra were recorded on a Varian Unity Inova 500 MHz spectrometer. MALDI-TOF mass spectrometric analyses were performed on a Bruker Autoflex mass spectrometer using a picolinic/3-hydroxypicolinic acid mixture as the matrix. ESI-MS were performed on a Applied Biosystem API 2000 mass spectrometer in positive mode. The ODN concentration was determined spectrophotometrically at $\lambda = 260$ nm and 90 °C, using the molar extinction coefficient $\epsilon = 57800 \text{ cm}^{-1}\text{M}^{-1}$ calculated for the unstacked oligonucleotide by the nearest neighbour mode.

1.12.2 Syntheses of linkers 8a-b.

8a. 0.34 g (3.6 mmol) of 1,2,3-propantriol dried by repeated coevaporations with anhydrous pyridine and then dissolved in 8 mL of the same solvent, were reacted with 2.5 g (7.2 mmol) of 4,4'-dimethoxytrytilchloride at R.T. for 12 h. The reaction was quenched by addition of water and the resulting mixture, taken to dryness and redissolved in benzene, was purified on a silica gel column giving 1.63 g (2.34 mmol, 65% yield) of 1,3- bis-(O-DMT)-propantriol, in mixture with the full protected derivative. The bis-tritylated compound was dissolved in dry CH_2Cl_2 (5 mL) and N,N-diisopropylethylamine was added (0.860 mL, 4.6 mmol) followed by 2-cyanoethyl-N,N-diisopropylchlorophosphoramidite (0.48 mL, 2.76 mmol). The mixture was stirred

for 1 h at R.T. then diluted with ethyl acetate (50 mL) and washed with saturated sodium chloride solution (4 × 25 mL). The organic phase was dried over sodium sulphate and evaporated to an oil in the presence of toluene (10 mL). The product was purified by short column chromatography on Kieselgel 60H (10 g) eluting with CH₂Cl₂/ethyl acetate/2,6-lutidine 50:50:2. (v/v/v) The product was dried to give a white powder (90% yields). ¹H-NMR (400 MHz) ppm (acetone, d₆) 1.05 (d, 12H, CHCH₃), 2.97 (m, 2H, CHCH₃), 3.52 (d, 4H, CH₂ODMT), 3.82 (s, 12H, OCH₃), 3.87 (m, 1H, CHOP), 4.05 (s, 2H, CH₂CN), 6.82-7.55 (m, 26H, aromatic protons). ESI-MS calculated for C₅₃H₅₉N₂O₈P m/z: 882.11, found: 883.40 (M + H)⁺.

8b. 0.34 g (3.6 mmol) of 1,2,3-propantriol dissolved in 8 mL of pyridine, were reacted with 0.325 g (0.9 mmol) of 4,4'-dimethoxytrytylchloride at R.T. for 12h to afford after purification the monotrityl derivative as main product (0.343 g, 0.8 mmol, 80%). This latter was protected at the remaining primary hydroxyl group by reaction with fluorenylmethoxycarbonylchloride (Fmoc-Cl 232 mg, 0.9 eq) in anhydrous CH₂Cl₂. Phosphoramidite derivative was prepared as just described for obtaining **8a**. ¹H-NMR (400 MHz) ppm (acetone, d₆): 1.05 (d, 12H, CHCH₃), 2.97 (m, 2H, CHCH₃), 3.52 (d, 2H, CH₂ODMT), 3.82 (s, 6H, 4OCH₃), 4.05 (s, 2H, CH₂CN), 4.14 (m, 1H, CHOP), 4.31(d, 2H, CH₂OFmoc), 4.46 (t, 1H, CH-fluorenyl), 4.78 (d, 2H, CH₂-fluorenyl), 6.80-7.65 (m, 21H, aromatic protons). ESI-MS calculated for C₄₇H₅₁ N₂O₈P m/z: 802.34, found: 803.80 (M + H)⁺.

1.12.3 Syntheses and Purifications of TEL-ODNs L1-2 and S1-2

50 mg of support **6** (0.18 meq/g) were used for each synthesis in the automated DNA synthesizer following standard phosphoramidite chemistry, using 45 mg/mL of solution of phosphoramidite **7a** in two coupling cycles for the synthesis of **L1**, or using **8a** (two coupling cycles) for the synthesis of **S1** followed by reaction with 3'-phosphoramidite (for **L1** and **S1**) or 5'-phosphoramidite (for **L2** and **S2**) nucleotide building block (six cycles, 45 mg/mL in anhydrous CH₃CN) to obtain the polymer bound ODN **10**. The coupling yields were consistently higher than 98% (by DMT spectrophotometric measurements). The solid support **10** was then treated with conc. aq. ammonia solution for 7 hours at 55 °C. The filtered solution and washings were concentrated under reduced pressure and purified by HPLC on a Nucleogel SAX column eluted with a linear gradient of the following buffers. Buffer A: 20 mM NaH₂PO₄, pH 7.0 containing 20% CH₃CN; buffer B: 1 M NaCl, 20 mM NaH₂PO₄, pH 7.0, containing 20% CH₃CN; linear gradient from 0 to 100% B in 30 min, flow rate 1mL/min. The collected products were desalted by gel filtration on a Sephadex G25 column eluted with H₂O/ethanol (9:1,v/v) to obtain, after lyophilization, pure **L1**, **L2**, **S1** and **S2** (82, 80, 74, and 76 OD₂₆₀ units, respectively). The TEL-ODNs were characterized by MALDI TOF-MS (negative mode): **L1** found: 8820 (calcd. 8821.7); **S1** found: 8225 (calcd. 8226.9).

1.12.4 Syntheses and purifications of TEL-ODNs 3 and 4

For the synthesis of **L3**, and **S3** 50 mg of support **6** (0.18 meq/g) was reacted, in the automated DNA synthesizer, with **7b** (for **L3**) or **8b** (for **S3**) following standard phosphoramidite chemistry yielding support **11** (0.17 meq/g of DMT groups). After removal of DMT protecting groups by DCA, the second coupling cycle was performed in the same manner using phosphoramidite **7a** (for **L3**) or **8a** (for **S3**) thus obtaining support **12** (0.30 meq/g of DMT groups). **12** was then subjected to six coupling cycles

using 3'-phosphoramidite nucleotide building blocks (45 mg/mL in CH₃CN), followed by final DMT removal and 5'-OH capping with Ac₂O, to yield ODN functionalized support **13**. The removal of Fmoc groups was achieved by treatment with piperidine/DMF solution (2:8, v/v, 30 min R.T.). The resulting support was then reacted with phosphoramidite **7a** or **8a** as above described thus obtaining **14** (0.27 meq/g of DMT groups). After removal of DMT protecting groups the second ODN domain was assembled by six coupling cycles with 5'-phosphoroamidite nucleotide building block as described for support **12** yielding the polymer bound ODN **15**.

For the synthesis of **L4** and **S4**, support **6** (50 mg) was functionalized with appropriate **7a** or **8a** and then **7b** or **8b**, as described before, yielding the tetra-branched support **16** (0.28 meq/g of DMT groups). After removal of the DMT protecting groups, the first two ODN chains were assembled, using 3'-phosphoramidite nucleotide building blocks. After capping of the terminal 5'-OH functions by Ac₂O treatment, the Fmoc groups were removed as previously described, and two successive ODN chains were assembled using 5'-phosphoroamidite nucleotide building blocks, thus obtaining the polymer bound ODN **17**. TEL-ODNs were detached from the supports **15** and **17**, deprotected and purified as previously described. After lyophilization, the final pure products **L3**, **S3**, **L4**, and **S4**. (65, 72, 69 and 80 OD₂₆₀ units, respectively) were characterized by MALDI TOF-MS (negative mode): **L3** found: 8820 (calcd. 8821.7); **S3** found: 8225 (calcd. 8226.9); **L4** found: 8820 (calcd. 8821.7); **S4** found: 8225 (calcd. 8226.9).

1.12.5 Preparation of Quadruple Helices (Annealing).

G-quadruplexes types **I**, **II**, **III** and **IV** were formed by dissolving **L1-4** and **S1-4** in the appropriate phosphate buffers and annealed by heating to 90 °C for 20 min followed by slow cooling to room temperature. The solutions were equilibrated at 25 °C for 24 hours before performing the experiments.

1.12.6 Native gel electrophoresis.

Native gel electrophoreses were run on 20% non-denaturing polyacrylamide gels in 1× TB buffer, pH 7.0 with 40 mM NaCl (or KCl). The TEL-ODNs were dissolved in 0.1 mM EDTA, 10 mM NaH₂PO₄, 30 mM NaCl (40mM Na⁺ buffer), or 0.1 mM EDTA, 10 mM NaH₂PO₄, 70 mM NaCl (80mM Na⁺ buffer) at a quadruplex concentration of 400 μM or 10 μM and annealed as described earlier. Samples were loaded at a final concentration of 200 μM TEL-ODNs in a buffer solution containing 6% glycerol that was added just before gel loading. The gels were run at room temperature at constant voltage (100V) for 2.5 h. The bands were visualized by UV shadowing and after "stain all" colouration.

1.12.7 CD Experiments.

G-quadruplexes CD spectra were collected using a Jasco J-715 spectropolarimeter using a 0.1 cm path length quartz cuvette at 25 °C. The ODNs were prepared at a quadruplex concentration of 1.0×10^{-5} M in the appropriate buffer. Spectra were collected over a wavelength range of 200 - 320 nm with a scanning speed of 100 nm/min, a response time of 16 s, and a bandwidth of 2.0 nm. A background scan of buffer alone was subtracted from all scans. CD thermal denaturation experiments

were followed by recording the CD values at 264 nm in a temperature range of 25-90 °C at a heating rate of 0.5 °C/min.

1.12.8 ¹H NMR Experiments.

¹H NMR data were collected on Unity INOVA 500 and Mercury VX 400 Varian spectrometers equipped with a broadband inverse probe with z-field gradient, and processed using the Varian VNMR software package. 1D NMR spectra were acquired as 16384 data points with a recycle delay of 1.0 s at temperatures of 25, 45, 65 and 85 °C. Data sets were zero filled to 32768 points prior to Fourier transformation and apodized with a shifted sinebell squared window function. Pulsed-field gradient DPGSE sequence was used for H₂O suppression. All NMR samples were prepared at 0.5 mM quadruplex concentration in H₂O/D₂O (9:1, v/v) in 10 mM KH₂PO₄, 0.2 mM potassium EDTA and 70 mM KCl (K⁺ buffer) and 10 mM NaH₂PO₄, 0.2 mM sodium EDTA or 70 mM NaCl (Na⁺ buffer).

1.12.9 Molecular Modelling.

The conformational features of the TEL-ODNs **S1-4** have been explored by means of a molecular modelling study. All the calculations were performed on a personal computer running the HyperChem 7.5 suite of programs. The AMBER force field using AMBER 99 parameter set was used. The initial coordinates for the starting model of [d(TGGGGT)]₄ G-quadruplex were taken from the NMR solution structure of the [d(TTGGGGT)]₄ G-quadruplex (Protein Data Bank entry number 139D), choosing randomly one of the four available structures. The initial [d(TGGGGT)]₄ G-quadruplex model were built by deletion of the 5'-end thymidine residue in each of the four TTGGGGT strands. The complete structures of **S1-4** were then built using the HyperChem 7.5 building tool. Partial charges for each atom of the TEL were assigned using the Gasteiger-Marsili algorithm implemented in the QSAR module of HyperChem suite. The resulting coordinates of the TEL atoms were energy-minimized in vacuum keeping all DNA coordinates frozen (500 cycles of the steepest descent method). The calculations were performed using a distance-dependent macroscopic dielectric constant of 4^{*} ϵ_r , and an infinite cut-off for nonbonded interactions to partially compensate for the lack of solvent used. Hydrogen bond and glycosidic torsion angle constraints were used according to NMR and CD data. Upper and lower distance limits of 2.0 Å and 1.7 Å for hydrogen-acceptor distance, and 3.0 Å and 2.7 Å for donor-acceptor distance were employed (20 kcal/mol·Å²). Glycosidic torsion angles were constrained to a range of -160°/-70° as required for a parallel G-quadruplex having all guanines in the *anti* orientation (16 Kcal/mol·Å²). In each case, the entire system was energy minimized using the conjugate gradient method until convergence to an rms gradient of 0.1 kcal/mol·Å was reached. In the next step the coordinates of all the thymidines and TEL atoms were subjected to a restrained molecular dynamics simulation. The system was initially heated from 0 to 1000 K during the first 33 ps of simulation, the simulation then proceeded for 250 ps at 1000 K and was followed by 24 ps of cooling to 273 K. Finally, all the restraints were removed and the systems were energy minimized using 1000 cycles of the steepest descent method followed by the conjugate gradient method until convergence to a rms gradient of 0.1 kcal/mol·Å.

References

- ¹ W. Guschlbauer, J. F. Chantot, D. Thiele *J. Biomol. Struct. Dyn.* **1990**, 8, 491 – 511.
- ² M. Gellert, M. N. Lipsett, D. R. Davies *Proc. Natl. Acad. Sci. USA* **1962**, 48, 2013 – 2018.
- ³ Maizels, N. et al *Nat Struct Mol Biol* **2006** 13, 1055–1059.
- ⁴ Petraccone, L., Barone, G., Giancola, C. *Curr Med Chem Anticancer Agents* **2006** 5, 463–475.
- ⁵ De Cian, A., Mergny, J.L. *Nucleic Acids Res* **2007**, 35, 2483–2493.
- ⁶ Wang, Y., Patel, D.J. *Structure* **1993**, 1, 263–282.
- ⁷ Parkinson, G.N., Lee, M.P.H., Neidle, S. *Nature* **2002**, 417, 876–880
- ⁸ a) Ambrus, A., Chen, D., Dai, J., Jones, R.A., Yang, D. *Biochem* **2005**, 44, 2048–2048, b) Luu, K.N., Phan, A.T., Kuryavyy, V., Lacroix, L., Patel, D.J. *J Am Chem Soc* **2006**, 128, 9963–9970.
- ⁹ T. Simonsson *Biol. Chem.*, **2001**, 382, 621 – 628.
- ¹⁰ Hardin, C. C.; Henderson, E.; Watson, T.; Prosser, J.K. *Biochemistry* **1991**, 30, 4460–4472.
- ¹¹ Cech, T. R. *Nature* **1988**, 332, 777–778.
- ¹² Sen, D.; Gilbert, W. *Curr. Opin. Struct. Biol.* **1991**, 1, 435–438.
- ¹³ Marathias, V. M.; Bolton, P. H. *Biochemistry* **1999**, 38, 4355–4364.
- ¹⁴ Sen, D.; Gilbert, W. *Methods in Enzymol.* **1992**, 211, 191–199.
- ¹⁵ Wang, Y.; Patel, D. J. *Structure* **1994**, 2, 1141–1156.
- ¹⁶ Marathias, V. M.; Bolton, P. H. *Biochemistry* **1999**, 38, 4355–4364.
- ¹⁷ Kang, C.; Zhang, X.; Ratliff, R.; Moyzis, R.; Rich, A. *Nature* **1992**, 356, 126–131.
- ¹⁸ Wang, Y.; Patel, D. J. *J. Mol. Biol.* **1995**, 251, 76–94.
- ¹⁹ Fahlman, R. P.; Sen, D. *J. Mol. Biol.* **1998**, 280, 237–244.
- ²⁰ Töhl, J.; Eimer, W. *Biophys. Chem.* **1997**, 67, 177–186.
- ²¹ Kang, C.; Zhang, X.; Ratliff, R.; Moyzis, R.; Rich, A. *Nature* **1992**, 356, 126–131.
- ²² Hud, N. V.; Smith, F. W.; Anet, F. A. L.; Feigon, J. *Biochemistry* **1996**, 35, 15383–15390
- ²³ Sen, D.; Gilbert, W. *Biochemistry* **1992**, 31, 65–70.
- ²⁴ Miura, T.; Benevides, J. M.; Thomas, G. J. *J. Mol. Biol.* **1995**, 248, 233–238.
- ²⁵ Hardin, C. C.; Henderson, E.; Watson, T.; Prosser, J. K. *Biochemistry* **1991**, 30, 4460–4472.
- ²⁶ Boynton, A. L.; McKeehan, W. L.; Whitfield, J.F.; Eds. *Ions, Cell Proliferation and Cancer*; Academic **1982**.
- ²⁷ Lau, Y.-T.; Yassin, R.R.; Horowitz, S.B. *Science* **1988**, 240, 1321–1323.
- ²⁸ Roomans, G.; Von Euler, A. *Cell Biol. Int.* **1996**, 20, 103–109.
- ²⁹ Famulok, M. *Curr. Opin. Chem. Biol.* **1999**, 9, 324 – 329.
- ³⁰ Padmanabhan, K.; Tulinsky, A. *Acta Crystallogr. Sect. D* **1996**, 52, 272 – 282.
- ³¹ Kelly, J. A.; Feigon, J.; Yeates, T. O. *J. Mol. Biol.* **1996**, 256, 417 – 422.
- ³² Vairamani, M.; Gross, M. L. *J. Am. Chem. Soc.* **2003**, 125, 42 – 43.
- ³³ Jing, N. J.; Rando, R. F. et al. *Biochemistry* **1997**, 36, 12498 – 12505.
- ³⁴ Jing, N. J.; Marchand, C.; Liu, J. et al. *J. Biol. Chem.* **2000**, 275, 21 460 – 21467.
- ³⁵ Wyatt, J. R. Vickers, T. A. et al. *Proc. Natl. Acad. Sci. USA* **1994**, 91, 1356 – 1360.
- ³⁶ a) Wen, J.-D.; Gray, D. M. *Biochemistry* **2002**, 41, 11438 – 11448; b) Wen J.-D., Gray, C.W. ;. Gray, D. M *Biochemistry* **2001**, 40, 9300 – 9310; c) Tarrago-Litvak, L.; Litvak, S.; Andreola, M. L. *J. Mol. Biol.* **2002**, 324, 195 – 203.
- ³⁷ Dapic, V., Bates, P. J. et al. *Biochemistry* **2002**, 41, 3676 – 3685.
- ³⁸ Padmanabhan, K.; Tulinsky, A. *Acta Crystallogr. Sect. D* **1996**, 52, 272 – 282.
- ³⁹ Dai, J.X., Dexheimer, T.S., Chen, D., Carver, M., Ambrus, A., Jones, R.A., Yang, D.Z. *J Am Chem Soc* **2006**, 128, 1096–1098.
- ⁴⁰ Seenisamy, J., Rezler, E.M., Powell, T.J., Tye, D., Gokhale, V., Joshi, C.S., Siddiqui-Jain, A., Hurley, L.H. *J Am Chem Soc* **2004**, 126, 8702–8709.
- ⁴¹ Phan, A.T. , Kuryavyy, V., Burge, S., Neidle, S., Patel, D.J. *J Am Chem Soc* **2007** 129, 4386–4392.
- ⁴² Maizels, N. *Nat Struct Mol Biol* **2006**, 13, 1055–1059.
- ⁴³ Huppert, J.L., Balasubramanian, S. *Nucleic Acids Res* **2005**, 33, 2908–2916.
- ⁴⁴ Siddiqui-Jain, A., Grand, C.L., Bearss, D.J., Hurley, L.H. *Proc Natl Acad Sci USA* **2002**, 99, 11593–11598.
- ⁴⁵ Zimmerman, S. B. *J. Mol. Biol.* **1976**, 106, 663 – 672.

- ⁴⁶ Marotta, S. P.; Tamburri, P. A.; Sheardy R. D. *Biochemistry* **1996**, 35, 10484 – 10492.
- ⁴⁷ Marsh, T. C.; Henderson, E. *Biochemistry* **1994**, 33, 10718 –10724.
- ⁴⁸ Charles, J. A. M.; McGown, L. B. *Electrophoresis* **2002**, 23, 1599 – 1604.
- ⁴⁹ Nutiu, R.; Li, Y. F. *J. Am. Chem. Soc.* **2003**, 125, 4771 – 4778.
- ⁵⁰ Mergny, J.-L.; Maurizot, J.-C. *ChemBioChem* **2001**, 2, 124 – 132.
- ⁵¹ Alberti, P.; Mergny, J.-L. *Proc. Natl. Acad. Sci. USA* **2003**, 100, 1569 – 1573.
- ⁵² Mao, C. D.; Sun, W. Q.; Shen, Z. Y. & Seeman, N. C. *Nature* **1999**, 397, 144–146.
- ⁵³ Yurke, B.; Tuberfield, A. J.; Mills, A. P., Jr.; Simmel, F. C. & Neunmann, J. L. *Nature* **2000**, 406, 605–608.
- ⁵⁴ Barboiu, M. & Lehn, J. M. *Proc. Natl. Acad. Sci. USA* **2002**, 99, 5201–5206.
- ⁵⁵ Parkinson, G.N. *Quadruplex Nucleic Acids*; RSC Publishing: London, **2006**; Chapter 1.
- ⁵⁶ Patel D.J.; Phan, A.T.; Kuryavii, V. *Nucleic Acids Res* **2007**, 35, 7429–7455.
- ⁵⁷ Riou, J.-F.; Gomez, D.; Morjani, H.; Trentesaux, C. *Quadruplex Nucleic Acids*; RSC Publishing: London, **2006**; Chapter 6.
- ⁵⁸ Dexheimer, T.S.; Fry, M.; Hurley, L.H. *Quadruplex Nucleic Acids*; RSC Publishing: London, **2006**; Chapter 7.
- ⁵⁹ Huppert, J. *Quadruplex Nucleic Acids*; RSC Publishing: London, **2006**; Chapter 8.
- ⁶⁰ Pileur, F.; Andreola, M.-L.; Dausse, E.; Michel, J.; Moreau, S.; Yamada, H.; Gaidamarov, S.A.; Crouch, R.J.; Toulmé, J.J.; Cazenave, C. *Nucleic Acids Res* **2003**, 31, 5776–5788.
- ⁶¹ Wang, K.Y.; McCurdy, S.; Shea, R.J.; Swaminathan, S.; Bolton, P.H. *Biochemistry* **1993**, 32, 1899–1904.
- ⁶² Chou, S.-H.; Chin, K.-H.; Wang A. H.-J. *Trends Biochem Sci* **2005**, 30, 231-234.
- ⁶³ Levesque, D.; Beaudoin, J.-D.; Roy, S.; Perreault, J.-P. *Biochemical J* **2007**, 403, 129-138.
- ⁶⁴ Girvan, A.C.; Teng, Y.; Casson, L.K.; Thomas, S.D.; Jueliger, S.; Ball, M.W.; Klein, J.B.; Pierce, W.M.Jr.; Barve, S.S.; Bates, P.J. *Mol Canc Therapeut* **2006**, 5, 1790-1799.
- ⁶⁵ Phan, A.T.; Kuryavii, V.; Luu, K.N.; Patel D.J. *Quadruplex Nucleic Acids*; RSC Publishing: London, **2006**; Chapter 3.
- ⁶⁶ Bhavesh, N.S.; Patel, P.K.; Karthikeyan, S.; Hosur, R.V. *Biochem Biophys Res Comm* **2004**, 317, 625-633 and references cited therein.
- ⁶⁷ Oliviero G.; Amato J.; Borbone N.; Galeone A.; Varra M.; Piccialli G.; Mayol L. *Biopolymers* **2006**, 81, 194-201 and references cited therein.
- ⁶⁸ Searle, M.S.; Williams, H.E.L.; Gallagher, C.T.; Grant, R.J.; Stevens, M.F.G. *Org Biomol Chem* **2004**, 2, 810-812 and references cited therein.
- ⁶⁹ Chen, J.; Zhang, R.L.; Min, J.M.; Zhang, L.H.; *Nucleic Acids Res* **2002**, 30, 3005–3014.
- ⁷⁰ Virgilio, A.; Esposito, V.; Randazzo, A.; Mayol, L.; Galeone, A. *Bioorg Med Chem* **2005**, 13, 1037-1044.
- ⁷¹ Risitano, A.; Fox, K.R. *Nucleic Acids Res* **2004**, 32, 2598-2606.
- ⁷² Rachwal, P.A.; Findlow, I.S.; Werner, J.M.; Brown, T.; Fox, K.R. *Nucleic Acids Res* **2007**, 35, 4214-4222.
- ⁷³ Rachwal, P.A.; Brown, T.; Fox, K.R. *FEBS Lett* **2007**, 581, 1657-1660.
- ⁷⁴ Bugaut, A.; Balasubramanian, S. *Biochemistry* **2008**, 47, 689-697.
- ⁷⁵ Oliviero, G.; Borbone, N.; Galeone, A.; Varra, M.; Piccialli, G.; Mayol, L. *Tetrahedron Lett* **2004**, 45, 4869-4872.
- ⁷⁶ Oliviero G.; Amato J.; Borbone N.; Galeone A.; Petraccone, L.; Varra M.; Piccialli G.; Mayol L. *Bioconjugate Chem* **2006**, 17, 889-898.
- ⁷⁷ Petraccone, L.; Erra, E.; Esposito, V.; Randazzo, A.; Mayol, L.; Nasti, L.; Barone, G., and Giancola, C. *Biochemistry* **2004**, 43, 4877-4884.
- ⁷⁸ Jin, R.; Gaffney, B. L.; Wang, C.; Jones, R. A., and Breslauer, K. J. *Proc. Natl. Acad. Sci. U.S.A* **1992**, 89, 8832-8836.
- ⁷⁹ Dapic', V.; Abdomerovic', V.; Marrington, R.; Pederby, J.; Rodger, A.; Trent, J. O., and Bates, P. J. *Nucleic Acids Res.* **2003**, 31, 2097-2170.
- ⁸⁰ Hardin, C. C.; Perry, A. G., and White, K. *Biopolymers* **2001**, 56, 147-194. 971.
- ⁸¹ Rankin, S.; Reszka, A. P.; Huppert, J.; Zloh, M.; Parkinson, G. N.; Todd, A. K.; Ladame, S.; Balasubramanian, S.; Neidle, S. *J. Am. Chem. Soc.* **2005**, 127, 10584-10589.
- ⁸² Jing, N.; Rando, R. F.; Pommier, Y.; Hogan, M. E. *Biochemistry* **1997**, 36, 12498-12505.
- ⁸³ Feigon, J.; Koshlap, K.M.; Smith, F.W. *Methods in Enzymology* **1995**, 225-255.
- ⁸⁴ Feigon, J. *Encyclopedia of Nuclear Magnetic Resonance* **1996**, 1726-1731.

-
- ⁸⁵ Breslauer, K. J., Frank, R., Blocker, H., and Marky, L. A. *Proc. Natl. Acad. Sci. U. S.A* **1986**, 83, 3746-3750.
- ⁸⁶ Hwang, T. L.; Shaka, A. J. *J. Magn. Res.* **1995**, A112, 275-279.
- ⁸⁷ Dalvit, C. J. *Biomol. NMR* **1998**, 11, 437-444.
- ⁸⁸ Cornell, W. D., Cieplack, P., Bayly, C. I., Gould, I. R., Merz, K. M., Ferguson, D. M., Spellmeyer, D. C., Fox, T., Caldwell, J. W., and Kollman, P. A. *J. Am. Chem. Soc.* **1995**, 117, 5179-5197.
- ⁸⁹ Gasteiger, J., and Marsili, M. *Tetrahedron* **1980**, 36, 3219-3228.

Chapter 2

Synthesis of combinatorial libraries of nucleosides, specifically inosine analogues

Introduction

Nucleoside research has historically been an area of keen interest for small molecule drug discovery due predominately to the medicinal value and biological importance of these molecules. Apart from being the genomic building blocks, nucleosides interact with roughly one-third of the protein classes in the human genome, including polymerases, kinases, reductases, motor proteins, membrane receptors, and structural proteins, all targets of biological importance.

The binding motifs of these nucleosides are associated with a broad array of targets of therapeutic importance in biological systems. It was early recognized that, introducing diversity into the carbohydrate or the base subunits of nucleosides, represents promising strategies to identify specific receptor ligands, enzyme inhibitors, or nucleoside function modifiers. Nucleoside analogues, showing very complex and interesting structures, have been isolated from t-RNA (5-methylcytidine, 3'-methyluridine), marine organism and several other microbiological forms. Naturally occurring nucleosides analogues demonstrate selective activities, such as protein synthesis inhibitors (puromycin), glycosyl transferase inhibitors (tunicamycin), methyl transferase inhibitors (sinefungin) and antibiotic activity (coformicine A and adenomicine). The discovery that some nucleoside analogues can possess biological activities has been a significant breakthrough especially in antiviral and anticancer chemotherapy. In this regard, the isolation from natural sources, but especially synthetic work have lead to the discovery of a large variety of new analogues. After decades of drug discovery and development effort from hundreds of academic laboratories and pharmaceutical companies, approximately 50-nucleoside- and nucleotide-related drugs, have been approved by the US Food and Drug Administration, and pushed to the market, and over 80 nucleosides/nucleotides are in the (pre) clinical studies for various therapeutic indications, including antiviral¹, anticancer², antibiotic³ and antifungal⁴.

In the search for antiviral nucleoside analogues, structural modifications of the heterocyclic bases and/or modifications on the sugar moiety of natural nucleosides, can be attempted. In the latter, the main modifications involved changes in the (2-deoxy)-D-ribofuranose moiety like, inversion of hydroxyl group configurations, their substitution/functionalisation by various synthetic groups, or cleavage of the sugar ring leading to acyclic nucleosides. Other structural modifications have also been attempted such as replacement by a methylene group or a sulfur atom of the endocyclic oxygen, transposition of the latter and/or additional insertion of a second heteroatom in the sugar moiety. Currently, nucleoside analogues are prominent drugs in the management of several viral infections. The nucleoside analogues at present formally approved for the treatment of viral infections are shown in **Figure 2.1** Acyclovir is an important antiviral in hepatitis C (HCV) treatment, while Lamivudine (3'-thiocytydine, 3TC) is a nucleoside analogue used for treatment of hepatitis B virus (HBV), the 5-iodouridine is employed in Herpes Simplex infections (HSV). Furthermore, it must be considered that the most commonly used anti-HIV drugs are nucleoside analogues, including Zidovudine (AZT, azidothymidine), Hivid

(ddC, zalcitabine), Zerit (d4T, stavudine) and some others, all possessing high activity in antiretroviral therapies⁴. They mimic natural nucleosides and target a unique, but complex viral polymerase that is essential for viral replication. Some nucleosides show also antiproliferative properties, for example arabinosylcytidine and 5-azacytidine are both utilized in the treatment of leukaemia, while 5-fluorouracil (5-FU) is employed in breast tumour (**Figure 2.1**).

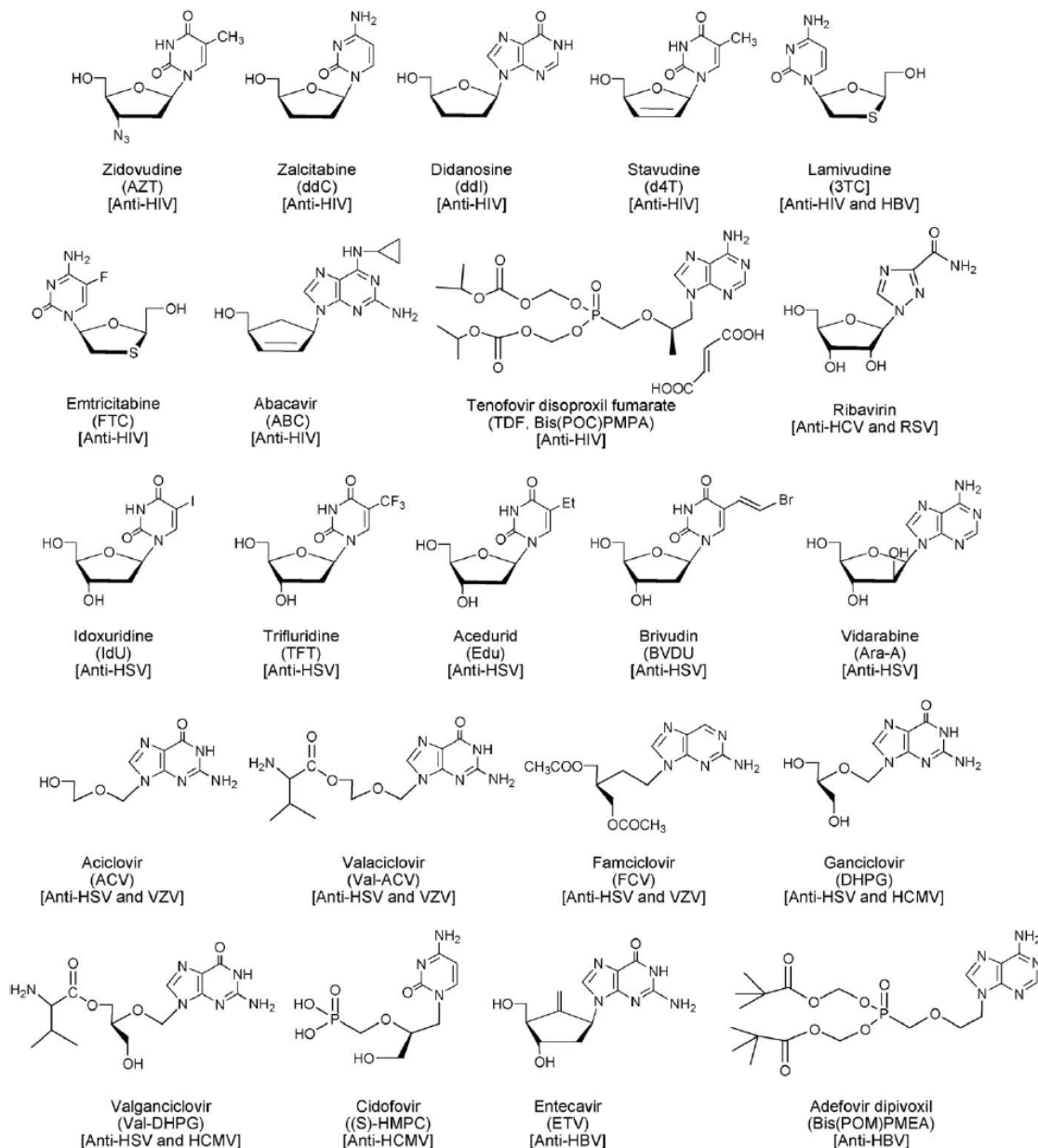


Figure 2.1: Nucleoside analogues currently used in antiviral therapy.

For salvage to be efficient, mediated transport of nucleosides and nucleobases across the plasma membrane has to occur. Then metabolic activation of nucleosides and nucleobases takes place, modulating their pharmacological action. The biochemical mechanism can be of various type, but in most cases the 5'-phosphorylation of the sugar moiety is the first step. The nucleoside 5'-phosphate is then converted into a triphosphate derivative that inhibits, in different way, the replication of DNA or RNA. However, some drugs such as AZT, ddI, 3TC etc. rapidly

develop drug resistance and show mitochondrial, bone-marrow and other toxicity. The increasing resistance of pathogens, the often severe side effects of nucleosides in chemotherapy, and the lack of selective ligands for adenosine receptor subclasses, despite extensive medicinal chemistry research, emphasizes the need for nucleoside analogues in high number and diversity. In addition, the availability of high-throughput screening capabilities, together with the combinatorial synthesis of small organic molecule libraries, offers a unique opportunity to accelerate the discovery of novel pharmaceutical targets and leads, especially, with biologically privileged scaffolds, such as nucleosides in hand.

2.1. Nucleoside analogues

The design of selective, specific and non-toxic antiviral, but also anticancer agents, has presented extraordinary challenges compared with the design of other antimicrobial agents. This is primarily because, in contrast to bacteria and parasites that are equipped with their own metabolic machinery for reproduction and growth, viruses rely on the host cellular machinery for replication and propagation. Consequently, there are few virus-specific molecular targets that are amenable to antiviral intervention. In addition, drug resistance to antiviral agents is a major problem as many viruses mutate rapidly under the selective pressure of the antiviral therapy. In recent times, however, and largely owing to the AIDS epidemic and advances in molecular virology, the structure and function of a few virus-specific molecular targets such as proteases and helicases have been revealed.

Furthermore, in the past decade, a repertoire of discovery tools in terms of structure and mechanism-based drug design, such as elucidations on *nucleoside analogues uptake and export, their activation, mechanism of action and mitochondrial toxicity*, have provided novel strategies for the design of antiviral agents against new molecular targets. In this regard different sites of diversity on both purine- and pyrimidine-nucleoside scaffolds have been introduced, schematically represented in **Figure 2.2**, bearing a myriad of functional groups. Generally, nucleosides analogues can be catalogued in “**Base-modified**” and “**Sugar-modified**” nucleoside analogues.

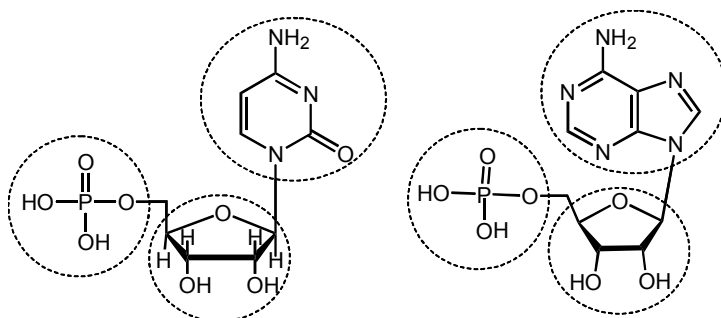


Figure 2.2: Nucleoside, nucleotide modifications

Notwithstanding these advances, progress in the discovery of new antiviral therapeutics has remained slow, and current antiviral chemotherapy is heavily dependent on a “cocktail” of antiviral agents. New antiviral agents, with unique mechanisms of action, are urgently needed, given the propensity of viruses to mutate rapidly under the selective pressure of chemotherapy. In the last years, the combinatorial chemistry has emerged as very efficient tool to produce a large number of new molecules differing in punctiform manner around a core structure of

active compounds. Solid phase combinatorial strategies have been mainly used in the nucleoside field.

2.2. Nucleoside analogue uptake

The intracellular concentration of nucleosides and nucleobases is of great importance for the success of antiviral and anticancer therapies and, to some extent, it is the result of the metabolic background of the specific cell line used for infection studies, its particular suit of enzymes and transporters. Transporter-mediated pathways are involved in either the uptake or the efflux of nucleoside and nucleobase derivatives. From a biochemical point of view, four different types of transport processes for nucleoside-related drugs are involved: 1) equilibrative uniport; 2) substrate exchange; 3) concentrative Na^+ - or H^+ -dependent uptake and finally 4) substrate export through primary ATP-dependent active efflux pump. These mechanisms are mainly related to the following set of transporter families: Concentrative Nucleoside Transporter (CNT), Equilibrative Nucleoside Transporter (ENT), Organic Anion Transporter (OAT) and Organic Cation Transporter (OCT), Peptide Transporter (PEPT) and Multidrug Resistance Protein (MRP)⁵. The scheme in figure 4.3 shows an idealistic epithelial cell expressing all known nucleoside-based antiviral drug transporters, emphasizing their location, either apical or basolateral, which ensure, when necessary, vectorial flux of substrates across the epithelium. Although information regarding the plasma membrane domains, in which they are inserted, has recently become available, the location for some specific transporters, such as Multidrug Resistance Proteins (MRP8) is still in doubt and so they are shown at the lateral side of the cell.

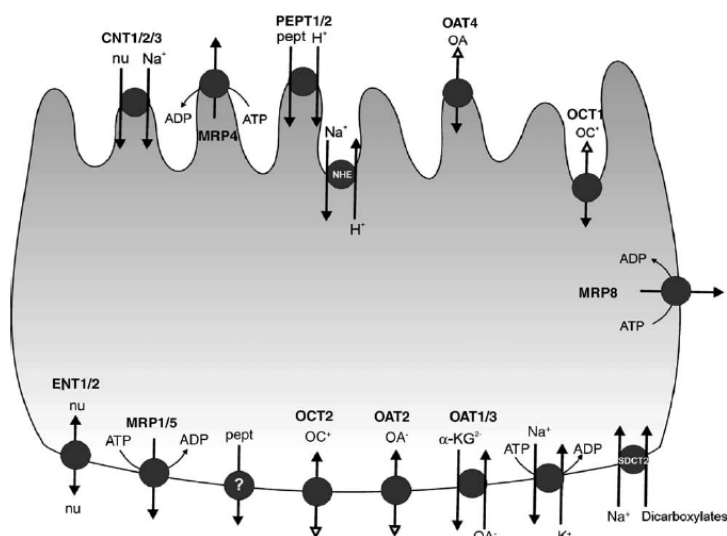


Figure 2.3: Major transporters implicated in the uptake and efflux of nucleoside-derived drugs used in antiviral therapy. A model of an idealized polarized epithelial cell, with the apical and basolateral membrane domains.

Equilibrative uniport works down the substrate concentration gradient and thus, it is in principle a reversible mechanism that responds only to the transmembrane substrate gradient tending to equilibrate it. This would be the case for the basolateral Equilibrative Nucleoside Transporter (ENT) carriers. The working model for an exchanger, particularly an obligatory exchanger, implies that efficient translocation of the substrate occurs only if both molecules are bound at both sides of the membrane to allow substrate exchange. An example of this mechanism depicted in **Figure 2.3**

is that the Organic Anion Transporter, also located at the basolateral plasma membrane, which exchanges an extracellular organic anion with a dicarboxylic acid, such as alphaketoglutarate. This process may be thermodynamically favourable, due to the ability of certain cells to concentrate dicarboxylates thanks to a complementary transporter, such as SDCT2 (also show in **Figure 2.3**), which allows the cell to concentrate alpha-ketoglutarate in a Na^+ -dependent manner. The latter is an example of the fourth mechanism of transport processes listed above. Coupling with Na^+ also occurs for other transporters, such as Concentrative Nucleosides Transporters (CNTs), implicated in the uptake of natural nucleosides, whereas H^+ -dependent uptake is involved into Peptide Transporters (PEPTs). These two basic mechanisms of concentrative transport, Na^+ - and H^+ -dependent, require tight coupling with carriers responsible for the immediate recovery of the ionic transmembrane gradients, the Na^+ , K^+ -ATPase and the Na^+/H^+ exchanger. In contrast to these secondary and tertiary active transport mechanism, ATP-dependent primary export pumps, responsible for antiviral drug efflux, have recently been identified. This would be the case of the Multidrug Resistance Protein isoforms (MRPs), shown in **Figure 2.3**, which mediates efflux, also in an energy-dependent manner, against substrate concentration, thanks to a direct coupling with ATP hydrolysis. The hypothesis that transporters belonging to the same gene family are responsible for the uptake of structurally related compounds is valid, at least for those responsible for uptake processes other than export pumps such as MRPs. Nevertheless, structurally related molecules can often be substrates of completely unrelated carrier proteins. However, when natural substrates are modified for pharmacological purposes, the spectrum of transporter proteins able to recognize them may vary.

2.3. Nucleoside analogue activation

Phosphorylation is required for mutagenesis and nucleotide metabolism interference. Nucleosides are phosphorylated by intracellular kinases to their active fraudulent nucleoside triphosphate (TP) analogue form, which compete with the natural dNTP for incorporation into the elongating proviral DNA. Since all current nucleoside-TP analogues lack a 3'-hydroxyl group, incorporation results in chain termination. The fact that a specific nucleoside-TP analogue competes with its natural nucleotide each time, and also it appears in the active site near the reverse-transcribing viral RNA chain, produces multiple opportunities for their blockade during a single round of reverse transcription. The long intracellular half-life of many nucleoside-TP analogues can result in a significant post-antibiotic effect⁶. Factors that influence their efficacy and dose frequency include the drug concentration versus time profile in plasma (pharmacokinetics), the efficiency of cellular uptake of the nucleoside analogues, levels of phosphorylation to their correspondent TP-derivatives, and their inhibition constant (K_i) with the target (viral DNA-polymerases, reverse transcriptase, respectively in DNA and RNA viruses).

2.4. Mechanism of action of nucleoside analogues

Although all orally available drugs target the viral polymerase, nucleoside analogues have different mechanisms of action on the viral genome replication machinery. Several drugs such as adefovir, entecavir and amdoxovir inhibit the priming of reverse transcription, a unique enzymic reaction that results in the synthesis of a

short DNA primer covalently attached to a conserved tyrosine residue of the viral polymerase. Other compounds inhibit the elongation of viral minus-strand DNA, such as lamivudine, emtricitabine and elvucitabine. The mechanism of action of clevudine involves a weak effect on the priming reaction but a stronger inhibitory activity on plus-strand DNA synthesis. The mechanism of action of telbivudine has not been described so far. Based on these distinct modes of action, one may speculate that the combination of drugs targeting different steps of viral genome replication may lead to an additive or synergic effect⁷. Therefore, the evaluation of the combination of drugs such as emtricitabine and clevudine, which are under clinical investigation, is relevant for the future development of combination therapy. Nucleoside analogues are also an emerging field of novel anticancer drugs, that is revolutionizing cancer therapy. In addition to inhibiting DNA replication by one or more mechanisms, these compounds may produce effects subsequent to their incorporation into the DNA; for example, premature DNA chain termination, structural lesions in the DNA product, and effects on transcription of modified DNA. Since charged nucleotides were believed normally do not enter the cells and considered ineffective as drugs, nucleosides have proved critical as therapeutic agents. Nucleosides and their analogues are precursors, that are intracellularly phosphorylated ('activated') into nucleotides (dNTPs), and act to inhibit or are incorporated by DNA polymerases *in vivo* (Figure 2.4).

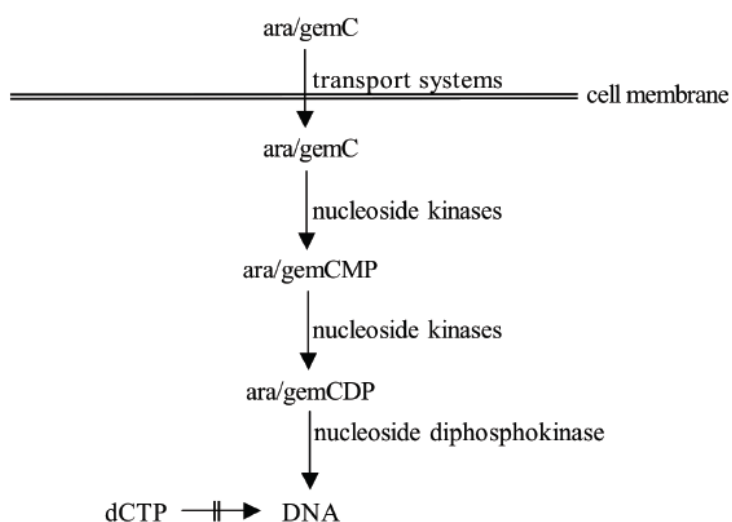


Figure 2.4: The intracellular formation of nucleotide triphosphate for araC and gemcitabine (gemC), as well as, their incorporation into new DNA.

Some two of these nucleoside analogues are currently used in chemotherapy or are in clinical trials or development. Examples include arabinofuranosylcytosine (araC)⁸ and 5-FU (the first for the treatment of non-solid tumors like leukemia, while the latter involved in breast tumour treatment), and 2',2'-difluorodeoxycytosine (gemcitabine)⁹ (for treatment of various non-solid and solid tumours, Figure 2.5). Promising applications of nucleotides analogues in antiviral and anticancer therapy are currently evaluated.

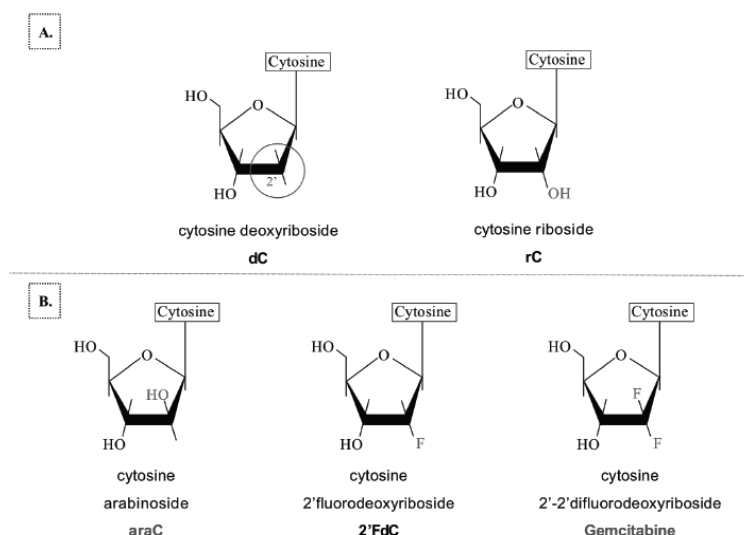


Figure 2.5: Nucleoside structures highlighting the differences on the groups on the 2'-carbon of the ribose-ring. **A.** Naturally occurring nucleosides dCTP and rCTP, and **B.** sugar-modified nucleoside analogues, araC, 2'FdC and gemcitabine.

2.5. Mitochondrial toxicity of nucleoside analogues

Generally, the mechanism of action of nucleoside analogues is based upon the intracellular phosphorylation to their 5'-triphosphate form which can interact with virus-specific polymerases, acting as a competitive inhibitor or an alternate substrate for these target enzymes, usually preventing further viral nucleic acid chain elongation. Long-term toxicities associated with nucleosides phosphorylation may be related to over-activation of this process. Elevated cell activation results in high nucleic acid synthesis and an up-regulation of kinases that phosphorylate nucleosides. Most of the clinical manifestations, resemble mitochondrial disease, and histological evidence, demonstrates abnormal mitochondria (mt) and/or mtDNA depletion in affected tissues. Studies show that nucleoside tri-phosphates competitively inhibit mtDNA polymerase gamma in vitro, the sole enzyme responsible for the base excision repair of oxidative damage to mitochondrial DNA. This in turn may decrease the number of mitochondrial respiratory chain proteins, inhibit aerobic respiration, induce oxidative stress, increase mutation in mtDNA, and result in mitochondrial and/or tissue failure, evidenced by the toxic accumulation of non-esterified fatty acids, dicarboxylic acids and free radical damage.

2.6. Nucleotide analogues

Since the discovery that monophosphorylated forms of nucleosides can be carried in cells by the Multidrug Resistance Proteins (MRP), and known that, monophosphorylated (MP) derivatives show smallest drug-induced cytotoxicity, AZT MP (Schuetz et al. 1999), d4T MP (Reid et al., 2003) and 5-FU MP (Guo et al., 2003) have been synthesized and evaluated in MRP uptake, in their activities and toxicities. Adefovir dipivoxil (ADV), the first prototype nucleotide analogue, has been approved recently for HBV therapy¹⁰. ADV seems relatively non-toxic upon longer-term use, overcome viral resistance to chemotherapy, and prevent viral replication rebound following cessation of therapy. Towards this objective, there is genuine optimism that selected nucleotide analogues could become front-line agents to be

used in combination with nucleosides and other agents in antiviral therapy producing improved pharmacological effects. Furthermore, nucleotide analogues can be useful tools in investigating the DNA polymerase mechanism. Considering the irreplaceable role of DNA polymerases in numerous important molecular biological core technologies, future potentials for biotechnological applications could be envisaged for nucleotide analogues. However, all these promising applications are limited by the broad tissue distribution of MRP proteins, including endothelia, most epithelia, smooth muscle and immune system cells (Adachi et al., 2002). However, the list of tissues and/or cell types is increasing, although there is discrepancy between the detection of the mRNA and the corresponding protein. Unfortunately, although the pharmacology of these transporter proteins is being studied, there is little information about the regulation of MRP activity, with the exception of the evidence that specific isoforms can be over-expressed in particular tumours.

2.7. Solid-phase synthesis of nucleoside analogues

A variety of different modified nucleosides derivatives, above reported, were synthesized by the classical approaches in solution, which is expensive and time consuming. Combinatorial synthesis of large diverse libraries and high-throughput screening technologies have recently emerged as powerful drug discovery paradigms. Various solid-phase, solution-phase¹¹, liquid phase¹², and third-phase combinatorial approaches have been successfully utilized for the generation of different oligomeric and small molecule libraries for a wide range of biological screenings. Unfortunately, these power technologies, especially parallel solid-phase combinatorial strategies¹³, have not been applied to the nucleoside chemistry for small molecule drug discovery yet although di/tri-and oligonucleotides¹⁴ were synthesized on solid support, and the modified solid supports have been used as acylating agent to acylate nucleosides derivatives¹⁵. Several key considerations had to be taken into account in order to develop a strategy for the combinatorial solid-phase synthesis of nucleosides analogues in high number and short period of time, to explore wide biological activities: i) most applicable linkers do not meet the general requirements for the solid phase synthesis of nucleoside libraries: stable enough under the required reaction conditions during synthesis, and labile enough to be cleaved easily from solid support without affecting nucleoside products; ii) limited positions on nucleoside can be attached on solid support; iii) limited types of reactions can be utilized and limited number of sites can be utilized and limited number of sites can be combinatorialized on the nucleoside skeletons, which prevent the generation of large diverse nucleoside libraries; iv) it is more difficult to get high quality and purity nucleoside libraries without purification compared to other small molecule libraries. Only in the most recent years, a variety of solid phase combinatorial strategies have been reported for the preparation of nucleoside and small oligonucleotide analogues libraries. In these approaches both the chemical stability and the position of the linkage with the polymeric support, play an important role in the selection of the chemical treatments allowing the nucleobase or sugar-phosphate modifications. For example, a solid support binding uridine or thymidine nucleosides by the acid labile 5'-O-trityl linkage has been used to prepare libraries of N-4-alkylated cytidine derivatives¹⁶. Another recently reported nucleoside functionalized support uses an alkaline labile 5'-O-succinyl linkage to bind the 6-chloro-2-nitro inosine derivative to produce a set of N-6- or N-2 alkylated adenosine derivatives¹⁷. Also the 2',3'-acetal linkage has been used to bind purine and

pyrimidine nucleosides to a solid support which has employed to introduce chemical diversities both on the base (C-6 of purine and C-4 of pyrimidine) and on the 5'-ribose position¹⁸. In another approach, a pyrimidine or purine nucleoside is anchored to the polymeric support by the N-3 or N-1 base position, respectively, through a N-alkyl- β -thioether function¹⁹⁻²¹, which results stable to both the acidic and basic conditions. The above supports have been used to prepare 2', 3'-ribose modified nucleoside or nucleotide analogues. Furthermore, CPG support loading 5'-DMT-nucleosides by the classical 3'-succinyl linkage²²⁻²³ or by a 3' acyloxyaryl phosphate linker²⁴ have been successful exploited to prepare very large nucleic-acid-bases (NABTM) libraries of nucleosidic 5'-phosphoramidate derivatives, and nucleic acid fragments to be tested in their antiviral activity²⁵.

2.8. The aim of the work

Although hundreds of purine and pyrimidine nucleosides were synthesized for a variety of biological and biomedical studies only a handful of N1-alkylated-inosine derivatives and the corresponding 2',3'- seco-nucleosides were reported.

To thoroughly explore the biological and biomedical properties of these analogues, the design and synthesis of these derivatives were performed by combinatorializing the N1-(2,4-dinitro)-phenyl derivatized position with a variety of amino building blocks, obtaining a first small library of N1-alkylated inosine and AICAR derivatives. Moreover, the supports bearing N1-alkylated inosine and AICAR derivatives, furnished, by a solid phase cleavage of the 2', 3' ribose bond, a set of new N1-alkylated-2',3'-secoinosine derivatives and AICAR derivative ones, in high yields.

2.9. Chemistry

In an effort to enlarge the nucleoside chemical reactivity on the solid phase, and thus the number of obtainable structurally diverse analogues, the synthesis and exploitation of the new acid labile nucleoside functionalized supports **4** and **5**, which bind the N-1-dinitrophenyl-inosine derivatives **2** or **3** through the ribose 5'-position, is reported. These supports have been employed in the solid phase synthesis of the N-1 substituted inosine **8a-e**, **9a-e**, the related 2', 3'-seconucleoside derivatives **11a-e** and the AICAR derivatives **14** and **15**. The solid phase strategy, here proposed, is based on our previous studies on the C-2 reactivity of N-1-dinitrophenyl-2'-deoxy-inosine towards N-nucleophiles²⁶⁻²⁷, to obtain N-1 substituted inosine and AICAR derivatives. The reported reaction mechanism (**Figure 2.6**) indicates that, when a strong electron-withdrawing group, such as the 2,4-dinitrophenyl (DNP), nitro group²⁸ (NO₂) or arylsulfonyl²⁹ one (ArS) is attached to the N-1 atom of the hypoxanthine ring, the C-2 carbon become electrophilic enough to react with amino nucleophiles (R-NH₂), leading to N1 substituted inosine derivative, by a fast opening and re-closure of the six terms purine cycle. It is to be noted that, as a consequence of the purine rearrangement, the endocyclic N-1 atom is substituted by the nitrogen atom of the nucleophilic reactant. This purine reactivity has been also exploited by others to introduce a modified base into oligonucleotides³⁰.

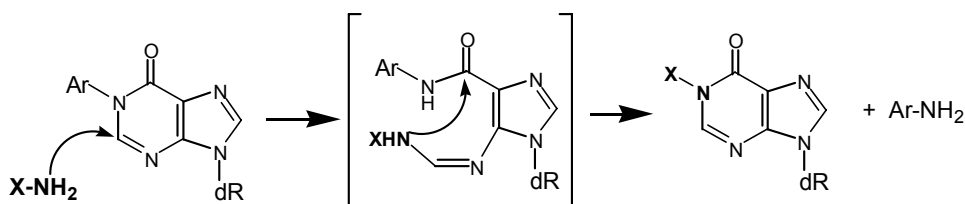
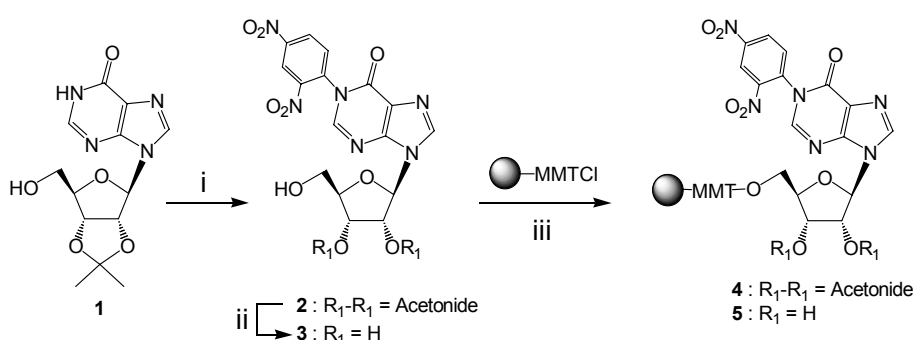


Figure 2.6: The nitrogen of nucleophile substitutes the purine N-1 nitrogen.

To exploit this reaction in a solid phase strategy to obtain a small library of N-1 alkyl inosine derivatives, we bound the 1-(2,4-dinitrophenyl)-2',3'-O-isopropylideneinosine **2**, or the corresponding unprotected inosine derivative **3** to the commercially available polystyrenemonomethoxytrityl chloride (MMTCl) resin by 5'-O-trityl ether linkage (**iii**, **Scheme 2.1**).



Scheme 2.1: Acid labile N-1-(2,4-dinitrophenyl)-nucleoside functionalized supports **4** and **5**

Inosine derivative **2** was synthesized by the reaction of the commercially available 2',3'-O-isopropylidene inosine (**1**) with 2,4-dinitrochlorobenzene (DNCIB), essentially as previously described³¹(**i**, **Scheme 2.1**). The 2',3'-deprotected-inosine-derivative **3**, was obtained treating **2** with aqueous formic acid (5 h, r.t., 90 % yield, **Scheme 2.1**, **ii**). The reaction of the MMTCl polystyrene resin (1.3 meq/g) with **2** or **3** (2 equiv.) in anhydrous pyridine at room temperature and in presence of 4-(N,N-dimethylamino)-pyridine (DMAP), afforded the support **4** or **5** respectively, in almost quantitative yields (**iii**, **Scheme 2.1**). The structure and the loading of the supports **4** and **5** were confirmed analyzing, by NMR and quantitative UV experiments, the released inosine derivatives **2** and **3**, respectively, by treatment with 2% TFA in DCM (8 min r.t.).

Support **4** and **5** were then reacted with several N-nucleophiles ($R_2\text{-NH}_2$, **Table 2.1** entry **a-e**) to give supports **6a-e** and **7a-e**, respectively (scheme 4.2). In a typical reaction, 100 mg (0.13 mmol) of support **4** (or **5**), swollen in DMF, was left in contact with the $R_2\text{-NH}_2$ nucleophile (5.0 mmol) in 1.5 mL of DMF under shaking (8 h, at 50 °C). After washings with DMF and MeOH, the support was dried under reduced pressure and the reaction yield was evaluated detaching the nucleoside material from a weighted amount of resin. The reaction of **4** or **5** with ethylenediamine (**Table 2.1**, entry **f**) furnished, as expected, the supports **12** and **13** bearing 2'-3'-isopropylidene-AICAR and AICAR, respectively, in almost quantitative yields. The structure of the support **6**, **7**, **12**, and **13** were ascertained analyzing and purifying by HPLC, ^1H NMR and MS analyses the corresponding detached crude materials **8**, **9**, **14**, and **15**. The product yields and the ^1H NMR data are reported in **Table 2.1**.



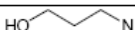
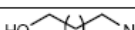
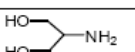
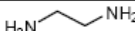
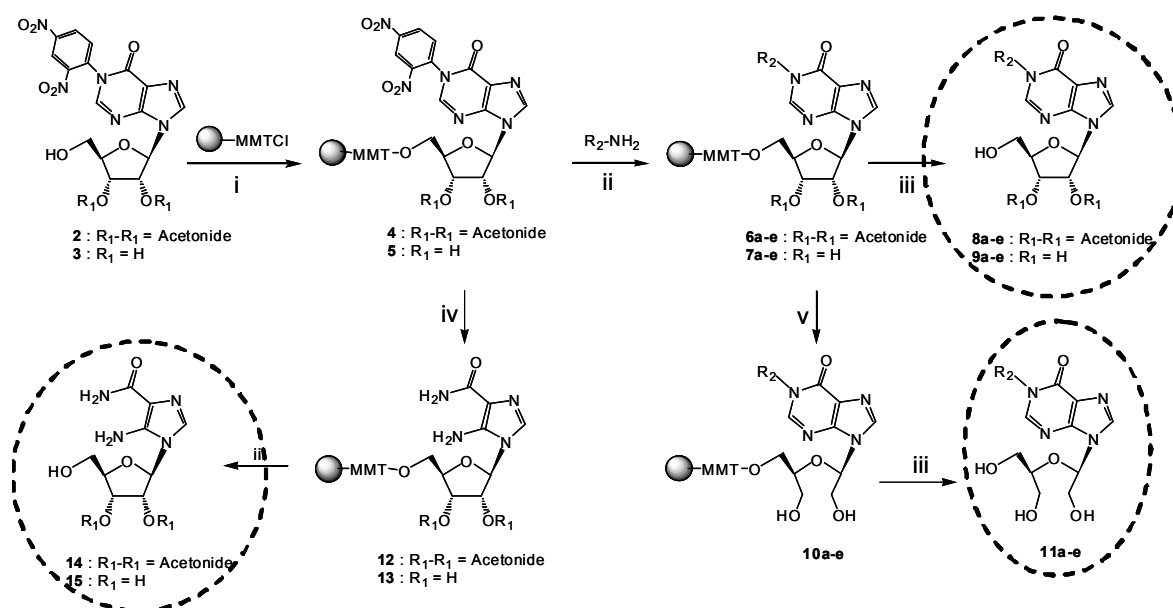
Entry	R ₂ -NH ₂	8, 9, 14, 15 Yield ^a (%)	9a-e and 15 ¹ H NMR ^b		11a-e Yield ^c (%)	¹ H NMR ^b	
			H-2; H-8; H-1'	R ₂ moiety		H-2; H-8; H-1' (seco)	R ₂ moiety
a		8 (98)	8.41; 8.36;	4.12; 1.76;	11a (85)	8.30; 8.26;	4.00; 1.75;
		9 (98)	6.02	1.40; 0.98		6.04	1.38; 0.96
b		8 (96)	8.42; 8.26;	4.19; 3.82	11b (85)	8.28; 8.24;	4.20; 3.83
		9 (95)	6.01			6.04	
c		8 (98)	8.41; 8.32;	4.20; 3.60;	11c (84)	8.31; 8.26;	4.21; 3.60;
		9 (96)	6.02	1.98		6.03	1.98
d		8 (98)	8.40; 8.35;	4.12; 3.56	11d (82)	8.33; 8.27;	4.11; 3.55;
		9 (98)	6.02	1.81; 1.59; 1.42		6.03	1.79; 1.58; 1.43
e		8 (92)	8.38; 8.32;	3.98 (2CH ₂ OH);	11e (75)	8.29; 8.04;	4.02 (2CH ₂ OH)
		9 (90)	6.00	3.92 (CH)		6.05	3.95 (CH)
f		1 (98)	8.04;		N.T.	N.T.	
		1 (98)	5.66				

Table 2.1: Reactions of the support **2** Products **4**, **6**, and **8**. N.T: not tested

^a Starting from resin **2**. ^b 400 MHz, (CD₃OD) significant protons at ppm. ^c Starting from resin **3**.

The second goal of this research work was aimed to combining the set of the base modified nucleoside (support **7**) with a ribose modification (**Scheme 2.2**).



Scheme 2.2: i: **2** or **3** (1.5 eq) in pyridine (1.5 mL/250 mg of resin), DMAP (0.05eq.), 24 h r.t; ii: R-NH₂/DMF (1:1,w/w), 8 h 50 °C; iii: TFA 5% solution in DCM; iv: EDA/DMF (1:1, w/w) 8 h 50 °C; v: NaIO₄ (50 eq.) in DMF/H₂O (1:1,v/v), 12 h, 60 °C; resin washings and treatment with NaBH₄ (20 eq.) in EtOH, 2 h, r.t.

As indicative example, the well known C2'-C3' bond oxidative cleavage of the ribose moiety by reaction with metaperiodate followed by the reduction of the di-aldehyde derivative which leads to 2',3'-seconucleosides³², was examined. In a typical reaction the support **7a-e** (100 mg, 0.13 mmol) was left in contact with a solution of NaIO₄ (1.3 mmol) in DMF/H₂O (1.5 mL, 1:1,v/v) and shaken for 12 h at 60 °C. The resulting

support, after washings with DMF and EtOH, was treated with NaBH₄ (2.6 mmol) in 1.5 mL of EtOH and shaken for 2.0 h at r.t. After washings, the resin **10a-e** was dried under reduced pressure and analyzed by detachment of the nucleoside material by TFA treatment. HPLC analyses indicated that the 2',3'-secoinosine derivatives **11a-e** were obtained in 75-85% yield. The structures of **11a-e** were confirmed by ¹H-NMR (Table 2.1) and MS analyses. The above oxidative cleavage performed in EtOH/H₂O (at several ratios and temperatures) afforded the seco-nucleosides in lower reaction yields most probably due to the scanty swelling of the polystyrene matrix in these solvents mixtures.

2.10. Conclusions

In conclusion, the synthesis of new N-1-dinitrophenyl-inosine based solid supports (**4** and **5**) in which the nucleoside are anchored to a MMT-polystyrene resin by the 5' position, was performed. The supports **4** and **5**, reacting at C-2 position of the purine base with R-NH₂ nucleophiles, were converted in the N-1 alkylated inosine supports (**6** and **7**) and AICAR derivatives supports (**12** and **13**) in very high yields. The detachment of the nucleosidic material, from the above supports, furnished small libraries of N-1 alkylated inosine (**8a-e** and **9a-e**) and AICAR derivatives (**14-15**), having the ribose moiety both protected and unprotected at the 2',3'-hydroxyl functions, in high purities (90-98%). In a further solid-phase reaction, the set of the N-1 alkylated inosine of the supports **7a-e** were combined with the cleavage of the 2',3'-ribose bond. These reactions furnished the new group of solid supports **10a-e** bearing base modified acyclo-nucleosides. Supports **10a-e** released, under acidic conditions, N-1 alkylated-2',3'-secoinosine derivatives **11a-e** in good purity (75-85 %). It reasonable to suppose that the supports **6**, **7**, **10**, **12** and **13**, bearing a nucleoside derivative can be fruitfully utilized in a combinatorial manner to introduce a number of further derivatizations/conjugations both on the 1-(hydroxyalkyl) function and/or on the ribose or seco-ribose moieties. Briefly, this research work reports the parallel solid-phase combinatorial approach for the rapid synthesis of new N1-alkylated inosine and N1-alkylated-2',3'-secoinosine derivative libraries. MMT-Cl polystyrene resin was confirmed to be an efficient solid support for nucleoside library synthesis. Hydroxyl groups at the 5'-position were preferentially involved into attach the nucleoside scaffold onto the MMT-Cl polystyrene resin. The DNP group is an excellent leaving group for various nucleophilic substitutions on the inosine base to synthesize high quality nucleoside libraries. The method seems good also to prepare a N1-alkylated-2',3'-secoinosine collection. All these new inosine derivatives, with various modifications at N1-position and at 2',3'-bond of the sugar moiety, will be screened against a wide range of biological assays. Further studies are currently in progress in this direction to obtain new and largest libraries of nucleoside analogues.

2.11 Experimental Session

2.11.1 General Methods

4-Methoxytrityl chloride resin (1% divinylbenzene, 200–400 mesh, 1.3 mmol g⁻¹ substitution) was purchased from CBL Patras, Greece. Anhydrous solvents were used for reactions. All the other reagents were obtained from commercial sources and were used without further purification. The reactions on solid phase were performed using glass columns (10 mm diameter, 100 mm length) with fused-in sintered glass-disc PO (bore of plug 2.5 mm), which were shaken on an orbital shaker, or round bottom flask, when reactions were performed at high temperatures. The ¹H NMR spectra were performed on a Varian Mercury Plus 400 MHz using CD₃OD and CDCl₃ as solvents; chemical shifts were reported in parts per million (δ) relative to residual solvent signals: CD₂HOD 3.31, CHCl₃ 7.26. The UV spectra were recorded on a Jasco V-530 UV spectrophotometer. Mass spectra were recorded on an Applied Biosystems API 2000 mass spectrometer using electron spray ionization (ESI) technique in positive mode. Column chromatography was performed on silica gel (Merck, Kieselgel 60, 0.063–0.200 mm). Analytic TLC detections were performed using F254 silica gel plates (0.2 mm, Merck). TLC spots were detected under UV light (254 nm).

Abbreviations: DMF = N,N-dimethylformamide, Py = pyridine, MeOH = methanol, EtOH = ethanol, DNCIB = 2,4-dinitrochlorobenzene, K₂CO₃ = potassium carbonate, MMT-Cl = 4-methoxytrityl chloride polystyrene resin, DMAP = 4,4'-dimethylaminopyridine, NaIO₄ = sodium *m*-periodate, NaBH₄ = sodium borohydride, s's = singlets, d's = doublets, m's = multiplets, q's = quartets

2.11.2 General Procedures

***N*-1-(2,4-dinitrophenyl)-2',3'-O-isopropylideneinosine (compound 2).** A mixture of **1** (1.0 g, 2.6 mmol), DNCIB (1.87 g, 8.1 mmol) and K₂CO₃ (897 mg, 6.5 mmol) was stirred in anhydrous DMF (16 mL) at 80 °C for 2.5 h. After cooling, the mixture was filtered and the solid was washed with CHCl₃. The filtrate and washings, evaporated to dryness under reduced pressure, were purified on a silica gel column eluted with increasing amount of CH₃OH in CHCl₃ (from 0 to 5%) to give 1.208 g of **2** (as 1: 1 mixture of atropoisomers at N-1-phenyl bond) as pale yellow amorphous solid (98% yield).

2, ¹H-NMR (400 MHz) ppm (CDCl₃) 1.30 (s, 3H, CH₃), 1.45 (s, 3H, CH₃), 3.65–4.0 (m, 2H, 2x5'-H), 4.5 (m, 1H, 4'-H), 5.10 (m, 1H, 3'-H), 5.30 (m, 1H, 2'-H), 6.00 (m, 1H, 1'-H), 7.70 (m, 1H, *o*-H), 8.10 (m, 2H, H-8, H-2), 8.70 (m, 1H, *m*-H), 9.00 (m, 1H, *m*-H); ESI-MS calculated *m/z*: 474.11, (C₁₉H₁₈N₆O₉), found: 513.50 (M + H)⁺.

***N*-1-(2,4-dinitrophenyl)-inosine (compound 3).** A solution of **2** (500 mg, 1.05 mmol) in aqueous HCO₂H (60%, 14 mL) was stirred at 50 °C for 2 h. After the solvent was evaporated under reduced pressure and the residue was purified on a silica gel column eluted with increasing amount of CH₃OH in CHCl₃ (from 0 to 20%) to give 451 mg, 99% of **3**.

3, ¹H-NMR (400 MHz) ppm (CD₃OD) 3.72–3.95 (m, 2H, 2x5'-H), 3.9 (m, 1H, 4'-H), 4.15 (m, 1H, 3'-H), 4.35 (m, 1H, 4'-H), 4.60–4.70 (m, 1H, 2'-H), 6.10 (m, 1H, 1'-H), 8.00 (m, 1H, *orto*-H), 8.50 (m, 2H, H-8, H-2), 8.76 (m, 1H, *meta*-H), 9.06 (m, 1H, *meta*-H); ESI-MS calculated *m/z*: 434.08 (C₁₆H₁₄N₆O₉), found: 435.32 (M + H)⁺.

Support 4. A suspension of MMT-Cl resin (500 mg, 0.65 mmol, 1.3 mmol/g), N-1-(2,4-dinitrophenyl)-2',3'-O-isopropylideneinosine, **2** (370 mg, 0.78 mmol, 1.2 eq), DMAP (6 mg, 0.05 mmol) in 1.5 mL of anhydrous pyridine was shaken at room temperature for 24 h. The resin was filtered and washed sequentially with pyridine-DMF (1:1 v/v, three times) and then with dichloromethane (three times). The obtained resin was dried under vacuum for 1h.

1.0 mL of a solution of 2% TFA in CH₂Cl₂ was added to 20 mg of weighted resin. The reaction mixture was shaken for 8 min, then the solution was filtered into a vial. The resin was washed with CH₂Cl₂, and filtered. The combined filtered were evaporated in vacuo. Quantitative UV experiment was performed on detached nucleoside (λ_{max} = 245 nm, ϵ = 20100, H₂O). The solid support **4** was obtained in almost quantitative yield (1.26 mmol g⁻¹, 97%).

Support 5. A suspension of MMT-Cl resin (1.0 g, 1.3 mmol, 1.3 mmol/g), N-1-(2,4-dinitrophenyl)-inosine, **3** (676 mg, 1.56 mmol), DMAP (12 mg, 0.1 mmol) in 1.5 mL of anhydrous pyridine was shaken at room temperature for 24h. The resin was filtered and washed sequentially with pyridine-DMF (1:1 v/v, three times) and then with dichloromethane (three times). The obtained resin was dried under vacuum for 1h.

1.0 mL of a solution of 2% TFA in CH₂Cl₂ was added to 20 mg of weighted resin. The reaction mixture was shaken for 8 min, then the solution was filtered into a vial. The resin was washed with CH₂Cl₂, and filtered. The combined filtered were evaporated in vacuo. Quantitative UV experiment was performed on detached nucleoside (λ_{max} = 245 nm, ϵ = 20100, H₂O). The solid support **4** was obtained in almost quantitative yield (1.26 mmol g⁻¹, 97%).

2.11.3 Synthesis of N-1-alkylated-inosine library

Support 6a-f. Approximately 80 mg (0.1 mmol) of starting resin **4** was dispensed in 6 reaction wells. To each well of resin were added 100 μ L of anhydrous DMF and 0.5mL of the (**a-e**) appropriate amine (see **Table 1**) in DMF. The reaction mixtures were shaken for 4h at 50°C, then filtered and washed with DMF (three times), MeOH-DMF (1:1 v/v, four times), MeOH (three times), MeOH-CH₂Cl₂ (1:1 v/v, four times), and finally with dichloromethane (two times). The resultant resins **6a-f** were dried under nitrogen.

Cleavage. Compounds 8a-e and 14. To the dried resin in each well was added 2 mL of a solution of 2% TFA in CH₂Cl₂. The reaction mixtures were shaken for 8 min, then the solution were filtered into a pre-labeled and pre-weighted vials. The resins were washed with MeOH, and filtered in the same corresponding vials. To the combined filtrates was added toluene. The solvents were evaporated under vacuum to provide compounds **8a-e**. The reaction of **4** with ethylenediamine (**Table 1**, entry **f**) furnished, as expected, the support **12**, bearing the 2',3'-isopropylidene-AICAR which corresponding detached form **14** was obtained in almost quantitative yields.

8a= 98% yields starting from resin **4**; ¹H-NMR (400 MHz) ppm (CD₃OD) 0.98 (t, 3H, CH₃), 1.36 (s, 3H, CH₃), 1.60 (s, 3H, CH₃), 1.40-1.76 (m's, 4H, 2xCH₂), 3.66-3.80 (m, 2H, 2x5'-H), 4.12 (t, 2H, CH₂N), 4.32-4.39 (m, 1H, 4'-H), 5.00 (m, 1H, 3'-H), 5.26 (m, 1H, 2'-H), 6.02 (d, 1H, 1'-H), 8.36-8.41 (s's, 1H each, H-8, H-2). ESI-MS calculated m/z: 364.17 (C₁₇H₂₄N₄O₅) found: 364.35 (M + H)⁺.

8b= 92% yields starting from resin **4**; ¹H-NMR (400 MHz) ppm (CD₃OD) 1.36 (s, 3H, CH₃), 1.60 (s, 3H, CH₃), 1.94-2.04 (m, 2H, CH₂), 3.66-3.80 (m, 2H, 2x5'-H), 3.82 (t, 2H, CH₂O), 4.19 (t, 2H, CH₂N), 4.32-4.39 (m, 1H, 4'-H), 5.00 (m, 1H, 3'-H), 5.26 (m, 1H, 2'-H), 6.01 (d, 1H, 1'-H), 8.26-8.41 (s's, 1H each, H-8, H-2). ESI-MS calculated m/z: 352.11 (C₁₅H₂₀N₄O₆) found: 353.28 (M + H)⁺.

8c= 98% yields starting from resin **4**; ¹H-NMR (400 MHz) ppm (CD₃OD) 1.36 (s, 3H, CH₃), 1.60 (s, 3H, CH₃), 1.94-2.04 (m, 2H, CH₂), 3.60 (t, 2H, CH₂O), 3.66-3.80 (m, 2H, 2x5'-H), 4.20 (t, 2H, CH₂N), 4.32-4.39 (m, 1H, 4'-H), 5.00 (m, 1H, 3'-H), 5.26 (m, 1H, 2'-H), 6.02 (d, 1H, 1'-H), 8.32-8.41 (s's, 1H each, H-8, H-2). ESI-MS calculated m/z: 366.15 (C₁₆H₂₂N₄O₆) found 367.32 (M + H)⁺.

8d= 98% yields starting from resin **4**; ¹H-NMR (400 MHz) ppm (CD₃OD) 1.37 (s, 3H, CH₃), 1.40-1.49 (m, 2H, CH₂), 1.42-1.81 (m's, 9H, CH₃, 3xCH₂), 3.56 (t, 2H, CH₂O), 3.67-3.80 (m, 2H, 2x5'-H), 4.12 (t, 2H, CH₂N), 4.33-4.39 (m, 1H, 4'-H), 5.00 (m, 1H, 3'-H), 5.26 (m, 1H, 2'-H), 6.02 (d, 1H, 1'-H), 8.35-8.40 (s's, 1H each, H-8, H-2). ESI-MS calculated m/z: 394.19 (C₁₈H₂₆N₄O₆) found: 395.44 (M + H)⁺.

8e= 92% yields starting from resin **4**; ¹H-NMR (400 MHz) ppm (CD₃OD) 1.37 (s, 3H, CH₃), 1.60 (s, 3H, CH₃), 3.67-3.80 (m, 2H, 2x5'-H), 3.92 (m, 1H, CHN), 3.98 (m's, 4H, 2xCH₂O), 4.35 (m, 1H, 4'-H), 5.28 (m, 1H, 2'-H), 6.00 (d, 1H, 1'-H), 8.32-8.38 (s's, 1H each, H-8, H-2). ESI-MS calculated m/z: 382.15 (C₁₆H₂₂N₄O₇) found: 382.32 (M + H)⁺.

14= 98% yields starting from resin **4**; ¹H-NMR (400 MHz) ppm (CD₃OD) 1.37 (s, 3H, CH₃), 1.60 (s, 3H, CH₃), 3.67-3.80 (m, 2H, 2x5'-H), 4.35 (m, 1H, 4'-H), 5.28 (m, 1H, 2'-H), 5.66 (d, 1H, 1'-H), 8.04 (s, 1H, H-2). ESI-MS calculated m/z: 298.13 (C₁₂H₁₈N₄O₅) found: 299.23 (M + H)⁺.

Support 7a-f. Approximately 150 mg (0.15mmol) of starting resin **5** was dispensed in 6 reaction wells. To each well of resin were added 100μL of anhydrous DMF and 0.5 mL of the appropriate amine (see **Table 1**) in DMF. The reaction mixtures were shaken for 4 h at 50 °C, then filtered and washed with DMF (three times), MeOH-DMF (1:1 v/v, four times), MeOH (three times), MeOH-CH₂Cl₂ (1:1 v/v, four times), and finally with CH₂Cl₂ (two times). The resultant resins **7a-f** were dried under nitrogen. An half of each one resin (**7a-f**) was dispensed in other 6 reaction wells and cleaved. The remaining ones were stored as starting material for synthesis of the N-1-alkylated-2',3'-secoinosine library.

Cleavage. Compounds 9a-e and 15. To the dried resin in each well was added 2 mL of a solution of 2% TFA in CH₂Cl₂. The reaction mixtures were shaken for 8 min, then the solution were filtered into a pre-labeled and pre-weighted vials. The resins were washed with MeOH, and filtered in the same corresponding vials. To the combined filtrates was added toluene. The solvents were evaporated under vacuum to provide compounds **9a-e**. The reaction of **5** with ethylenediamine (**Table 1**, entry **f**) furnished, as expected, the support **13** bearing the AICAR compound, which corresponding detached form **15** was obtained in almost quantitative yields.

9a= 98% yields starting from resin **5**; $^1\text{H-NMR}$ (400 MHz) ppm (CD_3OD) 0.98 (t, 3H, CH_3), 1.40-1.76 (m's, 4H, $2\times\text{CH}_2$), 3.72-3.95 (m, 2H, $2\times 5'\text{-H}$), 4.12 (t, 2H, CH_2N), 4.15 (m, 1H, $3'\text{-H}$), 4.35 (m, 1H, $4'\text{-H}$), 4.60-4.70 (m, 1H, $2'\text{-H}$), 6.02 (m, 1H, $1'\text{-H}$), 8.36-8.41 (s's, 1H each, H-8, H-2). ESI-MS calculated m/z: 324.15 ($\text{C}_{14}\text{H}_{20}\text{N}_4\text{O}_5$) found: 325.35 ($\text{M} + \text{H}$) $^+$.

9b= 95% yields starting from resin **5**; $^1\text{H-NMR}$ (400 MHz) ppm (CD_3OD) 3.72-3.95 (m, 2H, $2\times 5'\text{-H}$), 3.82 (t, 2H, CH_2O), 4.19 (t, 2H, CH_2N), 4.15 (m, 1H, $3'\text{-H}$), 4.35 (m, 1H, $4'\text{-H}$), 4.60-4.70 (m, 1H, $2'\text{-H}$), 6.01 (m, 1H, $1'\text{-H}$), 8.26-8.42 (s's, 1H each, H-8, H-2). ESI-MS calculated 312.11 ($\text{C}_{12}\text{H}_{16}\text{N}_4\text{O}_6$) found 313.28, ($\text{M} + \text{H}$) $^+$.

9c= 96% yields starting from resin **5**; $^1\text{H-NMR}$ (400 MHz) ppm (CD_3OD) 1.98 (m, 2H, CH_2), 3.60 (t, 2H, CH_2O), 3.72-3.95 (m, 2H, $2\times 5'\text{-H}$), 4.20 (t, 2H, CH_2N), 4.15 (m, 1H, $3'\text{-H}$), 4.35 (m, 1H, $4'\text{-H}$), 4.60-4.70 (m, 1H, $2'\text{-H}$), 6.02 (m, 1H, $1'\text{-H}$), 8.32-8.41 (s's, 1H each, H-8, H-2). ESI-MS calculated m/z: 326.12 ($\text{C}_{13}\text{H}_{18}\text{N}_4\text{O}_6$) found: 327.20 ($\text{M} + \text{H}$) $^+$.

9d= 98% yields starting from resin **5**; $^1\text{H-NMR}$ (400 MHz) ppm (CD_3OD) 1.42-1.81 (m's, 6H, $3\times\text{CH}_2$), 3.56 (t, 2H, CH_2O), 3.72-3.95 (m, 2H, $2\times 5'\text{-H}$), 4.12 (t, 2H, CH_2N), 4.15 (m, 1H, $3'\text{-H}$), 4.35 (m, 1H, $4'\text{-H}$), 4.60-4.70 (m, 1H, $2'\text{-H}$), 6.02 (m, 1H, $1'\text{-H}$), 8.35-8.40 (s's, 1H each, H-8, H-2). ESI-MS calculated m/z: 354.15 ($\text{C}_{15}\text{H}_{22}\text{N}_4\text{O}_6$) found: 355.45 ($\text{M} + \text{H}$) $^+$.

9e= 90% yields starting from resin **5**; $^1\text{H-NMR}$ (400 MHz) ppm (CD_3OD) 3.92 (m, 1H, CHN), 3.98 (m's, 4H, $2\times\text{CH}_2\text{O}$), 3.72-3.95 (m, 2H, $2\times 5'\text{-H}$), 4.15 (m, 1H, $3'\text{-H}$), 4.35 (m, 1H, $4'\text{-H}$), 4.60-4.70 (m, 1H, $2'\text{-H}$), 6.00 (m, 1H, $1'\text{-H}$), 8.32-8.38 (s's, 1H each, H-8, H-2). ESI-MS calculated m/z: 342.12, ($\text{C}_{13}\text{H}_{18}\text{N}_4\text{O}_7$), found: 342.30, ($\text{M} + \text{H}$) $^+$.

15= 98% yields starting from resin **5**; $^1\text{H-NMR}$ (400 MHz) ppm (CD_3OD) 3.72-3.95 (m, 2H, $2\times 5'\text{-H}$), 4.15 (m, 1H, $3'\text{-H}$), 4.35 (m, 1H, $4'\text{-H}$), 4.60-4.70 (m, 1H, $2'\text{-H}$), 5.66 (m, 1H, $1'\text{-H}$), 8.04 (m, 2H, H-2). ESI-MS calculated m/z: 258.10 ($\text{C}_9\text{H}_{14}\text{N}_4\text{O}_5$) found: 259.30 ($\text{M} + \text{H}$) $^+$.

2.11.4 Synthesis of N-1-alkylated-2',3'-secoinosine derivative library

Support 10a-e. The resins **7a-e** (75 mg of each one, 0.075 mmol) were treated with a solution of NaIO_4 (168mg, 0.75mmol) in $\text{DMF}/\text{H}_2\text{O}$ (1.5 mL, 1:1 v/v), and shaken for 12 h at 60 °C. The resulting supports after washings with DMF and EtOH , were left in contact with a solution of NaBH_4 (60 mg, 1.5 eq) in 1.5 mL of $\text{EtOH}-\text{H}_2\text{O}$ (1:1, v/v) for 2 h at room temperature. After washings with EtOH , the obtained supports **10a-e** were dried under reduced pressure and analyzed detaching the nucleoside material by TFA treatment.

Cleavage. Compounds 11a-e. To the dried resin in each well was added 2 mL of a solution of 2% TFA in CH_2Cl_2 . The reaction mixtures were shaken for 8 min, then the solution were filtered into a pre-labeled and pre-weighted vials. The resins were washed with MeOH , and filtered in the same corresponding vials. To the combined filtrates was added toluene. The solvents were evaporated under vacuum to provide compounds **11a-e**.

11a= 85% yields starting from resin **7a**; $^1\text{H-NMR}$ (400 MHz) ppm (CD_3OD) 0.96 (t, 3H, CH_3), 1.38-1.75 (m's, 4H, $2\times\text{CH}_2$), 3.20 (m, 1H, 4'-H), 3.90 (m's, 4H, $2\times\text{CH}_2\text{O}$), 4.00 (t, 2H, CH_2N), 4.22 (m, 2H, CH_2O), 6.04 (t, 1H, 1'-H), 8.26-8.30 (s's, 1H each, H-8, H-2). ESI-MS calculated m/z: 326.16 ($\text{C}_{14}\text{H}_{22}\text{N}_4\text{O}_5$) found: 349.05 ($\text{M} + \text{Na}$) $^+$.

11b= 85% yields starting from resin **7a**; $^1\text{H-NMR}$ (400 MHz) ppm (CD_3OD) 3.20 (m, 1H, 4'-H), 3.83 (t, 2H, CH_2O), 3.90 (m's, 4H, $2\times\text{CH}_2\text{O}$), 4.20 (t, 2H, CH_2N), 4.40 (m, 2H, CH_2O), 6.04 (t, 1H, 1'-H), 8.24-8.28 (s's, 1H each, H-8, H-2). ESI-MS calculated m/z: 326.16 ($\text{C}_{14}\text{H}_{22}\text{N}_4\text{O}_5$) found: 349.05 ($\text{M} + \text{Na}$) $^+$.

11c= 84% yields starting from resin **7a**; $^1\text{H-NMR}$ (400 MHz) ppm (CD_3OD) 1.98 (m, 2H, CH_2), 3.20 (m, 1H, 4'-H), 3.60 (t, 2H, CH_2O), 3.90 (m's, 4H, $2\times\text{CH}_2\text{O}$), 4.21 (t, 2H, CH_2N), 4.40 (m, 2H, CH_2O), 6.03 (t, 1H, 1'-H), 8.26-8.31 (s's, 1H each, H-8, H-2). ESI-MS calculated m/z: 326.16 ($\text{C}_{14}\text{H}_{22}\text{N}_4\text{O}_5$) found: 349.05 ($\text{M} + \text{Na}$) $^+$.

11d= 82% yields starting from resin **7a**; $^1\text{H-NMR}$ (400 MHz) ppm (CD_3OD) 1.43-1.79 (m's, 6H, $3\times\text{CH}_2$), 3.20 (m, 1H, 4'-H), 3.55 (t, 2H, CH_2O), 3.90 (m's, 4H, $2\times\text{CH}_2\text{O}$), 4.11 (t, 2H, CH_2N), 4.40 (d, 2H, 2'-H), 6.03 (t, 1H, 1'-H), 8.25-8.28 (s's, 1H each, H-8, H-2). ESI-MS calculated m/z: 326.16 ($\text{C}_{14}\text{H}_{22}\text{N}_4\text{O}_5$) found: 349.05 ($\text{M} + \text{Na}$) $^+$.

11e= 75% yields starting from resin **7a**; $^1\text{H-NMR}$ (400 MHz) ppm (CD_3OD) 3.20 (m, 1H, 4'-H), 3.90 (m, 4H, $2\times\text{CH}_2\text{O}$), 3.95 (m, 1H, CHN), 4.02 (m's, 4H, $2\times\text{CH}_2\text{O}$), 4.40 (m, 2H, CH_2O), 6.05 (t, 1H, 1'-H), 8.29-8.04 (s's, 1H each, H-8, H-2). ESI-MS calculated m/z: 326.16 ($\text{C}_{14}\text{H}_{22}\text{N}_4\text{O}_5$) found: 349.05 ($\text{M} + \text{Na}$) $^+$.

References

1. (a) Miura, S.; Izuta, S. *Current Drug Targets* **2004**, *5*, 191-195; (b) Parker, W.B.; Secrist, J.A.; Waud, W.R. *Current Opinion in Investigational Drugs*, **2004**, *5*, 592-596; (c) Szafraniec, S.I.; Stachnick, K.J.; Skierski, J.S. *Acta Poloniae Pharmaceutica* **2004**, *61*, 297-306.
2. (a) Lagoja, I.M. *Chemistry & Biodiversity*, **2005**, *2*, 1-50; (b) Kimura K.; Bugg, T.D.H. *Nat. Prod. Rep.* **2003**, *20*, 252-273; (c) Rachakonda, S.; Cartee, L. *Current Medicinal Chemistry*, **2004**, *11*, 775-793.
3. (a) In *Antiviral Nucleosides*; Chu, C.K., Ed.; Elsevier: , 2003; (b) Simons, C.; Wu, Q.; Htar, T.T. *Current Topics in Medicinal Chemistry* **2005**, *5*, 1191-1203; (c) De Clercq, E.; Neyts, J. *Rev. Med. Virol.* **2004**, *14*, 289-300.
4. Mathè, C.; Gosselin, G.; *Antiviral research* , **2006**, *71*, 276-281
5. Pastor-Anglada, M.; Cano-Soldado, P.; *Virus Research*, **2005**, *107*, 151-164
6. Schinazi, R.; Hernandez-Santiago, B.; *Antiviral research* , **2006**, *71*, 322-334
7. Zoulim, F.; *Journal of Antimicrobial Chemotherapy*, **2005**, *55*, 608–611
8. Plunkett, W., Huang, P.; *Semin. Oncol.*, **1996**, *22* (4 Suppl 11), 3-10
9. Plunkett, W., Huang, P.; *Semin. Oncol.*, **1996**, *23* (5 Suppl 10), 3-15
10. Rivkin, A.M.; *Ann.Pharmacother.*, **2004**, *38*, 625-633
11. Houghten, R.A.; Pinilla, C.; *J.Med.Chem.*, **1999**, *42*, 3743
12. An, H.; Cook, P.D.; *Chem.Rev.*, **2000**, *100*, 3311
13. Reed, N.N.; Janda, K.D.; *Org.Lett.*, **2000**, *2*, 1311
14. Nakamura, H.; Linclau, B.; *J.Am.Chem.Soc.*, **2001**, *123*, 10119
15. Jin, Y.; Chen, X.L.; *Bioorg.Med.Chem.Lett.*, **2001**, *11*, 2057
16. Becauge, S.L.; *Methods Mol. Biol.*, **1993**, *20*, 33
17. Ding, Y.; Habib, Q.; Shaw, S.Z.; Li, D.Y.; . *J. Comb. Chem.* **2003**, *5*, 851-859.
18. Rodenko, B.; Wanner, M.J.; *J. Chem. Soc., Perkin Trans. 1* **2002**, 1247-1252
19. Epple, R.; Kudirka, R.; Greenberg, W.A. *J. Comb. Chem.* **2003**, *5*, 292-310.
20. de Champdoré M.; De Napoli, L.; et al.; *Chem. Commun.* **1997**, 2079-2082.
21. De Napoli, L.; Di Fabio, G.; et al.; *D. Synlett* **2004**, *11*, 1975-1979.
22. Zhou, W.; Roland, A.; et al.; *Tetrahedron Lett.* **2000**, *41*, 441-445.
23. Jin, Y.; Roland, A., et al.; *Bioorganic & Medicinal Chemistry Letters* **2000**, *10*, 1921-1925
24. Roland, A.; Xiao, Y.; Jin, Y.; Iyer, R.P. *Tetrahedron Lett.* **2001**, *42*, 3669-3672
25. Jin, Y.; Chen, X., et al.; *Bioorganic & Medicinal Chemistry Letters* **2001**, *11*, 2057-2060.
26. De Napoli, L.; Messere, A.; Montesarchio, D.; Piccialli, G. *J. Org. Chem.* **1995**, *60*, 2251-2253.
27. De Napoli, L.; Messere, A., et al.; *J. Chem. Soc., Perkin Trans. 1* **1997**, 2079-2082.
28. N Ariza, X.; Bou, V.; Villarasa, J. *J. Am. Chem. Soc.* **1995**, *117*, 3665-3673
29. Terraza, M.; Ariza, X.; Farràs, J.; Villarrasa, J.; *Chem. Commun.* **2005**, 3968-3970
30. Narukulla, R.; Shuker, D.E.G.; Xu, Y.-Z. *Nucleic Acids Research* **2005**, *33*, 1767-1778
31. Galeone, A.; Mayol, L., et al.; *Eur. J. Org. Chem.* **2002**, 4234-4238.
32. Kumar, A.; Walker, R. T. *Tetrahedron* **1990**, *46*, 3101–3110.

Chapter 3

Synthesis of N-4-alkyl and ribose-modified AICAR analogues on solid support

Introduction

Nucleosides and their phosphorylated counterparts constitute an important class of biomolecules possessing a pivotal role in cellular metabolism and signal transmission. For example, they are involved in nucleic acid replication and in a very wide number of interactions with enzymes, structural proteins, and other biological targets of therapeutic importance. Many nucleoside analogues are currently used in therapy antivirals¹ and others are active compounds exhibiting antineoplastic², antibiotic, and antifungal properties³. The research of new active nucleosides is still very dynamic and promising; substances such as nelarabine⁴, entecavir⁵, clofarabine⁶ and azacitidine⁷ are examples of anticancer and antiviral drugs recently approved by U.S. FDA. Particular attention has recently been paid to 5-aminoimidazole-4-carboxamide-1- β -D-ribofuranoside (AICAR) since its 5'-phosphorylated derivative (ZMP), a key biosynthetic precursor of purine nucleotides, is an activator of AMP-activated protein kinase (AMPK)⁸. A possible therapeutic importance of its exploitation arises from the fact that the AICAR-induced AMPK activation strongly inhibits the basal and the insulin-stimulated glucose uptake, the lipogenesis, the glucose oxidation, as well as the lactate production in fat cells⁹. It has been also found that the control of protein kinase C (PKC) activation is correlated with the pathogenesis of diabetic retinopathy¹⁰.

Long-term exercise is well known to improve the glucose homeostasis and insulin action in insulin-resistant subjects and is one of the cornerstones in the treatment of Type 2 diabetes mellitus. Furthermore, it has been shown that regular exercise can partly prevent or delay the onset of the disease¹¹. The ameliorated insulin sensitivity after exercise is mainly due to enhanced insulin action on skeletal muscle, the predominant tissue for insulin-stimulated glucose disposal. In skeletal muscle, insulin stimulation leads to activation of a specific intracellular signaling cascade involving the insulin receptor substrate (IRS) family, the lipid kinase phosphatidylinositol (PI) 3-kinase, and also the serine/threonine kinase PKB/Akt.¹²

Activation of the insulin-signaling cascade leads to a recruitment of the insulin-sensitive glucose transporter (GLUT-4) from an intracellular pool to the surface membrane, thus allowing glucose to enter cell. This transport of glucose across the sarcolemma through GLUT-4 is thought to be the rate-limiting step for glucose utilization.

The 5'-AMP-activated protein kinase (AMPK) has recently been suggested as a potential candidate in the signaling process in response to exercise. Interestingly, both long-term treatment of rats with AICAR, which is an AMPK activator resulted in enhanced expression of GLUT-4 in skeletal muscles. Furthermore, the increased GLUT-4 expression is associated with a concomitant fiber type-related increase in the level of maximally insulin-stimulated glucose uptake¹³, suggesting that at least parts of this beneficial adaptation to long-term exercise can be mimicked through chronic AMPK activation.

Furthermore, the extracellular role of adenosine and other nucleosides as endogenous cell function modulators indicates the adenosine receptors as significant targets with wide therapeutic potential. In this context, AICAR has been indicated as a promising prodrug, which induces benefits in patients suffering from autism,

cerebral palsy, insomnia, schizophrenia, and other neuropsychiatric symptoms generally associated to chronic low levels of adenosine¹⁴.

The de novo purine biosynthetic pathway consist of 10 enzymatic reactions that convert 5'-phosphoribosyl-1-pyrophosphate to IMP (Inosine-5'-monophosphate). This pathway is used by virtually all organisms to produce purine nucleotides that are essential for many cellular processes. Consequently, this pathway has attracted considerable attention for the development of inhibitors, in particular for cancer chemotherapy since rapid dividing cells require large amounts of purines. The penultimate and final reactions of this pathway are catalyzed by a bifunctional protein with two distinct active sites: 5-aminoimidazole-4-carboxamide ribonucleotide transformylase (AICAR Tfase)¹⁵ and inosine monophosphate cyclohydrolase (IMP CHase). AICAR Tfase catalyzes the transfer of the formyl group from (6*R* α S)-10-formyltetrahydrofolate (10-f-H₄F) to ZMP producing 5-formyl-ZMP, which is then subsequently cyclized by IMP CHase to form IMP¹⁶ (**Figure 3.1**).

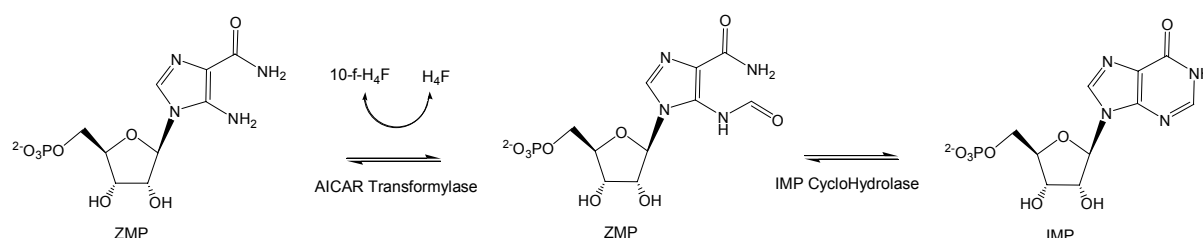


Figure 3.1 Reactions catalyzed by AICAR Tfase and IMP CHase.

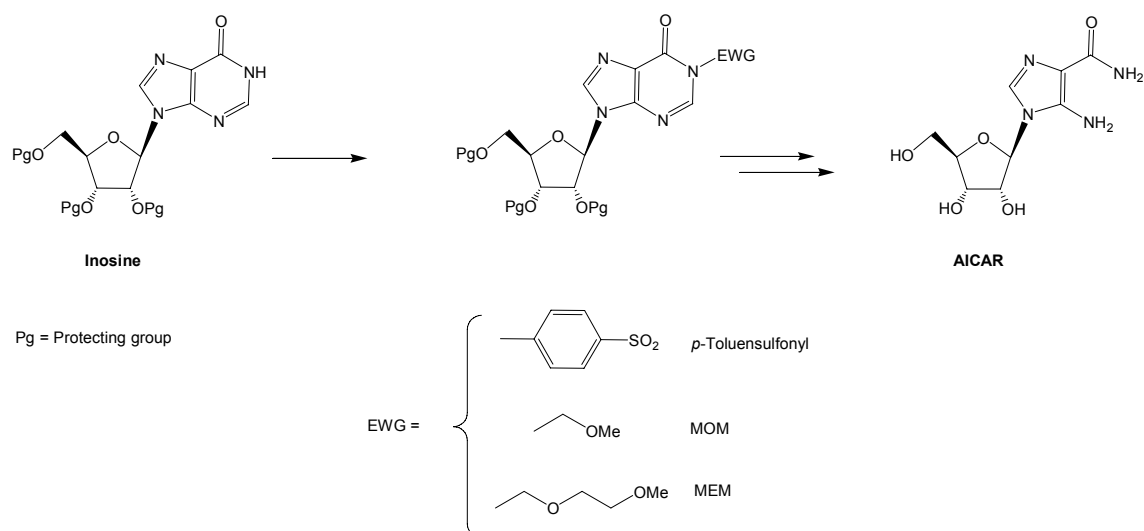
3.1 Chemical synthesis of AICAR and its derivatives

In recent years, the syntheses of a number of AICAR derivatives, such as the 2-aryl¹⁷ 4-N-benzyl¹⁸, 4-substituted¹⁹, 5-substituted²⁰, 5-hydroxyl (Bredinin)²¹, triazolyl-ribose (Ribavirin)²², 2',3'-secoriboside derivatives²³ have been reported in the literature.

Recently, the production of large nucleoside analogue libraries has emerged as an important synthetic goal to chase the high efficiency and velocity of the current biological screenings. In this frame, the solid-phase synthesis, associated with a combinatorial approach, offers the advantage of combining the rapid synthesis with an easily obtainable molecular diversity around a single core scaffold.

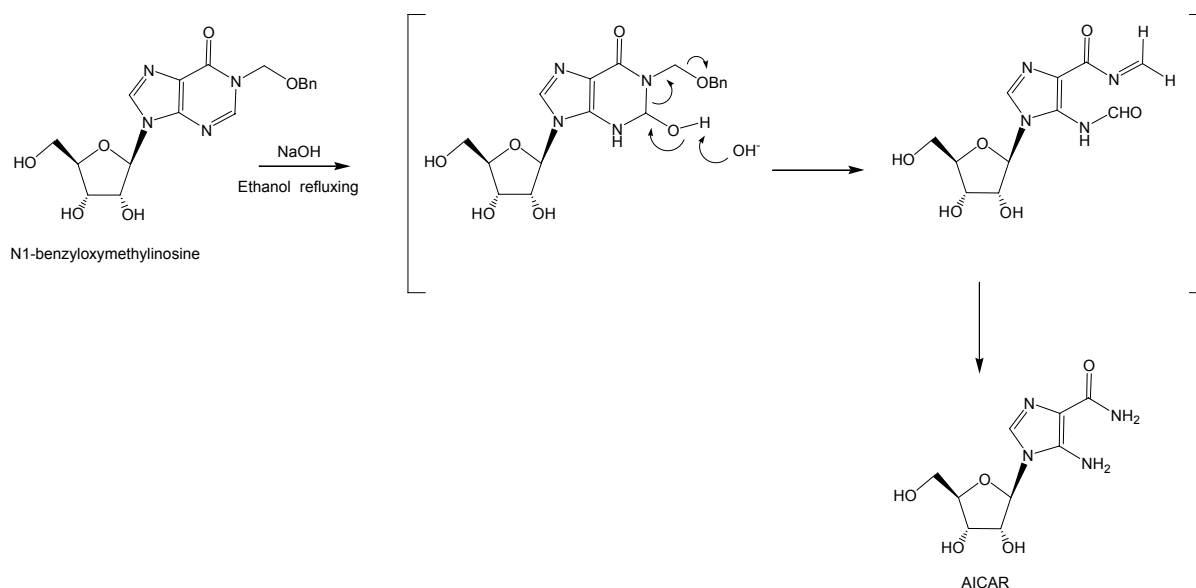
The synthesis of AICAR from inosine by using *p*-toluensulfonyl or methoxymethyl (MOM) groups as N-1-substituents was describe by Shaw²⁴. According to this report, treatment of these N-1-substituted inosines by aqueous alkali in refluxing ethanol could simultaneously open the pyrimidine ring and remove the N-1-substituent to afford the AICAR.

A more recent paper make use of a (2-methoxyethoxy)methyl (MEM) as the substituent of choice to perform this transformation from inosine to AICAR²⁵ (**Scheme 3.1**).



Scheme 3.1 Synthesis of AICAR from Inosine.

In this paper Kohyama presumed that the ring-opening reaction proceeded prior to the deprotection of benzyloxymethyl group since inosine was non detected during this alkaline hydrolysis. The formamidine moiety of N1-benzyloxymethylinosine is considered to be hydrolyzed, followed by elimination of benzyl alcohol, to imine intermediate, which is then converted to AICAR (**Scheme 3.2**).



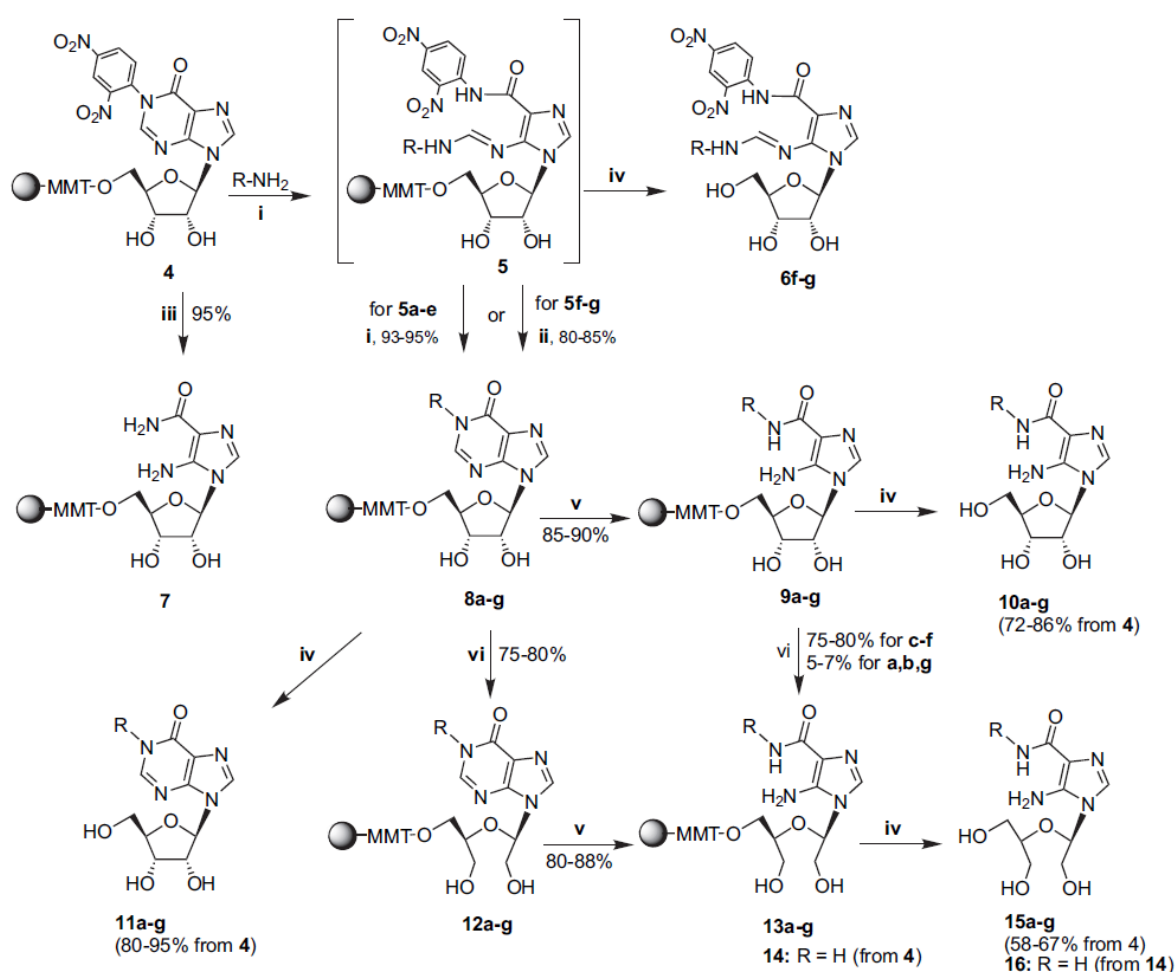
Scheme 3.2 Degradation of N1-benzyloxymethylinosine to AICAR

In 2006, Casanova et al.²⁶ performed a synthesis to obtain N-4-alkyl AICAR analogues on the basis of the known reactivity of position 1 of inosine. Thus, treatment of inosine with the corresponding alkyl, allyl, benzyl halide in dimethylacetamide (DMAC) and in presence of 1,8-diazabicyclo[5.4.0]undec-7-ene (DBU)²⁷ afforded the N-1-substituted inosines (56-89% yields) that, treated with NaOH 5 M in refluxing ethanol afforded N-4-alkyl AICAR derivatives (46-53% yield).

3.2 The aim of the work

The production of large nucleoside analogue libraries has emerged as an important synthetic goal to chase the high efficiency and velocity of the current biological screenings. In this frame, the solid-phase synthesis, associated with a combinatorial approach, offers the advantage of combining the rapid synthesis with an easily obtainable molecular diversity around a single core scaffold.

Here a new solid-phase synthetic strategy is reported, to obtain AICAR analogue libraries. The methodology has been tested in the synthesis of the two small AICAR libraries **10a–g** and **15a–g** (**Scheme 3.3**) where the nucleosides are modified on the 4-carboxamide residue or both at the 4-carboxamide and the ribose moiety, respectively.



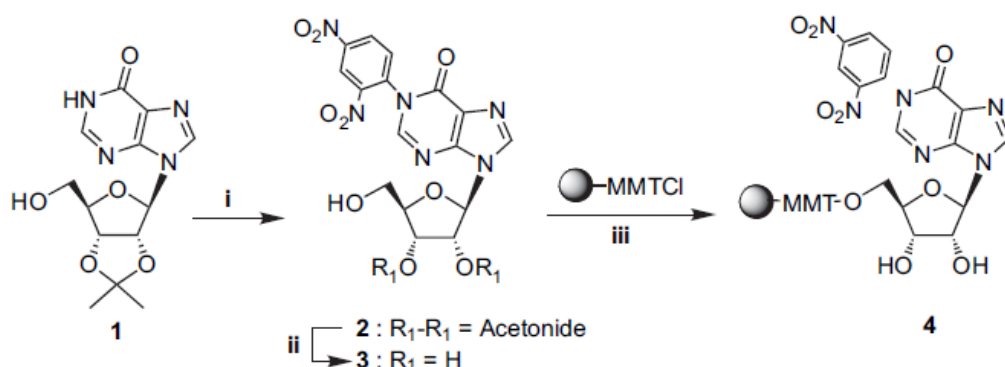
Scheme 3.3 (i) R-NH₂ (38.0 equiv) in DMF, 8 h, 50 °C; (ii) 1 M K₂CO₃ in DMF, 15 h, 50 °C; (iii) EDA/DMF (1:1, w/w) 8 h, 50 °C; (iv) 2% TFA solution in DCM; (v) 5 M NaOH in EtOH, 6 h, reflux; (vi) NaIO₄ (10 equiv) in DMF/H₂O (1:1, v/v), 12 h, 60 °C or Pb(OAc)₄ (15 equiv), in DCM, 2 h, rt; resin washings and treatment with NaBH₄ (20 equiv) in EtOH, 2 h, rt.

Our synthetic approach uses as starting material the recently proposed N-1-dinitrophenyl-inosine solid support **4** synthesized as depicted in **Scheme 3.3**. Support **4** reacting with R-NH₂ nucleophiles is converted into N-1 alkyl-inosine solid supports **8a–g** from which the AICAR libraries **10a–g** and **15a–g** could be obtained (**Scheme 3.3**). Previously, we utilized support **4** to prepare small libraries of N-1

alkyl-inosines and their corresponding 2',3'-secoriboside derivatives²⁸ We also demonstrated that when **4** reacts with ethylenediamine (EDA), the AICAR support **7** can be obtained in an almost quantitative yield^{28,29}.

Under alkaline conditions, N-1 alkyl-inosines react at the C-2 of the purine system to give 4-N-alkyl AICAR derivatives by pyrimidine ring cleavage and concomitant extrusion of the C-2 carbon itself. Therefore, we decided to extend this process to the solid-phase chemistry aiming at two main targets: (i) to efficiently prepare a set of 4-N-alkyl AICAR derivatives (**10a–g**) as well as the corresponding precursor solid supports (**9a–g**) from N-1 alkyl-inosine supports **8a–g**; (ii) to combine the set of AICAR derivatives with a ribose modification (2',3'-secoribosyl derivatives) thus producing the new kind of products **15a–g**, as well as the related solid supports **13a–g**, which are in turn potentially useful for further AICAR derivatization/ modification.

Support **4** was obtained by binding 1-(2,4-dinitrophenyl)-inosine **3** (**Scheme 3.4**) to the commercially available polystyrenemonomethoxytrityl chloride (MMTCl) resin by 5'-O-trityl ether linkage. Inosine derivative **3** was synthesized by the reaction of the commercially available 2'-3'-O-isopropylidene inosine **2** with 2,4 dinitrochlorobenzene (DNCB), followed by 2'-3' deprotection by aqueous formic acid treatment as previously described²⁸.



Scheme 3.4 (i) DNCB (2.2 equiv), K₂CO₃ (2.0 equiv), 2 h, 80 °C; (ii) HCOOH/H₂O (6:4, v/v), 4 h, rt; (iii) **3** (1.5 equiv) in pyridine (1.5 mL/250 mg of resin), DMAP (0.2 equiv), 24 h rt.

The reaction of the MMTCl resin (1.3 mequiv g⁻¹) with **3** in the presence of 4-(N,N-dimethylamino)pyridine (DMAP), in anhydrous pyridine, afforded support **4** in almost quantitative yield. Reaction of **4** with several N-nucleophiles (R-NH₂, **Table 3.1**) furnished the N-1 alkylinosine supports **8a–g**. In the above reactions, the R-NH₂ nucleophiles react with the strongly activated purine C-2 atom to give the open intermediates **5** possessing an N-alkyl formamidinium group. The successive fast ring re-closure, favored by the loss of 2,4-dinitroaniline as leaving group, led to N-1-alkyl-inosines **8a–e** (93–95% yields). We observed that in the case of sterically hindered amines (entries **f** and **g**), the reaction stopped at intermediate products **5**, which, after detachment from the support, could be isolated and characterized (**6f** and **g**).

As previously demonstrated, treatment with carbonate in DMF (at 50 °C) converted these open-pyrimidine species **5** in the N-1-alkyl-inosine supports **8f** and **g** (80–85% yields) by the six-membered ring re-closure³⁰. Reaction yields obtained for **8a–g** were evaluated quantifying the N-1-alkyl-inosines **11a–g** released from a weighted amount of supports **8a–g** by treatment with 2% (v/v) TFA in DCM taking into account that the starting support **4** had a nucleoside functionalization of 1.26 mequiv g⁻¹.

Entry	R-NH ₂	6, 11, Yield ^a (%)	10, 15, Yield ^a (%)
a		6 (NI), 11 (95)	10 (81), 15 (60)
b		6 (NI), 11 (95)	10 (83), 15 (67)
c		6 (NI), 11 (93)	10 (84), 15 (63)
d		6 (NI), 11 (95)	10 (86), 15 (69)
e		6 (NI), 11 (94)	10 (83), 15 (62)
f		6 (90), 11 (85)	10 (76), 15 (59)
g		6 (85), 11 (80)	10 (72), 15 (58)

NI: not isolated.

^a Starting from support 4.

Table 3.1 reaction on the support 4.

The corresponding N-4-alkyl AICAR supports **9a–g** were then obtained by cleavage of the pyrimidine ring in supports **8a–g** by NaOH treatment (5 M in EtOH, reflux, 85–90% reaction yields). TFA treatment of supports **9a–g** released the crude AICAR derivatives **10a–g**, which were purified by HPLC. The overall yield (starting from support 4) of the pure obtained nucleosides **10** and **11** are reported in **Table 3.1**. The structures and the purity of the products were confirmed by ¹H NMR spectroscopy and ESI-MS data. In a typical reaction starting from 20 mg of solid support 4, and considering an average molecular weight of 320 g mol⁻¹, 6–7 mg of each crude AICAR derivatives **10a–g** could be obtained in 70–85% purity.

Next, we explored the possibility of performing the 2',3'-oxidative cleavage of the ribose moiety in supports **9a–g**. In a first attempt, we employed the previously tested²⁸ reaction conditions, namely sodium metaperiodate followed by borohydride reduction of the di-aldehyde products. In a typical reaction, the supports **9a–g** were left in contact with a solution of NaIO₄ (10 equiv excess) in DMF/H₂O and shaken for 12 h at 60 °C. The resulting supports, after washing, were treated with NaBH₄ in EtOH and shaken for 2.0 h at room temperature to give supports **13a–g** that were analyzed by detaching the nucleosidic material by TFA treatment.

The HPLC analyses and purifications indicated that the above reactions, leading to **15c–f**, proceeded with 75–80% yields, whereas complex reaction mixtures were obtained for supports **13a,b,g** leading to very low quantities of the corresponding products **15a,b,g** (5–7% yields). These results suggest that the presence of the 4-N-(ω-hydroxyalkyl) portion on the AICAR supports **9a,b,g** leads to large side reactions when the products were reacted with sodium metaperiodate. In the case of AICAR support 7, the reaction furnished support 14 from which the AICA-2',3'-secoriboside **16** could be obtained in 70% overall yield (from 4) after the usual TFA treatment.

This prompted us to test the alternative pathway where the C2–C3 scission of the ribose moiety, with formation of 2',3'-secoribosides **12a–g**, was accomplished prior to

the pyrimidine ring degradation. Following this route, ribose cleavage of **8a–g** furnished **12a–g** in good reaction yields (75–80%, from **8**), which in turn were converted into the pyrimidine-degraded supports **13a–g** from which the products **15a–g** were obtained as described above (80–88% yields from **12**). The success of this pathway demonstrated that the presence of a 2',3'-secoribosyl moiety does not interfere with the alkaline degradation of the purine ring leading to the AICA heterocyclic system. Though a 75–80% yield for the ribose cleavage could seem acceptable, we considered this result not completely satisfactory for a solid-phase reaction supporting a combinatorial synthetic strategy. In fact, the above reaction causes a reduction in the overall yield and purity of the derivatives **15a–g** (60–70% yields from **4**). In order to further improve the yield of the C2–C3 bond cleavage in ribose, lead tetraacetate (LTA)³¹ was used in DCM or DMF. Though the process was accomplished at several LTA/**8a–g** ratios and varying the reaction time, no significant improvement of the 2',3'-secoribosyl derivatives **12a–g** was obtained after the usual NaBH₄ treatment (60–65% yields). However, it is to be noted that in both oxidative cleavage procedures (i.e., sodium metaperiodate or LTA) the predominant side products resulted to be the corresponding unreacted inosines **11a–g**.

3.3 Biological results

All compounds were tested for their effect on cellular proliferation using a human breast cancer cell line (MCF-7). The proliferative effects were evaluated in the absence of 5% fetal calf serum (FCS), while the anti-proliferative effects were evaluated in the absence of serum. The proliferation was evaluated by a standard colorimetric procedure (MTT test)³² after 24 and 48 h in triplicate using 1 mM of each compound dissolved in water or in 10% ethanol to improve solubility. The toxicity of the 10:90 ethanol/water solution was tested separately. No significant effect on proliferation was observed for any compound tested. Further experiments using different conditions and cell lines are currently undergoing.

3.4 Conclusions

In conclusion, we have successfully utilized the N-1-dinitrophenyl- inosine solid support **4**, where the nucleoside is anchored to an MMT-polystyrene resin by the 5'-ribose position, to synthesize small libraries of inosine and AICAR derivatives. The following solid-phase reactions have been carried out on this support and its derivatives: (i) the N-1 alkylation of purine by reaction of **4** with a variety of amines (90–95% yields); (ii) the alkaline cleavage of the N-1-alkyl-inosine base leading to AICAR derivatives (85–90% yields); (iii) the 2',3'-oxidative cleavage of the ribose moiety (75–80% yields). The proposed synthetic pathways allowed the preparation of small libraries of the N-1 alkyl-inosines **11a–g**, N-4-alkyl AICAR derivatives **10a–g**, and the corresponding 2',3'-secoriboside derivatives **15a–g**. It is to be noted that the reported solid-phase reactions proceed with yields comparable to, or higher than, those obtainable from the corresponding procedures in solution. Furthermore, the proposed solid-phase procedures furnished a new group of solid supports bearing inosine derivatives (**8a–g**, **12a–g**) or AICAR derivatives (**9a–g**, **13a–g**), which can be utilized in a combinatorial manner to achieve a number of further derivatizations/conjugations both on the imidazolyl residue and/or on the ribose or 2',3'-secoribose moiety.

3.5. Experimental

3.5.1. General

4-Methoxytrityl chloride resin (1% divinylbenzene, 200–400 mesh, 1.3 mmol g⁻¹ substitution) was purchased from CBL Patras, Greece. Anhydrous solvents were used for reactions. All the other reagents were obtained from commercial sources and were used without further purification. The reactions on solid phase were performed using glass columns (10 mm diameter, 100 mm length) with fused-in sintered glass-disc PO (bore of plug 2.5 mm), which were shaken on an orbital shaker, or round bottom flask, when reactions were performed at high temperatures. Mps were determined on a Reichert Thermovar apparatus. IR spectra were collected on a Jasco FT-IR-430 spectrometer. The ¹H NMR spectra were performed on a Varian Mercury Plus 400 MHz using CD₃OD and CDCl₃ as solvents; chemical shifts were reported in parts per million (δ) relative to residual solvent signals: CD₂HOD 3.31, CHCl₃ 7.26. RP-HPLC analyses of crude products were carried out on a Jasco UP-2075 Plus pump using a 5 mm, 4.8x150 mm C-18 reversephase column eluted with a linear gradient of CH₃CN in 0.1 M TEAB (pH 7.0, from 0 to 60% in 60 min, flow 1.0 mL min⁻¹) equipped with a Jasco UV-2075 Plus UV detector. The UV spectra were recorded on a Jasco V-530 UV spectrophotometer. Mass spectra were recorded on an Applied Biosystems API 2000 mass spectrometer using electron spray ionization (ESI) technique in positive mode. The High Resolution MS were recorded on a Bruker APEX II FT-ICR mass spectrometer using electron spray ionization (ESI) technique in positive mode. Column chromatography was performed on silica gel (Merck, Kieselgel 60, 0.063–0.200 mm). Analytic TLC detections were performed using F254 silica gel plates (0.2 mm, Merck). TLC spots were detected under UV light (254 nm).

Abbreviations: DMF = N,N-dimethylformamide, Py = pyridine, MeOH = methanol, EtOH = ethanol, DNCIB = 2,4-dinitrochlorobenzene, K₂CO₃ = potassium carbonate, MMT-Cl = 4-methoxytrityl chloride polystyrene resin, DMAP = 4,4'-dimethylaminopyridine, NaIO₄ = sodium *m*-periodate, NaBH₄ = sodium borohydride, NaOH = sodium hydroxide, LTA = lead tetraacetate, s's = singlets, d's = doublets, m's = multiplets, q's = quartets

3.5.2 Synthesis

1-(2,4-Dinitrophenyl)-2',3'-O-isopropylideninosine (2)

A mixture of 2',3'-O-isopropylideninosine (**1**) (1.00g, 3.24 mmol), DNCIB (820 mg, 4.05 mmol), and K₂CO₃ (560 mg, 4.05 mmol) was suspended in anhydrous DMF (5 mL) and stirred at 80 °C for 3 h. The reaction was monitored by TLC (CHCl₃/MeOH, 95:5). After cooling, the mixture was filtered and the solid was washed with CHCl₃. The filtrates and washings, collected and evaporated to dryness, were purified on a silica gel column eluted with increasing amounts of MeOH in CHCl₃ (from 0 to 5%) to give **2** as a pale yellow amorphous solid consisting of a 1:1 mixture of atropisomers at the N(1)–phenyl bond (1.20 g, 80%); mp 235–237 °C; ν_{max} (CHCl₃) 3417, 3106, 1710, 1538, 1348 cm⁻¹; ¹H NMR δ H (CDCl₃) 9.04 (br s, 1H, H-3 DNP), 8.72–8.62 (m, 1H, H-5 DNP), 8.11, 8.14 (2' s, 2H, H-2 and H-8), 7.81–7.72 (m, 1H, H-6 DNP),

6.07–5.96 (m, 1H, H-1'), 5.22–5.11 (m, 1H, H-2'), 5.10–5.02 (br s, 1H, H-3'), 4.53 (br s, 1H, H-4'), 4.02–3.75 (m, 2H, H-5'_{a,b}), 2.90 (br s, 1H, OH, exchange with D₂O), 1.64, 1.39 (2s, 6H, 2CH₃); UV (MeOH) λ_{max} 246 nm, ϵ = 20,200; HRESIMS calcd for C₁₉H₁₈N₆NaO₉: 497.1033, found: 497.1056 (M+Na)⁺.

1-(2,4-Dinitrophenyl)inosine (3)

Compound **2** (1.20 g, 2.60 mmol) was dissolved in HCOOH/H₂O (6:4, v/v, 16 mL) and left at room temperature for 4 h. The reaction was monitored by TLC (CHCl₃/MeOH, 6:4). The mixture was evaporated to dryness to furnish **3** (1.13 g, 99%) as a pale yellow amorphous solid that constituted a 1:1 mixture of atropisomers at the N(1)–phenyl bond. The product was used without further purification; mp 210–212 °C; ν_{max} (neat) 3402, 3098, 1704, 1546, 1343, 1217 cm⁻¹; ¹H NMR δ H (CD₃OD) 9.05 (s, 1H, H-3 DNP), 8.82–8.72 (m, 1H, H-5 DNP), 8.49, 8.52 (2s, 2H, H-2 and H-8), 8.08–7.98 (m, 1H, H-6 DNP), 6.14–6.06 (m, 1H, H-1'), 4.70–4.60 (m, 1H, H-2'), 4.40–4.32 (m, 1H, H-3'), 4.19–4.12 (m, 1H, H-4'), 3.94–3.74 (m, 2H, H-5'_{a,b}); UV (H₂O) λ_{max} 246 nm, ϵ = 20,100; HRESIMS calcd for C₁₆H₁₄N₆NaO₉: 457.0720, found: 457.0715 (M+Na)⁺.

3.5.3. General procedure for the scaffold synthesis

Loading of 3 on solid support

1-(2,4-Dinitrophenyl)inosine (**3**) (1.13 g, 2.60 mmol) was evaporated with dry pyridine (3x1.5 mL) and then coupled with the MMTCl resin (1.30 g, 1.69 mmol), and swollen with dry pyridine (8 mL) in the presence of DMAP (0.35 mmol, 42.0 mg) for 24 h at room temperature. The resin was filtered and washed with CH₂Cl₂ (3x5 mL), CH₂Cl₂/MeOH (1:1, v/v, 3x5 mL), and MeOH (3x5 mL), and finally dried in vacuo. The reaction yield was evaluated by cleavage of the nucleoside from the solid support by treatment with 2% (v/v) TFA in DCM (8 min, rt) followed by quantitative UV experiment (**3**, λ_{max} = 246 nm, ϵ = 20,100, H₂O). The solid support **4** was obtained in almost quantitative yield (1.26 mmol g⁻¹, 97%).

Treatment of solid support 4 with N-nucleophiles a–g (products 8a–g, 11a–g)

Solid support **4** (100 mg, 0.13 mmol), previously swollen in DMF, was left in contact with amines **a–g** (5.0 mmol) in DMF (1.5 mL) under shaking for 8 h at 50 °C. The reaction of **4** with amines **a–e** furnished, after usual washings, supports **8a–e**. In the case of amines **f** and **g**, after detachment from the support as described above, intermediates **6f** and **g** could be obtained, after HPLC purification, in 90 and 85% yields, respectively. Alternatively, supports **5f–g** were treated with a 1 M solution of K₂CO₃ in DMF (15 h, 50 °C) thus giving supports **8f** and **g**. After filtration and washings with DMF (3x5 mL), DMF/MeOH (1:1, v/v, 3x5 mL), and MeOH (3x5 mL), supports **8a–g** were dried under reduced pressure. The yields of N-1-alkyl-inosines **11a–g** (80–95%, from **4**, **Table 3.1**) were calculated by quantifying the products obtained by HPLC purification of the crude nucleoside material released from a weighted amount of resin (as described above) and taking into account that the starting support **4** had a 1.26 mol g⁻¹ nucleoside functionalization.

Formation of 4-N-alkyl AICAR derivatives 10a–g

Supports **8a–g** (100 mg, 0.10–0.12 mmol) were treated with NaOH (5 M in EtOH) for 6 h at reflux. After filtration and washings with EtOH (3x5 mL), EtOH/H₂O (1:1, v/v, 3x5 mL), H₂O (3x5 mL), and MeOH (3x5 mL), supports **9a–g** were dried under reduced pressure. The reaction yields (8/9, 80–90%) and the overall yields of 4-N-alkyl AICAR derivatives **10a–g** (72–86% from **4**) were evaluated on isolated products after HPLC purification of the material released from a weighted amount of resin, as described above. ¹H NMR spectra (see later) confirmed the purity of the products.

Formation of 4-N-alkyl AICA-2',3'-secoriboside derivatives 15c–f (pathway 9→13→15)

Supports **9c–f** (100 mg, 0.09–0.11 mmol) were left in contact with a solution of NaIO₄ (235 mg, 1.1 mmol) in DMF/H₂O (1.5 mL, 1:1, v/v) and shaken for 12 h at 60 °C. The resulting supports, after washings with DMF (3x5 mL), DMF/H₂O (1:1, v/v, 3x5 mL), H₂O (3x5 mL), and then with EtOH (3x5 mL), were treated with NaBH₄ (2.2 mmol) in EtOH (1.5 mL) and shaken for 2.0 h at room temperature. After filtration and washings with EtOH (3x5 mL), EtOH/H₂O (1:1, v/v, 3x5 mL), H₂O (3x5 mL), and MeOH (3x5 mL), supports **13c–f** were dried under reduced pressure. Reaction yields (9→13, 75–80%, **Table 3.1**) were evaluated by HPLC analysis and purification of the crude 4-N-alkyl AICA-2',3'-secoriboside derivatives **15c–f** released from a weighted amount of resin, as describe above. The same reactions, performed on **9a,b,e** furnished very low quantities of the corresponding **15a,b,e**.

Formation of 4-N-alkyl AICA-2',3'-secoriboside derivatives 15a–g (pathway 8→12→13→15)

Supports **8a–g** (100 mg, 0.10–0.12 mmol) were left in contact with a solution of NaIO₄ (235 mg, 1.1 mmol) in DMF/H₂O (1.5 mL, 1:1, v/v) and shaken for 12 h at 60 °C. The resulting supports, after washings with DMF (3x5 mL), DMF/H₂O (1:1, v/v, 3x5 mL), H₂O (3x5 mL), and then with EtOH (3x5 mL), were treated with NaBH₄ (2.2 mmol) in EtOH (1.5 mL) and shaken for 2.0 h at room temperature. After filtration and washings with EtOH (3x5 mL), EtOH/ H₂O (1:1, v/v, 3x5 mL), H₂O (3x5 mL), and MeOH (3x5 mL), supports **12a–g** were dried under reduced pressure. Reaction yields (8→12, 75–80%) were evaluated by HPLC analysis and purification of the crude 1-N-alkyl-inosine-2',3'-secoriboside derivatives released from a weighted amount of resin, as described above. Alternatively, supports **8a–g** (100 mg, 0.10–0.12 mmol) were left into contact with a solution of LTA (235 mg, 1.1 mmol) in DCM (1.5 mL) and shaken for 24 h at room temperature. The resulting supports, after usual washings, were treated with NaBH₄ (2.2 mmol) in EtOH (1.5 mL) as described above, thus obtaining supports **12a–g** in 60–65% reaction yield (8→12) calculated by HPLC on the released material. Then, supports **12a–g** were treated with 5 M NaOH in EtOH as described above for the reaction 8→9 thus giving supports **13a–g**. The TFA treatment of **13a–g** furnished **15a–g** (80–88% from **12a–g**), which were purified by HPLC as described above for **10a–g**. The overall yields of pure **15a–g** (from **4**) resulted to be in the range 58–67% (**Table 3.1**).

3.5.4 Synthesized scaffolds

5-[(Cyclohexylamino)methyleneamino]-1-(β-D-ribofuranosyl) imidazole-4[N-(2,4-dinitrophenyl)]carboxamide (6f)

Amorphous solid, mp over 250 °C (decomp.); ν_{\max} (neat) 3423, 3302, 2917, 1656, 1204, 1111 cm^{-1} ; ^1H NMR δH (CDCl_3) 12.36 (s, 1H, NH, exchange with D_2O), 9.18–9.13 (m, 2H, H-6 and H-3 DNP), 8.70 (br s, 1H, H-2), 8.48 (dd, 1H, $J = 9.8, 2.4$ Hz, H-5 DNP), 7.47 (s, 1H, CH=N), 5.78 (br s, 1H, H-1'), 4.62–4.59 (m, 1H, H-2'), 4.38–4.41 (m, 2H, H-30, H-4'), 3.94–3.87 (m, 2H, 2H-5'), 3.45 (br s, 1H, CHN), 2.20–1.20 (m, 10H, 5CH₂); UV (MeOH) λ_{\max} 275 nm, $\varepsilon = 13,300$; HRESIMS calcd for $\text{C}_{22}\text{H}_{27}\text{N}_7\text{NaO}_9$: 556.1768, found: 556.1779 ($\text{M}+\text{Na}$)⁺.

5-[(1R,2S,3R,4R)-2,3-Dihydroxy-4-((hydroxymethyl)-cyclopentyl)aminomethyleneamino]-1-(β -D-ribofuranosyl)imidazole- 4-[N-(2,4-dinitrophenyl)]carboxamide (6g)

Amorphous solid, mp over 250 °C (decomp.); ν_{\max} (neat) 3430, 3320, 2904, 1668, 1264, 1128 cm^{-1} ; ^1H NMR δH (CDCl_3) 9.20 (d, 1H, H-5 DNP), 9.03 (s, 1H, H-3 DNP), 8.64 (s, 1H, H-2), 8.42 (d, 1H, H-6 DNP), 7.73 (s, 1H, CHN), 6.03 (d, 1H, H-1'), 4.63–4.60 (m, 1H, H-2'), 4.40–4.36 (m, 2H, H-3', H-2'), 4.22–4.18 (m, 2H, H-4', H-3'), 3.76–3.72 (m, 2H, CH₂O), 3.62–3.59 (m, 2H, CH₂O), 3.23–3.20 (m, 1H, H-1''), 2.02–1.98 (m, 2H, H-4'', H-5''_a), 1.62–1.59 (m, 1H, H-5''_b), 1.18 (s, 3H, CH₃), 1.31 (s, 3H, CH₃); UV (CHCl_3) λ_{\max} 276 nm, $\varepsilon=12,900$; HRESIMS calcd for $\text{C}_{25}\text{H}_{31}\text{N}_7\text{NaO}_{12}$: 644.1928, found: 644.1945 ($\text{M}+\text{Na}$)⁺.

1-(3-Hydroxypropyl)inosine (11a)

Amorphous solid, mp 215–218 °C; ν_{\max} (neat) 3390, 2930, 1700, 1450, 1232 cm^{-1} ; ^1H NMR δH (CD_3OD) 8.41 (br s, 1H, H-2), 8.34 (s, 1H, H-8), 6.00 (d, 1H, $J = 5.0$ Hz, H-1'), 4.64–4.60 (m, 1H, H-2'), 4.34–4.29 (m, 1H, H-3'), 4.20 (t, 2H, $J=4.0$ Hz, CH₂N), 4.15–4.11 (m, 1H, H-4'), 3.86 (dd, 1H, $J=12.2, 2.6$ Hz, H-5'_a), 3.75 (dd, 1H, $J=12.2, 2.6$ Hz, H-5'_b), 3.60 (t, 2H, $J=6.3$ Hz, CH₂O), 2.03–1.94 (m, 2H, CH₂CH₂N); UV (MeOH) λ_{\max} 249 nm, $\varepsilon=9900$; HRESIMS calcd for $\text{C}_{13}\text{H}_{19}\text{N}_4\text{O}_6$: 327.1305, found: 327.1291 ($\text{M}+\text{H}$)⁺.

1-(5-Hydroxypentyl)inosine (11b)

Amorphous solid, mp over 250 °C (decomp.); ν_{\max} (neat) 3375, 2929, 1679, 1427, 1240 cm^{-1} ; ^1H NMR δH (CD_3OD) 8.40 (br s, 1H, H-2), 8.35 (s, 1H, H-8), 6.02 (d, 1H, $J=5.5$ Hz, H-1'), 4.64–4.60 (m, 1H, H-2'), 4.33–4.29 (m, 1H, H-3'), 4.14–4.08 (m, 3H, H-4', CH₂N), 3.87 (dd, 1H, $J=12.1, 2.6$ Hz, H-5'_a), 3.75 (dd, 1H, $J=12.1, 2.6$ Hz, H-5'_b), 3.60 (t, 2H, $J=6.2$ Hz, CH₂O), 1.85–1.77 (m, 2H, CH₂), 1.61–1.56 (m, 2H, CH₂), 1.48–1.38 (m, 2H, CH₂); UV (MeOH) λ_{\max} 249 nm, $\varepsilon=10,000$; HRESIMS calcd for $\text{C}_{15}\text{H}_{22}\text{N}_4\text{NaO}_6$: 377.1437, found: 377.1453 ($\text{M}+\text{Na}$)⁺.

1-Propylinosine (11c)

Amorphous solid, mp 185–187 °C; ν_{\max} (neat) 3324, 3302, 1702, 1240 cm^{-1} ; ^1H NMR δH (CD_3OD) 8.43 (br s, 1H, H-2), 8.35 (s, 1H, H-8), 6.01 (d, 1H, $J=5.5$ Hz, H-1'), 4.64–4.60 (m, 1H, H-2'), 4.34–4.31 (m, 1H, H-3'), 4.18–4.11 (m, 1H, H-4'), 4.07 (t, 2H, $J=7.3$ Hz, CH₂N), 3.87 (dd, 1H, $J=12.5, 2.6$ Hz, H-5'_a), 3.75 (dd, 1H, $J=12.5, 2.6$ Hz, H-5'_b), 1.83–1.78 (m, 2H, CH₂CH₃), 0.98 (t, 3H, $J=7.0$ Hz, CH₃); UV (MeOH) λ_{\max}

252 nm, $\epsilon=9700$; HRESIMS calcd for $C_{13}H_{18}N_4NaO_5$: 333.1175, found: 333.1207 (M_p+Na)⁺.

1-Butylinosine (11d)

Amorphous solid, mp 170–172 °C; ν_{\max} (neat) 3334, 3296, 1693, 1384, 1232 cm^{-1} ; 1H NMR δH (CD₃OD) 8.41 (br s, 1H, H-2), 8.36 (s, 1H, H-8), 6.02 (d, 1H, $J=5.5$ Hz, H-1'), 4.64–4.60 (m, 1H, H-2'), 4.34–4.30 (m, 1H, H-3'), 4.14–4.08 (m, 3H, H-4', CH₂N), 3.87 (dd, 1H, $J=12.1, 2.6$ Hz, H-5'_a), 3.75 (dd, 1H, $J=12.1, 2.6$ Hz, H-5'_b), 1.80–1.71 (m, 2H, CH₂), 1.45–1.35 (m, 2H, CH₂), 0.98 (t, 3H, $J=7.7$ Hz, CH₃); UV (MeOH) λ_{\max} 252 nm, $\epsilon=9800$; HRESIMS calcd for $C_{14}H_{21}N_4O_5$: 325.1512, found: 325.1490 (M+H)⁺.

1-Benzylinosine (11e)

Amorphous solid, mp 217–220 °C (lit.³³ 219–222 °C); ν_{\max} (neat) 3383, 3298, 1698, 1490, 1212 cm^{-1} ; 1H NMR δH (CD₃OD) 8.44, 8.33 (2s, 2H, H-2, H-8), 7.32–7.26 (m, 5H, Ph), 6.00 (d, 1H, $J=5.9$ Hz, H-1'), 5.29 (s, 2H, CH₂Ph), 4.69–4.63 (m, 1H, H-2'), 4.33–4.30 (m, 1H, H-3'), 4.13–4.09 (m, 1H, H-4'), 3.87 (dd, 1H, $J=12.5, 2.9$ Hz, H-5'_a), 3.75 (dd, 1H, $J=12.5, 2.9$ Hz, H-5'_b); UV (MeOH) λ_{\max} 249 nm, $\epsilon=10,100$; HRESIMS calcd for $C_{17}H_{18}N_4NaO_5$: 381.1175, found: 381.1173 (M+Na)⁺.

1-Cyclohexylinosine (11f)

Amorphous solid, mp 188–191 °C; ν_{\max} (neat) 3344, 3286, 1706, 1368, 1238 cm^{-1} ; 1H NMR δH (CD₃OD) 8.37, 8.32 (2s, 2H, H-2, H-8), 6.00 (d, 1H, $J=5.9$ Hz, H-1'), 4.64–4.60 (m, 1H, H-2'), 4.34–4.30 (m, 1H, H-3'), 4.22–4.19 (m, 1H, CHN), 4.11–4.10 (m, 1H, H-4'), 3.85 (dd, 1H, $J=12.0, 2.9$ Hz, H-5'_a), 3.72 (dd, 1H, $J=12.0, 2.9$ Hz, H-5'_b), 2.00–1.30 (m, 10H, 5CH₂); UV (MeOH) λ_{\max} 246 nm, $\epsilon=9800$; HRESIMS calcd for $C_{16}H_{23}N_4O_5$: 351.1668, found: 351.1699 (M+H)⁺.

1-[(1R,2S,3R,4R)-2,3-(Isopropylidenedioxy)-4(hydroxymethyl)cyclopentyl]inosine (11g)

Amorphous solid, mp over 250 °C (decomp.); ν_{\max} (neat) 3380, 3298, 1685, 1703, 1430, 1210; 1H NMR δH (CD₃OD) 8.40 (br s, 1H, H-2), 8.36 (s, 1H, H-8), 6.04 (d, 1H, $J=5.4$ Hz, H-10), 5.23–5.19 (m, 1H, H-200), 4.73–4.70 (m, 1H, H-300), 4.60–4.58 (m, 2H, H-1'', H-2'), 4.33–4.29 (m, 1H, H-3'), 4.10–4.09 (m, 1H, H-4'), 3.75–3.83 (m, 4H, H-5'_{a,b}, H-6''_{a,b}), 2.40–2.12 (m, 3H, H-4'', H-5''_{a,b}), 1.16 (s, 3H, CH₃), 1.30 (s, 3H, CH₃); UV (MeOH) λ_{\max} 253 nm, $\epsilon=9500$; HRESIMS calcd for $C_{19}H_{26}N_4NaO_8$: 461.1648, found: 461.1620 (M+Na)⁺.

5-Amino-1-(β -D-ribofuranosyl)imidazole-4-[N-(3-hydroxypropyl)]carboxamide (10a)

Amorphous solid, mp over 250 °C (decomp.); ν_{\max} (neat) 3402, 3322, 1678, 1220 cm^{-1} ; 1H NMR δH (CD₃OD) 7.31 (s, 1H, H-2), 5.54 (d, 1H, $J=6.6$ Hz, H-1'), 4.50–4.45 (m, 1H, H-2'), 4.24–4.20 (m, 1H, H-3'), 4.06–4.03 (m, 1H, H-4'), 3.79 (dd, 1H, $J=12.1, 2.6$ Hz, H-5'_a), 3.74 (dd, 1H, $J=12.1, 2.6$ Hz, H-5'_b), 3.63 (t, 2H, $J=6.2$ Hz, CH₂O),

3.31 (2H, CH₂N, partly covered by solvent signal), 1.81–1.74 (m, 2H, CH₂); UV (MeOH) λ_{max} 268 nm, ε =10,700; HRESIMS calcd for C₁₂H₂₀N₄NaO₆: 339.1280, found: 339.1302 (M+Na)⁺.

5-Amino-1-(β -D-ribofuranosyl)imidazole-4-[N-(5-hydroxypentyl)]carboxamide (10b)

Amorphous solid, mp over 250 °C (decomp.); ν_{max} (neat) 3409, 3338, 2934, 1623, 1255 cm⁻¹; ¹H NMR δ H (CD₃OD) 7.38 (s, 1H, H-2), 5.56 (d, 1H, J =6.2 Hz, H-1'), 4.50–4.46 (m, 1H, H-2'), 4.23–4.19 (m, 1H, H-3'), 4.08–4.05 (m, 1H, H-4'), 3.77–3.72 (m, 2H, H-5'_{a,b}), 3.55 (t, 2H, J =6.2 Hz, CH₂O), 3.31 (2H, CH₂N, partly covered by solvent signal), 1.62–1.55 (m, 4H, 2CH₂), 1.48–1.42 (m, 2H, CH₂); UV (MeOH) λ_{max} 268 nm, ε =10,900; HRESIMS calcd for C₁₄H₂₄N₄NaO₆: 367.1594, found: 367.1586 (M+Na)⁺.

5-Amino-1-(β -D-ribofuranosyl)imidazole-4-(N-propyl)carboxamide (10c)

Amorphous solid, mp 202–205 °C; ν_{max} (neat) 3330, 2980, 1702, 1210, 1166 cm⁻¹; ¹H NMR δ H (CD₃OD) 7.36 (s, 1H, H-2), 5.54 (d, 1H, J =6.6 Hz, H-1'), 4.50–4.45 (m, 1H, H-2'), 4.24–4.20 (m, 1H, H-3'), 4.09–4.06 (m, 1H, H-4'), 3.79 (dd, 1H, J =11.7, 2.6 Hz, H-5'_a), 3.74 (dd, 1H, J =11.7, 2.6 Hz, H-5'_b), 3.31 (2H, CH₂N, partly covered by solvent signal), 1.63–1.57 (m, 2H, CH₂CH₃), 0.98 (t, 3H, J =7.3 Hz, CH₃); UV (MeOH) λ_{max} 267 nm, ε =10,400; HRESIMS calcd for C₁₂H₂₀N₄NaO₅: 323.1331, found: 323.1324 (M+Na)⁺.

5-Amino-1-(β -D-ribofuranosyl)imidazole-4-(N-butyl)carboxamide (10d)

Amorphous solid, mp 222–225 °C; ν_{max} (neat) 3398, 3347, 1702, 1239, 1120 cm⁻¹; ¹H NMR δ H (CD₃OD) 7.32 (s, 1H, H-2), 5.52 (d, 1H, J =5.5 Hz, H-1'), 4.50–4.46 (m, 1H, H-2'), 4.20–4.16 (m, 1H, H-3'), 4.13–4.10 (m, 1H, H-4'), 3.79 (dd, 1H, J =12.5, 2.9 Hz, H-5'_a), 3.74 (dd, 1H, J =12.5, 2.9 Hz, H-5'_b), 3.31 (2H, CH₂N, partly covered by solvent signal), 1.60–1.51 (m, 2H, CH₂), 1.45–1.36 (m, 2H, CH₂), 0.96 (t, 3H, J =7.3 Hz, CH₃); UV (MeOH) λ_{max} 267 nm, ε =10,300; HRESIMS calcd for C₁₃H₂₂N₄NaO₅: 337.1488, found: 337.1480 (M+Na)⁺.

5-Amino-1-(β -D-ribofuranosyl)imidazole-4-(N-benzyl)carboxamide (10e)

Amorphous solid, mp 170–173 °C (lit.³³ 171–172 °C); ν_{max} (neat) 3334, 3256, 1456, 1696, 1198 cm⁻¹; ¹H NMR δ H (CD₃OD) 7.38–7.30 (m, 6H, Ph, H-2), 5.55 (d, 1H, J =6.6 Hz, H-1'), 4.54–4.48 (s, 3H, CH₂Ph, H-2'), 4.19–4.16 (m, 1H, H-3'), 4.08–4.05 (m, 1H, H-4'), 3.79 (dd, 1H, J =12.1, 2.9 Hz, H-5'_a), 3.74 (dd, 1H, J =12.1, 2.9 Hz, H-5'_b); UV (MeOH) λ_{max} 270 nm, ε =11,400; HRESIMS calcd for C₁₆H₂₀N₄NaO₅: 371.1331, found: 371.1325 (M+Na)⁺.

5-Amino-1-(β -D-ribofuranosyl)imidazole-4-(N-cyclohexyl)carboxamide (10f)

Amorphous solid, mp 210–212 °C; ν_{max} (neat) 3320, 3295, 1689, 1197, 1172 cm⁻¹; ¹H NMR δ H (CD₃OD) 7.35 (s, 1H, H-2), 5.54 (d, 1H, J =7.0 Hz, H-1'), 4.50–4.45 (m, 1H,

H-2'), 4.24–4.19 (m, 1H, H-3'), 4.07–4.04 (m, 1H, H-4'), 3.82–3.72 (m, 3H, H-5'_{a,b}, CHN), 2.00–1.30 (m, 10H, 5CH₂); UV (MeOH) λ_{max} 267 nm, $\epsilon=10,800$; HRESIMS calcd for C₁₅H₂₄N₄NaO₅: 363.1644, found: 363.1635 (M+Na)⁺.

5-Amino-1-(*b*-D-ribofuranosyl)imidazole-4-[N-((1*R*,2*S*,3*R*,4*R*)-2,3-isopropylidenedioxy)-4-(hydroxymethyl)cyclopentyl]carboxamide (10g)

Amorphous solid, mp over 250 °C (decomp.); ν_{max} (neat) 3349, 3325, 1706, 1217, 1122 cm⁻¹; ¹H NMR δ H (CD₃OD) 7.37 (br s, 1H, H-2), 5.57 (d, 1H, *J*=5.5 Hz, H-1'), 5.19–5.15 (m, 1H, H-2''), 4.55–4.40 (m, 3H, H-2', H-1'', H-3''), 4.26–4.22 (m, 1H, H-3'), 4.13–4.09 (m, 1H, H-4'), 3.80–3.68 (m, 4H, H-5'_{a,b}, H-6''_{a,b}), 2.30–2.10 (m, 3H, H-4'', H-5''_{a,b}), 1.18 (s, 3H, CH₃), 1.31 (s, 3H, CH₃); UV (MeOH) λ_{max} 268 nm, $\epsilon=10,500$; HRESIMS calcd for C₁₈H₂₈N₄NaO₈: 451.1805, found: 451.1812 (M+Na)⁺.

5-Amino-1-[1-(1,3-dihydroxypropan-2-yloxy)-2-hydroxyethyl]imidazole-4-[N-(3-hydroxypropyl)]carboxamide (15a)

Amorphous solid, mp over 250 °C (decomp.); ν_{max} (neat) 3378, 3327, 1698, 1220 cm⁻¹; ¹H NMR δ H (CD₃OD) 7.34 (s, 1H, H-2), 5.60 (t, 1H, *J*=5.7 Hz, H-1'), 3.87–3.83 (m, 2H, CH₂O), 3.75–3.64 (m, 2H, CH₂O), 3.61–3.49 (m, 5H, CH, 2CH₂O), 3.31 (2H, CH₂N, partly covered by solvent signal), 1.80–1.75 (m, 2H, CH₂); UV (MeOH) λ_{max} 268 nm, $\epsilon=10,200$; HRESIMS calcd for C₁₂H₂₂N₄NaO₆: 341.1437, found: 341.1445 (M+Na)⁺.

5-Amino-1-[1-(1,3-dihydroxypropan-2-yloxy)-2-hydroxyethyl]imidazole-4-[N-(5-hydroxypentyl)]carboxamide (15b)

Amorphous solid, mp over 250 °C (decomp.); ν_{max} (neat) 3370, 3323, 1702, 1210 cm⁻¹; ¹H NMR δ H (CD₃OD) 7.35 (s, 1H, H-2), 5.62 (t, 1H, *J*=5.9 Hz, H-1'), 3.95–3.85 (m, 2H, CH₂O), 3.78–3.64 (m, 2H, CH₂O), 3.60–3.50 (m, 5H, CH, 2CH₂O), 3.32 (2H, CH₂N, partly covered by solvent signal), 1.64–1.54 (m, 4H, 2CH₂), 1.48–1.38 (m, 2H, CH₂); UV (MeOH) λ_{max} 268 nm, $\epsilon=10,100$; HRESIMS calcd for C₁₄H₂₆N₄NaO₆: 369.1750, found: 369.1756 (M+Na)⁺.

5-Amino-1-[1-(1,3-dihydroxypropan-2-yloxy)-2-hydroxyethyl]imidazole-4-(*N*-propyl)carboxamide (15c)

Amorphous solid, mp 225–229 °C; ν_{max} (neat) 3384, 3332, 1705, 1264, 1176 cm⁻¹; ¹H NMR δ H (CD₃OD) 7.36 (s, 1H, H-2), 5.62 (t, 1H, *J*=3.3 Hz, H-1'), 3.90–3.83 (m, 2H, CH₂O), 3.78–3.62 (m, 2H, CH₂O), 3.61–3.49 (m, 3H, CH, CH₂O), 3.30 (2H, CH₂N, partly covered by solvent signal), 1.65–1.56 (m, 2H, CH₂), 0.96 (t, 3H, *J*=7.2 Hz, CH₃); UV (MeOH) λ_{max} 267 nm, $\epsilon=10,300$; HRESIMS calcd for C₁₂H₂₂N₄NaO₅: 325.1488, found: 325.1480 (M+Na)⁺.

5-Amino-1-[1-(1,3-dihydroxypropan-2-yloxy)-2-hydroxyethyl]imidazole-4-(*N*-butyl)carboxamide (15d)

Amorphous solid, mp 218–222 °C; ν_{max} (neat) 3398, 3340, 1702, 1241, 1160 cm⁻¹; ¹H NMR δ H (CD₃OD) 7.34 (s, 1H, H-2), 5.60 (t, 1H, *J*=3.3 Hz, H-1'), 3.91–3.84 (m, 2H,

CH₂O), 3.79–3.65 (m, 2H, CH₂O), 3.61–3.49 (m, 3H, CH, CH₂O), 3.31 (2H, CH₂N, partly covered by solvent signal), 1.60–1.51 (m, 2H, CH₂), 1.46–1.32 (m, 2H, CH₂), 0.96 (t, 3H, *J*=7.2 Hz, CH₃); UV (MeOH) λ_{max} 267 nm, ϵ = 10,300; HRESIMS calcd for C₁₃H₂₄N₄NaO₅: 339.1644, found: 339.1640 (M+Na)⁺.

5-Amino-1-[1-(1,3-dihydroxypropan-2-yloxy)-2-hydroxyethyl]imidazole-4-(N-benzyl)carboxamide (15e)

Amorphous solid, mp over 250 °C (decomp.); ν_{max} (neat) 3367, 3331, 1705, 1264, 1176 cm⁻¹; ¹H NMR δ H (CD₃OD) 7.36–7.28 (m, 6H, Ph, H-2), 5.60 (t, 1H, *J*=5.6 Hz, H-1'), 4.51 (s, 2H, CH₂Ph), 3.96–3.84 (m, 2H, CH₂O), 3.78–3.64 (m, 2H, CH₂O), 3.61–3.49 (m, 3H, CH, CH₂O); UV (MeOH) λ_{max} 270 nm, ϵ = 11,200; HRESIMS calcd for C₁₆H₂₂N₄NaO₅: 373.1488, found: 373.1476 (M+Na)⁺.

5-Amino-1-[1-(1,3-dihydroxypropan-2-yloxy)-2-hydroxyethyl]imidazole-4-(N-cyclohexyl)carboxamide (15f)

Amorphous solid, mp 210–213 °C; ν_{max} (neat) 3367, 3302, 1708, 1164 cm⁻¹; ¹H NMR δ H (CD₃OD) 7.33 (s, 1H, H-2), 5.59 (t, 1H, *J*=5.5 Hz, H-1'), 3.94–3.84 (m, 2H, CH₂O), 3.80–3.65 (m, 3H, CH₂O, CHN), 3.61–3.49 (m, 3H, CH, CH₂O), 2.00–1.30 (m, 10H, 5CH₂); UV (MeOH) λ_{max} 267 nm, ϵ = 10,800; HRESIMS calcd for C₁₅H₂₆N₄NaO₅: 365.1801, found: 365.1810 (M+Na)⁺.

5-Amino-1-[1-(1,3-dihydroxypropan-2-yloxy)-2-hydroxyethyl]imidazole-4-[N-((1*R*,2*S*,3*R*,4*R*)-2,3-isopropylidenedioxy)-4(hydroxymethyl)cyclopentyl]carboxamide (15g)

Amorphous solid, mp over 250 °C (decomp.); ν_{max} (neat) 3404, 3387, 1693, 1287, 1193 cm⁻¹; ¹H NMR δ H (CD₃OD) 7.25 (s, 1H, H-2), 5.60 (t, 1H, *J*=4.7 Hz, H-1'), 5.20–5.17 (m, 1H, H-2''), 4.56–5.50 (m, 2H, H-1'', H-3''), 3.93–3.86 (m, 2H, CH₂O), 3.80–3.67 (m, 2H, CH₂O), 3.61–3.49 (m, 5H, CH, 2CH₂O), 2.36–2.10 (m, 3H, H-4'', H-5''_{a,b}), 1.32 (s, 3H, CH₃), 1.20 (s, 3H, CH₃); UV (MeOH) λ_{max} 268 nm, ϵ = 10,200; HRESIMS calcd for C₁₈H₃₀N₄NaO₈: 453.1961, found: 453.1969 (M+Na)⁺.

References

- ¹ Antiviral Nucleosides: *Chiral Synthesis and Chemotherapy*; Chu, C. K., Ed.; Elsevier: Amsterdam, The Netherlands, **2003**; (b) Simons, C.; Wu, Q.; Htar, T. T. *Curr. Top. Med. Chem.* **2005**, *5*, 1191–1203; (c) De Clercq, E.; Neyts, J. *Rev. Med. Virol.* **2004**, *14*, 289–300.
- ² (a) Lagoja, I. M. *Chem. Biodivers.* **2005**, *2*, 1–50; (b) Kimura, K.; Bugg, T. D. H. *Nat. Prod. Rep.* **2003**, *20*, 252–273; (c) Rachakonda, S.; Cartee, L. *Curr. Med. Chem.* **2004**, *11*, 775–793; (d) Knapp, S. *Chem. Rev.* **1995**, *95*, 1859–1876.
- ³ Miura, S.; Izuta, S. *Curr. Drug Targets* **2004**, *5*, 191–195; (b) Parker, W. B.; Secrist, J. A.; Waud, W. R. *Curr. Opin. Investig. Drugs* **2004**, *5*, 592–596; (c) Szafraniec, S. I.; Stachnick, K. J.; Skierski, J. S. *Acta Pol. Pharm.* **2004**, *61*, 223–232.
- ⁴ Gandhi, V.; Keating, M. J.; Bate, G.; Kirkpatrick, P. *Nat. Rev. Drug Discov.* **2006**, *5*, 17–18.
- ⁵ Matthews, S. J. *Clin. Ther.* **2006**, *28*, 184–203.
- ⁶ Pui, C. H.; Jeha, S.; Kirkpatrick, P. C. *Nat. Rev. Drug Discov.* **2005**, *4*, 369–370.
- ⁷ Kaminskas, E.; Farrell, A.; Abraham, S.; Baird, A.; Hsieh, L. S.; Lee, S. L.; Leighton, J. K.; Patel, H.; Rahman, A.; Shidhara, R.; Wang, Y. C.; Pazdur, R. *Clin. Cancer Res.* **2005**, *11*, 3604–3608.
- ⁸ Rutter, G. A.; Silva Xavier, G.; Leclerc, I. *Biochem. J.* **2003**, *375*, 1–16.
- ⁹ Gaidhu, M. P.; Fediuc, S.; Ceddia, R. B. *J. Biol. Chem.* **2006**, *281*, 25956–25964.
- ¹⁰ Frank, R. N. *Am. J. Ophthalmol.* **2002**, *133*, 693–698.
- ¹¹ Knowler, W. C.; Barrett-Connor, E.; Fowler, S. E.; Hamman, R. F.; Lachin, J. M.; Walker, E. A., and Nathan, D. M. *N. Engl. J. Med.* **2002**, *346*, 393–403.
- ¹² Alessi, D. R., and Cohne, P. *Curr. Opin. Genet. Dev.* **1998**, *8*, 55–62.
- ¹³ Buhl, E. S.; Jessen, N.; Schmitz, O.; Pedersen, S. B.; Pedersen, O.; Holman, G. D., and Lund, S. *Diabetes*, **2001**, *50*, 12–17.
- ¹⁴ Lara, D. R.; Dall'Igna, O. P.; Ghisolfi, E. S.; Brunstein, M. G. *Prog. Neuropsychopharmacol. Biol. Psychiatry* **2006**, *30*, 617–629.
- ¹⁵ Yamazaki, A.; Kumashiro, I.; Takenishi, T., and Ikenara, M., *Chem. Pharm. Bull.* **1968**, *16*, 2172–2181.
- ¹⁶ Wall, M.; Hoon Smith, J., and Benkovic, S. J. *Biochemistry* **2000**, *39*, 11303–11311.
- ¹⁷ Kohyama, N.; Katashima, T.; Yamamoto, Y. *Synthesis* **2004**, *17*, 2799–2804.
- ¹⁸ Ulrich, S. M.; Sallee, N. A.; Shokat, K. M. *Bioorg. Med. Chem. Lett.* **2002**, *12*, 3223–3227.
- ¹⁹ Wall, M.; Shim, J. H.; Benkovic, S. J. *Biochemistry* **2000**, *39*, 11303–11311.
- ²⁰ (a) Minakawa, N.; Kojima, N.; Sasaki, T.; Matsuda, A. *Nucleosides Nucleotides* **1996**, *15*, 251–263; (b) Minakawa, N.; Takeda, T.; Sasaki, T.; Matsuda, A.; Ueda, T. *J. Med. Chem.* **1991**, *34*, 778–786.
- ²¹ Mizuno, A.; Tsujino, M.; Takada, M.; Hayashi, M.; Atsumi, K. *J. Antibiot. (Tokyo)* **1974**, *27*, 775–782.
- ²² Sidwell, R. W.; Huffman, J. H.; Khare, G. P.; Allen, L. B.; Witkowski, J. T.; Robins, R. K. *Science* **1972**, *177*, 705–706.
- ²³ Kalman, T. I.; Houston, D. M. *Nucleosides Nucleotides* **1989**, *8*, 899–902.
- ²⁴ Shaw, E. J. *Am. Chem. Soc.* **1959**, *81*, 6021–6022.
- ²⁵ Kohyama, N.; Yamamoto, Y. *Synthesis* **2003**, 2639–2642.
- ²⁶ Casanova, E.; Hernández, A. I.; Priego E. M.; Liekens, S.; Camarasa, M. J.; balzarini, J., and Pérez-Pérez, M. J. *J. Med. Chem.* **2006**, *49*, 5562–5570.
- ²⁷ Hyde, R. M.; Broom, A. D.; Buckheit, R. W. *J. Med. Chem.* **2003**, *46*, 1878–1885.
- ²⁸ Oliviero, G.; Amato, J.; Borbone, N.; D'Errico, S.; Piccialli, G.; Mayol, L. *Tetrahedron Lett.* **2007**, *48*, 397–400.
- ²⁹ De Napoli, L.; Messere, A.; Montesarchio, D.; Piccialli, G.; Varra, M. *J. Chem. Soc., Perkin Trans. 1* **1997**, 2079–2082.
- ³⁰ (a) De Napoli, L.; Messere, A.; Montesarchio, D.; Piccialli, G. *J. Org. Chem.* **1995**, *60*, 2251–2253; (b) Fukuoka, M.; Shuto, S.; Minakawa, N.; Ueno, Y.; Matsuda, A. *J. Org. Chem.* **2000**, *65*, 5238–5248.
- ³¹ For general accounts on lead tetraacetate reactions, see: (a) Criegee, R. *Oxidation in Organic Chemistry*; Wiberg, K. B., Ed.; Academic: New York, NY, **1965**; Part A; (b) Sheldon, R. A.; Kochi, J. K. *Org. React.* **1972**, *19*, 279–421; (c) Mihailovic, M. L.; Cekovic, Z.; Lorenc, L. *Organic Synthesis by Oxidation with Metal Compounds*; Mijs, W. J., De Jonge, C. R. H. I., Eds.; Plenum: New York, NY, **1986**; pp 741–816.
- ³² Hussain, R. F.; Nouri, A. M.; Oliver, R. T. *J. Immunol. Methods* **1993**, *15*, 86–89.
- ³³ Shaw, E. J. *Am. Chem. Soc.* **1958**, *80*, 3899–3902.

Chapter 4

Solid phase synthesis of cADPR analogs

Introduction

Cyclic ADP-ribose (cADPR) was discovered in 1987 as a Ca^{2+} mobilizing metabolite of the well known coenzyme β -nicotinamide adenine dinucleotide (NAD) by Lee and co-workers¹. The cyclic structure of cADPR was initially predicted to originate from a N-glycosyl linkage between the anomeric carbon of the ribose, which in the precursor NAD is linked to nicotinamide, and the amino/imino group at C6 of the adenine moiety². Spectroscopic data³ and finally a crystal structure revealed cyclization between the anomeric C1' of this ribose moiety (commonly termed "northern ribose" while the ribose linked to N-9 of adenine is called the "southern" ribose; **Figure 4.1**) and the N1 of the adenine ring⁴. For clarity atoms of "northern ribose" will be marked as double prime ("') while atoms in the southern ribose will be marked as a single prime ('). Later, Jacobson and co-workers investigated the UV spectral properties of cADPR as a function of pH, compared them with those of N1- and N6-alkylated adenines and concluded that the structure should be the N1-cyclized ADP-ribose (**Figure 4.1**). Sekine and co-workers did a detailed investigation of the structure of cADPR in aqueous solution using NMR⁵. They concluded that the glycosyl torsion angle of the adenosine moiety is in the *syn* conformation and that the ribose of adenosine ("southern ribose") and the "northern ribose" have the C2-endo and the flat conformation, respectively.

Besides D-*myo*-inositol 1,4,5-triphosphate (InsP_3) and nicotinic acid adenine dinucleotide phosphate (NAADP), cADPR is one of the principal Ca^{2+} -releasing second messengers involved in cellular Ca^{2+} homeostasis. Changes in the cellular Ca^{2+} homeostasis are among the fundamental signalling processes in multicellular organisms. Such changes occur in response to extracellular signals, e.g. hormones, mediators, cell-cell contacts or physical stimuli, and represent one of the most important, powerful and versatile intracellular signal transducers. Changes in cellular Ca^{2+} homeostasis finally in meaningful physiological response of the cell. Thus, intracellular Ca^{2+} signalling is one of the most important transduction systems to integrate physiological responses of multicellular organisms.

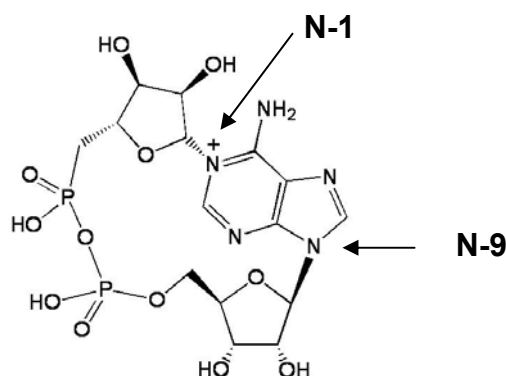


Figure 4.1. cADPR

The cADPR/ Ca^{2+} signalling system is active in diverse cellular systems, including smooth, skeletal and cardiac muscle, neuronal and neuronal-related cells,

hemopoietic cells, acinar cells, and oocytes⁶. Because the cADPR/Ca²⁺ signalling system was also observed in protozoa and plant cells, it appears to be a phylogenetically old and conserved system. As for the InsP₃/Ca²⁺ signalling system, in several cell types extracellular stimuli activate cADPR-forming enzymes called ADPRC (ADP-ribosyl cyclases) and thereby induce the formation of cADPR (**Figure 4.2**). G-protein coupling and Tyr phosphorylation have been implicated in ADPRC activation^{7,8}.

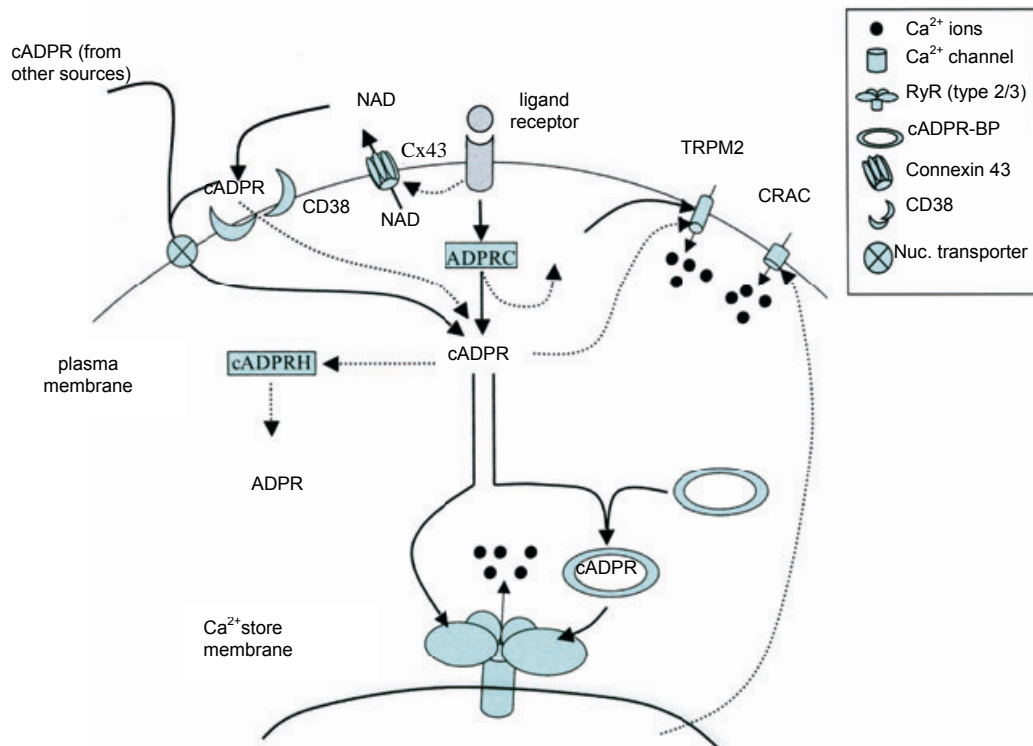
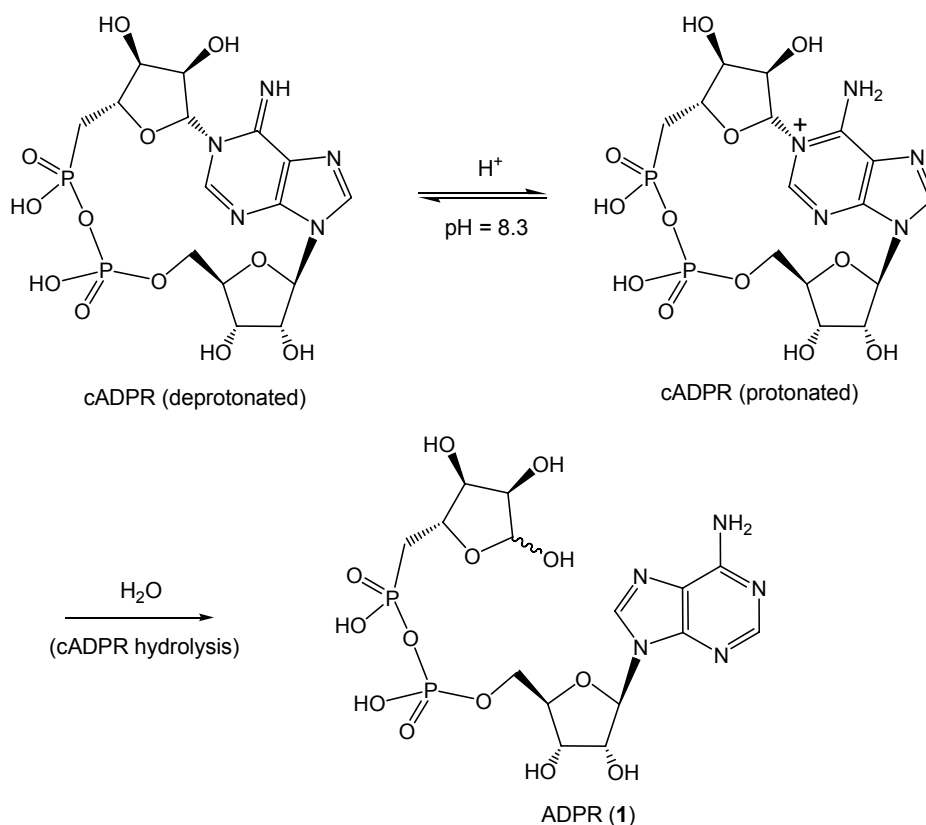


Figure 4.2. Receptor-mediated formation, metabolism and site of action of cADPR. Dotted lines indicate minor pathway or relations not generally accepted or proven. Cx43, connexin 43, CRAC, Ca²⁺ release-activated Ca²⁺ channel, cADPRH, cADPR-hydrolase.

The enzymes responsible for the synthesis of cADPR are still a matter of debate. An ADPRC that acts mainly as a cyclizing enzyme has been purified and cloned more than 10 years ago from the ovotestis of *Aplysia californica*^{9,10}. Mammalian homologues of this enzyme are the membrane proteins CD38 and CD157. After their discovery it was surprising to note that their catalytic sites are located outside of the cell (or in intracellular vesicles), but obviously not in direct contact to the substrate NAD and the intracellular Ca²⁺ release channel sensitive to cADPR, the ryanodine receptor (RyR). This situation has been described as the 'topological paradox' of the cADPR/Ca²⁺ signalling system¹¹. De Flora and coworkers have worked out a potential solution for this problem. They found that NAD can leave the cell via connexin 43 hemichannels. Outside the cell (or inside CD38 containing vesicles) NAD is then converted, at least in part, to cADPR. Evidence was presented that both CD38 and nucleoside transporters act as cADPR-transporting proteins (**Figure 4.2**). This system in principle represents a solution for the topological paradox.

cADPR has the characteristic 18-membered cyclic structure including a pyrophosphate linkage. Although pyrophosphate linkages, e.g. the linkage in NAD⁺, can often be readily cleaved enzymatically, cADPR is resistant to pyrophosphatases from various sources¹², probably due to its unusual cyclic structure. However,

treatment of cADPR with *t*-BuOK in DMSO selectively cleaved the pyrophosphate linkage. Under neutral conditions, cADPR is in a zwitterionic form with a positive charge around the N1-C6-N6 moiety ($pK_a = 8.3$), making the molecule extremely unstable. The charged adenine moiety attached to the anomeric carbon of the "northern" ribose can be a very efficient leaving group. Accordingly, cADPR is readily hydrolyzed at the unstable N1-ribose linkage of its adenine moiety to produce ADPribose (ADPR, **1**), even in neutral aqueous solution (**Scheme 4.1**)¹³. Under physiological conditions, cADPR is also hydrolyzed at the N1-ribose linkage by cADPR hydrolase to give the inactive ADPR (**1**)¹³.



Scheme 4.1. The protonated and deprotonated forms of cADPR and its hydrolysis in aqueous media.

cADPR analogs can be used effectively in proving the mechanism of cADPR-mediated Ca^{2+} signaling pathways. Agonists or antagonists of cADPR are also expected to be lead structures for the development of drugs, since cADPR has been shown to play important physiological roles, such as insulin release from β -cells¹⁴. Therefore, the synthesis of cADPR analogs has been extensively investigated¹⁵. However, because of the unique structure and instability of cADPR, chemical synthesis of cADPR and its analogs has proved to be rather difficult. Consequently cADPR analogs have been synthesized predominantly by enzymatic and chemo-enzymatic methods using ADP-ribosyl cyclase-catalyzed cyclization under mild neutral conditions¹⁶. In recent years, on the other hand, methods for the chemical synthesis of cADPR analogs have been extensively studied, and useful cADPR analogs, which could not be prepared by the enzymatic and chemo-enzymatic methods, have been synthesized¹⁶.

4.1. Enzymatic and chemo-enzymatic synthesis

Before discussing the chemical synthesis, I will briefly describe the enzymatic and chemo-enzymatic methods using ADP-ribosyl cyclase, by which a variety of cADPR analogs have been prepared since the discovery of cADPR. ADP-ribosyl cyclase, which is responsible for the biosynthesis of cADPR from β -NAD⁺, is present in all tissues, from mammalian species to marine invertebrates¹³. The well-known mammalian ADP-ribosyl cyclase, the lymphocyte antigen CD38, has both cADPR synthesizing and hydrolyzing activities¹⁷. The ADP-ribosyl cyclase from *Aplysia Californica* catalyzes a stoichiometric conversion of β -NAD⁺ to cADPR. The cyclase is commercially available and has been widely used for the synthesis of cADPR analogs. The enzyme mediates the intramolecular ribosylation of β -NAD⁺ and some modified β -NAD⁺ analogs, prepared chemically or enzymatically, at the N1-position of the purine moiety to yield cADPR or the corresponding analogues¹⁸. For example, using this method, cADPR analogs modified at the 8-position of the adenine ring and at the 2'- or 3'-position of the "southern" ribose¹⁹ (**Figure 4.3**), have been prepared from the corresponding β -nicotinamide dinucleotide-type precursors. The method also provided the aristeromycin congener, cArisDPR (**2**)²⁰ and 3-deaza-cADPR (**3**)²¹. Furthermore, a "northern" ribose modified analog, 2"-NH₂-cADPR (**4**) was synthesized by this method. Biological evaluation of these analogs has identified some analogs as useful biological tools; e.g. the effective antagonist 8-NH₂-cADPR (**5**)²², 3-deaza-cADPR (**3**)²¹ and the membrane permeable antagonist 8-Br-7-deazacADPR (**6**)²³. One drawback of the enzymatic and chemo-enzymatic procedures is that these methods require preparation of the nicotinamide dinucleotide-type precursors as the substrates, the synthesis of which is often troublesome. More importantly, the analogs that can be obtained by these methods are limited due to the substrate-specificity of the ADP-ribosyl cyclase. Furthermore, even though the enzyme catalyzes the cyclization of the NAD⁺ analogs, in some cases the newly formed N-ribosyl bond is not attached to the N1 nitrogen of the purine ring: e.g. the products of the enzymatic reaction of the inosine and guanosine analogs of β -NAD⁺ are not the desired N1-cyclized products **7** and **8**, but rather the N7-cyclized products **9** and **10**, respectively (**Figure. 4.3**)²⁴. It is likely that the enzymatic cyclization of NAD⁺ and its analogs occurs at the most nucleophilic position of the purine bases, i.e. the N1 of adenine and 8-substituted adenine bases or the N7 of the guanine and hypoxanthine bases.

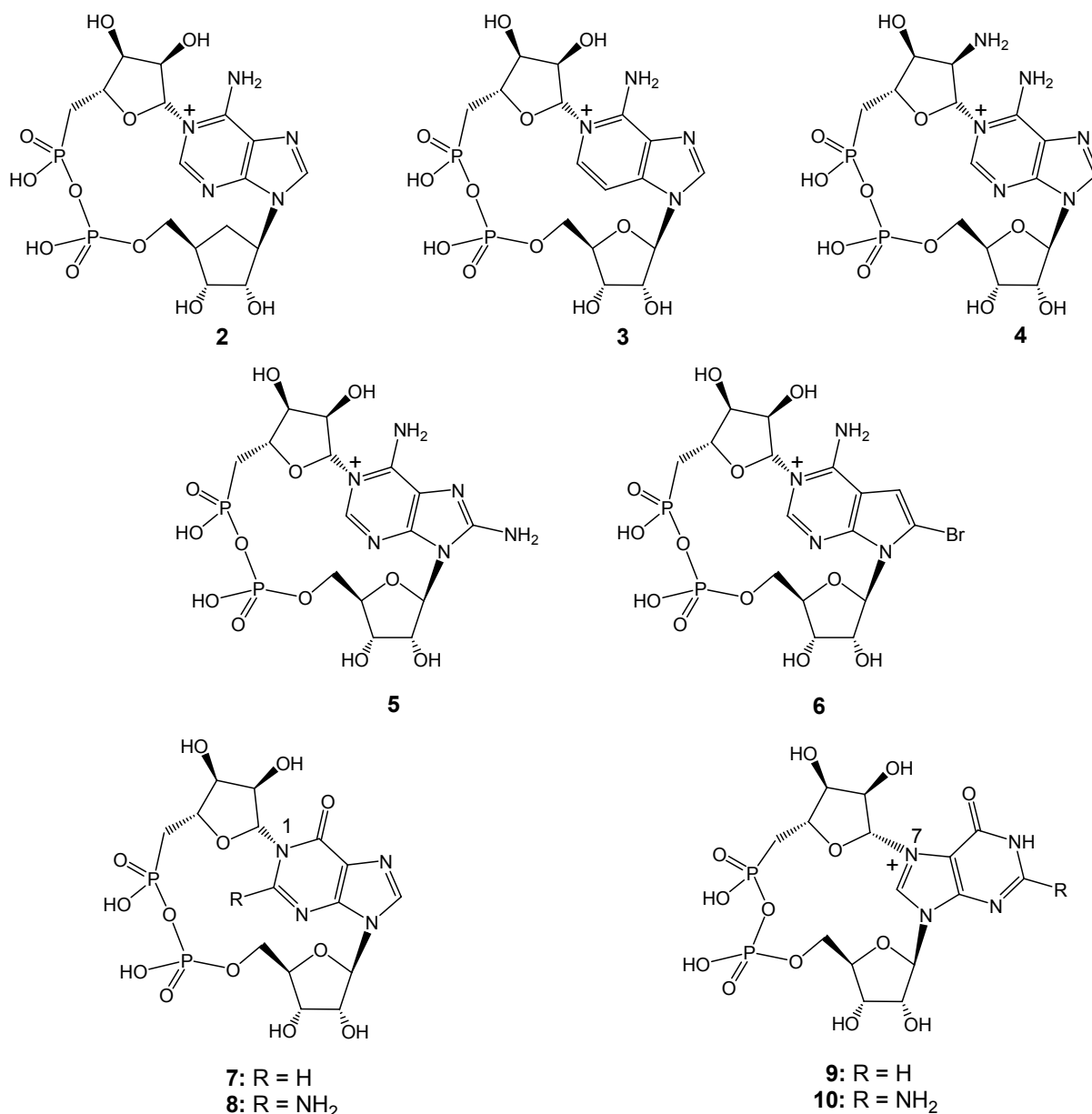


Figure 4.3. cADPR analogs synthesized by the enzymatic and chemo-enzymatic methods.

4.2. Chemical synthesis

The total synthesis of cADPR itself may not be of importance, since cADPR is easily prepared by the enzymatic synthesis from β -NAD⁺. On the other hand, because of the limitations of the enzymatic and chemoenzymatic methods described above, development of effective chemical synthetic methods for the preparation of a greater variety of cADPR analogs is required. Considerable efforts have been devoted to the chemical synthesis of cyclic ADP-carbocyclic-ribose (cADPcR, **11**) and its related compounds, for example the inosine congener cIDP carbocyclic-ribose (cIDPcR, **12**), in which the ring oxygen in the "northern" ribose is replaced by a methylene unit (**Figure. 4.4**). Since they lack the unstable N1-ribosyl linkage of cADPR, these carbocyclic analogs should be resistant to both enzymatic and chemical hydrolysis,

while still preserving most of the functional groups of cADPR, except for the ring oxygen.

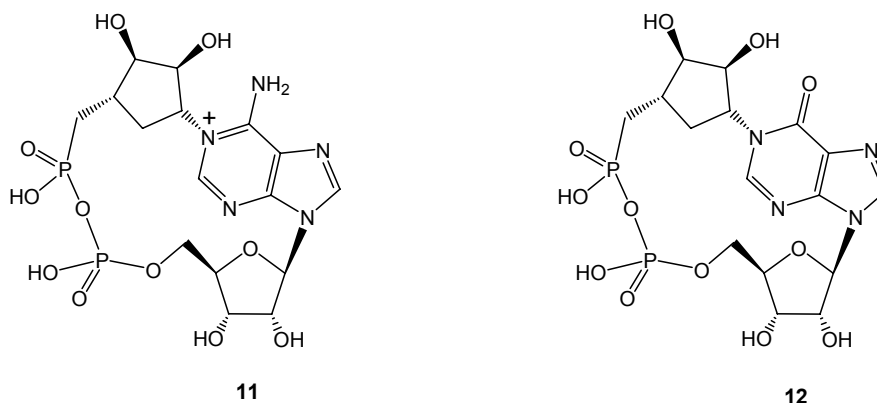


Figure 4.4. Cyclic ADP-carbocyclic-ribose (cADPcR, **11**) and its inosine congener cIDPcR (**12**).

Therefore, they should have a conformation similar to that of cADPR. Accordingly, these analogs are expected to be very stable mimics of cADPR. These carbocyclic analogs lacking the N1-glycosyl linkage could not be synthesized by the enzymatic or the biomimetic method, because both these intramolecular ribosylations with NAD⁺-type substrates probably proceed via an oxocarbenium intermediate **13** (Figure 4.5), or its enzymatically stabilized equivalent.

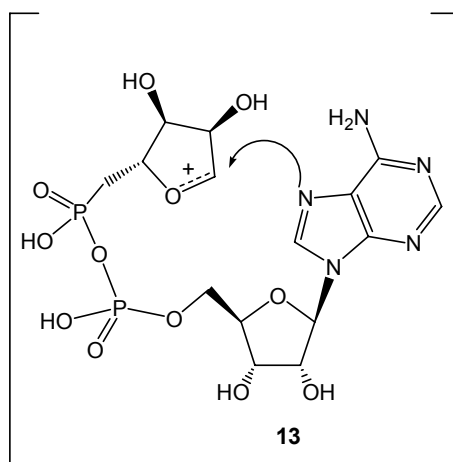
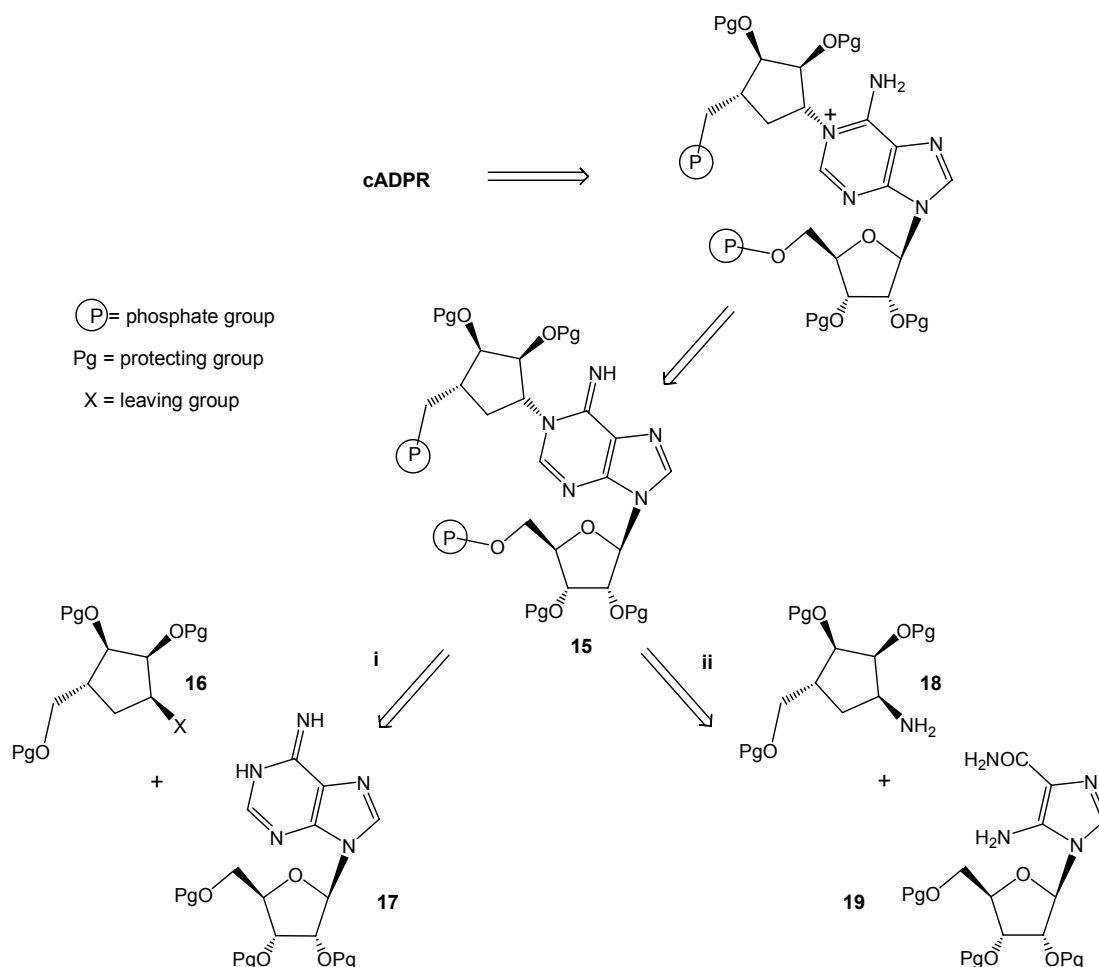


Figure 4.5. Oxocarbenium intermediate (**13**) forming probably during enzymatic synthesis of cADPR.

4.3. Synthetic strategy

cADPR (Figure 4.1) has the 18-membered ring consisting of an adenine, two riboses, and a pyrophosphate, that connects the two primary hydroxyl groups of the "southern" and "northern" riboses. In the synthesis of cADPR and its analogs, construction of the large 18-membered ring structure should be the key step. The highly-polar phosphate moiety seems to be detrimental to purification and reactions, and therefore it should be introduced later in the synthetic process, after which the construction of the large 18-membered ring could be accomplished by the intramolecular condensation of the two phosphate groups. A typical synthetic strategy, showing the retro-synthesis of cADPcR (**11**), is illustrated in **Scheme 4.2**.

All of the studies on the chemical synthesis of cADPR and its analogs reported so far have employed strategies similar to the one shown in **Scheme 4.2**. Although the key step of the synthesis is the intramolecular condensation forming the pyrophosphate linkage, an efficient construction of the N1-ribosyl (or carbocyclic-ribosyl) purine nucleoside structure, such as **15**, is also essential. Two strategies for constructing the N1- substituted structures can be considered: i.e. i) the N1- selective nucleophilic substitution between a purine nucleoside (**17**) derivative and an electrophile having a leaving group at the 1-position of the ribose (or carbocyclic-ribose) derivative (**16**), or ii) condensation with an imidazole nucleoside (**19**) and 1-amino ribose (or carbocyclic-ribose) derivative (**18**) (**Scheme 4.2**).

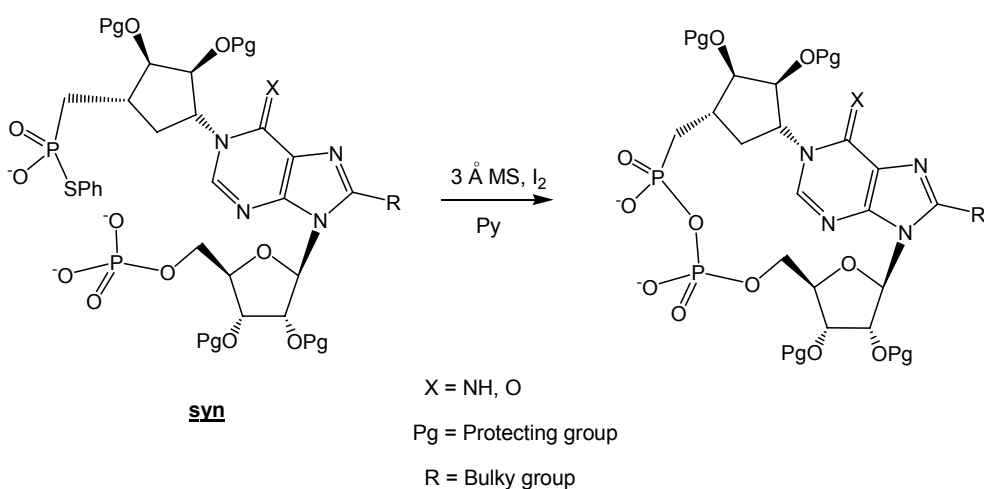


Scheme 4.2. The retrosynthetic analysis of cADPCr (**11**).

The N1-selective glycosylation of inosine derivatives has been studied by several groups²⁵, probably because cyclic inosine-diphosphate (cIDPR, **7**), the inosine congener of cADPR, could not be prepared by the above enzymatic cyclization even if, in 2003, Potter et al. synthesized enzymatically 8-Br-N1-cIDPR considering that the presence of bulky Br group at 8 position of nucleobase were sufficient to bring hypoxanthine N1 in spatial proximity to the anomeric carbon of the northern ribose²⁶. The chemical synthesis of cIDPR and its analogs was also thought to be easier than that of the corresponding adenine congeners. The non-charged N1-substituted hypoxanthine structure can be more stable than the positively charged N1-

substituted adenine moiety of the adenine congeners, during the reaction and purification steps.

Matsuda's group developed a total synthetic approach to construct cADPR analogues. They found an efficient intramolecular cyclization for the construction of cyclopyrophosphate, the key reaction of all synthetic route. Their strategy was to introduce a bulky group into the 8-position of purine nucleoside; this maneuver can restrict the conformation of diphosphate intermediate in a *syn* form in which the two phosphate moieties are close to each other and facilitate intramolecular condensation. Matsuda and co-workers performed the intramolecular condensation between a phenylthiophosphate and a phosphomonoester²⁷, using I₂/3 Å MS as a promoter in pyridine to obtain cyclic compound in quantitative yield²⁸, (**Scheme 4.3**). The usual condensation between two phosphomonoesters using EDC [N-(3-Dimethylaminopropyl)-N'-ethylcarbodiimide hydrochloride] as promoter failed or gave rise to very low yield of cyclic compounds.



Scheme 4.3: Matsuda's strategy for total synthesis of cADPRcR and cIDPcR.

Several cIDPR analogs, the structures of which are shown in **Figure 4.6**, have been synthesized based on the established synthetic strategy.

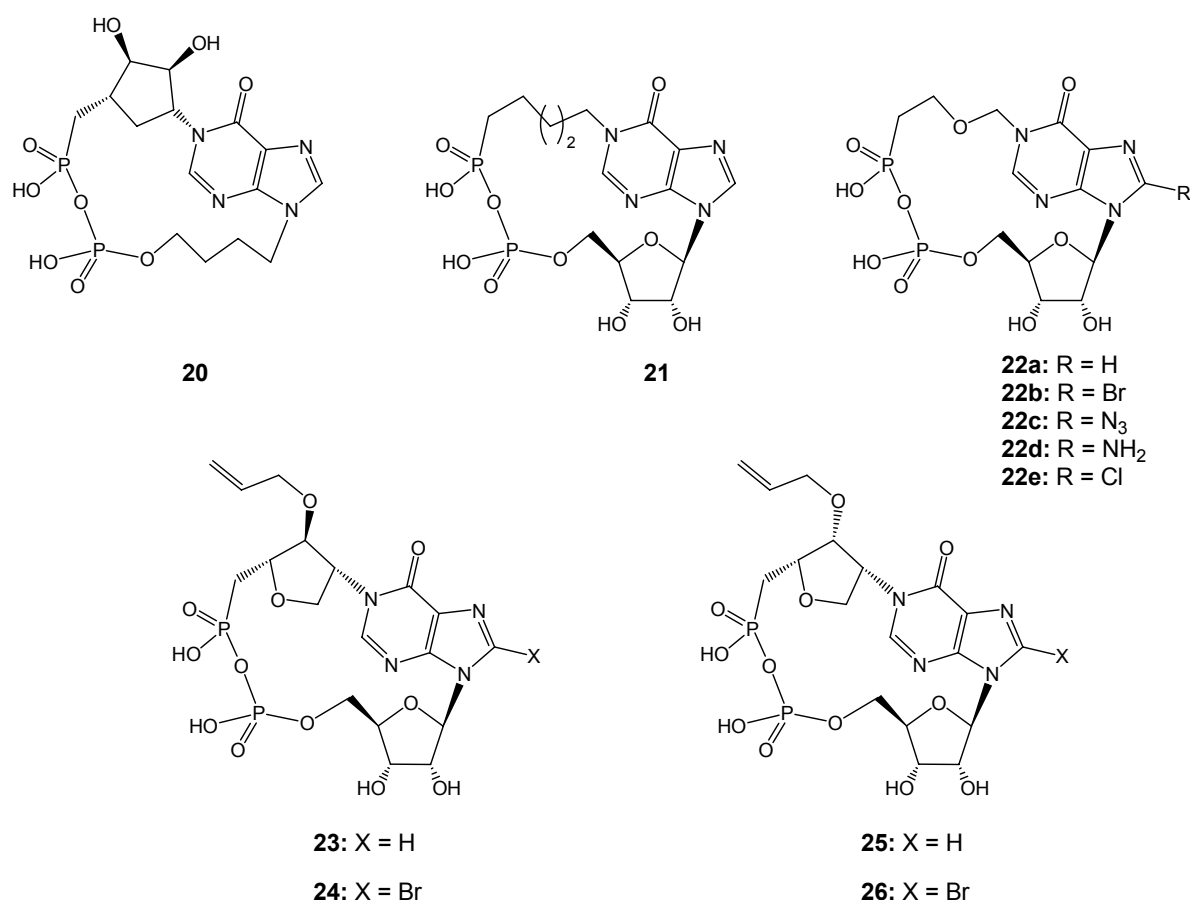
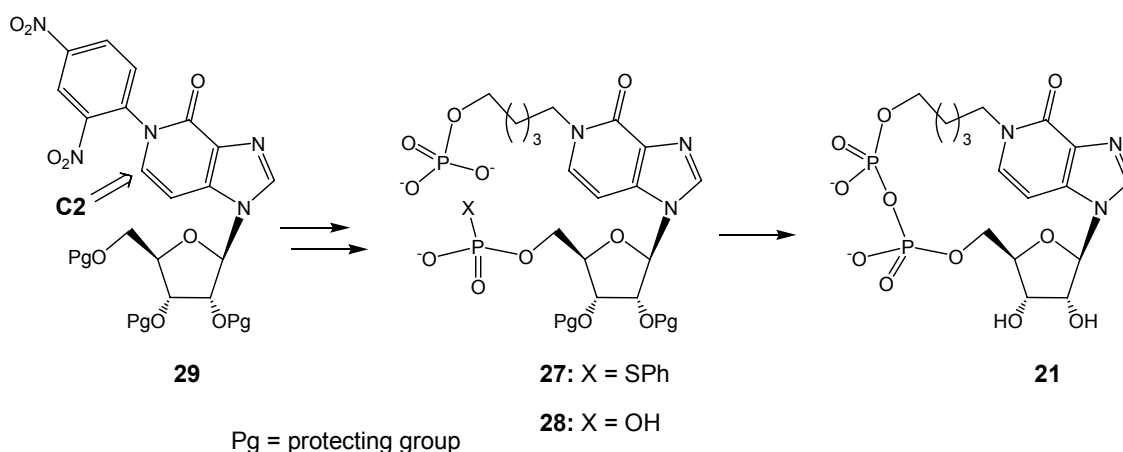


Figure 4.6. Chemically synthesized cIDPR analogs.

We synthesized the cIDPcR analog **20**, the "southern" ribose of which was replaced by a butyl group²⁹, and analog **21** where the "northern" ribose was replaced by a pentyl group³⁰ (**Figure 4.6**).

Considering, for example, the synthesis of **21**, the key intramolecular condensation occurred effectively using I₂/MS 3A-promoted method with the phenylthiophosphate substrate **27**. Surprisingly, the intramolecular condensation also occurred in high yield by the usual EDC-promoted method with the corresponding bisphosphate **28**. Conformational flexibility of the bisphosphate **28** due to the acyclic N1-pentyl chain may enable the cyclization to proceed.

The synthesis of **21** was performed treating N1-(2,4-dinitrophenyl)inosine intermediate **29** with 5-amino-1-pentanol via nucleophilic addition of amine at the C2-position of nucleobase followed by rearrangement (**Scheme 4.4**). This new method for construction of N-1 Inosine derivatives was clearly superior to method using S_N2-type condensation (**Scheme 4.2, i**).



Scheme 4.4. Synthesis of cIDPR analog **21**.

4.4. Structural cADPR analogues for SAR elucidation

According to the biosynthesis of cADPR from β -NAD⁺, a variety of cADPR analogues were obtained by the enzymatic and chemo-enzymatic approach using nicotinamide dinucleotide-type precursors and ADP-ribosyl cyclase for the synthesis of the cyclic pyrophosphate. cADPR analogues with a substitution at the 8-position of the adenine ring (including 8-Br, -NH₂, -CH₃, and -OMe)²² were found to be antagonist of cADPR. 8-Br-cADPR, although not as potent as 8-NH₂-cADPR, has been shown to be cell-permeant and can be used as a valuable tool. 7-deaza-8-Br-cADPR is a cell-permeant antagonist and is about twice as effective as 8-Br-cADPR⁸. 7-Deaza-cADPR was a partial agonist in sea urchin egg homogenates and 3-deaza-cADPR was about 70-fold more potent in sea urchin egg homogenates, as compared to cADPR³¹. In the case of the N1-coupled cyclic inosine diphosphate ribose mimics (cIDPR), different functional groups at the 8-position resulted in completely different biological activities; for example 8-Br-cIDPR acts as membrane-permeant agonist of Ca²⁺ signalling. However, due to the limitation of substrate-specificity of the ADP-ribosyl cyclase, the enzymatic and chemo-enzymatic method cannot be used for the construction of a larger variety of mimics modified in the northern or southern ribose moiety of cADPR. To build up a more detailed structure-activity profile for the calcium-releasing activity of cADPR, a method for the total syntheses of cADPR and its mimics is urgently needed.

Matsuda's group developed a total synthetic approach to construct cADPR analogues^{25e}. They found an efficient intramolecular cyclization for the construction of pyrophosphate. In this way they synthesized cIDP-carbocyclic-ribose (cIDPcR) and cyclic ADP-carbocyclic-ribose (cADPcR). cADPcR, in which the 4'-oxo in the northern ribose moiety of cADPR was substituted by a methylene group caused a significant release of Ca²⁺ in sea urchin eggs; in the same system, cADPcR is 3-4 times more potent than cADPR while 8-substituted analogues were less efficacious. Carbocyclic analogs were synthesized expecting to possess properties of both the stable carbocyclic analogs and the antagonistic 8-substituted cADPR analogs. These compounds were assayed for their calcium mobilizing effects as well as cADPR-evoked calcium release with sea urchin egg homogenates³². Surprisingly, although 8-NH₂-cADPR is a potent antagonist, the corresponding carbocyclic analog 8-NH₂-cADPcR was shown to be a potent full agonist with EC₅₀ value two times less than of cADPR.

8-Cl- and 8-N₃-cADPR analogs were also full agonists, though these were weaker than 8-NH₂cADPR²².

In mammalian cells, cADPR acted much more weakly, as compared to sea urchin system³³. However, it was found that cIDPR showed only an insignificant Ca²⁺-mobilizing effect (EC₅₀>10⁶ μM), and 8-Br-cIDPR was almost inactive in sea urchin egg homogenates¹⁶.

Rat brain microsomes were one of the first mammalian cell preparations in which cADPR was shown to trigger Ca²⁺ release. Nucleotides **23**, **24**, **25**, and **26** were tested for their abilities to release calcium from rat brain microsomes. In addition, Ca²⁺ mobilizing effect of extracellular added compounds were analyzed in intact HeLa cells. cADPR or the syntetic samples **23**, **24**, **25**, and **26** induced Ca²⁺ release from brain microsomes with a threshold concentration of less than 15 μM under these experimental conditions. Ca²⁺ was soon requested into microsomes. It is interesting that 8-nonsubstitued analogues have more potent calcium-modulating activity than the corresponding 8-bromo cIDPR mimics. In addition to their activity in broken cell preparations, these cIDPR mimics modified at the N1-ribosyl moiety were also active in intact HeLa cells. The natural compound cADPR (200 μM) itself exhibited no Ca²⁺ releasing activity, presumably because it cannot cross the cell membrane. Taken together, these data suggest that the modification in the northern ribose moiety of cADPR could retain the calcium release activity and also increase the membrane permeability of cADPR. It seems that N1-ribosyl moiety and the 6-amino group in cADPR are not critical structural factors for biological activity. The data indicated that further modification in the northern ribose might also work, for example, a mimic of cADPR with complete replacement of northern ribose with an ether strand (cIDPRE, **22a**). A series of 8-substitued cIDPRE were also reported (**22b-e**). The results indicate that cIDPRE permeates the plasma membrane, releases calcium from an intracellular, cADPR-sensitive Ca²⁺ store, and subsequently initiates Ca²⁺ release-activated Ca²⁺ entry. The Ca²⁺-releasing activity of cIDPRE resulted in a lower efficacy of cIDPRE as compared to cADPR. Analogues of cIDPRE modified at C8 position of inosine had strikingly differential effects: while 8-N₃-cIDPRE and 8-NH₂-cIDPRE were similiarly effective in their agonistic activity as compared to cIDPRE, the halogenated derivatives 8-Br- and 8-Cl-cIDPRE did not significantly elevate [Ca²⁺]. Comparison of the calcium-release activities of different cIDPRE derivatives revealed a remarkable structure-activity relationship: while any functional group larger than the natural H at C8 in cADPR turned the molecule into a cADPR antagonist, for example 8-NH₂-cADPR, 8-Br-cADPR and so on, in the case on cyclic IDP-ribose mimics, different functional groups at the 8-position resulted in completely different biological activities.

Thus, cIDPRE, 8-NH₂-, and N₃-cIDPRE are novel important agonist tools similiarly suitable for studying the structure-activity relationship of cADPR and for use as membrane permeant cADPR mimics in intact cells.

Concerning modifications on the southern ribose moiety of cADPR, it was found that the 3'-hydroxyl group was essential for calcium release in the sea urchin egg system, whereas the 2'-hydroxyl group was not. O-methylation of the 3'-hydroxyl group generated an antagonist¹⁹ (**30**, **Figure 4.7**). The stable cyclic aristeromycin dipshosphoribose (c-Aris DPR, **31**) contains a replacement of the southern ribose with a carbocyclic five-membered ring and is an agonist slightly more potent as compared to cADPR in the T-lymphocyte system²⁰. Comparison of the calcium-release activities of cIDPRE and cADPR revealed that the greater flexibility of the whole molecule introduced by replacement of the northern ribose by the ether strand

either still allows fitting into the binding site or allows the functional groups to support a conformation much more like cADPR. Because of the same structure of the northern and southern ribose occurring in cADPR, it appeared interesting to synthesize the cIDPR analog with replacement of both northern and southern ribose using two ether strand. The evaluation of the biological activity of cIDP-DE (**32**) indicates that it is a membrane permeant analog of cADPR with agonistic properties. In saponin-permeabilized Jurkat T cells, cIDP-DE releases Ca^{2+} from intracellular stores but was much weaker as compared to cADPR. Regardless of this weak direct effect, a pronounced activity of cIDP-DE on Ca^{2+} signalling was observed in intact Jurkat T cells. The biological activity of cIDP-DE in Jurkat cells was quite similar to cIDPRE (**22a**) in terms of (i) Ca^{2+} release activity in permeabilized cells and (ii) induction of both Ca^{2+} release and Ca^{2+} entry in a Ca^{2+} -free/ Ca^{2+} -reintroduction protocol. The Ca^{2+} -mobilizing activity was also confirmed in cardiac myocytes freshly prepared from mouse heart. The similarity of cIDP-DE and cIDPRE, especially in induction of Ca^{2+} signalling in intact T cells, indicate that the further replacement of the southern ribose by the second ether bridge in cIDP-DE did not significantly influence its biological activity.

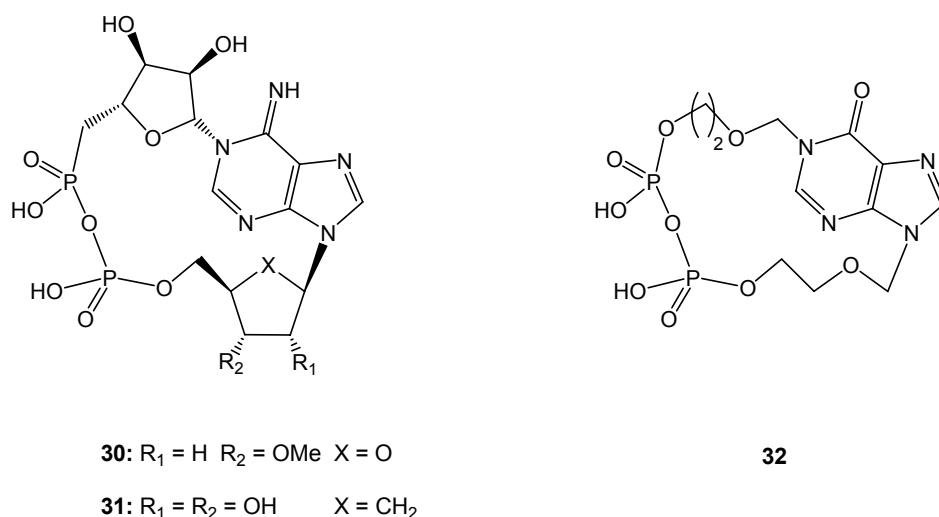


Figure 4.7. The structure of 3'-O-methyl cADPR, c-ARIS-DPR and cIDP-DE.

4.5. Cellular effect and metabolic stability of cADPR derivatives

Cyclic ADP-ribose (cADPR) is a Ca^{2+} mobilizing cyclic nucleotide active in many cell types and tissues, both in animals, protists and plants. The role of cADPR as an important transducer in human cell types implies that analogues of the molecule may become relevant as therapeutic agents in future. The biological activity and metabolic stability of a number of such analogues have been studied³⁴. Alterations in adenine base resulted in metabolic stable analogues: 3-deaza-cADPR is a potent and hydrolysis-resistant agonist, whereas 7-deaza-cADPR is also resistant to hydrolysis, but only a partial agonist. Modifications of the 8-position of adenine usually resulted in antagonists; thus, further substitution of 7-deaza-cADPR at the 8-position converted the partial agonist 7-deaza-cADPR into the membrane-permeant, hydrolysis resistant antagonist 7-deaza-8-Br-cADPR. Metabolic stability was also achieved by converting either the 'southern' or the 'northern' ribose into carbocyclic moieties; the resulting analogues cyclic aristeromycin diphosphoribose and cyclic

adenosine diphospho-carbocyclic-ribose were biologically active, although at different magnitude, and hydrolysis-resistant. Likewise, 2''-amino-cADPR, modified in the 'northern' ribose, was a potent and hydrolysis-resistant agonist.

Despite the wide acceptance of cADPR as a second messenger, its metabolism is still an enigma as the only well-described mammalian enzymes, CD38 and CD157, catalyse both the formation and breakdown of cADPR. In addition, the active sites of CD38 and CD157 are localized in the extracellular space (or in intracellular vesicles), making a direct involvement of these enzymes in the intracellular metabolism of cADPR difficult. However, to solve this topological paradox, transport systems for the export of nicotinamide adenine dinucleotide (NAD^+) and the import of cADPR have been described in some cell types. Recently, N1-cyclic inosine diphosphoribose (N1-clDPR) and its derivatives have been introduced as stable mimics of cADPR.

N1-clDPR has recently been shown to mobilize Ca^{2+} from intracellular stores with an effector concentration for half-maximum response (EC_{50}) of approximately 33 mM.

The natural nucleotide cADPR gave almost identical results indicating that the replacement of the imino-group at C6 by an oxo-group does not change binding and interaction properties of the nucleotide at its receptor protein. As both compounds are very polar, only few experiments were conducted with intact cells; as expected, no Ca^{2+} mobilization was observed. 8-Br-N1-clDPR induced a transient Ca^{2+} mobilization in intact cells; however, its Ca^{2+} -releasing activity in permeabilized cells was very low. The latter may indicate that 8-Br-N1-clDPR acts via a mechanism distinct from the one induced by cADPR and is presently under investigation. The compounds N1-clDPRE and N1-clDP-DE were less effective in permeabilized cells as compared to the maximal Ca^{2+} release obtained with cADPR. Concentrations of 100 mM for N1-clDPRE and 500 mM for N1-clDP-DE did not even reach the magnitude of Ca^{2+} release obtained by cADPR. In intact cells, the EC_{50} for N1-clDPRE was approximately 500 mM, while an exact EC_{50} for N1-clDP-DE could not be determined since at 1mM extracellular concentration there was still no saturation of the effect; however, it did not appear reasonable to further increase the concentration (**Table 4.1**)³⁵.

Antagonistic effects were not observed with any inosine based analogues of cADPR (data not shown).

Compound	EC_{50} (μM)	
	Permeabilized cell	Intact cell
cADPR	33	ND
N1-clDPR	33	ND
8-Br-N1-clDPR	ND	Active
N1-clDPRE	>100	Approx. 500
N1-clDP-DE	>500	>500

Table 4.1: Effects of N1-CIDPR and some its derivatives on Ca^{2+} mobilization in Jurkat T cells.

As N1-clDPR and some of its derivatives displayed Ca^{2+} mobilizing properties in mammalian cells (**Table 4.1**), these compounds are well suited as novel tools for

signal-transduction research and may further serve as starting material for the synthesis of novel pharmaceutical compounds. The latter ideally are metabolically stable to maintain a constant effective concentration during therapy. The stability of N1-clDPR was studied under identical conditions as above for cADPR.

To study the metabolism of cADPR by CD38, the nucleotide was incubated with intact Jurkat T-lymphocytes. These cells express CD38 as an integral type 2 membrane protein with the active site located in the extracellular space). The well-described cADPR-hydrolase activity of CD38 resulted in a slow decrease of cADPR with a concomitant increase in the hydrolysis product adenosine 5'-diphosphoribose (ADPR).

As CD38 was the only enzyme capable of hydrolysing cADPR to ADPR to some extent, the cyclic inosine nucleotides were incubated with intact Jurkat T cells in a similar manner as for cADPR. Experiments in which CD38 expressed on Jurkat T cells was used were confirmed by replacement of the Jurkat cells by mouse recombinant soluble CD38. Data (**Figure 4.8**) confirm the idea that substitution of the amino/imino- group at C6 by an oxo-group, thus converting the bond between N1 and C1'' at the northern ribose into a much more chemically stable, amide bond, produces compounds that are also biologically stable. In fact cADPR was digested for 60% to ADPR within 18 h (**Figure 4.8a**) while there was no decrease in the peak area of N1-clDPR at the same time (**Figure 4.8b**).

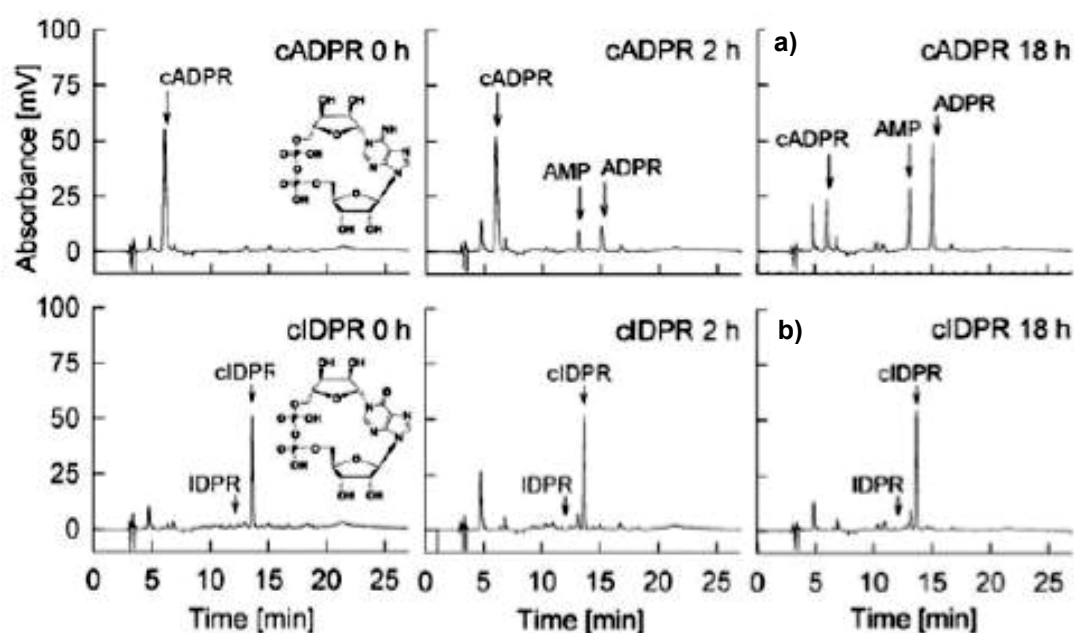


Figure 4.8. RP-HPLC profiles of metabolism of CADPR and N1-clDPR by CD38. cADPR (50 μM) or N1-clDPR (50 μM) were incubated at RT either with 1×10^{-7} Jurkat T-lymphocytes for the times indicated with recombinant soluble mouse CD38 (0.75 $\mu\text{g mL}^{-1}$).

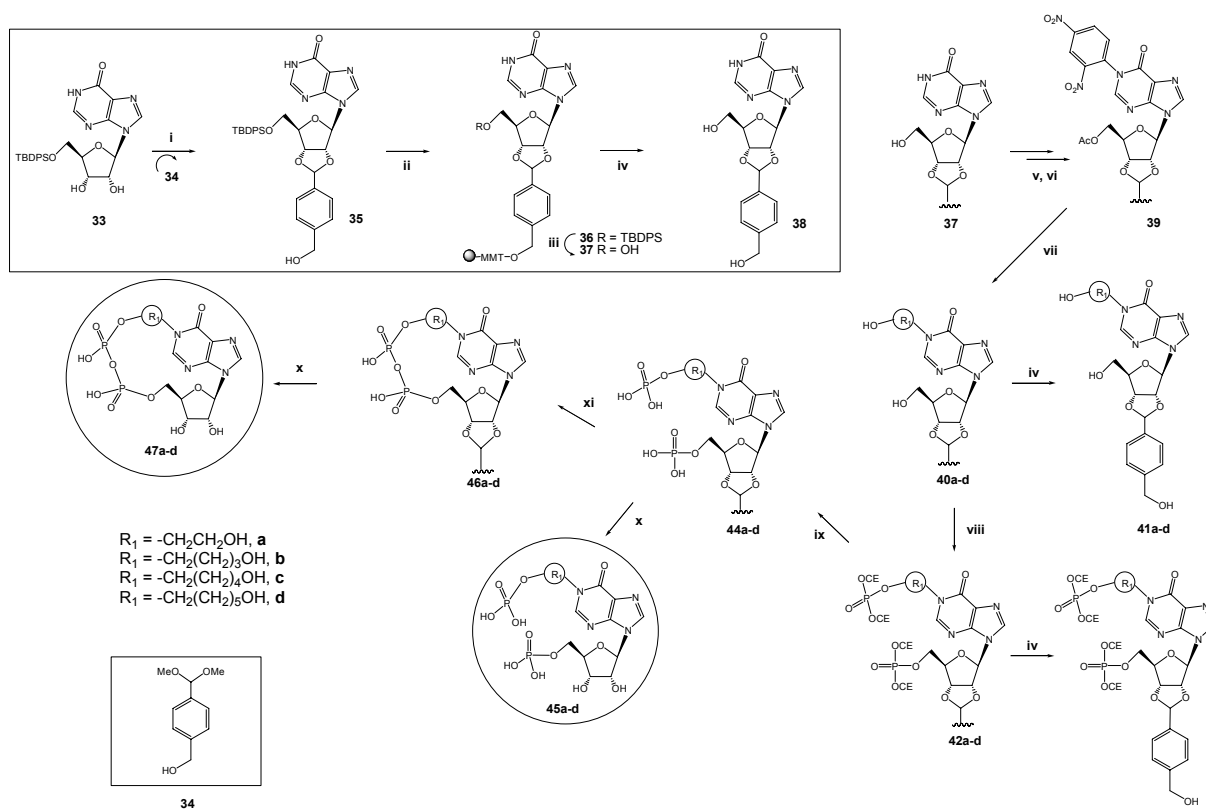
CADPR, N1-clDPR and the analogues were incubated with the autonomously proliferating Jurkat T-lymphoma cells. Whereas cADPR and 8-Br-N1-clDPR had no effect on proliferation, there was a dose dependent inhibition of proliferation by N1-clDPR, N1-clDP-DE and N1-clDPRE. These antiproliferative effects of N1-clDPR and N1-clDPRE was further studied in primary T cells. Surprisingly, only a very modest and statistically not significant effect on proliferation induced by myelin-basic

protein in primary rat T cells was observed (data not shown). To find out whether the difference observed was due to the different species involved (human Jurkat T cells vs primary rat T cells), a similar experiment was carried out using human myelin-basic protein-specific T cells. Again, at the concentrations of N1-cIDPR and N1-cIDPRE almost completely blocking autonomous proliferation of Jurkat T-lymphoma cells no effect on the proliferation was observed in the human primary T cells (data not shown).

Although the endogenous second messenger cADPR was degraded by CD38-type ADPRC, N1-cIDPR and its analogues were metabolically stable. Along with the proven Ca^{2+} -mobilizing activity of these compounds and the newly discovered inhibitory effects on proliferation of T-lymphoma cells, but not on primary T cells, their metabolic stability is another advantage for the development of new tools for signal-transduction research and potentially also for the design of novel pharmaceutical compounds.

4.6. The aim of the work

The chemical synthesis and in particular the total synthetic approach proposed for the great part of these analogues, makes use of multistep and time-consuming solution processes which require the purification of the products after each reaction step. In an effort to facilitate the chemical synthesis of these substances, and to enlarge the number of accessible structurally diverse analogues, we report here a new and general solid-phase approach to prepare N-1-alkyl analogues of cIDPR (**47a-d**, **Scheme 4.5**) in good yields.



Scheme 4.5: Reagents and conditions: i) 4-(hydroxymethyl)-benzaldehyde dimethyl acetal (**34**) (5.0 equiv), *p*-TsOH (0.5 equiv), DCM, 7 h, reflux; ii) MMTCl resin, **35** (1.5 equiv), Py (1.5 mL/250 mg of resin) DMAP (0.2 equiv) 24 h, r.t.; iii) NH_4F (30 equiv), MeOH, reflux, 7 h, v) Ac_2O (10 equiv), Py 30 min., r.t.; vi) DNCB (5 equiv), K_2CO_3 (5 equiv), 3 h, 80 °C.; vii) $\text{OH-R}_1\text{-NH}_2$ (40 equiv), DMF, 8 h, 50 °C; viii) a) DCEA (20 equiv), 1-*H*-tetrazole (20 equiv), THF, 24 h, r.t., b) *t*-BuOOH (20 equiv), THF, rt, 3 h; ix) $\text{NH}_3\text{-MeOH}$ (1:1, v/v, 24 h, 55 °C; xi) CDI (1.0 equiv) DMF, 15 h, r.t.; iv) TFA 2% in DCM, 8 min, r.t., x) TFA 2% in DCM, 8 min, r.t. followed by H_2O washings, 5 min.

Our synthetic approach use as key intermediate solid support **36** in which 5'-TBDPS-inosine **33** is bound to the solid matrix by a 2',3'-acetal linkage. **36** was then converted in two steps in the N-1-dinitrophenyl-inosine solid support **39** possessing a C-2 purine atom very reactive towards N-nucleophiles and easily convertible into N-1-alkyl-inosine derivatives, as previously reported.³⁶ Following that approach, the reaction of support **39** with several ω -hydroxyalkylamines ($\text{HO}-(\text{CH}_2)_n\text{-NH}_2$, **a-d**, **Table 4.2**) furnished the N-1-alkyl-inosine supports **40a-d** which were in turn

converted into the phosphate derivative **42a-d** in high yields. After the complete deprotection of the phosphate groups, the intramolecular cyclization was performed by pyrophosphate bond formation, treating support **42a-d** with carbonyldiimidazole (CDI). After detachment from the solid matrix, the target N-1-alkyl-analogues of cIDPR (**47a-d**) could be obtained in 25-30 % overall yields (**Table 4.2**).

The intramolecular cyclization can be considered the key step in the chemical synthesis of cADPR, cIDPR and their derivatives, requiring the closure of a 18-membered cycle. For this purpose the most employed method uses the condensation between a S-phenyl phosphorothioate and a phosphomonoester groups promoted by AgNO₃. However, the above procedure requires two distinct phosphorylation reactions and suitable protection/deprotection steps of the involved alcoholic functions. In our synthetic strategy we successfully use the intramolecular condensation of two phosphomonoester functions (**44a-d**) which could be prepared by a one-step bis-phosphorylation reaction of **40a-d**. In this work we have also investigated the effect of the alkyl amine length on the cyclization yields and the reaction conditions for the pyrophosphate bond formation.

Support **36** was prepared binding the 4-(hydroxymethyl)-2',3'-benzylidene-5'-TBDPS-inosine **35** to the polystyrenemonomethoxytrityl chloride (MMTCl) resin by a benzyl-O-trityl ether linkage. In this way inosine is bound to the trityl resin by a benzylidene linker having two acid labile functions: a benzyl-trityl ether and a 2',3'-acetal linkage both selectively cleavable by treatment with anhydrous acids or aqueous acids, respectively. Inosine derivative **35** was synthesized by reaction of **33** with 4-(hydroxymethyl)-benzaldehyde dimethyl acetal in the presence of catalytic amounts of *p*-TsOH (85% yield). The reaction of commercially available MMTCl resin (1.3 meq/g) with **35**, performed in anhydrous pyridine in the presence of 4-(N,N-dimethylamino)-pyridine (DMAP), afforded support **36** in almost quantitative yield. Deprotection of the 5'-OH function, performed by NH₄F treatment, furnished the support **38** in over 95% yield.

In previous papers we demonstrated that N-1-(2,4-dinitrophenyl)-inosine, both in solution³⁷ or 5'-bound to a polymeric support^{36b}, is a good precursor to alkylate the N-1-atom of the purine ring of inosine by reaction with primary alkylamines. In particular, reaction of the C-2 carbon with amino nucleophiles (R₁-NH₂) leads to the opening of the six member ring through the cleavage of the (N-1)-(C-2) bond. The successive fast ring re-closure, favoured by the loss of the 2,4-dinitroaniline as the leaving group, furnishes the N-1-alkyl inosine derivatives in high yields. Therefore, N-1-(2,4-dinitrophenyl)-inosine-containing support **39** was synthesized by reaction of **37** (previously protected on 5'-OH with acetyl group), suspended in DMF, with 2,4-dinitrochlorobenzene (DNCB, 5 equiv) in the presence of K₂CO₃ (5 equiv). In this way **39** was obtained in high yields (93-95%) thus demonstrating that this unprecedented solid-phase inosine reaction can successfully replace the time-consuming step required for the preparation of N-1-(2,4-dinitrophenyl)-inosine before its loading onto the solid support.^{36b} Reaction of **39** with several ω -hydroxyalkylamines (HO-(CH₂)_n-NH₂, n = 2→**a**, 4→**b**, 5→**c**, n = 6→**d**, **Table 4.2**) furnished the N-1-alkyl-inosine supports **40a-d** in 90-92% yields. In a typical reaction, 100 mg (0.12 mmol) of support **39**, swollen in DMF, was left in contact with the amine (5.0 mmol, DMF, 8 h, 50 °C). After washings with DMF and MeOH, the support was dried under reduced pressure and the reaction yield, as well as the structures of the N-1-alkyl-inosines were ascertained analyzing the plates TLC purified nucleoside material **41a-d** released from a weighed amount of resin by treatment with a 2% TFA solution in dry DCM (8 min, r.t.).

Treatment of **40a-d** with N,N-diisopropyl-bis-(2-cianoethyl)phosphoramidite³⁸ (DCEA, 20 equiv) in the presence of 1-*H*-tetrazole (20 equiv) in dry THF, followed by oxidation with *t*-BuOOH in dry THF furnished the bis-phosphate derivatives **42a-d** in 90-92 % yield. The complete deprotection of phosphates was achieved by treating **42a-d** with NH₃(aq)-MeOH (1:1, v/v, 24 h, 55 °C) followed by washings with H₂O and MeOH. The dried support **44a-d** was treated with 2% TFA in DCM and washed with water. The combined filtrate solution and washings, dried under reduced pressure, furnished the N-1-alkyl-inosine-diphosphate derivative **45a-d** (Table 4.2) whose structures were confirmed, after HPLC purification, by spectroscopic data.

Good cyclization yields (40-45% from **44a-d**) were observed treating **44a-d** with carbonyldiimidazole (CDI, 2.0 equiv, DMF, 24 h, 60 °C). In particular, we also observed that cyclization yields is slightly affected by the N-1-polymethylene chain length with best yields obtained with the shorter chain **44a**. It is to be noted that notwithstanding pseudo-dilution conditions characterizing the solid-phase cyclizations, variable amounts of polymeric species were obtained (20-30%). These species are formed by intermolecular pyrophosphate bond formation, as demonstrated from HPLC and MS analyses of the detached nucleotide material (data not shown). Finally, cleavage of the **47a-d** from the solid support was achieved by acidic treatment as described for derivatives **45a-d**. The structures of all HPLC purified final products were confirmed by ¹H-, ³¹P-NMR and ESI-MS. In a typical reaction sequence, starting from 50 mg of solid support **36** (1.2 mmol/g) and considering an average molecular weight of 480 g/mol, 2-3 mg of pure **47a-d** could be obtained (25-30% overall yield from **36**).

In conclusion, we have successfully investigated the practical solid-phase synthesis of N-1-alkyl-substituted analogues of cIDPR by using solid support **36**, where the inosine is anchored to a MMT-polystyrene resin by a benzylidene linker. The utility of this approach lies in the fact that it furnishes a general and fast synthetic methodology for i) nucleoside analogues; ii) their phosphorylated derivatives; iii) intramolecular solid-phase pyrophosphate bond formation. Particular attention has been devoted to the latter reaction which, after optimization, could lead to satisfactory cyclization yield by pyrophosphate bond formation. In our opinion this unprecedented solid-phase approach can be generally applied to the synthesis of a several cIDPR derivatives also combining a number of derivatization on the purine moiety.

N-1-alkyl moiety	40a-d (from 36) yield (%)	42a-d (from 36) yield (%)	44a-d (from 36) yield (%)	46a-d (from 36) yield (%)
a (CH ₂) ₂	90	77	77	30
b (CH ₂) ₄	92	78	78	28
c (CH ₂) ₅	90	77	77	26
d (CH ₂) ₆	91	79	79	25

Table 4.2. Products and reaction yields.

4.7. Experimental Session

4.7.1. General

4-Methoxytrityl chloride resin (1% divinylbenzene, 200–400 mesh, 1.3 mmol g⁻¹ substitution) was purchased from CBL Patras, Greece. Anhydrous solvents were used for reactions. All the other reagents were obtained from commercial sources and were used without further purification. The reactions on solid phase were performed using glass columns (10 mm diameter, 100 mm length) with fused-in sintered glass-disc PO (bore of plug 2.5 mm), which were shaken on an orbital shaker, or round bottom flask, when reactions were performed at high temperatures.. The ¹H NMR spectra were performed on a Varian Mercury Plus 400 MHz using CD₃OD and D₂O as solvents; chemical shifts were reported in parts per million (δ) relative to residual solvent signals: CD₂HOD 3.31, HDO 4.80, ³¹P NMR spectra (H₃PO₄ 85% as an external standard) were performed on Varian Unity Inova 500 MHz. RP-HPLC analyses of crude products were carried out on a Jasco UP-2075 Plus pump using a 5 mm, 4.8 x 150 mm C-18 reverse phase column eluted with a linear gradient of CH₃CN in 0.1 M TEAB (pH 7.0, from 0 to 60% in 60 min, flow 1.0 mL min⁻¹) equipped with a Jasco UV-2075 Plus UV detector. The UV spectra were recorded on a Jasco V-530 UV spectrophotometer. Mass spectra were recorded on an Applied Biosystems API 2000 mass spectrometer using electron spray ionization (ESI) technique. Column chromatography was performed on silica gel (Merck, Kieselgel 60, 0.063–0.200 mm); preparative plate chromatography was performed using F254 silica gel plates (0.5 mm, Merck), plates were developed in this system of solvents: [AcOEt-MeOH (85:15, v/v)], analytic TLC detections were performed using F254 silica gel plates (0.2 mm, Merck). TLC spots were detected under UV light (254 nm). Cationic exchanges were performed on Dowex 50W X8 (Na⁺ form, 50-100 mesh, Fluka).

The following abbreviations were used throughout the text: Ac₂O = acetic anhydride, AcOEt = ethyl acetate, CDI = 1, 1'-carbonyldiimidazole, CH₂Cl₂ = dichloromethane, DCEA = N,N-diisopropyl-bis-(2-cianoethyl)phosphoramidite, DMAP = 4-(N,N-dimethylamino)-pyridine, DMF = N,N-dimethylformamide, DNCB = 2,4-dinitrochlorobenzene, EtOH = ethanol, K₂CO₃ = potassium carbonate, MeOH = methanol, NH₄F = ammonium fluoride, Py = pyridine, TEAB = triethylammonium bicarbonate, TBDPSCI = *tert*-butyldiphenylchlorosilane, *t*-BuOOH = *tert*-butyl hydroperoxide, TFA = trifluoroacetic acid, THF = tetrahydrofuran, *p*TsOH = *p*-toluenesulfonic acids, 's =, singlets, d's = doublets, m's = multiplets, q's = quartets.

4.7.2. Synthesis

Compound 35

A mixture of **33** (1.00 g, 1.97 mmol), 4-(Hydroxymethyl)benzaldehyde dimethyl acetal **34** (4.60 g, 25.3 mmol), and *p*-TsOH (460 mg, 2.53 mmol) was refluxed in anhydrous DCM (13 mL mL) and for 7 h. The reaction was monitored by TLC (AcOEt/MeOH, 95:5). After cooling, the solvent was evaporated and the crude was purified on a silica gel column eluted with increasing amounts of MeOH in AcOEt (from 0 to 5%) to give **35** as a white amorphous solid (0.86 g, 70%), ¹HNMR δ_H (CD₃OD) 8.40 (s, 1H, H-2), 7.80 (s, 1H, H-8), 7.62-7.25 (m, 12H, arom.), 6.35 (d, 1H, H-1'), 6.00 (s, 1H, CHPh),

5.50 (m, 1H, H-2'), 5.10 (m, 1H, H-3'), 4.63 (s, 2H, CH₂Ph), 4.56 (m, 1H, H-4'), 3.89-3.78 (m, 2H, H-5'), 1.02 (s, 9H, 3xCH₃). ESI-MS calculated for C₃₅H₃₈N₄O₅Si 622.26, found 645.31 (M + Na)⁺.

Loading of compound **35** on solid support

Compound **35** (0.86 g, 1.38 mmol) was evaporated with dry Py (3 x 1.5 mL) and then coupled with the MMTCl resin (1.30 g, 1.66 mmol), in dry Py (8 mL) in the presence of DMAP (0.35 mmol, 42.0 mg) for 24 h at room temperature. The resin was filtered and washed with DCM (3x5 mL), DCM/MeOH (1:1, v/v, 3x5 mL), and MeOH (3x5 mL), and finally dried in vacuo. The reaction yield was evaluated by cleavage of the nucleoside from the solid support and from acetal linkage by treatment with 2% (v/v) TFA in DCM (8 min, rt) followed by treatment with H₂O (30'). Quantitative UV experiment was performed on detached inosine ($\lambda_{\text{max}} = 248 \text{ nm}$, $\epsilon = 12200$, H₂O). The solid support **36** was obtained in almost quantitative yield (1.26 mmol g⁻¹, 97%).

Support **37**

Support **36** (1.00 g, 1.30 mmol) was suspended in MeOH (20 mL) and then NH₄F (1.45 g, 40 mmol) was added in one portion. The reaction was refluxed for 7 h. After cooling, the resin was filtered and washed with MeOH (3x5 mL), DCM/MeOH (1:1, v/v, 3x5 mL), and DCM (3x5 mL), and finally dried in vacuo. Support **37** was obtained and the yield of the reaction (98%) was calculated quantifying the product **38** obtained by TLC plate purification (see General) of the crude nucleoside material released from a weighted amount of resin (as described above) and taking into account that the starting support **36** had a 1.26 mol g⁻¹ nucleoside functionalization.

Compound **38**: ¹HNMR δ_{H} (CD₃OD) 8.36 (s, 1H, H-2), 8.08 (s, 1H, H-8), 7.57 (d, 1H, arom), 7.43 (d, 1H, arom), 6.36 (d, 1H, H-1'), 6.04 (s, 1H, CH), 5.42 (m, 1H, H-2'), 5.13 (m, 1H, H-3'), 4.65 (s, 2H, CH₂Ph), 4.52 (m, 1H, H-4'), 3.77 (m, 2H, 2xH-5'); ESI-MS calculated for C₁₈H₁₈N₄O₆ 386.12 found 409.18 (M + Na)⁺.

Support **39**

Support **37** (0.50 g, 0.65 mmol) was suspended in Py (3 mL) and Ac₂O (0.60 mL, 6.5 mmol) and was shaken for 30' at RT; the resin was filtered and washed with DCM (3x5 mL), DCM/MeOH (1:1, v/v, 3x5 mL), and MeOH (3x5 mL), and finally dried in vacuo. The obtained support was suspended in dry DMF (16 mL) and then DNCB (0.66 g, 3.25 mmol) and K₂CO₃ (0.45 g, 3.25 mmol) were added in one portion. The reaction was stirred at 80 °C for 3 h. After cooling, the resin was washed with DMF (3x5 mL), DMF/MeOH (1:1, v/v, 3x5 mL), and MeOH (3x5 mL), and finally dried in vacuo. The resin **39** was used for the next step without detachment of nucleoside material from solid support.

Supports **40a-d**

Solid support **39** (4x100 mg, 0.12 mmol), previously swollen in DMF, was left in contact with amines **a-d** (Table 4.2, 5.0 mmol) in DMF (1.5 mL) under shaking for 8 h at 50 °C. The solid supports **40a-d** were filtered and washed with DMF (3x5 mL), DMF/MeOH (1:1, v/v, 3x5 mL), and MeOH (3x5 mL), and finally dried in vacuo.

The yields of N-1-alkyl-inosines **41a-d** (from **36**, **Table 4.2**) were calculated by quantifying the products obtained by plates TLC purification (see General) of the crude nucleoside material released from a weighted amount of resin (as described above) and taking into account that the starting support **36** had a 1.26 mol g⁻¹ nucleoside. ¹H-NMR spectra (see later) confirmed the purity of the products **41a-d**.

Supports 42a-d

Solid supports **40a-d** (4x100 mg, 0.10-0.12 mmol), previously swollen in dry THF, were treated with DCEA (650 mg, 2.4 mmol) in dry THF (1.5 mL) under shaking for 24 h at RT. The obtained solid supports were filtered and washed with THF (3x5 mL), THF/MeOH (1:1, v/v, 3x5 mL), and MeOH (3x5 mL), and finally dried in vacuo. After treatment with *t*-BuOOH (5-6 M in decane, 216 μ L, 2.4 mmol) in THF (1.5 mL) for 3 h at RT and after washings with THF (3x5 mL), THF/MeOH (1:1, v/v, 3x5 mL), and MeOH (3x5 mL), solid supports **42a-d** were obtained.

The yields of compounds **43a-d** (from **36**, **Table 4.2**) were calculated by quantifying the products obtained by plates TLC purification (see General) of the crude nucleoside material released from a weighted amount of resin (as described above) and taking into account that the starting support **36** had a 1.26 mol g⁻¹ nucleoside. ¹H-NMR spectra (see later) confirmed the purity of the products **43a-d**.

Supports 44a-d

Solid supports **42a-d** (4x100 mg, 0.09-0.11 mmol) were shaken with NH₃(aq)-MeOH solution (1:1, v/v, 1.5 mL) for 24 h at 55 °C. The solid support **44a-d** were filtered and washed with H₂O (3x5 mL), MeOH/H₂O (1:1, v/v, 3x5 mL), MeOH (3x5 mL), and finally dried in vacuo. The yields of compounds **45a-d** (from **36**, **Table 4.2**) were calculated by quantifying the products obtained by HPLC purification (see General) of the crude nucleoside material released from a weighted amount of resin (as described above) and taking into account that the starting support **36** had a 1.26 mol g⁻¹ nucleoside. ¹H-NMR spectra (see later) confirmed the purity of the products **45a-d**.

Support 46a-d

Solid supports **44a-d** (4x100 mg, 0.09-0.11 mmol) were left in contact with a mixture of CDI (32 mg, 0.20 mmol) in DMF (0.4 mL) for 15 h at RT. The solid supports **46a-d** were filtered and washed with DMF (3x5 mL), DMF/MeOH (1:1, v/v, 3x5 mL), and MeOH (3x5 mL), and finally dried in vacuo. The yields of compounds **47a-d** (from **36**, **Table 4.2**) were calculated by quantifying the products obtained by HPLC purification (see General) of the crude nucleoside material released from a weighted amount of resin (as described above) and taking into account that the starting support **36** had a 1.26 mol g⁻¹ nucleoside. ¹H-NMR spectra (see later) confirmed the purity of the products **47a-d**.

4.7.3 Synthesized scaffolds

Compound 41a

Oil, $^1\text{H-NMR}$ δ_{H} (CD_3OD) 8.35 (s, 1H, H-2), 8.32 (s, 1H, H-8), 7.57 (d, 2H, arom), 7.43 (d, 2H, arom), 6.03 (d, 1H, H-1'), 6.04 (s, 1H, CHPh), 5.42 (m, 1H, H-2'), 5.17 (m, 1H, H-3'), 4.65 (s, 2H, CH_2Ph), 4.52 (m, 1H, H-4'), 4.20 (t, 3H, CH_2N), 3.84-3.76 (m, 5H, CH_2O , 2xH-5'), ESI-MS calculated for $\text{C}_{20}\text{H}_{22}\text{N}_4\text{O}_7$ 430.15 found 453.19 ($\text{M} + \text{Na}$) $^+$

Compound 41b

Oil, $^1\text{H-NMR}$ δ_{H} (CD_3OD) 8.35 (s, 2H, H-2, H-8), 7.58 (d, 1H, arom), 7.43 (d, 1H, arom), 6.34 (d, 1H, H-1'), 6.03 (s, 1H, CH), 5.40 (m, 1H, H-2'), 5.11 (m, 1H, H-3'), 4.65 (s, 2H, CH_2Ph), 4.51 (m, 1H, H-4'), 4.14 (t, 2H, CH_2N), 3.77 (m, 2H, 2xH-5'), 3.60 (t, 2H, CH_2O), 1.85 (m, 2H, CH_2), 1.59 (m, 2H, CH_2), ESI-MS calculated for $\text{C}_{22}\text{H}_{26}\text{N}_4\text{O}_7$ 458.18 found 481.22 ($\text{M} + \text{Na}$) $^+$.

Compound 41c

Oil, $^1\text{H-NMR}$ δ_{H} (CD_3OD), 8.35 (s, 1H, H-8), 8.34 (s, 1H, 8-H), 7.57 (d, 1H, arom), 7.43 (d, 1H, arom), 6.34 (d, 1H, H-1'), 6.03 (s, 1H, CH), 5.41 (m, 1H, H-2'), 5.11 (m, 1H, H-3'), 4.65 (s, 2H, CH_2Ph), 4.52 (m, 1H, H-4'), 4.12 (t, 2H, CH_2N), 3.76 (m, 2H, 2xH-5'), 3.56 (t, 2H, CH_2O), 1.81 (m, 2H, CH_2), 1.59 (m, 2H, CH_2), 1.44 (m, 2H, CH_2), ESI-MS calculated for $\text{C}_{23}\text{H}_{28}\text{N}_4\text{O}_7$ 472.20 found 500.24 ($\text{M} + \text{Na}$) $^+$.

Compound 41d

Oil, $^1\text{H-NMR}$ δ_{H} (CD_3OD), 8.36 (s, 1H, H-2), 8.32 (s, 1H, H-8), 7.58 (d, 1H, arom), 7.44 (d, 1H, arom), 6.34 (d, 1H, H-1'), 6.04 (s, 1H, CH), 5.41 (m, 1H, H-2'), 5.11 (m, 1H, H-3'), 4.65 (s, 2H, CH_2Ph), 4.53 (m, 1H, H-4'), 4.12 (t, 2H, CH_2N), 3.80 (m, 2H, 2xH-5'), 3.54 (t, 2H, CH_2O), 1.80 (m, 2H, CH_2), 1.55 (m, 2H, CH_2), 1.42 (m, 4H, 2x CH_2). ESI-MS calculated for $\text{C}_{24}\text{H}_{30}\text{N}_4\text{O}_7$ 486.21 found 509.26 ($\text{M} + \text{Na}$) $^+$.

Compound 43a

Oil, $^1\text{HNMR}$ δ_{H} (CD_3OD) 8.37 (s, 1H, H-2), 8.25 (s, 1H, H-8), 7.57 (d, 2H, arom), 7.43 (d, 2H, arom), 6.41 (d, 1H, H-1'), 6.07 (s, 1H, CH), 5.60 (m, 1H, H-2'), 5.28 (m, 1H, H-3'), 4.64 (m, 3H, H-4', CH_2Ph), 4.47-4.36 (m, 2H, 2x5'-H), 4.31-4.17 (m, 12H, 4x $\text{OCH}_2\text{CH}_2\text{CN}$, CH_2N , $\text{CH}_2\text{OP}(\text{OCE})_2$), 2.92-2.82 (m, 8H, 4x $\text{OCH}_2\text{CH}_2\text{CN}$), $^{31}\text{P-NMR}$ δ (D_2O) -1.55, -1.67. ESI-MS calculated for $\text{C}_{32}\text{H}_{36}\text{N}_8\text{O}_{13}\text{P}_2$ 802.19.12 found 825.24 ($\text{M} + \text{Na}$) $^+$.

Compound 43b

Oil, $^1\text{H-NMR}$ δ_{H} (CD_3OD) 8.38 (s, 1H, H-2), 8.25 (s, 1H, H-8), 7.57 (d, 2H, arom), 7.43 (d, 2H, arom), 6.42 (d, 1H, H-1'), 6.05 (s, 1H, CH), 5.60 (m, 1H, H-2'), 5.26 (m, 1H, H-3'), 4.65 (m, 3H, H-4', CH_2Ph), 4.48-4.36 (m, 2H, 2x5'-H), 4.32-4.15 (m, 12H, 4x $\text{OCH}_2\text{CH}_2\text{CN}$, CH_2N , $\text{CH}_2\text{OP}(\text{OCE})_2$), 2.92-2.82 (m, 8H, 4x $\text{OCH}_2\text{CH}_2\text{CN}$), 1.92 (m, 2H, CH_2), 1.86 (m, 2H, CH_2), $^{31}\text{P-NMR}$ δ (D_2O) -1.55, -1.67. ESI-MS calculated for $\text{C}_{34}\text{H}_{40}\text{N}_8\text{O}_{13}\text{P}_2$ 830.22 found 853.27 ($\text{M} + \text{Na}$) $^+$.

Compound 43c

Oil, $^1\text{H-NMR}$ δ_{H} (CD_3OD) 8.35 (s, 1H, H-2), 8.22 (s, 1H, H-8), 7.57 (d, 2H, arom), 7.43 (d, 2H, arom), 6.40 (d, 1H, H-1'), 6.05 (s, 1H, CH), 5.61 (m, 1H, H-2'), 5.29 (m, 1H, H-3'), 4.62 (m, 3H, H-4', CH_2Ph), 4.48-4.36 (m, 2H, 2x5'-H), 4.32-4.15 (m, 12H, 4x $\text{OCH}_2\text{CH}_2\text{CN}$, CH_2N , $\text{CH}_2\text{OP}(\text{OCE})_2$), 2.90-2.81 (m, 8H, 4x $\text{OCH}_2\text{CH}_2\text{CN}$), 1.92 (m, 2H, CH_2), 1.86 (m, 2H, CH_2) 1.59 (m, 2H, CH_2), $^{31}\text{P-NMR}$ δ (D_2O) -1.54, -1.68. ESI-MS calculated for $\text{C}_{35}\text{H}_{42}\text{N}_8\text{O}_{13}\text{P}_2$ 844.23 found 867.31 ($\text{M} + \text{Na}$) $^+$.

Compound 43d

Oil, $^1\text{H-NMR}$ δ_{H} (CD_3OD) 8.38 (s, 1H, H-2), 8.25 (s, 1H, H-8), 7.57 (d, 2H, arom), 7.43 (d, 2H, arom), 6.42 (d, 1H, H-1'), 6.01 (s, 1H, CH), 5.60 (m, 1H, H-2'), 5.24 (m, 1H, H-3'), 4.63 (m, 3H, H-4', CH_2Ph), 4.48-4.36 (m, 2H, 2x5'-H), 4.32-4.15 (m, 12H, 4x $\text{OCH}_2\text{CH}_2\text{CN}$, CH_2N , $\text{CH}_2\text{OP}(\text{OCE})_2$), 2.92-2.82 (m, 8H, 4x $\text{OCH}_2\text{CH}_2\text{CN}$), 1.92 (m, 4H, 2x CH_2), 1.86 (m, 4H, 2x CH_2), $^{31}\text{P-NMR}$ δ (D_2O) -1.55, -1.67. ESI-MS calculated for $\text{C}_{36}\text{H}_{44}\text{N}_8\text{O}_{13}\text{P}_2$ 858.25 found 881.24 ($\text{M} + \text{Na}$) $^+$.

Compound 45a

Solid (sodium salt), $^1\text{H-NMR}$ δ_{H} (D_2O) 8.50 (1H, bs, H-2); 8.45 (1H, s, H-8); 6.16 (d, 1H, H-1'); 4.77 (1H, m, H-2'); 4.45 (1H, m, H-3'), 4.38 (m, 3H, CH_2O , H-4'); 4.13 (m, 4H, $\text{CH}_2\text{-N}$ and 2xH-5'), $^{31}\text{P-NMR}$ δ (D_2O) 0.40, -0.11. ESI-MS calculated for $\text{C}_{12}\text{H}_{18}\text{N}_4\text{O}_{12}\text{P}_2$ 472.04 found 471.06 ($\text{M} - \text{H}$) $^-$.

Compound 45b

Solid (sodium salt), $^1\text{H-NMR}$ δ_{H} (D_2O) 8.45 (bs, 1H, H-2); 8.40 (1H, s, H-8); 6.12 (d, 1H, H-1'); 4.77 (1H, m, H-2'); 4.47 (1H, m, H-3'), 4.35 (m, 1H, H-4'); 4.16 (m, 2H, $\text{CH}_2\text{-N}$), 4.07 (m, 2H, CH_2O), 3.87 (m, 2H, 2xH-5'), 1.87 (m, 2H, CH_2), 1.67 (m, 2H, CH_2), $^{31}\text{P-NMR}$ δ (D_2O) 0.51, -0.20. ESI-MS calculated for $\text{C}_{14}\text{H}_{22}\text{N}_4\text{O}_{12}\text{P}_2$ 500.07 found 499.10 ($\text{M} - \text{H}$) $^-$.

Compound 45c

Solid (sodium salt), $^1\text{H-NMR}$ δ_{H} (D_2O) 8.42 (bs, 1H, H-2); 8.38 (1H, s, H-8); 6.11 (d, 1H, H-1'); 4.77 (1H, m, H-2'); 4.47 (1H, m, H-3'), 4.35 (m, 1H, H-4'); 4.11 (m, 4H, CH_2N , CH_2O), 3.83 (m, 2H, 2xH-5'), 1.81 (m, 2H, CH_2), 1.59 (m, 2H, CH_2), 1.44 (m, 2H, CH_2), $^{31}\text{P-NMR}$ δ (D_2O) 0.42, -0.16. ESI-MS calculated for $\text{C}_{15}\text{H}_{24}\text{N}_4\text{O}_{12}\text{P}_2$ 514.09, found 513.15 ($\text{M} - \text{H}$) $^-$.

Compound 45d

Solid (sodium salt), $^1\text{H-NMR}$ δ_{H} (D_2O) 8.50 (bs, 1H, H-2); 8.40 (1H, s, H-8); 6.13 (d, 1H, H-1'); 4.77 (1H, m, H-2'); 4.50 (1H, m, H-3'), 4.37 (m, 1H, H-4'); 4.14 (m, 2H, $\text{CH}_2\text{-N}$), 4.06 (m, 2H, CH_2O), 3.82 (m, 2H, 2xH-5'), 1.82 (m, 2H, CH_2), 1.62 (m, 2H, CH_2), 1.41 (m, 4H, 2x CH_2), $^{31}\text{P-NMR}$ δ (D_2O) 0.46, -0.17. ESI-MS calculated for $\text{C}_{16}\text{H}_{26}\text{N}_4\text{O}_{12}\text{P}_2$ 528.10 found 528.11 ($\text{M} - \text{H}$) $^-$.

Compound 47a

Solid (sodium salt), $^1\text{H-NMR}$ δ_{H} (D_2O) 8.39 and 8.21 (s, 1 H each, H-2 and H-8), 6.04 (br. s, 1 H, H-1'), 5.38 (m, 1 H, H-2'), 4.50 (m, 1 H, H-3'), 4.31 (m, 1 H, H-4'), 3.96 and 3.84 (m's, 2 H each, CH_2O and CH_2N), 3.76 (m, 2 H, 2xH-5'), ^{31}P NMR δ (D_2O) -10.21, -11.12. ESI-MS calculated for $\text{C}_{12}\text{H}_{16}\text{N}_4\text{O}_{11}\text{P}_2$ 454.03 found 453.06 ($\text{M} - \text{H}$) $^-$.

Compound 47b

Solid (sodium salt), $^1\text{H-NMR}$ δ_{H} (D_2O) 8.39 and 8.21 (s, 1 H each, H-2 and H-8), 6.04 (br. s, 1 H, H-1'), 5.38 (m, 1 H, H-2'), 4.50 (m, 1 H, H-3'), 4.31 (m, 1 H, H-4'), 3.96 and 3.84 (m's, 2 H each, CH_2O and CH_2N), 3.76 (m, 2 H, 2xH-5'), 1.85, 1.58 (m's, 2 H each, methylene groups), ^{31}P NMR δ (D_2O) -10.34, -11.25. ESI-MS calculated for $\text{C}_{14}\text{H}_{20}\text{N}_4\text{O}_{11}\text{P}_2$ 482.06 found 481.09 ($\text{M} - \text{H}$) $^-$.

Compound 47c

Solid (sodium salt), $^1\text{H-NMR}$ δ_{H} (D_2O) 8.39 and 8.21 (s, 1 H each, H-2 and H-8), 6.04 (br. s, 1 H, H-1'), 5.38 (m, 1 H, H-2'), 4.50 (m, 1 H, H-3'), 4.31 (m, 1 H, H-4'), 3.96 and 3.84 (m's, 2 H each, CH_2O and CH_2N), 3.76 (m, 2 H, 2xH-5'), 1.85, 1.58 and 1.32 (m's, 2 H each, methylene groups), ^{31}P NMR δ (D_2O) -10.30, -11.45. ESI-MS calculated for $\text{C}_{15}\text{H}_{22}\text{N}_4\text{O}_{11}\text{P}_2$ 496.08 found 495.12 ($\text{M} - \text{H}$) $^-$.

Compound 47d

Solid (sodium salt), $^1\text{H-NMR}$ δ_{H} (D_2O) 8.39 and 8.21 (s, 1 H each, H-2 and H-8), 6.04 (br. s, 1 H, H-1'), 5.38 (m, 1 H, H-2'), 4.50 (m, 1 H, H-3'), 4.31 (m, 1 H, H-4'), 3.96 and 3.84 (m's, 2 H each, CH_2O and CH_2N), 3.76 (m, 2 H, 2xH-5'), 1.85, 1.58 (m's 2H each, methylene groups), 1.42 (m, 4 H, methylene groups), ^{31}P NMR δ (D_2O) -10.29, -11.11. ESI-MS calculated for $\text{C}_{16}\text{H}_{24}\text{N}_4\text{O}_{11}\text{P}_2$ 510.09 found 509.02 ($\text{M} - \text{H}$) $^-$.

References

- ¹ Clapper, D.L.; Walseth, T.F.; Dargie, P.J.; Lee, H.C. *J. Bio. Chem.* **1987**, *262*, 9561–9568.
- ² Lee, H.C.; Walseth, T.F.; Bratt, G.T.; Hayes, R.N.; Clapper, D.L. *J. Bio. Chem.* **1989**, *264*, 1608–1615.
- ³ Kim, H.; Jacobson, E.L.; Jacobson, M.K. *Biochem. Biophys. Res. Commun.* **1993**, *194*, 1143–1147.
- ⁴ Lee, H.C.; Aarhus, R.; Levitt, D. *Nat. Struct. Biol.* **1994**, *1*, 143–144.
- ⁵ Wada, T.; Inageda, K.; Aritomo, K.; Tokita, K.; Nishina, H.; Takahashi, K.; Katada, T.; Sekine, M. *Nucleosides Nucleotides* **1995**, *14*, 1301–1341.
- ⁶ Guse, A.H. *Curr. Mol. Medical* **2004**, *4*, 239–248.
- ⁷ Higashida, H. *FEBS Lett.* **1997**, *418*, 355–356.
- ⁸ Guse, A.H.; da Silva, C.P.; Berg, I.; Skapenko, A.L.; Weber, K.; Heyer, P. *et al. Nature*, **1999**, *398*, 70–73.
- ⁹ Hellmich, M.R.; Strumwasser, F. *Cell. Regul.* **1991**, *2*, 193–202.
- ¹⁰ Glick, D.L.; Hellmich, M.R.; Beushausen, S.; Tempest, P.; Bayley, H.; Strumwasser, F. *Cell. Regul.* **1991**, *2*, 211–218.
- ¹¹ De Flora, A.; Franco, L.; Guida, L.; Bruzzone, S.; Usai, C.; Zocchi, E.; *Chem. Immunol.* **2000**, *75*, 79–88.
- ¹² Gu, Q.-M.; Sih, C. J. *J. Am. Chem. Soc.* **1994**, *116*, 7481–7486.
- ¹³ Lee, H. C.; Aarhus, R. *Biochem. Biophys. Acta* **1993**, *1164*, 68–74.
- ¹⁴ Takasawa, S.; Nata, K.; Yonekura, H.; Okamoto, H. *Science* **1993**, *259*, 370–373.
- ¹⁵ Zhang, F.-J.; Gu, Q.-M.; Sih, C. J. *Bioorg. Med. Chem.* **1999**, *7*, 653–654.
- ¹⁶ For more detailed references: Shuto, S.; Matsuda, A. *Curr. Med. Chem.* **2004**, *11*, 827–845.
- ¹⁷ Howard, M.; Grimaldi, J. C.; Bazan, J. F.; Lund, F. E.; Santos-Argumedo, L.; Parkhouse, R. M.; Walseth, T. F.; Lee, H. C. *Science* **1993**, *262*, 1056–1059.
- ¹⁸ For example(a) Zhang, F.-J.; Sih, C. J. *Bioorg. Med. Chem. Lett.* **1995**, *5*, 1701–1706; Ashamu, G. A.; Galione, A.; Potter, B. V. L. *J. Chem. Soc., Chem. Commun.* **1995**, 1359–1356; (b) Thomas, J. M.; Summerhill, R. J.; Fruen, R. J.; Bradley, R. C.; Grant C. G. A. *Curr. Biol.* **2002**, *12*, 2018–2022.
- ¹⁹ Ashamu, G. A.; Sethi, J. K.; Galione, A.; Potter, B. V. L. *Biochemistry* **1997**, *36*, 9509–9517.
- ²⁰ Bailey, B. C.; Fortt, S. M.; Summerhill, R. J.; Galione, A.; Potter, B.V. L. *FEBS Lett.* **1996**, *379*, 227–230.
- ²¹ Wong, L.; Aarhus, R.; Lee, H. C.; Walseth, T. F. *Biochim. Biophys. Acta* **1999**, *1472*, 555–564.
- ²² Walseth, T. F.; Lee, H. C. *Biochem. Biophys. Acta* **1993**, *1178*, 235–242.
- ²³ Sethi, J. K.; Empson, R. M.; Bailey, V. C.; Potter, B. V. L.; Galione, A. *J. Biol. Chem.* **1997**, *272*, 16358–16363.
- ²⁴ Graeff, R. M.; Walseth, T. J.; Fryxell, K.; Branton, W. D.; Lee, H.C. *J. Biol. Chem.* **1994**, *269*, 30260–30267; Zhang, F.-J.; Sih, C. J. *Tetrahedron Lett.* **1995**, *36*, 9289–9292.
- ²⁵ a) Aritomo, K.; Urashima, C.; Wada, T.; Sekine, M. *Nucleosides Nucleotides* **1996**, *15*, 1–16; b) De Napoli, L.; Di Fabio, G.; Messere, A.; Montesarchio, D.; Piccialli, G.; Varra, M. *J. Chem. Soc., Perkin 1*, **1999**, 3489–3493; d) De Capua, A.; De Napoli, L.; Di Fabio, G.; Messere, A.; Montesarchio, D.; Piccialli, G. *Nucleosides Nucleotides* **2000**, *19*, 1289–1299; e) Shuto, S.; Shirato, M.; Sumita, Y.; Ueno, Y.; Matsuda, A. *J. Org. Chem.* **1998**, *63*, 1986–1994.
- ²⁶ Wagner, G. K.; Black, S.; Guse, A. H.; Potter, B. V. L. *Chem. Comm.* **2003**, *70*, 1944–1945.
- ²⁷ (a) Nakagawa, I.; Kony, S.; Ohtani, S.; Hata, T. *Synthesis* **1980**, 556–557. (b) Sekine, M.; Kamimura, T.; Hata, T. *J. Chem. Soc., Perkin 1* **1985**, 997–1000. (c) Sekine, M.; Nishiyama, S.; Kamimura, T.; Osaki, Y.; Hata, T. *Bull. Chem. Soc. Jpn.* **1985**, *58*, 850–860. (d) Fukuoka, K.; Suda, F.; Suzuki, R.; Ishikawa, M.; Takaku, H.; Hata, T. *Nucleosides Nucleotides* **1994**, *13*, 1557–1567.
- ²⁸ Fukuoka, M.; Shuto, S.; Minakawa, N.; Ueno, Y.; Matsuda, A. *J. Org. Chem.* **2000**, *65*, 5238–5248.
- ²⁹ Galeone, A.; Mayol, L.; Oliviero, G.; Piccialli, G.; Varra, M. *Tetrahedron* **2002**, *58*, 363–368.
- ³⁰ Galeone, A.; Mayol, L.; Oliviero, G.; Piccialli, G.; Varra, M. *Eur. J. Org. Chem.* **2002**, 4234–4238.
- ³¹ Bailey, V. C.; Sethi, J. K.; Fortt, S. M.; Galione, A.; Potter, B. V. L. *Chem. Biol.* **1997**, *4*, 51.
- ³² Shuto, S.; Fukuoka, M.; Kudoh, T.; Garnham, C.; Galione, A.; Potter, B. L. V. Matsuda, A. *J. Med. Chem.* **2004**, *446*, 1980–1988.
- ³³ Guse, A. H.; Cakir-kiefer, C.; Fukoka, M.; Shuto, S.; Weber, K.; Bailey, V. C.; Matsuda, A.; Mayer, G. W.; Oppenheimer, N.; Schuber, F.; Potter, B. V. L. *Biochemistry*, **2002**, *41*, 6744–6751.
- ³⁴ Guse A. H. *Curr Med Chem.* **2004**, *11*: 847–855.
- ³⁵ Kirchberger, T.; Wagner, G.; Xu, J.; Cordiglieri, C.; Wang, P.; Gasser, A.; Fliegert, R.; Bruhn, S.; Flugel, A.; Lund, F. E.; Zhang, L. H.; Potter, B. V. L.; Guse, A. H. *Br. J. Pharmacol.* **2006**, *149*, 337–344.

-
- ³⁶ a) L. De Napoli, A. Messere, D. Montesarchio, G. Piccialli, *J. Org. Chem.*, **1995**, 60, 2251-2253, b) G. Oliviero, J. Amato, N. Borbone, S. D'Errico, G. Piccialli, L. Mayol, *Tetrahedron Lett.* **2007**, 48, 397-400, c) M. Terrazas, X. Ariza, J. Farràs, J. Vilarrasa, *Chem. Commun*, **2005**, 3968-3970.
- ³⁷ A. Galeone, L. Mayol, G. Oliviero, G. Piccialli, M. Varra, *Eur. J. Org. Chem.* **2002**, 4234-4238.
- ³⁸ a) Uhlmann, E., Engels, J. *Tetrahedron Lett.* **1986**, 27, 1023-1026, b) Ahmadviebi, Y., Parang, K. *Org Lett.* **2005**, 7, 5589-5592.

Appendix

Publications

Synthesis of N-1 and ribose modified inosine analogues on solid support, Oliviero, G.; Amato, J.; Borbone, N.; D'Errico, S.; Piccialli, G.; and Mayol, L. *Tetrahedron Letters* **2007**, 48, 397-400.

A General Approach to the Synthesis of 1-Deoxy-L-iminosugars, Guaragna, A.; D'Errico, S.; D'Alonzo, D.; Pedatella, S.; Palumbo, G. *Organic Letters*. **2007**, 9, 3473-3476.

Synthesis of a new ribose modified analogue of cyclic inosine diphosphate ribose, Oliviero, G.; Borbone, N.; Amato, J.; D'Errico, S.; Piccialli, G.; Varra, M.; Mayol, L. *Nucleosides Nucleotides & Nucleic Acids* **2007**, 26, 1321-1324.

Synthesis and characterization of tetra-end linked oligonucleotides capable of forming monomolecular G-quadruplexes, Borbone, N.; Oliviero, G.; Amato, J.; D'Errico, S.; Galeone, G.; Piccialli, G.; Mayol, L. *Nucleosides Nucleotides & Nucleic Acids* **2007**, 26, 1231-1236.

Solid phase synthesis of nucleobase and ribose modified inosine nucleoside analogues, Oliviero, G.; Amato, J.; D'Errico, S.; Borbone, N.; Piccialli, G.; Mayol, L. *Nucleosides Nucleotides & Nucleic Acids* **2007**, 26, 1649-1652.

Synthesis of 4-N-alkyl and ribose-modified AICAR analogues on solid support. Oliviero, G.; Amato, J.; Borbone, N.; D'Errico, S.; Piccialli, G.; Bucci, E.; Piccialli, V.; Mayol, L. *Tetrahedron* **2008**, 64, 6475-6481.

Synthesis of N-1-alkyl analogues of cyclic inosine diphosphate ribose (cIDPR) by a new solid phase approach. Oliviero, G.; D'Errico, S.; Borbone, N.; Amato, J.; Piccialli, V.; Varra, M.; Piccialli, G.; Mayol, L. *Nucleic Acids Symposium Series* **2008**, 52, 573-574.

Ligand binding to tetra-end-linked (TGGGGT)₄ G-quadruplexes: an electrospray mass spectroscopy study. Amato, J.; Oliviero, G.; Borbone, N.; D'Errico, S.; Piccialli, G.; Mailliet, P.; Rosu, F.; De Pauw, E.; Gabelica, V. *Nucleic Acids Symposium Series* **2008**, 52, 165-166.

Oral Communications

Una rapida sintesi in fase solida di nuove collezioni nucleosidiche a potenziale attività antitumorale ed antivirale, D'Errico S.; Oliviero, G.; Amato, J.; Borbone, N.; Piccialli, G.; Piccialli, V.; Mayol, L. Giornate Scientifiche Polo delle Scienze e delle Tecnologie per la Vita, Napoli (Italia) Facoltà di Farmacia, 20-21 Settembre 2007.

Synthesis of N-1 and ribose modified inosine analogues on solid support

Giorgia Oliviero,^a Jussara Amato,^a Nicola Borbone,^b Stefano D'Errico,^a
Gennaro Piccialli^{a,*} and Luciano Mayol^b

^a*Facoltà di Scienze Biotecnologiche, Dipartimento di Chimica delle Sostanze Naturali, Università di Napoli Federico II,
via D. Montesano 49, Napoli 80131, Italy*

^b*Facoltà di Farmacia, Dipartimento di Chimica delle Sostanze Naturali, Università di Napoli Federico II,
via D. Montesano 49, Napoli 80131, Italy*

Received 11 October 2006; revised 9 November 2006; accepted 13 November 2006
Available online 1 December 2006

Abstract—Herein, we report the synthesis and the use of new *N*-1-dinitrophenyl-inosine based solid supports, in which the C-2 of the purine base is strongly activated toward the attack of *N*-nucleophiles. The synthesized supports, binding the nucleoside by a 5'-*O*-monomethoxytrityl function, have been used to accomplish the synthesis of a small library of *N*-1 alkylated inosine and AICAR derivatives. In addition, cleavage of the 2'-3' ribose bond of *N*-1 alkylated inosine derivatives anchored to the supports allowed to prepare a new set of *N*-1 alkylated-2',3'-secoinosine derivatives in high yields.

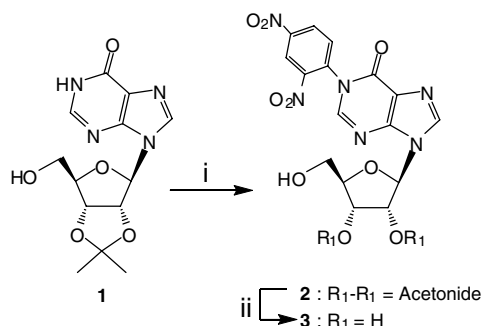
© 2006 Elsevier Ltd. All rights reserved.

Solid phase reactions have been extensively applied to a variety of organic reactions, furnishing an easy and rapid procedure for modifying functional groups and/or to conjugate specific molecules to target products. Solid phase reactions facilitate the synthesis of large libraries of compounds endowed with a series of molecular diversity motifs around a single core scaffold. Screening libraries of synthetic compounds for biological activity is currently the most widely used approach toward drug discovery. Nucleosides are biomolecules possessing a pivotal role in the metabolism. In fact, they are involved, as tri-phosphate derivatives, in the nucleic acid replications and in a very wide number of interactions with enzymes, structural proteins and other biological targets of therapeutic importance. In this light, it is not surprising that the most important antiviral drugs¹ currently used in therapy, and other active compounds exhibiting anti-neoplastic,² antibiotic, and antifungal properties,³ have been developed starting from this class of molecules. Recently, the interest toward large nucleoside libraries has emerged as an important synthetic goal to allow a

wide range of biological screenings. A variety of solid phase combinatorial strategies have been reported for the preparation of nucleoside and small oligonucleotide analogues libraries. In these approaches, both the chemical stability and the position of the linkage with the polymeric support play an important role in the selection of the chemical treatments allowing the nucleobase or sugar–phosphate modifications. For example, a solid support binding uridine or thymidine by the acid labile 5'-*O*-trityl function has been used to prepare libraries of *N*-4-alkylated cytidine derivatives.⁴ Another recently reported nucleoside-bearing support has exploited the alkaline labile 5'-*O*-succinyl linkage to bind the 6-chloro-2-nitro-inosine to synthesize a set of *N*-6- or *N*-2-alkylated adenosine derivatives.⁵ Also the 2',3'-acetal linkage has been used to bind nucleosides to a solid matrix which has been employed to introduce chemical diversities both on the base (C-6 of purine and C-4 of pyrimidine) and on the 5'-ribose position.⁶ In another approach, recently proposed by some of us, a purine or pyrimidine nucleoside was anchored to the solid support by the *N*-3 or *N*-1 base position, respectively, through a *N*-alkyl- β -thioether function^{7,8} which resulted stable to both the acidic and basic conditions. The above supports have been used to synthesize 2',3'-ribose modified nucleoside or nucleotide analogues. Furthermore, controlled pore glass (CPG) supports, loading

Keywords: Nucleoside analogues; Solid phase synthesis; Combinatorial chemistry.

* Corresponding author. Tel.: +39 081 678541; fax: +39 081 678552;
e-mail: piccialli@unina.it



Scheme 1. Reagents and conditions: (i) DNCB (2.2 equiv), K_2CO_3 (2.0 equiv) 2 h, 80 °C; (ii) $\text{HCOOH}/\text{H}_2\text{O}$ (6:4, v/v), 4 h, rt.

5'-DMT-nucleosides by the classical 3'-succinyl linkage^{9–11} or by the 3'-acyloxyaryl phosphate linker,¹² have been successfully exploited to prepare very large nucleic-acid-bases (NABTM) libraries of 5'-phosphoramidate nucleoside derivatives and nucleic acid fragments to be tested in their antiviral activity.

In an effort to enlarge the nucleoside chemical reactivity on the solid phase and consequently the number of accessible structurally diverse analogues, we report here the synthesis and exploitation of the new nucleoside functionalized supports **4** and **5** which bind the *N*-1-dinitrophenyl-inosine derivatives **2** or **3** through the 5'-*O*-trityl function. These supports have been employed in the synthesis of the *N*-1 substituted inosine **8a–e**, **9a–e**, the related 2',3'-seconucleoside derivatives **11a–e** and the 5-aminoimidazole-4-carboxamide riboside (AICAR) derivatives **14** and **15**. The here proposed solid phase strategy is based on our previous studies on the C-2 reactivity of the *N*-1-dinitrophenyl-2'-deoxyinosine toward *N*-nucleophiles^{13,14} that allowed to obtain *N*-1 substituted inosine and AICAR derivatives. In particular, according to the reported reaction mechanism, when a strong electron-withdrawing group (such as the 2,4-dinitrophenyl, nitro,¹⁵ or arylsulfonyl¹⁶ group) is attached to the *N*-1 atom of the hypoxanthine ring, the C-2 carbon becomes electrophilic enough to react with amino nucleophiles ($\text{R}_2\text{-NH}_2$). This leads to the opening of the six membered ring through the cleavage of the (*N*-1)–(C-2) bond. The successive fast ring re-closure, favoured by the loss of the 2,4-dinitroaniline as the leaving group, furnished the *N*-1 alkyl inosine derivatives. It is to be noted that as a consequence of the purine rearrangement, the endocyclic *N*-1 atom is substituted by the nitrogen atom of the nucleophilic reactant. This purine reactivity has also been used by others to introduce modified purine bases into oligonucleotides.¹⁷ Thus, to obtain a small library of *N*-1 alkyl inosine derivatives, we bound the 1-(2,4-dinitrophenyl)-2',3'-*O*-isopropylideneinosine **2**, or the corresponding unprotected inosine derivative **3** (Scheme 1 and 2), to the commercially available polystyrenemonomethoxytrityl chloride (MMTCl) resin by 5'-*O*-trityl ether linkage. Inosine derivative **2** was synthesized by reaction of the commercially available 2',3'-*O*-isopropylidene inosine **1** with 2,4-dinitrochlorobenzene (DNCB) essentially as previously described.¹⁸ The 2'-3' deprotected inosine derivative **3**[†] was obtained treating **2** with aqueous for-

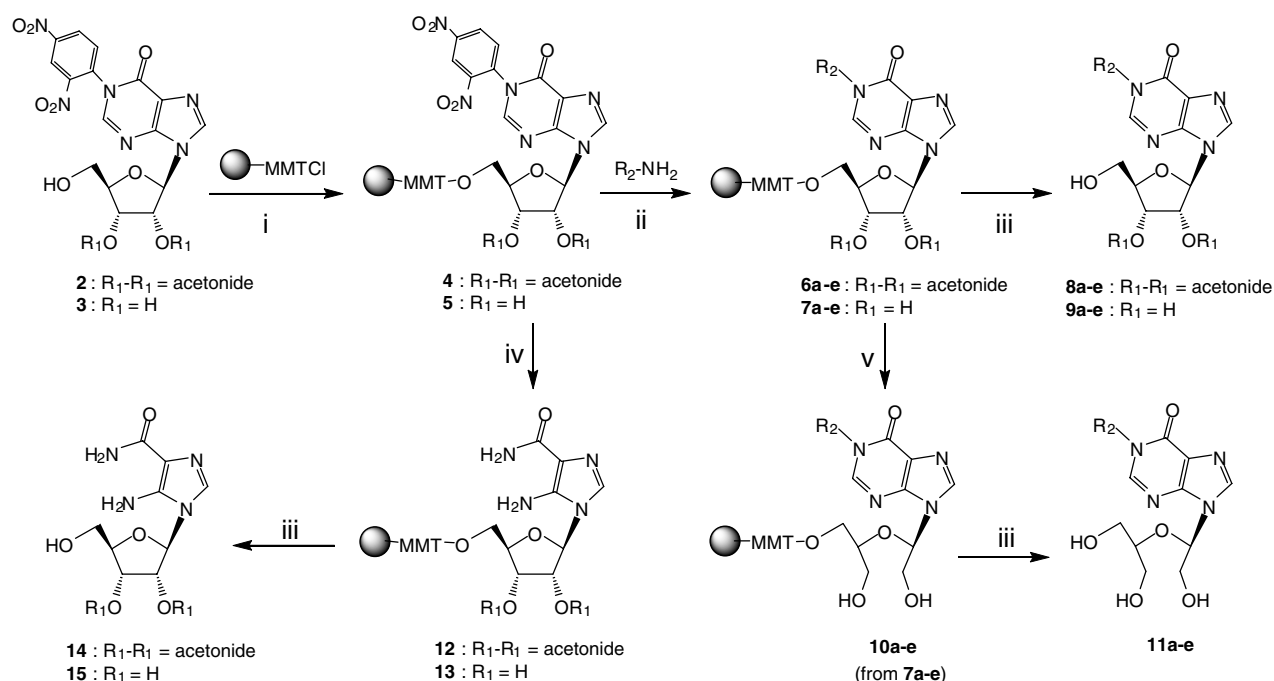
mic acid (90% yield). The reaction of the MMTCl polystyrene resin (1.3 mequiv/g) with **2** or **3** in anhydrous pyridine at room temperature and in the presence of 4-(*N,N*-dimethylamino)pyridine (DMAP) afforded support **4** or **5**, respectively, in almost quantitative yield. The structure and the loading of supports **4** and **5** were confirmed by NMR analysis and quantitative UV experiments, on the released inosine derivatives **2** and **3** obtained by treating the support with 2% TFA in DCM (8 min, rt). Supports **4** and **5** were then reacted with several *N*-nucleophiles ($\text{R}_2\text{-NH}_2$, Table 1, entries a–e) to give supports **6a–e** and **7a–e**, respectively. In a typical reaction, 100 mg (0.13 mmol) of support **4** (or **5**), swollen in DMF, was left in contact with the $\text{R}_2\text{-NH}_2$ nucleophile (5.0 mmol) in 1.5 mL of DMF under shaking (8 h, at 50 °C). After washings with DMF and MeOH, the support was dried under reduced pressure and the reaction yield was evaluated detaching the nucleoside material from a weighted amount of resin. The reaction of **4** or **5** with ethylenediamine (Table 1, entry f) furnished, as expected,¹⁴ supports **12** and **13** bearing the 2'-3'-isopropylidene-AICAR and the AICAR, respectively, in almost quantitative yields. The structure and the loading of supports **6**, **7**, **12**, and **13** were ascertained by analyzing with HPLC,[‡] ¹H NMR (Table 1) and MS[§] the corresponding detached *N*-1 alkyl inosine derivatives **8a–e**, **9a–e** as well as AICAR **14** and its derivative **15**. The purity and the yield of the above detached nucleosides, confirmed by HPLC analysis and quantitative UV experiments, resulted to be always over 90–95%, (Table 1). Starting from 20 mg of solid support (**4** or **5**), and considering an average molecular weight of 300 g/mol, 6–7 mg of each nucleoside derivative could be obtained in 90–98% purity, thanks to the almost quantitative reaction yields.

The second goal of this work was to combine the set of the *N*-1 alkylated inosine derivatives (from supports **7**) with a ribose modification. As an example we have examined the well known 2',3'-oxidative cleavage of the ribose moiety generally carried out by reaction with metaperiodate followed by reduction of the di-aldehyde derivative which leads to 2',3'-seconucleosides.¹⁹ In a typical reaction, supports **7a–e** (100 mg, 0.13 mmol) were left in contact with a solution of NaIO_4 (1.3 mmol) in DMF/ H_2O (1.5 mL, 1:1, v/v) and shaken for 12 h at 60 °C. The resulting support, after washings with DMF and EtOH, was treated with NaBH_4 (2.6 mmol) in

[†] Product **3**, as a 1:1 mixture of atropisomers at *N*-1 phenyl bond; ¹H NMR (400 MHz, CD_3OD): δ 9.05 (s, 1H, H-3 DNP); 8.77 (dd, 1H, H-5 DNP); 8.49, 8.49, 8.48, 8.40 (s's, H-2 and H-8); 8.02 (dd, 1H, H-6 DNP); 6.10 and 6.12 (d's, 0.5 H each, H-1'); 4.69 and 4.64 (dd's, 0.5 H each, H-2'); 4.35 (m, 1H, H-3'); 4.15 (m, 1H, H-4'); 3.88 and 3.77 (m, 1H each, H-5').

[‡] HPLC analyses: RP18 analytic column eluted with a linear gradient of CH_3CN in 0.1 M TEAB (pH 7.0, from 0% to 60% in 60 min, flow 1.0 mL/min).

[§] ESI MS data *m/z* (calcd): **9a** 325.2 ($\text{M}+\text{H}^+$) (324.1); **9b** 313.2 ($\text{M}+\text{H}^+$) (312.1); **9c** 327.1 ($\text{M}+\text{H}^+$) (326.1); **9d** 355.1 ($\text{M}+\text{H}^+$) (354.1); **9e** 343.2 ($\text{M}+\text{H}^+$) (342.1); **11a** 349.1 ($\text{M}+\text{Na}^+$) (326.2); **11b** 337.2 ($\text{M}+\text{Na}^+$) (314.1); **11c** 351.2 ($\text{M}+\text{Na}^+$) (328.1); **11d** 379.2 ($\text{M}+\text{Na}^+$) (356.2); **11e** 367.2 ($\text{M}+\text{Na}^+$) (344.1); **15** 259.0 ($\text{M}+\text{H}^+$) (258.1).



Scheme 2. Reagents and conditions: (i) compound **2** or **3** (1.5 equiv) in pyridine (1.5 mL/250 mg of resin), DMAP (0.2 equiv), 24 h, rt; (ii) R₂-NH₂ (38.0 equiv) in DMF, 8 h, 50 °C; (iii) TFA 2% solution in DCM; (iv) EDA/DMF (1:1, w/w) 8 h, 50 °C; (v) NaIO₄ (10 equiv) in DMF/H₂O (1:1, v/v), 12 h, 60 °C; resin washings and treatment with NaBH₄ (20 equiv) in EtOH, 2 h, rt.

Table 1. Reactions of the supports **4** and **5**; products **8**, **9**, **11**, **14**, and **15**

Entry	R ₂ -NH ₂	8 , 9 , 14 , 15 Yield ^a (%)	9a-e and 15 ¹ H NMR ^b		11a-e Yield ^c (%)	¹ H NMR ^b	
			H-2; H-8; H-1'	R ₂ Moiety		H-2; H-8; H-1' (<i>seco</i>)	R ₂ Moiety
a		8 (98) 9 (98)	8.41; 8.36; 6.02	4.12; 1.76; 1.40; 0.98	11a (85)	8.30; 8.26; 6.04	4.00; 1.75; 1.38; 0.96
b		8 (96) 9 (95)	8.42; 8.26; 6.01	4.19; 3.82	11b (85)	8.28; 8.24; 6.04	4.20; 3.83
c		8 (98) 9 (96)	8.41; 8.32; 6.02	4.20; 3.60; 1.98	11c (84)	8.31; 8.26; 6.03	4.21; 3.60; 1.98
d		8 (98) 9 (98)	8.40; 8.35; 6.02	4.12; 3.56; 1.81; 1.59; 1.42	11d (82)	8.33; 8.27; 6.03	4.11; 3.55; 1.79; 1.58; 1.43
e		8 (92) 9 (90)	8.38; 8.32; 6.00	3.98 (2CH ₂ OH); 3.92 (CH)	11e (75)	8.29; 8.04; 6.05	4.02 (2CH ₂ OH) 3.95 (CH)
f		1 (98) 1 (98)	8.04; 5.66		NT	NT	

^a Starting from resin **4** or **5** respectively; the yield is almost coincident with the purity degree of the product.

^b 400 MHz, (CD₃OD) significant protons at ppm.

^c Starting from resin **5**; the yield (before HPLC purification) is almost coincident with the purity degree of the product.

1.5 mL of EtOH and shaken for 2.0 h at rt. After washings, the obtained supports **10a-e** were dried under reduced pressure and analyzed by detaching the nucleoside material by TFA treatment. HPLC analyses indicated that the 2',3'-secuinucleoside derivatives **11a-e** were obtained in 75–85% yield and with almost the same purity degree. The sole side-products, obtained in 15–25% yields, were the corresponding uncleaved nucleoside. All the structures were confirmed by ¹H NMR (Table

1) and MS analyses.[§] When the above oxidative cleavage was performed in EtOH/H₂O (various solvent ratios and temperatures were used), the corresponding secunucleosides were obtained in lower yields, most probably due to the negligible swelling of the polystyrene matrix in these solvent mixtures.

In conclusion, we have reported the synthesis of new *N*-1-dinitrophenyl-inosine based solid supports (**4** and **5**) in

which the nucleosides are anchored to a MMT–polystyrene resin by the 5' position. Supports **4** and **5** were converted into the N-1 alkylated inosine supports (**6** and **7**) and AICAR derivatives supports (**12** and **13**) in very high yields, by reacting at C-2 position of the purine base with R–NH₂ nucleophiles. Detachment of the nucleosidic material from the above supports furnished, in high yields and purities, small libraries of N-1 alkylated inosines (**8a–e**, **9a–e**) and AICAR derivatives (**14** and **15**) (90–98%) possessing the ribose moiety either protected or unprotected at the 2'-3'-hydroxyl functions. In a further solid phase reaction, we have combined the set of the N-1 alkylated inosine of supports **7a–e** with the cleavage of the 2',3' ribose bond. These reactions furnished the new group of solid supports **10a–e** bearing the corresponding acyclo-nucleosides. Supports **10a–e** released, under acidic conditions, the N-1 alkylated-2',3'-secoinosine derivatives **11a–e** in good yields and purity (75–85%). In our opinion, supports **6**, **7**, **10**, **12**, and **13** bearing nucleoside derivatives with high purity degree can be fruitfully utilized in a combinatorial manner to obtain a number of further derivatizations/conjugations both on the 1-(ω -hydroxy-alkyl) function and/or on the ribose or secoribose moieties. Further studies are currently in progress in this direction to obtain new large libraries of nucleoside analogues that will be screened against a wide range of biological assays.

Acknowledgements

This work is supported by Italian MURST (PRIN 2005). The authors are grateful to Centro di Servizi Interdipartimentale di Analisi Strumentale (CSIAS) for supplying the NMR facilities.

References and notes

- (a) Chu, C. K. In *Antiviral Nucleosides*; Elsevier, 2003; (b) Simons, C.; Wu, Q.; Htar, T. T. *Curr. Top. Med. Chem.* **2005**, *5*, 1191–1203; (c) De Clercq, E.; Neyts, J. *Rev. Med. Virol.* **2004**, *14*, 289–300.
- (a) Lagoja, I. M. *Chem. Biodiv.* **2005**, *2*, 1–50; (b) Kimura, K.; Bugg, T. D. H. *Nat. Prod. Rep.* **2003**, *20*, 252–273; (c) Rachakonda, S.; Cartee, L. *Curr. Med. Chem.* **2004**, *11*, 775–793; (d) Knapp, S. *Chem. Rev.* **1995**, *95*, 1859–1876.
- (a) Miura, S.; Izuta, S. *Curr. Drug Targets* **2004**, *5*, 191–195; (b) Parker, W. B.; Secrist, J. A.; Waud, W. R. *Curr. Opin. Invest. Drugs* **2004**, *5*, 592–596; (c) Szafraniec, S. I.; Stachnick, K. J.; Skierski, J. S. *Acta Pol. Pharm.* **2004**, *61*, 223–232.
- Ding, Y.; Habib, Q.; Shaw, S. Z.; Li, D. Y.; Abt, J. W.; Hong, Z.; An, H. *J. Comb. Chem.* **2003**, *5*, 851–859.
- Rodenko, B.; Wanner, M. J.; Koomen, G.-J. *J. Chem. Soc., Perkin Trans. 1* **2002**, 1247–1252.
- Epple, R.; Kudirka, R.; Greenberg, W. A. *J. Comb. Chem.* **2003**, *5*, 292–310.
- de Champdoré, M.; De Napoli, L.; Di Fabio, G.; Messere, A.; Montesarchio, D.; Piccialli, G. *Chem. Commun.* **1997**, 2079–2082.
- De Napoli, L.; Di Fabio, G.; D'Onofrio, J.; Montesarchio, D. *Synlett* **2004**, *11*, 1975–1979.
- Zhou, W.; Roland, A.; Jin, Y.; Iyer, R. P. *Tetrahedron Lett.* **2000**, *41*, 441–445.
- Jin, Y.; Roland, A.; Zhou, W.; Fauchon, M.; Lyaku, J.; Iyer, R. P. *Bioorg. Med. Chem. Lett.* **2000**, *10*, 1921–1925.
- Jin, Y.; Chen, X.; Côté, M.-E.; Roland, A.; Korba, B.; Mounir, S.; Iyer, R. P. *Bioorg. Med. Chem. Lett.* **2001**, *11*, 2057–2060.
- Roland, A.; Xiao, Y.; Jin, Y.; Iyer, R. P. *Tetrahedron Lett.* **2001**, *42*, 3669–3672.
- De Napoli, L.; Messere, A.; Montesarchio, D.; Piccialli, G. *J. Org. Chem.* **1995**, *60*, 2251–2253.
- De Napoli, L.; Messere, A.; Montesarchio, D.; Piccialli, G.; Varra, M. *J. Chem. Soc., Perkin Trans. 1* **1997**, 2079–2082.
- Ariza, X.; Bou, V.; Vilarrasa, J. *J. Am. Chem. Soc.* **1995**, *117*, 3665–3673.
- Narukulla, R.; Shuker, D. E. G.; Xu, Y.-Z. *Nucleic Acids Res.* **2005**, *33*, 1767–1778.
- Terraza, M.; Ariza, X.; Farràs, J.; Vilarrasa, J. *Chem. Commun.* **2005**, 3968–3970.
- Galeone, A.; Mayol, L.; Oliviero, G.; Piccialli, G.; Varra, M. *Eur. J. Org. Chem.* **2002**, 4234–4238.
- For example see Kumar, A.; Walker, R. T. *Tetrahedron* **1990**, *46*, 3101–3110.

A General Approach to the Synthesis of 1-Deoxy-L-iminosugars

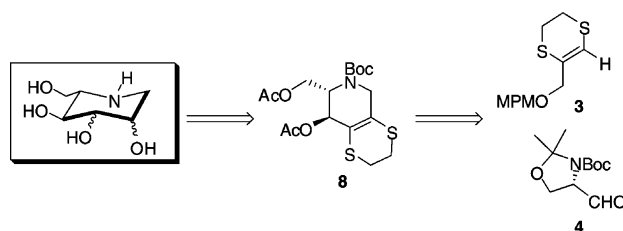
Annalisa Guaragna,* Stefano D'Errico, Daniele D'Alonzo, Silvana Pedatella, and Giovanni Palumbo

Dipartimento di Chimica Organica e Biochimica, Università di Napoli Federico II,
via Cynthia, 4 I-80126 Napoli, Italy

guaragna@unina.it

Received June 21, 2007

ABSTRACT



A stereoselective procedure for the preparation of non-naturally occurring deoxy iminosugars belonging to L-series has been developed. The synthesis involves the construction of the key intermediate bicycle pyridine **8**, available in few steps by the coupling of the heterocyclic synthon **3** and the readily available Garner aldehyde **4**.

Polyhydroxylated piperidines (commonly known as iminosugars or azasugars) represent sugar analogues with the nitrogen atom in place of the ring oxygen of the corresponding carbohydrate. Since their first discovery over 40 years ago, iminosugars have gained a great deal of attention as inhibitors of carbohydrate-processing enzymes glycosidases and glycosyltransferases. As extensively described,¹ their inhibitory aptitude has been linked with their structural resemblance to the glycone moiety of glycosides that interact with such enzymes.

As alterations in biosynthesis and function of these enzymes are implicated in a wide variety of diseases, the significant inhibitory properties of iminosugars make them excellent targets for medical intervention. Their prospective therapeutical uses range from diabetes² through cancer³ and viral diseases⁴ to metabolic and neurological disorders.⁵ As

a result, α -glucosidase inhibitors 1-deoxynojirimycin (DNJ, **1**) and *N*-butyl-1-deoxynojirimycin (NB-DNJ, Zavesca **2**) (Figure 1) have been shown to inhibit human immunodeficiency

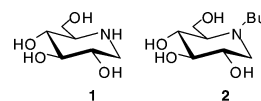


Figure 1. Bioactive iminosugars DNJ and NB-DNJ.

ciency virus (HIV) replication and HIV-mediated syncytium formation in vitro.⁶ Moreover, NB-DNJ has been the first iminosugar medicine to receive approval, in 2002 in the European Union and in 2003 in the United States, for use in patients with mild to moderate type 1 Gaucher disease.

The principal advances in total and stereoselective syntheses of such compounds have recently been reviewed.⁷ As reported, most syntheses have focused attention on the

* To whom correspondence should be addressed. Phone: + 39 081 674 118. Fax: + 39 081 674 119.

(1) (a) Stütz, A., Ed. *Iminosugars as Glycosidase Inhibitors*; Wiley-VCH: Weinheim, Germany, 1999. (b) Lillelund, V. H.; Jensen, H. H.; Liang, X.; Bols, M. *Chem. Rev.* **2002**, *102*, 515–553.

(2) Somsak, L.; Nagya, V.; Hadady, Z.; Docsa, T.; Gergely, P. *Curr. Pharm. Des.* **2003**, *9*, 1177–1189.

(3) Weiss, M.; Hettmer, S.; Smith, P.; Ladisch, S. *Cancer Res.* **2003**, *63*, 3654–3658.

(4) Greimel, P.; Spreitz, J.; Stütz, A. E.; Wrodnigg, T. M. *Curr. Topics Med. Chem.* **2003**, *3*, 513–523.

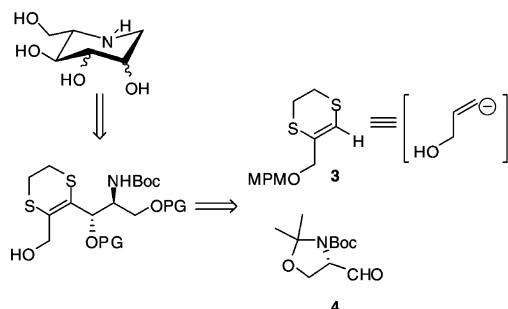
(5) Butters, T. D.; Dwek, R. A.; Platt, F. M. *Chem. Rev.* **2000**, *100*, 4683–4696.

(6) Ficher, P. B.; Collin, M.; Karlsson, G. B.; Lames, W.; Butters, T. D.; Davis, S. J.; Gordon, S.; Dwek, R. A.; Platt, F. M. *J. Virol.* **1995**, *69*, 5791–5797.

preparation of iminosugars with D-configuration, whereas few routes are available for the synthesis of their corresponding L-analogues.⁸ This fact is evidently due to the larger commercial availability of D-series sugars as starting materials, as well as to the fact that glycosides belonging to D-series are the natural substrates of almost all glycosidases. However, it is worth recalling that iminosugars mimicking the sugar moiety structure of the natural substrate are not always inhibitors of the corresponding glycosidase. D-manno-DNJ (DMJ) is known as a much better inhibitor of α -L-fucosidase than α -D-mannosidase; on the other hand L-*allo*-DNJ is a better inhibitor of α -D-mannosidase than D-DMJ.⁹ As recently shown,¹⁰ an explanation of this behavior could be found considering that D-enantiomers are competitive inhibitors of D-glycosidases, whereas their L-enantiomers are noncompetitive inhibitors of the same enzymes.

In the context of our ongoing program directed toward the achievement of a new synthetic methodology for the preparation of polyhydroxylated molecules, we have developed a versatile strategy for the synthesis of non-naturally occurring deoxy-iminopyranoses belonging to L-series, through a non-carbohydrate based route.

Scheme 1. Retrosynthetic Path



As outlined in Scheme 1, the synthesis involves the use of an heterocyclic synthon, the 5,6-dihydro-1,4-dithiin-2-yl-[(4-methoxybenzyl)oxy]methane¹¹ (**3**), a reagent capable of three-carbon homologation of electrophiles by the introduction of a fully protected allylic alcohol moiety, already

devoted to the preparation of several polyhydroxylated compounds.¹²

The synthesis began with the coupling of the in situ prepared C-3 lithiated carbanion of **3** with the Garner¹³ aldehyde **4** (Table 1) to afford a syn/anti diastereomeric

Table 1. Three-Carbon Homologation

solvent	catalyst (20%)	(anti/syn) dr	yield(%)
THF	none	60:40	83
THF	Ti(<i>O</i> - <i>i</i> -Pr) ₄	60:40	80
THF	Cp ₂ TiCl ₂	60:40	85
Et ₂ O	Cp ₂ TiCl ₂	70:30	49
Et ₂ O	ZnBr ₂	82:18	73
Et ₂ O	none	91:9	72

mixture of alcohols **5**. As highlighted in Table 1, the best stereoselectivity was achieved by the use of Et₂O without catalyst, providing *anti*-**5** in good stereoselectivity (91:9 dr). Interestingly, the stereochemical outcome of the reaction seemed to be mainly influenced by the nature of the solvent,¹⁴ whereas any significant stereoselective induction was not observed in the presence of the catalysts.¹⁵

The secondary alcohol¹⁶ *anti*-**5**, obtained by the coupling reaction, was separated from its diastereomer by flash chromatography; the stereochemical assignment at the newly generated C-4 was clearly deduced by X-ray analysis (Figure 2).

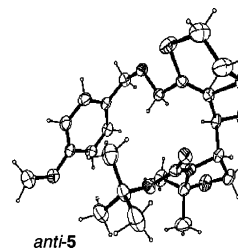


Figure 2. X-ray analysis of *anti*-**5**.

With the educt **5** in hand, our interest was focused on the achievement of key intermediate **9** (Scheme 2). To this purpose, we converted the alcohol **5** in its diacetate **6** by deprotection of the oxazolidine ring and acetylation of the

(7) For comprehensive reviews see: (a) Afarinkia, K.; Bahar, A. *Tetrahedron: Asymmetry* **2005**, *16*, 1239–1287. (b) Pearson, M. S. M.; Allaimat, M. M.; Fargeas, V.; Lebreton, J. *Eur. J. Org. Chem.* **2005**, 2159–2191. Carbohydrate-based routes to DNJ and congeners: (c) Asano, N.; Oseki, K.; Kizu, H.; Matsui, K. *J. Med. Chem.* **1994**, *37*, 3701–3706. (d) O'Brien, J. L.; Tosin, M.; Murphy, P. V. *Org. Lett.* **2001**, *3*, 3353–3356. (e) Spreidz, J. S.; Stütz, A. E.; Wrodnigg, T. M. *Carbohydr. Res.* **2002**, *337*, 183–191 and references cited therein. Non-carbohydrate based routes to DNJ and congeners: (f) Haukaas, M. H.; O'Doherty, G. A. *Org. Lett.* **2001**, *3*, 401–404. (g) Ruiz, M.; Ojea, V.; Ruanova, T. M.; Quintela, J. M. *Tetrahedron: Asymmetry* **2002**, *13*, 795–799. (h) Takahata, H.; Banba, Y.; Sasatani, M.; Nemoto, H.; Kato, A.; Adachi, I. *Tetrahedron* **2004**, *60*, 8199–8205 and literature cited therein.

(8) Meyers, A. I.; Andres, C. J.; Resek, J. E.; Woddall, C. C.; McLaughlin, M. A.; Lee, P. H.; Price, D. A. *Tetrahedron* **1999**, *55*, 8931–8952.

(9) Kato, A.; Kato, N.; Kano, E.; Adachi, I.; Ikeda, K.; Yu, L.; Okamoto, T.; Banba, Y.; Ouchi, H.; Takahata, H.; Asano, N. *J. Med. Chem.* **2005**, *48*, 2036–2044.

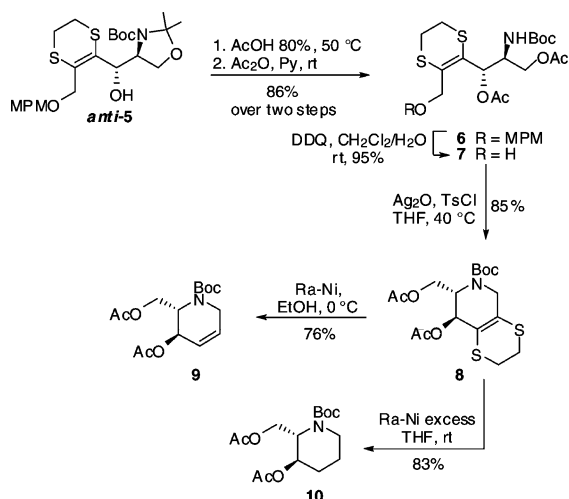
(10) Asano, N.; Ikeda, K.; Yu, L.; Kato, A.; Takebayashi, K.; Adachi, I.; Kato, I.; Ouchi, H.; Takahata, H.; Fleet, G. *Tetrahedron: Asymmetry* **2005**, *16*, 223–229.

(11) Guaragna, A.; Palumbo, G.; Pedatella, S. In *e-Encyclopedia of Reagents for Organic Synthesis*; Paquette, L. A., Ed.; John Wiley & Sons: New York, 2007. In press.

(12) (a) Caputo, R.; Guaragna, A.; Palumbo, G.; Pedatella, S. *J. Org. Chem.* **1997**, *62*, 9369–9371. (b) Caputo, R.; De Nisco, M.; Festa, P.; Guaragna, A.; Palumbo, G.; Pedatella, S. *J. Org. Chem.* **2004**, *69*, 7033–7037. (c) Guaragna, A.; Napolitano, C.; D'Alonzo, D.; Pedatella, S.; Palumbo, G. *Org. Lett.* **2006**, *8*, 4863–4866.

(13) Garner, P.; Park, J. M. *Org. Synth., Collected Vol. IX* **1998**, 300.

Scheme 2. Synthesis of the Key Intermediate **9**



crude residue (86% overall yield). Removal of MPM group by treatment of **6** with DDQ in a $\text{CH}_2\text{Cl}_2/\text{H}_2\text{O}$ (9:1) emulsion gave the primary alcohol **7** with an excellent yield (95%). Intramolecular cyclization was then carried out under mild conditions by treatment of **7** with $\text{Ag}_2\text{O}/\text{TsCl}$ in THF at 40 °C (85%). Finally, removal of the dithioethylene bridge on intermediate **8** was achieved by treatment with Raney-Ni in ethanol at 0 °C for 2 h leading to the olefin **9**. Moreover, when the reaction was carried out with a Raney-Ni excess in THF, at room temperature, the over-reduction product was obtained with a satisfactory yield (83%), affording the 1,2,3-trideoxy-L-iminosugar **10**.

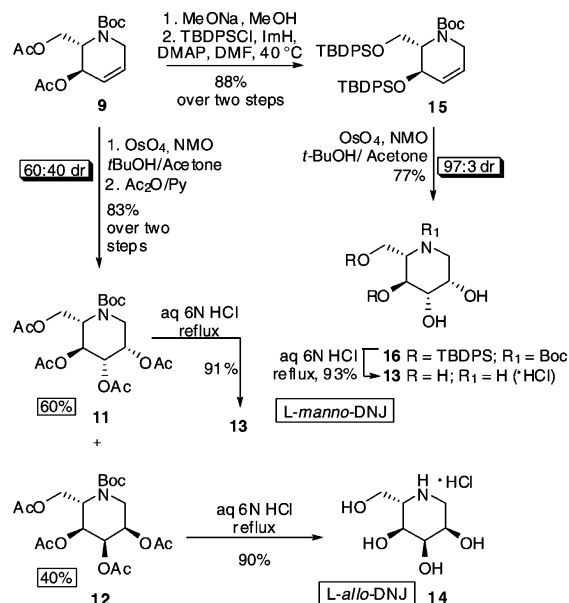
With the promising olefin **9** in hand our interest was directed to the stereoselective double-bond dihydroxylation (Scheme 3). Exposure of **9** to the common Upjohn conditions (OsO_4/NMO) followed by acetylation of the crude residue yielded a fully separable mixture of the protected *L*-manno-DNJ **11** and *L*-allo-DNJ **12** in low diastereomeric ratio (6:4). Both diastereomers were deprotected by means of refluxing aq 6 N HCl solution, obtaining deoxy-L-mannojirimycin (**13**) and deoxy-L-allonojirimycin (**14**) in remarkable yields (91% and 90%, respectively). Further attempts to improve the stereoselectivity of dihydroxylation reaction (i.e., using the bidentate complex $\text{OsO}_4/\text{TMEDA}$ ¹⁷ and the Sharpless catalysts¹⁸) showed no significant effects.¹⁹ The observed

(14) The solvent-dependent stereoselective effect should be related to the nature of the organolithium intermediate: as already reported (see farther on), a “nude” and more reactive ionic couple prevails in THF, while a less reactive non-ionized species is formed in Et_2O , driving the reaction towards a better stereoselective outcome: (a) Seyferth, D.; King, R. B. *Annual Surveys of Organometallic Chemistry*, Vol. 1–3, Elsevier Publishing Co.: Amsterdam, 1965–1967. (b) Maercker, A.; Roberts, J. D. *J. Am. Chem. Soc.* **1966**, *88*, 1742–1759.

(15) In all our experiments the reported syn stereoselection [Liang, X.; Andersch, J.; Bols, M. *J. Chem. Soc., Perkin Trans. I* **2001**, 2136–2157] was never observed. Because of the chemical characteristics of compound **5**, such discrepancy could be rationalized assuming that in the reaction medium the catalyst does not complex Garner aldehyde, but it can be sequestered by the negatively-charged heterocyclic system, without induction of stereoselectivity.

(16) An alternative numbering reported on the carbon skeleton has been employed to identify carbon atoms that will belong to the carbohydrate-like ring (see Table 1).

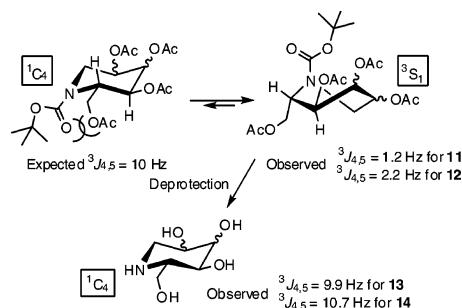
Scheme 3. Syn Dihydroxylation of **9**



low selectivity in the above dihydroxylation reactions might be attributed to the relatively small size of the C-4 acetyl group and thus both faces of the double bond were almost equally hindered. As a matter of fact, the replacement of the Ac groups of **9** with the much bigger TBDPS ethers (**15**, 88% overall yield, Scheme 3), afforded after dihydroxylation of **15**, under Upjohn conditions, the protected *L*-manno-DNJ **16** with a high stereoselectivity (97:3 dr). Then, treatment with aq 6 N HCl allowed removal of all protective groups to obtain deoxy-L-mannojirimycin (**13**) in 93% yield.

It is noteworthy to recall that the stereochemistry of compounds **13** and **14** is consistent with X-ray analysis of the *anti*-5 compound and with the spectroscopic data. However, observing the coupling constant values in the ^1H NMR spectra (Scheme 4), it is evident that the *N*-Boc

Scheme 4. Preferred Conformations for Compounds **11**, **12**

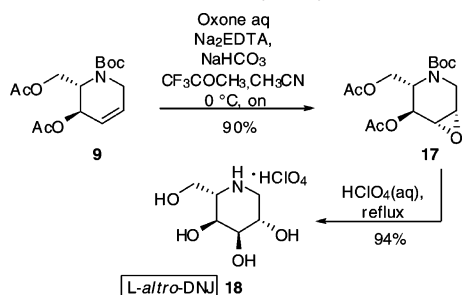


compounds **11** and **12** do not conform to the expected $^1\text{C}_4$ chair conformation, typical of *L*-sugars adopting a conformation close to $^3\text{S}_1$.²⁰

(17) Donohoe, T. J.; Blades, K.; Moore, P. R.; Waring, M. J.; Winter, J. J. G.; Helliwell, M.; Newcombe, N. J.; Stemp, G. *J. Org. Chem.* **2002**, *67*, 7946–7956.

The above successes led us to consider the anti dihydroxylation of the key olefin **9**. Treatment of this latter with in situ generated²¹ DMDO (oxone/trifluoroacetone) afforded exclusively the *anti*-epoxide **17** in 90% yield (Scheme 5).

Scheme 5. Anti Dihydroxylation of **9**



Ring opening²² of the 2,3-anhydro derivative **17** along with the removal of all protecting groups by means of

(18) Kolb, H. C.; VanNieuwenhze, M. S.; Sharpless, K. B. *Chem. Rev.* **1994**, *94*, 2483–2547.

(19) Wu, X.-D.; Khim, S.-K.; Zhang, X.; Cederstrom, E. M.; Mariano, P. S. *J. Org. Chem.* **1998**, *63*, 841–859.

(20) In the ¹C₄ chair form, a downward orientation is imposed on the *N*-Boc substituent owing to the nature of the ring nitrogen atom, resulting in a strong repulsive interaction with the nearly coplanar C-6 methylene group. An upward movement of the ring nitrogen relieves such repulsion leading to a ³S₁ conformation. For similar results see: (a) Kilonda, A.; Compennolle, F.; Hoornaert, G. J. *J. Org. Chem.* **1995**, *60*, 5820–5824. (b) Kazmaier, U.; Grandel, R. *Eur. J. Org. Chem.* **1998**, 1833–1840.

(21) Yang, D.; Wong, M.-K.; Yip, Y.-C. *J. Org. Chem.* **1995**, *60*, 3887–3889.

(22) On the basis of ¹H NMR coupling constant values we established that also **17** essentially exists in a ³S₁ conformation and that the formation of *trans*-diaxial ring opening product **18** could be explained assuming that the HClO₄ first removes the *N*-Boc group, allowing the chair inversion from ³S₁ to ¹C₄, and then leads to the epoxide cleavage.

refluxing HClO₄ gave the deoxy-L-altronojirimycin (**18**) in 94% yield.

In summary, a versatile pathway for the synthesis of L-deoxyiminosugars belonging to L-series has been opened up in this paper. Together with L-*manno*-, L-*allo*- and L-*altro*-deoxyiminosugars **13**, **14**, and **18**, whose synthesis has been described, this path will be profitably employed for the synthesis of all the epimers with *galacto* configuration, simply applying the same procedure on the *syn*-**5** diastereomer. Furthermore, the whole synthetic procedure so far described, carried out from **3** and the *ent*-**4** (prepared from D-serine) enables the preparation of D-series iminosugars as well.

Acknowledgment. This research has been supported by a Regione Campania grant to A.G. (L.R. 5/2002). ¹H and ¹³C NMR spectra and X-ray analysis were performed at Centro Interdipartimentale di Metodologie Chimico-Fisiche (CIMCF), Università di Napoli Federico II. Varian Inova 500 MHz instrument is property of Consorzio Interuniversitario Nazionale La Chimica per l'Ambiente (INCA) and was used in the frame of a project by INCA and M.I.U.R. (L. 488/92, Cluster 11-A). We are grateful to Dr Umberto Ciriello (ICI International Chemical Industry S.p.A.) for his collaboration to this work. We also thank Prof. Angela Tuzi (Dept. of Chemistry, University of Napoli) for X-ray analysis of *anti*-**5** compound.

Supporting Information Available: Experimental procedures, analytical data, X-ray crystallographic data (cif file) for *anti*-**5**, ¹H and ¹³C NMR spectra of all the new compounds. This material is available free of charge via the Internet at <http://pubs.acs.org>.

OL7014847

SYNTHESIS OF A NEW RIBOSE MODIFIED ANALOGUE OF CYCLIC INOSINE DIPHOSPHATE RIBOSE

Giorgia Oliviero, Nicola Borbone, Jussara Amato, Stefano D'Errico, Gennaro Piccialli, Michela Varra, and Luciano Mayol □ *Dipartimento di Chimica delle Sostanze Naturali, Università di Napoli "Federico II," Napoli, Italy*

□ *A new analogue of cyclic inosine diphosphate ribose (cIDPR), in which the N-1 and N-9 ribosyl moieties were substituted by an alkyl moiety and an hydroxy-alkyl chain, has been synthesized and characterized.*

Keywords cADPR; cIDPR; IP3; Ca^{2+}

INTRODUCTION

Cyclic ADP-ribose is an endogenous metabolite synthesized from NAD^+ by ADP-ribosyl cyclase in cells.^[1] In recent years cADPR has been attracting much attention because of its potent calcium-mobilizing activities as well as for its important role as a potent second messenger in cellular Ca^{2+} homeostasis, insulin secretion, and T-lymphocytes activation.^[2,3] It is also known to mobilize intracellular Ca^{2+} more actively than inositol-1,4,5-triphosphate (IP3) by a mechanism completely IP3 independent. Since Ca^{2+} ion regulate diverse cell functions, the cADPR signalling pathway may become a valuable target for pharmaceutical intervention.

cADPR is characterized by a very labile *N-1* glycosidic bond which is rapidly hydrolyzed, both enzymatically or not, to give ADP-ribose even in neutral aqueous solution. This biological and chemical instability can hinder the studies on cADPR aimed at elucidating its physiological role. Many nonhydrolyzable mimics of cADPR which retained a similar calcium release profile to that of cADPR are reported.^[4] Some structural modifications on cADPR adenine moiety make the mimic more potent than its parent—e.g. the 3-deaza-cADPR is 70-fold more potent than cADPR.^[5] Additional structural modification includes the pyrophosphate

Address correspondence to Giorgia Oliviero, Dipartimento di Chimica delle Sostanze Naturali, Università di Napoli "Federico II" via D. Montesano 49, Napoli I-80131, Italy. E-mail: golivier@unina.it

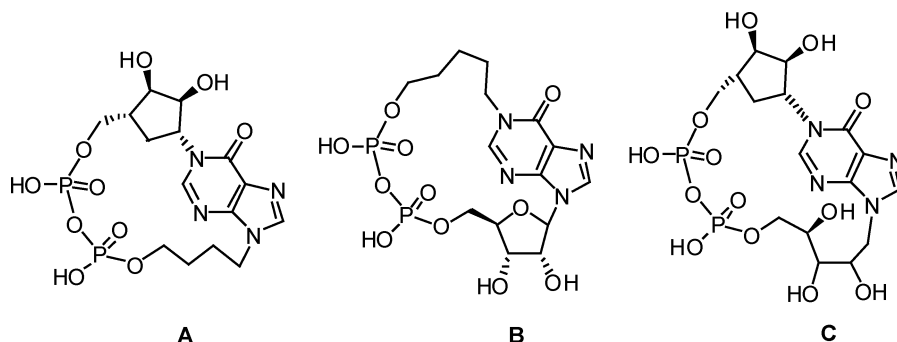
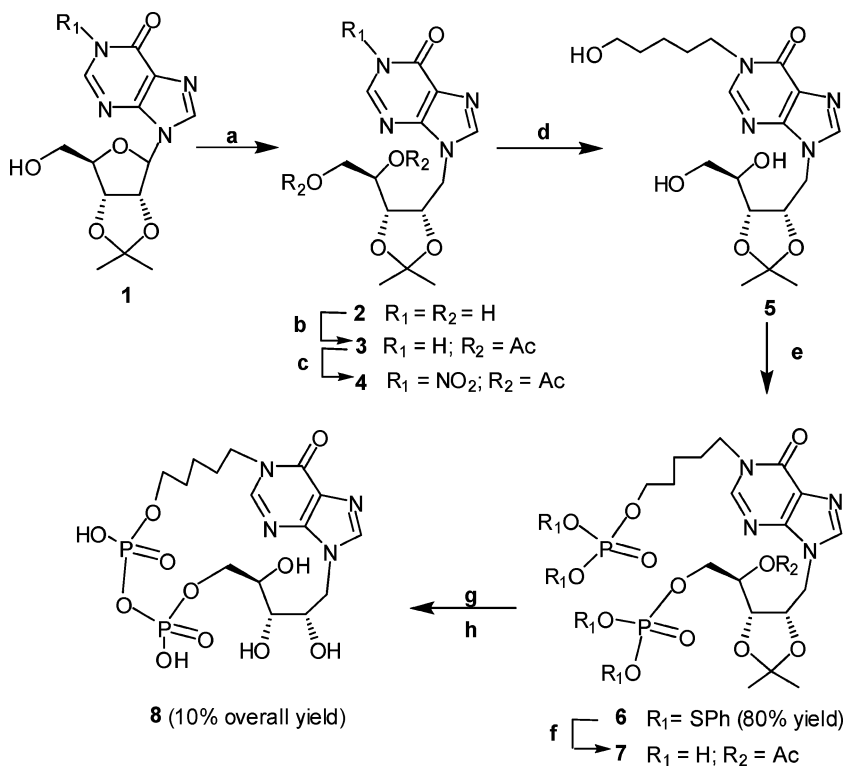


FIGURE 1 *N*-1 and/or *N*-9 modified analogues of cIDPR.

moiety. Cyclic adenosine triphosphate ribose was more potent in inducing Ca^{2+} release as compared to cADPR.^[6] Furthermore, *N*-1 deribosylated derivatives of cIDPR (methoxyethyl-8-substituted inosine) are found to be novel membrane permeant cADPR mimics causing the release of Ca^{2+} in human Jurkat T-lymphocytes.^[7] Recently we have proposed the syntheses of several analogues of cIDPR in which the *N*-1 or the *N*-9 ribosyl moiety has been replaced by an alkyl^[8,9] or hydroxyalkyl chain^[10] (products **A–C** Figure 1). To collect more information on the role of the *N*-1 and *N*-9 ribosyl moieties into Ca^{2+} release activity, we synthesized the new cIDPR analogue **8** (Scheme 1) containing a penthyl and an hydroxyalkyl chain at *N*-1 and *N*-9 hypoxanthine base positions, respectively.

The synthetic strategy adopted for **8** is shown in Scheme 1. The *N*-9 acyclic ribose inosine derivative **2** was obtained by reaction of the 2',3'-*O*-isopropylidene-inosine **1** with DIBALH.^[11] After protection of the alcoholic functions of **2** the *N*-1 nitro derivative **4** was obtained in good yield by reacting the diacetyl derivative **3** with ammonium nitrate and trifluoroacetic anhydride.^[12] The reaction of **4** with 5-amino-pentanol-1-ol furnished the derivative **5** which in turn was converted into the bis-phosphorylated compound **6** (80%) by treatment with *S,S*-diphenylphosphorodithioate (cyclohexylammonium salt) in the presence of 2,4,6-triisopropylbenzen-sulfonylchloride (TPSCl) and tetrazole in pyridine. In this reaction we observed the formation of the corresponding triphosphate derivative in 20% yield. **6** was acetylated at secondary alcoholic function and then treated with silver acetate to remove the phosphate protecting group.^[13] The obtained product **7** was purified by HPLC (RP18) before the cyclization step which was performed as previously described,^[10] thus obtaining **8** (10% overall yield starting from **1**), whose structure was confirmed by ¹H-NMR, ³¹P-NMR, and MS data. Studies on the biological activity of **8** are currently in progress.



SCHEME 1 Reagents and conditions: **a**) DIBALH, THF; **b**) Ac_2O , pyridine, r.t.; **c**) NH_4NO_3 , TFA, CH_2Cl_2 ; **d**) 5-aminopentanol, DMF, r.t. 8 hours; **e**) S,S-diphenylphosphorodithioate, TPSCI, pyridine, r.t., 8 hours; **f**) Ac_2O , AgAc, pyridine/ H_2O ; **g**) EDC, NMP, r.t.; 60 hours; **h**) aq. HCO_2H , r.t., 3.5 hours.

REFERENCES

- Hellmich, M.R.; Stumwasser, F. Purification and characterization of a molluscan egg-specific NADase, a second-messenger enzyme. *Cell. Regul.* **1991**, *2*, 193–202.
- Clapper, D.L.; Walset, T.F.; Dargie, P.J.; Lee, H.C. Pyridine nucleotide metabolites stimulate calcium release from sea urchin egg microsomes desensitized to inositol triphosphate. *J. Biol. Chem.* **1987**, *262*, 9561–9568.
- Shuto, S.; Matsuda, A. Chemistry of cyclic ADP-ribose and its analogs. *Curr. Med. Chem.* **2004**, *11*, 827–845.
- Lee, H.C. Physiological functions of cADPR and NAADP as calcium messengers. *Annu. Rev. Pharmacol. Toxicol.* **2001**, *41*, 317–345.
- Wong, L.; Aarhus, R.; Lee, H.C.; Walseth, T.F. Cyclic 3-deaza-adenosine diphosphoribose: A potent and stable analog of cyclic ADP-ribose. *Biochim. Biophys. Acta* **1999**, *1472*, 555–564.
- Zhang, F.J.; Yamado, S.; Gu, Q.M. Synthesis and characterization of cyclic ATP-ribose: A potent mediator of calcium release. *Bioorg. Med. Chem. Lett.* **1996**, *6*, 1203–1205.
- Gu, X.; Yang, Z.; Zhang, L.; Kunerth, S.; Fliegert, R.; Weber, K.; Guse, A. Synthesis and biological evaluation of novel membrane-permeant cyclic ADP-ribose mimics: N^1 -(5''-O-Phosphorylethoxy)methyl-5'-O-phosphorylinosine 5',5'-cyclicpyrophosphate (cIDPRE) and 8-substituted derivatives. *J. Med. Chem.* **2004**, *47*, 5674–5682.
- Galeone, A.; Mayol, L.; Oliviero, G.; Piccialli, G.; Varra, M. Synthesis of a novel *N-1* carbocyclic, *N-9* butyl analogue of cyclic ADP ribose (cADPR). *Tetrahedron* **2002**, *58*, 363–368.

9. Galeone, A.; Mayol, L.; Oliviero, G.; Piccialli, G.; Varra, M. Synthesis of a new N^1 -pentyl analogue of cyclic inosine diphosphate ribose (cIDPR) as a stable potential mimic of cyclic ADP ribose (cADPR). *Eur. J. Org. Chem.* **2002**, 24, 4234–4238.
10. Oliviero, G.; Amato, J.; Piccialli, G.; Varra, M.; Mayol, L. Synthesis of a new N -9 ribityl analogue of cyclic inosine diphosphate ribose (cIDPR) as a mimic of cyclic ADP ribose (cADPR). *Nucleosides Nucleotides Nucleic Acids* **2005**, 24, 735–738.
11. Hirota, K.; Monguchi, Y.; Kitade, Y.; Sajiki, H. Ribofuranose-ring cleavage of purine nucleosides with diisobutylaluminum hydride: Convenient method for the preparation of purine acyclonucleosides. *Tetrahedron* **1997**, 53, 16683–16698.
12. Ariza, X.; Bou, V.; Villarasa, J. A new route to ^{15}N -labeled, N -alkyl, and N -amino nucleosides via N -nitration of uridines and inosines. *J. Am. Chem. Soc.* **1995**, 117, 3665–3673.
13. Sekine, M.; Haoki, K.; Hata, T. Synthesis and properties of S,S -diaryl thymidine phosphorodithioates. *Bull. Chem. Soc. Jpn.* **1981**, 54, 3815–3827.

SYNTHESIS AND CHARACTERIZATION OF TETRA-END LINKED OLIGONUCLEOTIDES CAPABLE OF FORMING MONOMOLECULAR G-QUADRUPLEXES

Nicola Borbone, Giorgia Oliviero, Jussara Amato, Stefano D'Errico, Aldo Galeone, Gennaro Piccialli, and Luciano Mayol □ *Dipartimento di Chimica delle Sostanze Naturali, Università di Napoli "Federico II," Napoli, Italy*

□ *The chemical synthesis of two new G-rich Tetra-End-Linked-oligodeoxyribonucleotides (TEL-ODNs) as well as ¹H-NMR and CD spectra of the corresponding monomolecular quadruplexes (IVa and IVb) has been reported. The new TEL-ODNs, characterized by the presence of short branches in the linker moiety, could be very useful for the achievement of monomolecular quadruplexes with predetermined strand orientation.*

Keywords TEL-ODN; G-quadruplex; NMR

INTRODUCTION

DNA quadruple helices (quadruplexes) based on guanine (G) tetrads (Figure 1a) have recently emerged as biologically important structures.^[1] G-rich sequences, which are found primarily in telomeric region at the 3'-end of chromosomes, are able to fold into G-quadruplex structures. It has been suggested that quadruplex formation could inhibit the telomere maintenance provided by telomerase activity, thus affecting the lifespan of the cells of a number of cancer types characterized by a high level of telomerase expression.^[2] Furthermore, G-quadruplex structures are present in the scaffold of several aptamers provided with useful biological properties.^[3] G quadruplexes can be classified on the basis of the number and the polarity of the strands (Figure 1b–d), as well as for loop composition and conformation. Several studies have investigated the effect of loops on quadruplex stability and typology.^[4] We recently proposed the synthesis of a new class of modified tetra-end-linked G-rich ODNs (TEL-ODNs) capable of forming

This work is supported by Italian MURST (PRIN 2005). The authors are grateful to Centro di Servizi Interdipartimentale di Analisi Strumentale (CSIAS), for supplying the NMR facilities.

Address correspondence to Nicola Borbone, Dipartimento di Chimica, delle Sostanze Naturali, Università di Napoli "Federico II," via Domenico Montesano 49, Napoli 80131, Italy. E-mail: borbone@unina.it

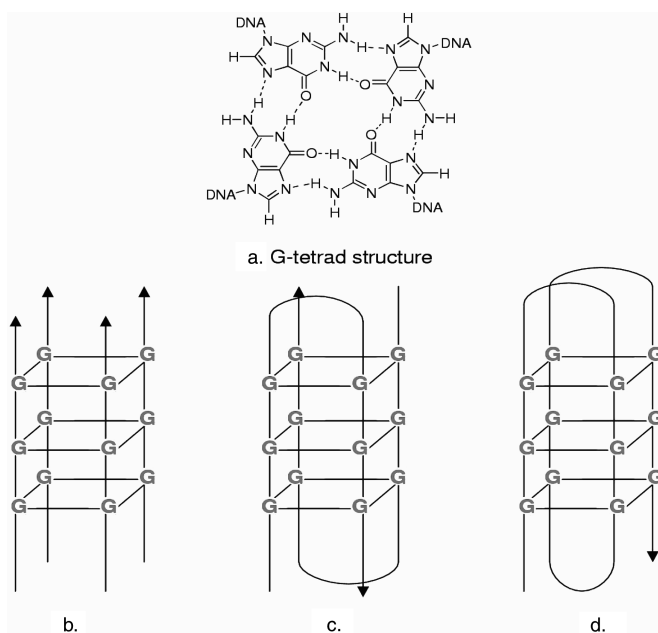
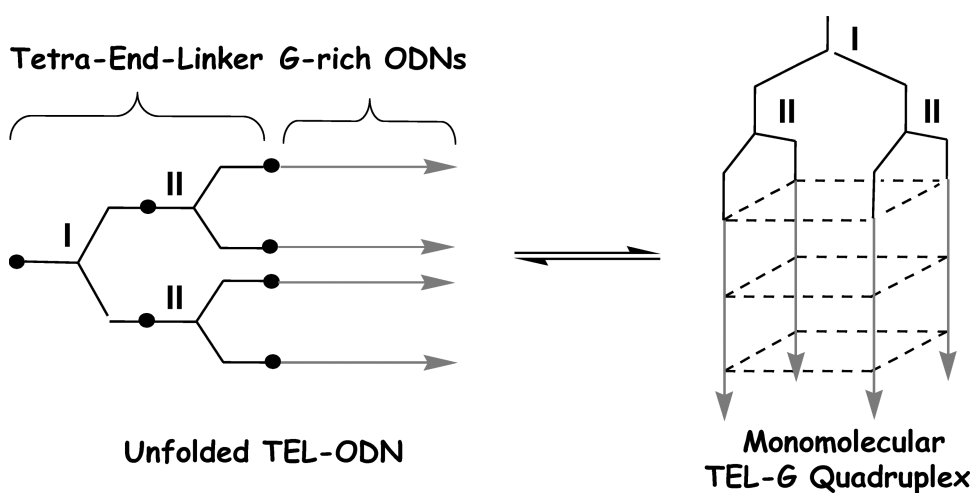
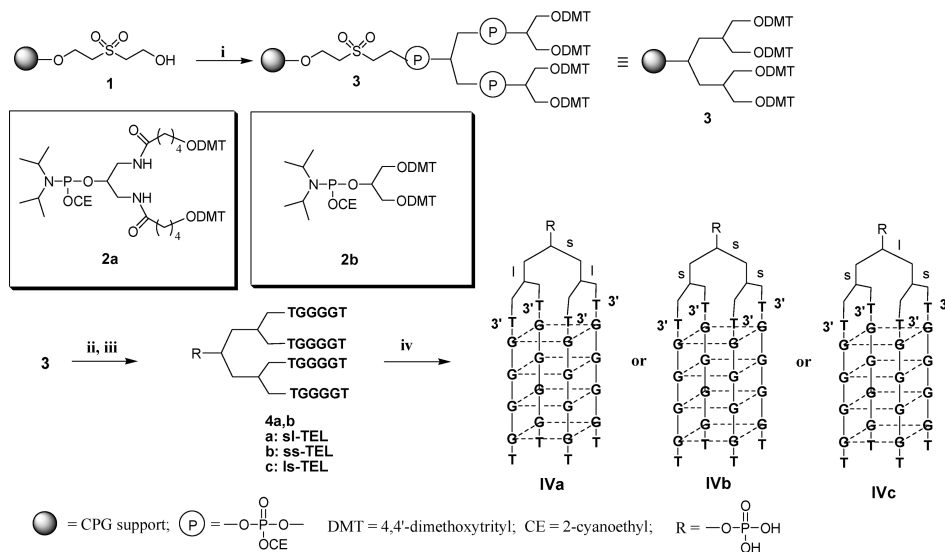


FIGURE 1 a) G-tetrad structure; b) tetramolecular parallel quadruplex; c) bimolecular antiparallel quadruplex; d) monomolecular antiparallel quadruplex.

monomolecular parallel G-quadruplexes characterized by faster kinetics and higher thermal stability than the correspondent tetramolecular counterparts (Scheme 1).^[5,6] Moreover, in the attempt to obtain monomolecular quadruplex structures characterized by predetermined strands stoichiometry and polarity, to be used as simple and stable models for structural studies



SCHEME 1 Schematic representation of unfolded (left) and folded (right) TEL-ODNs.



SCHEME 2 i) Two coupling procedures with **2a,b**; ii) ODN synthesis with 3'-phosphoramidites; iii) detachment and deprotection by NH_4OH conc. 32% (7 hours, 55°C); iv) HPLC purification and annealing.

on the quadruplex-ligand interaction, we recently synthesized a set of TEL-d(TGGGGT)₄ in which the ODN strands were linked with different orientations to the tetra-end linker. Structural studies performed on such compounds indicated that the TEL-d(TGGGGT)₄ assembled with two pairs of antiparallel ODN strands lead to parallel G-quadruplexes thanks to the considerable folding of the tetra-branched-linker around the whole quadruplex scaffold.^[7]

In this article, we report the syntheses of two new TEL-d(TGGGGT)₄ molecules (Scheme 2, **4a** and **4b**) characterized by the presence of one or three shorter branches in the TEL moieties (sl-TEL and ss-TEL, respectively). These structural features were chosen in the attempt to hinder the folding of the linker around the whole quadruplex structure thus forcing the predetermination of quadruplex strands polarity upon the basis of the relative orientation of the ODN strands into the TEL-ODN molecules.

RESULTS AND DISCUSSION

In the attempt to obtain monomolecular quadruplexes having predetermined strands polarity we designed the synthesis of two new tetra-branchedlinker moieties characterized by the shortening of the primary or both primary and secondary TEL branches (**sl-TEL** or **ss-TEL**, Scheme 2). To test if the sl-TEL and ss-TEL moieties were still able to allow the formation of stable quadruplex structures, we synthesized **4a** and **4b** via the

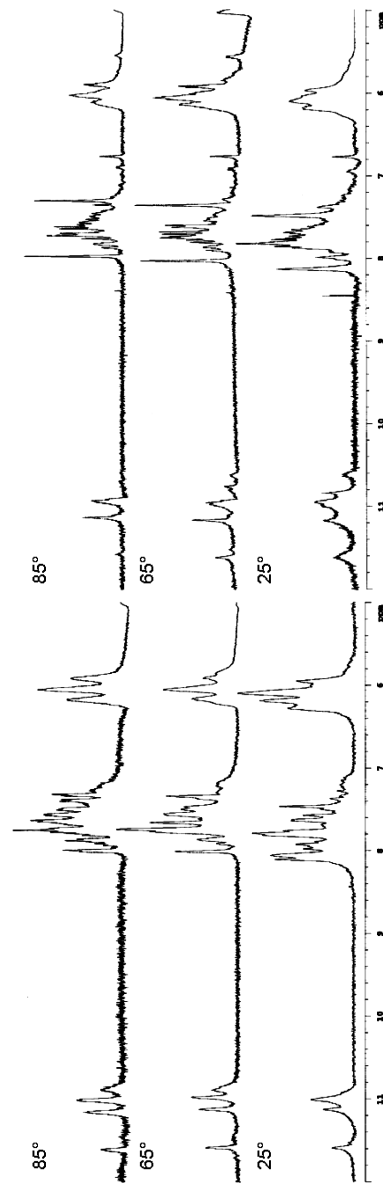


FIGURE 2 ¹H NMR spectra of **IVa** and **IVb** in 100 mM K⁺ buffer (500 MHz, H₂O/D₂O 9:1, v/v).

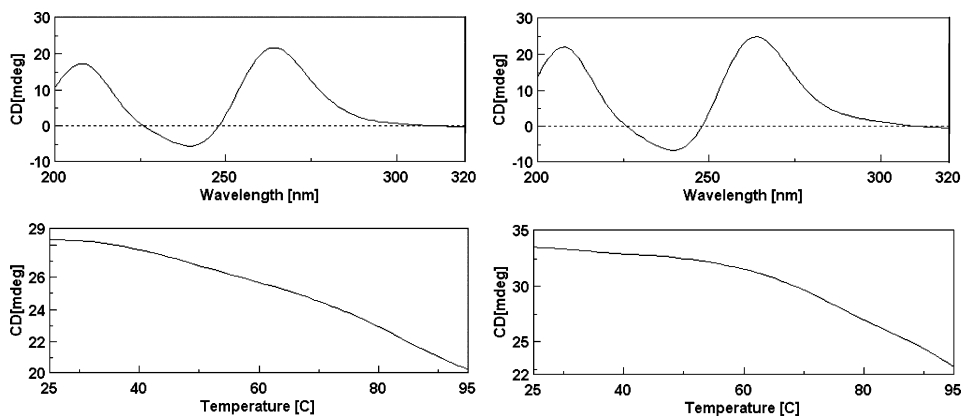


FIGURE 3 CD spectra (top; 25°C) and CD melting profiles (bottom; 264 nm, 1°C/minute) of **IVa** (left) and **IVb** (right) in 100 mM K⁺ buffer.

recently reported solid-phase procedure^[5] using the CPG support and the branching bi-functional linkers **2a** and **2b** as described in Scheme 2. We decided to not synthesize the ls-TEL-d(TGGGGT)₄ (**4c** in Scheme 2) because its primary branch is long enough to span the distance between the quadruplex edges, thus allowing the loss of strands polarity predetermination.

In order to assess if **4a** and **4b** could still fold into the quadruplex structures **IVa** and **IVb**, respectively, and if such were the case, to estimate their stabilities, we performed ¹H-NMR (at 25, 65, and 85°C using pulse field gradient WATERGATE^[8] sequences for H₂O suppression) and CD studies. Comparison of ¹H-NMR stacked spectra of **IVa** and **IVb** (Figure 2) showed that both adopted parallel quadruplex structures in the presence of K⁺ ions. However, it appeared that the presence of the ss-TEL moiety in **4b** lead to the lowering of the thermal stability of **IVb**, and to the partial loss of the magnetic equivalence between the imino protons in each G tetrad. On the other hand, **IVa**, characterized by the presence of the sl-TEL moiety, appeared to be very stable up to 85°C. Indeed, in the case of **IVa** no loss of imino protons magnetic equivalence was observed. Finally, the CD spectra and the CD melting curves were well in agreement with the NMR data (Figure 3). Upon the basis of these findings, the sl-TEL seems to be very promising for the achieving of monomolecular multistranded quadruplex structures characterized by both high thermal stability and predeterminable strands orientation. The synthesis of the antiparallel sl-TEL-d(TGGGGT)₄ is currently in progress in our laboratories.

REFERENCES

1. Neidle, S.; Parkinson, G. Telomere maintenance as a target for anticancer drug discovery. *Nat. Rev. Drug Disc.* **2002**, 1, 383–393.

2. Hazel, P.; Huppert, J.; Balasubramanian, S.; Neidle, S. Loop-length-dependent folding of G-quadruplexes. *J. Am. Chem. Soc.* **2004**, 126, 16405–16415.
3. Petraccone, L.; Barone, G.; Giancola, C. Quadruplex-forming oligonucleotides as tools in anticancer therapy and aptamers design: Energetic aspects. *Curr. Med. Chem.—Anti-Cancer Agents* **2005**, 5, 463–475.
4. Risitano, A.; Fox, K.R. Influence of loop size on the stability of intramolecular DNA quadruplexes, *Nucleic Acid Res.* **2004** 32, 2598–2606.
5. Oliviero, G.; Borbone, N.; Galeone, A.; Varra, M.; Piccialli, G.; Mayol, L. Synthesis and characterization of a bunchy oligonucleotide forming a monomolecular parallel quadruplex structure in solution, *Tetrahedron Lett.* **2004**, 45, 4869–4872.
6. Oliviero, G.; Amato, J.; Borbone, N.; Galeone, A.; Varra, M.; Piccialli, G.; Mayol, L. Synthesis and characterization of DNA quadruplexes containing T-tetrads formed by bunch-oligonucleotides. *Biopolymers* **2006**, 81, 194–201.
7. Oliviero, G.; Amato, J.; Borbone, N.; Galeone, A.; Petraccone, L.; Varra, M.; Piccialli, G.; Mayol, L. Synthesis and characterization of monomolecular DNA G-quadruplexes formed by tetra-end-linked oligonucleotides *Bioconjugate Chem.* **2006**, 17, 889–898.
8. Piotto, M.; Saudek, V.; Sklenar, V. Gradient tailored excitation for single-quantum NMR spectroscopy of aqueous solutions. *J. Biomol. NMR* **1992**, 2, 661–665.

SOLID PHASE SYNTHESIS OF NUCLEOBASE AND RIBOSE MODIFIED INOSINE NUCLEOSIDE ANALOGUES

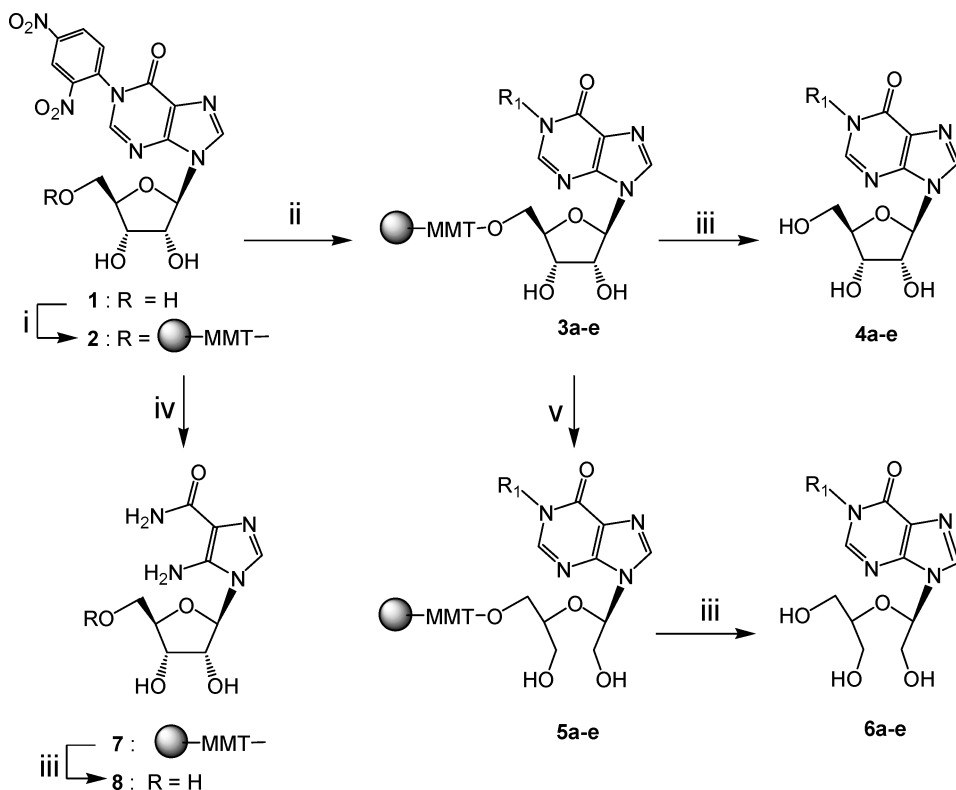
Giorgia Oliviero, Jussara Amato, Stefano D'Errico, Nicola Borbone, Gennaro Piccialli, and Luciano Mayol □ *Dipartimento di Chimica delle Sostanze Naturali, Università di Napoli Federico II, Napoli, Italy*

□ *The synthesis and the use of new N-1-dinitrophenyl-inosine based solid support is reported. The support, which binds the nucleoside by a 5'-O-monomethoxytrityl function, reacting with N-nucleophiles allowed the synthesis of a small library of N-1 alkylated inosine and AICAR derivatives. Moreover, the obtained supports, after the cleavage of the 2'-3' ribose bond, furnished a set of new N-1 alkylated-2'-3'-secoinosine derivatives in high yields.*

Keywords N-1-Dinitrophenyl-inosine based solid support; N-nucleophiles; 2'-3'-seconucleosides

Nucleosides are biomolecules possessing a pivotal role in the metabolism. In fact, they are involved, as tri-phosphate derivatives, in the nucleic acid replications and in a very wide number of interactions with enzymes, structural proteins, and nucleic acids. Furthermore, nucleosides are involved with a broad array of biological targets of therapeutic importance and a number of their derivatives exhibit antineoplastic,^[1] antibiotic,^[2] and antiviral properties.^[3] A variety of solid phase combinatorial strategies have been reported for the preparation of nucleoside and small oligonucleotide analogues libraries.^[4] In an effort to enlarge the nucleoside chemical reactivity on the solid phase, and, thus, the number of accessible structurally diverse analogues, we report here the new acid labile nucleoside functionalized support **2**, which binds the N-1-dinitrophenyl-inosine derivative **1** through the 5'-O-ribose position. These support has been employed in the solid phase synthesis of N-1 substituted inosine **4a–e**, the related 2'-,3'-seconucleoside derivatives **6a–e** and the 5-aminoimidazole-4-carboxamide riboside (AICAR) **8**. The solid phase strategy is based on our previous studies on the C-2 reactivity of N-1-dinitrophenyl-2'-deoxyinosine towards N-nucleophiles^[5,6] to obtain N-1 substituted inosine and AICAR derivatives.

Address correspondence to Giorgia Oliviero, Dipartimento di Chimica delle Sostanze Naturali, Università di Napoli Federico II, via D. Montesano 49, Napoli I-80131, Italy. E-mail: golivier@unina.it



SCHEME 1 i) **2** or **3** (1.5 eq.) in pyridine (1.5 mL/250 mg of resin), DMAP (0.2 eq.), 24 hours r.t.; ii) $R_1\text{-NH}_2$ /DMF (38.0 eq), 8 hours 50°C; iii) TFA 2% solution in DCM; iv) EDA/DMF (1:1, w/w) 8 hours 50°C; v) NaIO_4 (10 eq.) in DMF/ H_2O (1:1,v/v), 12 hours, 60°C; resin washings and treatment with NaBH_4 (20 eq.) in EtOH, 2 hours, r.t.

The reported reaction mechanism indicates that when a strong electron-withdrawing group (such as the 2,4-dinitrophenyl or the nitro group^[7]) is attached to the N-1 atom of the hypoxanthine ring, the C-2 carbon become electrophilic enough to react with amino nucleophiles ($R_1\text{-NH}_2$) leading to $R_1\text{-N-1}$ substituted inosine derivatives by a fast opening and re-closure of the six terms purine cycle.

Support **2** was obtained by reaction of the commercially available polystyrenemonomethoxytrityl chloride (MMTCl) with the 1-(2,4-dinitrophenyl)-inosine^[8] **1** (Scheme 1). The structure and the loading of the support **2** (1.2–1.3 meq/g) was confirmed analyzing, by ^1H NMR and quantitative UV experiments, the released inosine **1** by treatment with 2% TFA in DCM. The reaction of support **2** (100 mg, 0.13 mmol) with N-nucleophiles (5.0 mmol, $R_1\text{-NH}_2$, Table 1 entry **a–e**) in DMF (8 hours, at 50°C) gave supports **3a–e**. The reaction of **2** with ethylenediamine (Table 1, entry **f**) furnished, as expected,^[9] the support **7** bearing AICAR in almost quantitative yields. The structures of the supports **3a–e** and **7** were ascertained by HPLC, ^1H NMR, and MS analyses of the corresponding detached

TABLE 1 Reactions of the support **2** products **4**, **6**, and **8**. N.T.: not tested.

Entry	R ₁ -NH ₂	4a-e and 8 Yield ^a (%)	¹ H NMR ^b			¹ H NMR ^b		
			H-2; H-9; H-1'	R ₁ moiety	6a-e Yield ^c (%)	H-2; H-9; H-1'	R ₂ moiety	
a		4a , (98)	8.41; 8.36; 6.02	4.12; 1.76; 1.40; 0.98	6a (85)	8.30; 8.26; 6.04	4.00; 1.75; 1.38; 0.96	
b		4b , (96)	8.42; 8.26; 6.01	4.19; 3.82	6b (85)	8.28; 8.24; 6.04	4.20; 3.83	
c		4c , (97)	8.41; 8.32; 6.02	4.20; 3.60; 1.98	6c (84)	8.31; 8.26; 6.03	4.21; 3.60; 1.98	
d		4d , (98)	8.40; 8.35; 6.02	4.12; 3.56 1.81; 1.59; 1.42	6d (82)	4.21; 3.60; 1.98	4.11; 3.55; 1.79; 1.58; 1.43	
e		4e , (90)	8.38; 8.32; 6.00	3.98 (2CH ₂ OH); 3.92 (CH)	6e (75)	8.29; 8.04; 6.05	4.02 (2CH ₂ OH) 3.95 (CH)	
f		8 (98)	8.04; 5.66		N.T.	N.T.		

^aStarting from resin **2**.

^b400 MHz, (CD₃OD) significative protons at ppm.

^cStarting from resin **3**.

crude materials **4a–e** and **8**. The product yields and the ^1H NMR selected data are reported in Table 1. The second goal of this work was aimed to combining the set of the N-1 alkylations of the supports **3a–e** with the 2'-3'-oxidative cleavage of the ribose to obtain the related 2'-3'-seconucleoside derivatives.^[10] In a typical reaction the support **3a–e** (100 mg) was left in contact with a solution of NaIO_4 (1.3 mmol) in DMF/ H_2O (1:1,v/v) and shaken for 12 hours at 60°C . The resulting support was treated with NaBH_4 (2.6 mmol) in EtOH and shaken for 2.0 hours at room temperature. After washings, the resins **5a–e** were analyzed by detachment of the nucleosidic material by TFA treatment. HPLC analyses indicated that the 2'-3'-secoinosine derivatives **6a–e** were obtained in 75–85% yields. The structures of **6a–e** were confirmed by ^1H NMR (Table 1) and MS analyses.

In conclusion, we have reported the synthesis of the new N-1-dinitrophenyl-inosine based solid support **2**, which allowed the synthesis of small libraries of N-1 alkylated inosine derivatives **4a–e** and N-1 alkylated 2'-3'-secoinosine derivatives **6a–e** in good yields. Further studies are currently in progress in this direction to obtain new series of modified nucleoside analogues.

REFERENCES

1. a) Miura, S.; Izuta, S. *Current Drug Targets* **2004**, 5, 191–195; b) Parker, W.B.; Secrist, J.A.; Waud, W.R. *Current Opinion in Investigational Drugs* **2004**, 5, 592–596; c) Szafraniec, S.I.; Stachnick, K.J.; Skierski, J.S. *Acta Pol. Pharm.* **2004**, 61, 297–306.
2. a) Lagoja, I.M. *Chem. Biodiv.* **2005**, 2, 1–50; b) Kimura K.; Bugg, T.D.H. *Nat. Prod. Rep.* **2003**, 20, 252–273; c) Rachakonda, S.; Cartee, L. *Curr. Med. Chem.* **2004**, 11, 775–793.
3. (a) Chu, C.K., Ed. In *Antiviral Nucleosides*; Elsevier, New York; 2003; b) Simons, C.; Wu, Q.; Htar, T.T. *Curr. Top. Med. Chem.* **2005**, 5, 1191–1203; c) De Clercq, E.; Neyts, J. *Rev. Med. Virol.* **2004**, 14, 289–300.
4. For example see: a) Epple, R.; Kudirka, R.; Greenberg, W.A. *J. Comb. Chem.* **2003**, 5, 292–310; b) Ding, Y.; Habib, Q.; Shaw, S.Z.; Li, D.Y.; Abt, J.W.; Hong, Z.; An, H. *J. Comb. Chem.* **2003**, 5, 851–859; c) Rodenko, B.; Wanner, M.J.; Koomen, G.-J. *J. Chem. Soc., Perkin Trans. 1* **2002**, 1247–1252; d) Roland, A.; Xiao, Y.; Jin, Y.; Iyer, R.P. *Tetrahedron Lett.* **2001**, 42, 3669–3672.
5. De Napoli, L.; Messere, A.; Montesarchio, D.; Piccialli, G. *J. Org. Chem.* **1995**, 60, 2251–2253.
6. De Napoli, L.; Messere, A.; Montesarchio, D.; Piccialli, G.; Varra, M. *J. Chem. Soc., Perkin Trans. 1* **1997**, 2079–2082.
7. Ariza, X.; Bou, V.; Villarasa, J. *J. Am. Chem. Soc.* **1995**, 117, 3665–3673.
8. Galeone, A.; Mayol, L.; Oliviero, G.; Piccialli, G.; Varra, M. *Eur. J. Org. Chem.* **2002**, 4234–4238.
9. De Napoli, L.; Messere, A.; Montesarchio, D.; Piccialli, G.; Varra, M. *J. Chem. Soc., Perkin Trans. 1* **1997**, 2079–2082.
10. For example see: Kumar, A.; Walker, R.T. *Tetrahedron* **1990**, 46, 3101–3110.



Synthesis of 4-*N*-alkyl and ribose-modified AICAR analogues on solid support

Giorgia Oliviero^a, Jussara Amato^a, Nicola Borbone^b, Stefano D'Errico^a, Gennaro Piccialli^{a,*}, Enrico Bucci^c, Vincenzo Piccialli^d, Luciano Mayol^b

^a Facoltà di Scienze Biotecnologiche, Dipartimento di Chimica delle Sostanze Naturali, Università di Napoli Federico II, via D. Montesano 49, 80131 Napoli, Italy

^b Facoltà di Farmacia, Dipartimento di Chimica delle Sostanze Naturali, Università di Napoli Federico II, via D. Montesano 49, 80131 Napoli, Italy

^c Bioindustry Park del Canavese SpA, via Ribes 5, 10010 Colletterto Giacosa, Torino, Italy

^d Facoltà di Scienze MM.FF.NN., Dipartimento di Chimica Organica e Biochimica, Università di Napoli Federico II, via Cynthia 4, 80126 Napoli, Italy

ARTICLE INFO

Article history:

Received 15 November 2007

Received in revised form 2 April 2008

Accepted 17 April 2008

Available online 24 April 2008

Keywords:

AICAR

Nucleoside analogues

Solid-phase synthesis

Combinatorial chemistry

ABSTRACT

Herein, we report the solid-phase synthesis of several 5-aminoimidazole-4-(*N*-alkyl)carboxamide-1-ribosides (4-*N*-alkyl AICARs) and the corresponding 2',3'-secoriboside derivatives. The method uses the *N*-1-dinitrophenyl-inosine 5'-bonded to a solid support. This inosine derivative has the C-2 of the purine base strongly activated towards the attack of *N*-nucleophiles thus allowing the preparation of several *N*-1 alkylated inosine supports from which a small library of 4-*N*-alkyl AICAR derivatives has been synthesized. A set of new 4-*N*-alkyl AICA-2',3'-secoriboside derivatives have also been obtained in high yields by solid-phase cleavage of the 2',3'-ribose bond.

© 2008 Elsevier Ltd. All rights reserved.

1. Introduction

Nucleosides and their phosphorylated counterparts constitute an important class of biomolecules possessing a pivotal role in cellular metabolism and signal transmission. For example, they are involved in nucleic acid replication and in a very wide number of interactions with enzymes, structural proteins, and other biological targets of therapeutic importance. Many nucleoside analogues are currently used in therapy as antivirals¹ and others are active compounds exhibiting antineoplastic,² antibiotic, and antifungal properties.³ The research of new active nucleosides is still very dynamic and promising; substances such as nelarabine,⁴ entecavir,⁵ clofarabine,⁶ and azacitidine⁷ are examples of anticancer and antiviral drugs recently approved by U.S. FDA. Particular attention has recently been paid to 5-aminoimidazole-4-carboxamide-1-β-D-ribofuranoside (AICAR) since its 5'-phosphorylated derivative (ZMP), a key biosynthetic precursor of purine nucleotides, is an activator of AMP-activated protein kinase (AMPK).⁸ A possible therapeutic importance of its exploitation arises from the fact that the AICAR-induced AMPK activation strongly inhibits the basal and the insulin-stimulated glucose uptake, the lipogenesis, the glucose oxidation, as well as the lactate production in fat cells.⁹ It has been also found that the control of protein kinase C (PKC) activation is

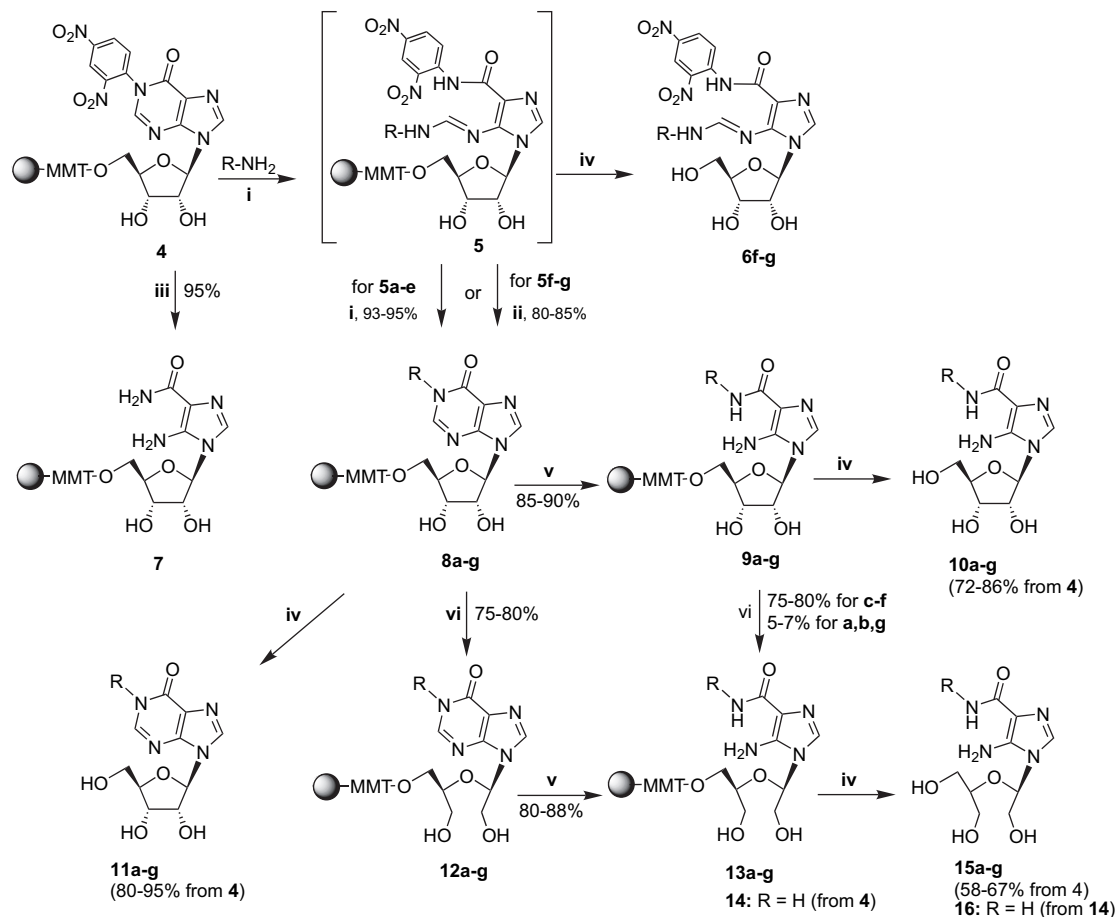
correlated with the pathogenesis of diabetic retinopathy.¹⁰ Furthermore, the extracellular role of adenosine and other nucleosides as endogenous cell function modulators indicates the adenosine receptors as significant targets with wide therapeutic potential. In this context, AICAR has been indicated as a promising prodrug, which induces benefits in patients suffering from autism, cerebral palsy, insomnia, schizophrenia, and other neuropsychiatric symptoms generally associated to chronic low levels of adenosine.¹¹ However, AICAR has short half-life in the cell, it does not efficiently cross the blood–brain barrier and is poorly adsorbed from the gastrointestinal tract. Consequently, the production of new AICAR derivatives is an appealing objective in the field of medicinal chemistry. In recent years, the syntheses of a number of AICAR derivatives, such as the 2-aryl,¹² 4-*N*-benzyl,¹³ 4-substituted,¹⁴ 5-substituted,¹⁵ 5-hydroxyl (Bredinin),¹⁶ triazolyl-riboside (Ribavirin),¹⁷ 2',3'-secoriboside derivatives,¹⁸ have been reported in the literature.

Recently, the production of large nucleoside analogue libraries has emerged as an important synthetic goal to chase the high efficiency and velocity of the current biological screenings. In this frame, the solid-phase synthesis, associated with a combinatorial approach, offers the advantage of combining the rapid synthesis with an easily obtainable molecular diversity around a single core scaffold.

In this paper, we report a new solid-phase synthetic strategy to obtain AICAR analogue libraries. The methodology has been tested in the synthesis of the two small AICAR libraries **10a–g** and **15a–g**

* Corresponding author. Tel.: +39 081 678541; fax: +39 081 678552.

E-mail address: picciall@unina.it (G. Piccialli).



Scheme 1. (i) $R-NH_2$ (38.0 equiv) in DMF, 8 h, 50 °C; (ii) 1 M K_2CO_3 in DMF, 15 h, 50 °C; (iii) EDA/DMF (1:1, w/w) 8 h, 50 °C; (iv) 2% TFA solution in DCM; (v) 5 M NaOH in EtOH, 6 h, reflux; (vi) $NaIO_4$ (10 equiv) in DMF/ H_2O (1:1, v/v), 12 h, 60 °C or $Pb(OAc)_4$ (15 equiv), in DCM, 2 h, rt; resin washings and treatment with $NaBH_4$ (20 equiv) in EtOH, 2 h, rt.

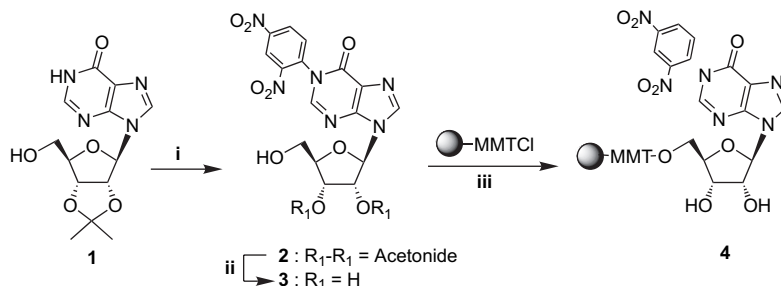
(Scheme 1) where the nucleosides are modified on the 4-carboxamide residue or both at the 4-carboxamide and the ribose moiety, respectively.

2. Results and discussion

Our synthetic approach uses as starting material the recently proposed *N*-1-dinitrophenyl-inosine solid support **4** synthesized as depicted in Scheme 2. Support **4** reacting with $R-NH_2$ nucleophiles is converted into *N*-1 alkyl-inosine solid supports **8a–g** from which the AICAR libraries **10a–g** and **15a–g** could be obtained (Scheme 1). In a previous paper, we utilized support **4** to prepare small libraries of *N*-1 alkyl-inosines and their corresponding 2',3'-secoriboside derivatives.¹⁹ We also demonstrated that when **4** reacts with ethylenediamine (EDA), the AICAR support **7** can be obtained in an almost quantitative yield.^{19,20} It is well known that, under alkaline


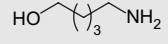
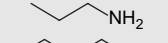
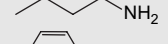
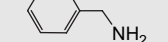
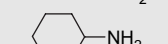
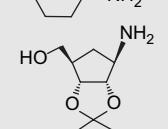
conditions, *N*-1 alkyl-inosines react at the C-2 of the purine system to give 4-*N*-alkyl AICAR derivatives by pyrimidine ring cleavage and concomitant extrusion of the C-2 carbon itself.²¹ Therefore, we decided to extend this process to the solid-phase chemistry aiming at two main targets: (i) to efficiently prepare a set of 4-*N*-alkyl AICAR derivatives (**10a–g**) as well as the corresponding precursor solid supports (**9a–g**) from *N*-1 alkyl-inosine supports **8a–g**; (ii) to combine the set of AICAR derivatives with a ribose modification (2',3'-secoribosyl derivatives) thus producing the new kind of products **15a–g**, as well as the related solid supports **13a–g**, which are in turn potentially useful for further AICAR derivatization/modification.

Support **4** was obtained by binding 1-(2,4-dinitrophenyl)-inosine **3** (Scheme 2) to the commercially available polystyrenemonomethoxytrityl chloride (MMTCl) resin by 5'-*O*-trityl ether linkage. Inosine derivative **3** was synthesized by the reaction



Scheme 2. (i) DNCB (2.2 equiv), K_2CO_3 (2.0 equiv), 2 h, 80 °C; (ii) $HCOOH/H_2O$ (6:4, v/v), 4 h, rt; (iii) **3** (1.5 equiv) in pyridine (1.5 mL/250 mg of resin), DMAP (0.2 equiv), 24 h rt.

Table 1
Reactions on the support **4**

Entry	R-NH ₂	6 , 11 , Yield ^a (%)	10 , 15 , Yield ^a (%)
a		6 (NI), 11 (95)	10 (81), 15 (60)
b		6 (NI), 11 (95)	10 (83), 15 (67)
c		6 (NI), 11 (93)	10 (84), 15 (63)
d		6 (NI), 11 (95)	10 (86), 15 (69)
e		6 (NI), 11 (94)	10 (83), 15 (62)
f		6 (90), 11 (85)	10 (76), 15 (59)
g		6 (85), 11 (80)	10 (72), 15 (58)

NI: not isolated.

^a Starting from support **4**.

of the commercially available 2'-3'-O-isopropylidene inosine **2** with 2,4-dinitrochlorobenzene (DNCB), followed by 2'-3' deprotection by aqueous formic acid treatment as previously described.¹⁹ The reaction of the MMTCl resin (1.3 mequiv g⁻¹) with **3** in the presence of 4-(*N,N*-dimethylamino)pyridine (DMAP), in anhydrous pyridine, afforded support **4** in almost quantitative yield. Reaction of **4** with several *N*-nucleophiles (R-NH₂, Table 1) furnished the *N*-1 alkyl-inosine supports **8a–g**. In the above reactions, the R-NH₂ nucleophiles react with the strongly activated purine C-2 atom to give the open intermediates **5** possessing an *N*-alkyl formamidine group. The successive fast ring re-closure, favored by the loss of 2,4-dinitroaniline as leaving group, led to *N*-1-alkyl-inosines **8a–e** (93–95% yields). We observed that in the case of sterically hindered amines (entries **f** and **g**), the reaction stopped at intermediate products **5**, which, after detachment from the support, could be isolated and characterized (**6f** and **g**). As previously demonstrated, treatment with carbonate in DMF (at 50 °C) converted these open-pyrimidine species **5** in the *N*-1-alkyl-inosine supports **8f** and **g** (80–85% yields) by the six-membered ring re-closure.²² Reaction yields obtained for **8a–g** were evaluated quantifying the *N*-1-alkyl-inosines **11a–g** released from a weighted amount of supports **8a–g** by treatment with 2% (v/v) TFA in DCM taking into account that the starting support **4** had a nucleoside functionalization of 1.26 mequiv g⁻¹. The corresponding 4-*N*-alkyl AICAR supports **9a–g** were then obtained by cleavage of the pyrimidine ring in supports **8a–g** by NaOH treatment (5 M in EtOH, reflux, 85–90% reaction yields). TFA treatment of supports **9a–g** released the crude AICAR derivatives **10a–g**, which were purified by HPLC. The overall yield (starting from support **4**) of the pure obtained nucleosides **10** and **11** are reported in Table 1. The structures and the purity of the products were confirmed by ¹H NMR spectroscopy and ESIMS data. In a typical reaction starting from 20 mg of solid support **4**, and considering an average molecular weight of 320 g mol⁻¹, 6–7 mg of each crude AICAR derivatives **10a–g** could be obtained in 70–85% purity.

Next, we explored the possibility of performing the 2',3'-oxidative cleavage of the ribose moiety in supports **9a–g**. In a first attempt, we employed the previously tested¹⁹ reaction conditions, namely sodium metaperiodate followed by borohydride reduction of the di-aldehyde products. In a typical reaction, the supports **9a–g** were left in contact with a solution of NaIO₄ (10 equiv excess) in DMF/H₂O and shaken for 12 h at 60 °C. The resulting supports, after washing, were treated with NaBH₄ in EtOH and shaken for 2.0 h at room temperature to give supports **13a–g** that were analyzed by detaching the nucleosidic material by TFA treatment. The HPLC

analyses and purifications indicated that the above reactions, leading to **15c–f**, proceeded with 75–80% yields, whereas complex reaction mixtures were obtained for supports **13a,b,g** leading to very low quantities of the corresponding products **15a,b,g** (5–7% yields). These results suggest that the presence of the 4-*N*-(ω-hydroxyalkyl) portion on the AICAR supports **9a,b,g** leads to large side reactions when the products were reacted with sodium metaperiodate. In the case of AICAR support **7**, the reaction furnished support **14** from which the AICA-2',3'-secoriboside **16**¹⁸ could be obtained in 70% overall yield (from **4**) after the usual TFA treatment. This prompted us to test the alternative pathway where the C2–C3 scission of the ribose moiety, with formation of 2',3'-secoribosides **12a–g**, was accomplished prior to the pyrimidine ring degradation. Following this route, ribose cleavage of **8a–g** furnished **12a–g** in good reaction yields (75–80%, from **8**), which in turn were converted into the pyrimidine-degraded supports **13a–g** from which the products **15a–g** were obtained as described above (80–88% yields from **12**). The success of this pathway demonstrated that the presence of a 2',3'-secoribosyl moiety does not interfere with the alkaline degradation of the purine ring leading to the AICA heterocyclic system. Though a 75–80% yield for the ribose cleavage could seem acceptable, we considered this result not completely satisfactory for a solid-phase reaction supporting a combinatorial synthetic strategy. In fact, the above reaction causes a reduction in the overall yield and purity of the derivatives **15a–g** (60–70% yields from **4**). In order to further improve the yield of the C2–C3 bond cleavage in ribose, lead tetraacetate (LTA)²³ was used in DCM or DMF. Though the process was accomplished at several LTA/**8a–g** ratios and varying the reaction time, no significant improvement of the 2',3'-secoribosyl derivatives **12a–g** was obtained after the usual NaBH₄ treatment (60–65% yields). However, it is to be noted that in both oxidative cleavage procedures (i.e., sodium metaperiodate or LTA) the predominant side products resulted to be the corresponding unreacted inosines **11a–g**.

2.1. Biological results

All compounds were tested for their effect on cellular proliferation using a human breast cancer cell line (MCF-7). The proliferative effects were evaluated in the absence of 5% fetal calf serum (FCS), while the anti-proliferative effects were evaluated in the absence of serum. The proliferation was evaluated by a standard colorimetric procedure (MTT test)²⁴ after 24 and 48 h in triplicate using 1 μM of each compound dissolved in water or in 10% ethanol to improve solubility. The toxicity of the 10:90 ethanol/water solution was tested separately. No significant effect on proliferation was observed for any compound tested. Further experiments using different conditions and cell lines are currently undergoing.

3. Conclusions

In conclusion, we have successfully utilized the *N*-1-dinitrophenyl-inosine solid support **4**, where the nucleoside is anchored to an MMT-polystyrene resin by the 5'-ribose position, to synthesize small libraries of inosine and AICAR derivatives. The following solid-phase reactions have been carried out on this support and its derivatives: (i) the *N*-1 alkylation of purine by reaction of **4** with a variety of amines (90–95% yields); (ii) the alkaline cleavage of the *N*-1 alkyl-inosine base leading to AICAR derivatives (85–90% yields); (iii) the 2',3'-oxidative cleavage of the ribose moiety (75–80% yields). The proposed synthetic pathways allowed the preparation of small libraries of the *N*-1 alkyl-inosines **11a–g**, 4-*N*-alkyl AICAR derivatives **10a–g**, and the corresponding 2',3'-secoriboside derivatives **15a–g**. It is to be noted that the reported solid-phase reactions proceed with yields comparable to, or higher than, those obtainable from the corresponding

procedures in solution. Furthermore, the proposed solid-phase procedures furnished a new group of solid supports bearing inosine derivatives (**8a–g**, **12a–g**) or AICAR derivatives (**9a–g**, **13a–g**), which can be utilized in a combinatorial manner to achieve a number of further derivatizations/conjugations both on the imidazolyl residue and/or on the ribose or 2',3'-secoribose moiety.

4. Experimental

4.1. General

4-Methoxytrityl chloride resin (1% divinylbenzene, 200–400 mesh, 1.3 mmol g⁻¹ substitution) was purchased from CBL Patras, Greece. Anhydrous solvents were used for reactions. All the other reagents were obtained from commercial sources and were used without further purification. The reactions on solid phase were performed using glass columns (10 mm diameter, 100 mm length) with fused-in sintered glass-disc PO (bore of plug 2.5 mm), which were shaken on an orbital shaker, or round bottom flask, when reactions were performed at high temperatures. Mps were determined on a Reichert Thermovar apparatus. IR spectra were collected on a Jasco FT-IR-430 spectrometer. The ¹H NMR spectra were performed on a Varian Mercury Plus 400 MHz using CD₃OD and CDCl₃ as solvents; chemical shifts were reported in parts per million (δ) relative to residual solvent signals: CD₂HOD 3.31, CHCl₃ 7.26. RP-HPLC analyses of crude products were carried out on a Jasco UP-2075 Plus pump using a 5 μ m, 4.8 \times 150 mm C-18 reverse-phase column eluted with a linear gradient of CH₃CN in 0.1 M TEAB (pH 7.0, from 0 to 60% in 60 min, flow 1.0 mL min⁻¹) equipped with a Jasco UV-2075 Plus UV detector. The UV spectra were recorded on a Jasco V-530 UV spectrophotometer. Mass spectra were recorded on an Applied Biosystems API 2000 mass spectrometer using electron spray ionization (ESI) technique in positive mode. The High Resolution MS were recorded on a Bruker APEX II FT-ICR mass spectrometer using electron spray ionization (ESI) technique in positive mode. Column chromatography was performed on silica gel (Merck, Kieselgel 60, 0.063–0.200 mm). Analytic TLC detections were performed using F₂₅₄ silica gel plates (0.2 mm, Merck). TLC spots were detected under UV light (254 nm).

4.2. Synthesis

4.2.1. 1-(2,4-Dinitrophenyl)-2',3'-O-isopropylideninosine (**2**)

A mixture of 2',3'-O-isopropylideninosine (**1**) (1.00 g, 3.24 mmol), 2,4-dinitrochlorobenzene (820 mg, 4.05 mmol), and K₂CO₃ (560 mg, 4.05 mmol) was suspended in anhydrous DMF (5 mL) and stirred at 80 °C for 3 h. The reaction was monitored by TLC (CHCl₃/MeOH, 95:5). After cooling, the mixture was filtered and the solid was washed with CHCl₃. The filtrates and washings, collected and evaporated to dryness, were purified on a silica gel column eluted with increasing amounts of MeOH in CHCl₃ (from 0 to 5%) to give **2** as a pale yellow amorphous solid consisting of a 1:1 mixture of atropisomers at the N(1)-phenyl bond (1.20 g, 80%); mp 235–237 °C; ν_{max} (CHCl₃) 3417, 3106, 1710, 1538, 1348 cm⁻¹; ¹H NMR δ_{H} (CDCl₃) 9.04 (br s, 1H, H-3 DNP), 8.72–8.62 (m, 1H, H-5 DNP), 8.11, 8.14 (2s, 2H, H-2 and H-8), 7.81–7.72 (m, 1H, H-6 DNP), 6.07–5.96 (m, 1H, H-1'), 5.22–5.11 (m, 1H, H-2'), 5.10–5.02 (br s, 1H, H-3'), 4.53 (br s, 1H, H-4'), 4.02–3.75 (m, 2H, H-5' a,b), 2.90 (br s, 1H, OH, exchange with D₂O), 1.64, 1.39 (2s, 6H, 2CH₃); UV (MeOH) λ_{max} 246 nm, ϵ =20,200; HRESIMS calcd for C₁₉H₁₈N₆NaO₉: 497.1033, found: 497.1056 (M+Na)⁺.

4.2.2. 1-(2,4-Dinitrophenyl)inosine (**3**)

Compound **2** (1.20 g, 2.60 mmol) was dissolved in HCOOH/H₂O (6:4, v/v, 16 mL) and left at room temperature for 4 h. The reaction was monitored by TLC (CHCl₃/MeOH, 6:4). The mixture was

evaporated to dryness to furnish **3** (1.13 g, 99%) as a pale yellow amorphous solid that constituted a 1:1 mixture of atropisomers at the N(1)-phenyl bond. The product was used without further purification; mp 210–212 °C; ν_{max} (neat) 3402, 3098, 1704, 1546, 1343, 1217 cm⁻¹; ¹H NMR δ_{H} (CD₃OD) 9.05 (s, 1H, H-3 DNP), 8.82–8.72 (m, 1H, H-5 DNP), 8.49, 8.52 (2s, 2H, H-2 and H-8), 8.08–7.98 (m, 1H, H-6 DNP), 6.14–6.06 (m, 1H, H-1'), 4.70–4.60 (m, 1H, H-2'), 4.40–4.32 (m, 1H, H-3'), 4.19–4.12 (m, 1H, H-4'), 3.94–3.74 (m, 2H, H-5' a,b); UV (H₂O) λ_{max} 246 nm, ϵ =20,100; HRESIMS calcd for C₁₆H₁₄N₆NaO₉: 457.0720, found: 457.0715 (M+Na)⁺.

4.3. General procedure for the scaffold synthesis

4.3.1. Loading of **3** on solid support

1-(2,4-Dinitrophenyl)inosine (**3**) (1.13 g, 2.60 mmol) was evaporated with dry pyridine (3 \times 1.5 mL) and then coupled with the MMTCl resin (1.30 g, 1.69 mmol), and swollen with dry pyridine (8 mL) in the presence of DMAP (0.35 mmol, 42.0 mg) for 24 h at room temperature. The resin was filtered and washed with CH₂Cl₂ (3 \times 5 mL), CH₂Cl₂/MeOH (1:1, v/v, 3 \times 5 mL), and MeOH (3 \times 5 mL), and finally dried in vacuo. The reaction yield was evaluated by cleavage of the nucleoside from the solid support by treatment with 2% (v/v) TFA in DCM (8 min, rt) followed by quantitative UV experiment (**3**, λ_{max} =246 nm, ϵ =20,100, H₂O). The solid support **4** was obtained in almost quantitative yield (1.26 mmol g⁻¹, 97%).

4.3.2. Treatment of solid support **4** with N-nucleophiles **a–g** (products **8a–g** and **11a–g**)

Solid support **4** (100 mg, 0.13 mmol), previously swollen in DMF, was left in contact with amines **a–g** (5.0 mmol) in DMF (1.5 mL) under shaking for 8 h at 50 °C. The reaction of **4** with amines **a–e** furnished, after usual washings, supports **8a–e**. In the case of amines **f** and **g**, after detachment from the support as described above, intermediates **6f** and **g** could be obtained, after HPLC purification, in 90 and 85% yields, respectively. Alternatively, supports **5f–g** were treated with a 1 M solution of K₂CO₃ in DMF (15 h, 50 °C) thus giving supports **8f** and **g**. After filtration and washings with DMF (3 \times 5 mL), DMF/MeOH (1:1, v/v, 3 \times 5 mL), and MeOH (3 \times 5 mL), supports **8a–g** were dried under reduced pressure. The yields of N-1-alkyl-inosines **11a–g** (80–95%, from **4**, Table 1) were calculated by quantifying the products obtained by HPLC purification of the crude nucleoside material released from a weighted amount of resin (as described above) and taking into account that the starting support **4** had a 1.26 mmol g⁻¹ nucleoside functionalization.

4.3.3. Formation of 4-N-alkyl AICAR derivatives **10a–g**

Supports **8a–g** (100 mg, 0.10–0.12 mmol) were treated with NaOH (5 M in EtOH) for 6 h at reflux. After filtration and washings with EtOH (3 \times 5 mL), EtOH/H₂O (1:1, v/v, 3 \times 5 mL), H₂O (3 \times 5 mL), and MeOH (3 \times 5 mL), supports **9a–g** were dried under reduced pressure. The reaction yields (**8** \rightarrow **9**, 80–90%) and the overall yields of 4-N-alkyl AICAR derivatives **10a–g** (72–86% from **4**) were evaluated on isolated products after HPLC purification of the material released from a weighted amount of resin, as described above. ¹H NMR spectra (see later) confirmed the purity of the products.

4.3.4. Formation of 4-N-alkyl AICA-2',3'-secoriboside derivatives **15c–f** (pathway **9** \rightarrow **13** \rightarrow **15**)

Supports **9c–f** (100 mg, 0.09–0.11 mmol) were left in contact with a solution of NaIO₄ (235 mg, 1.1 mmol) in DMF/H₂O (1.5 mL, 1:1, v/v) and shaken for 12 h at 60 °C. The resulting supports, after washings with DMF (3 \times 5 mL), DMF/H₂O (1:1, v/v, 3 \times 5 mL), H₂O (3 \times 5 mL), and then with EtOH (3 \times 5 mL), were treated with NaBH₄ (2.2 mmol) in EtOH (1.5 mL) and shaken for 2.0 h at room temperature. After filtration and washings with EtOH (3 \times 5 mL),

EtOH/H₂O (1:1, v/v, 3×5 mL), H₂O (3×5 mL), and MeOH (3×5 mL), supports **13c–f** were dried under reduced pressure. Reaction yields (**9**→**13**, 75–80%, Table 1) were evaluated by HPLC analysis and purification of the crude 4-*N*-alkyl AICA-2',3'-secoriboside derivatives **15c–f** released from a weighted amount of resin, as described above. The same reactions, performed on **9a,b,e** furnished very low quantities of the corresponding **15a,b,e**.

4.3.5. Formation of 4-*N*-alkyl AICA-2',3'-secoriboside derivatives **15a–g** (pathway **8**→**12**→**13**→**15**)

Supports **8a–g** (100 mg, 0.10–0.12 mmol) were left in contact with a solution of NaIO₄ (235 mg, 1.1 mmol) in DMF/H₂O (1.5 mL, 1:1, v/v) and shaken for 12 h at 60 °C. The resulting supports, after washings with DMF (3×5 mL), DMF/H₂O (1:1, v/v, 3×5 mL), H₂O (3×5 mL), and then with EtOH (3×5 mL), were treated with NaBH₄ (2.2 mmol) in EtOH (1.5 mL) and shaken for 2.0 h at room temperature. After filtration and washings with EtOH (3×5 mL), EtOH/H₂O (1:1, v/v, 3×5 mL), H₂O (3×5 mL), and MeOH (3×5 mL), supports **12a–g** were dried under reduced pressure. Reaction yields (**8**→**12**, 75–80%) were evaluated by HPLC analysis and purification of the crude 1-*N*-alkyl-inosine-2',3'-secoriboside derivatives released from a weighted amount of resin, as described above.¹⁹ Alternatively, supports **8a–g** (100 mg, 0.10–0.12 mmol) were left into contact with a solution of LTA (235 mg, 1.1 mmol) in DCM (1.5 mL) and shaken for 24 h at room temperature. The resulting supports, after usual washings, were treated with NaBH₄ (2.2 mmol) in EtOH (1.5 mL) as described above, thus obtaining supports **12a–g** in 60–65% reaction yield (**8**→**12**) calculated by HPLC on the released material. Then, supports **12a–g** were treated with 5 M NaOH in EtOH as described above for the reaction **8**→**9** thus giving supports **13a–g**. The TFA treatment of **13a–g** furnished **15a–g** (80–88% from **12a–g**), which were purified by HPLC as described above for **10a–g**. The overall yields of pure **15a–g** (from **4**) resulted to be in the range 58–67% (Table 1). ¹H NMR spectra (see later) confirmed the purity of the products.

4.4. Synthesized scaffolds

4.4.1. 5-[(Cyclohexylamino)methyleneamino]-1-(β-D-ribofuranosyl)imidazole-4-[*N*-(2,4-dinitrophenyl)]carboxamide (**6f**)

Amorphous solid, mp over 250 °C (decomp.); ν_{\max} (neat) 3423, 3302, 2917, 1656, 1204, 1111 cm⁻¹; ¹H NMR δ_{H} (CDCl₃) 12.36 (s, 1H, NH, exchange with D₂O), 9.18–9.13 (m, 2H, H-6 and H-3 DNP), 8.70 (br s, 1H, H-2), 8.48 (dd, 1H, *J*=9.8, 2.4 Hz, H-5 DNP), 7.47 (s, 1H, CH=N), 5.78 (br s, 1H, H-1'), 4.62–4.59 (m, 1H, H-2'), 4.38–4.41 (m, 2H, H-3', H-4'), 3.94–3.87 (m, 2H, 2H-5'), 3.45 (br s, 1H, CHN), 2.20–1.20 (m, 10H, 5CH₂); UV (MeOH) λ_{\max} 275 nm, ϵ =13,300; HRESIMS calcd for C₂₂H₂₇N₇NaO₉: 556.1768, found: 556.1779 (M+Na)⁺.

4.4.2. 5-[(1*R*,2*S*,3*R*,4*R*)-2,3-Dihydroxy-4-((hydroxymethyl)cyclopentyl)aminomethyleneamino]-1-(β-D-ribofuranosyl)imidazole-4-[*N*-(2,4-dinitrophenyl)]carboxamide (**6g**)

Amorphous solid, mp over 250 °C (decomp.); ν_{\max} (neat) 3430, 3320, 2904, 1668, 1264, 1128 cm⁻¹; ¹H NMR δ_{H} (CDCl₃) 9.20 (d, 1H, H-5 DNP), 9.03 (s, 1H, H-3 DNP), 8.64 (s, 1H, H-2), 8.42 (d, 1H, H-6 DNP), 7.73 (s, 1H, CHN), 6.03 (d, 1H, H-1'), 4.63–4.60 (m, 1H, H-2'), 4.40–4.36 (m, 2H, H-3', H-2'), 4.22–4.18 (m, 2H, H-4', H-3'), 3.76–3.72 (m, 2H, CH₂O), 3.62–3.59 (m, 2H, CH₂O), 3.23–3.20 (m, 1H, H-1''), 2.02–1.98 (m, 2H, H-4'', H-5''_a), 1.62–1.59 (m, 1H, H-5''_b), 1.18 (s, 3H, CH₃), 1.31 (s, 3H, CH₃); UV (CHCl₃) λ_{\max} 276 nm, ϵ =12,900; HRESIMS calcd for C₂₅H₃₁N₇NaO₁₂: 644.1928, found: 644.1945 (M+Na)⁺.

4.4.3. 1-(3-Hydroxypropyl)inosine (**11a**)

Amorphous solid, mp 215–218 °C; ν_{\max} (neat) 3390, 2930, 1700, 1450, 1232 cm⁻¹; ¹H NMR δ_{H} (CD₃OD) 8.41 (br s, 1H, H-2), 8.34 (s,

1H, H-8), 6.00 (d, 1H, *J*=5.0 Hz, H-1'), 4.64–4.60 (m, 1H, H-2'), 4.34–4.29 (m, 1H, H-3'), 4.20 (t, 2H, *J*=4.0 Hz, CH₂N), 4.15–4.11 (m, 1H, H-4'), 3.86 (dd, 1H, *J*=12.2, 2.6 Hz, H-5'_a), 3.75 (dd, 1H, *J*=12.2, 2.6 Hz, H-5'_b), 3.60 (t, 2H, *J*=6.3 Hz, CH₂O), 2.03–1.94 (m, 2H, CH₂CH₂N); UV (MeOH) λ_{\max} 249 nm, ϵ =9900; HRESIMS calcd for C₁₃H₁₉N₄O₆: 327.1305, found: 327.1291 (M+H)⁺.

4.4.4. 1-(5-Hydroxypentyl)inosine (**11b**)

Amorphous solid, mp over 250 °C (decomp.); ν_{\max} (neat) 3375, 2929, 1679, 1427, 1240 cm⁻¹; ¹H NMR δ_{H} (CD₃OD) 8.40 (br s, 1H, H-2), 8.35 (s, 1H, H-8), 6.02 (d, 1H, *J*=5.5 Hz, H-1'), 4.64–4.60 (m, 1H, H-2'), 4.33–4.29 (m, 1H, H-3'), 4.14–4.08 (m, 3H, H-4', CH₂N), 3.87 (dd, 1H, *J*=12.1, 2.6 Hz, H-5'_a), 3.75 (dd, 1H, *J*=12.1, 2.6 Hz, H-5'_b), 3.60 (t, 2H, *J*=6.2 Hz, CH₂O), 1.85–1.77 (m, 2H, CH₂), 1.61–1.56 (m, 2H, CH₂), 1.48–1.38 (m, 2H, CH₂); UV (MeOH) λ_{\max} 249 nm, ϵ =10,000; HRESIMS calcd for C₁₅H₂₂N₄NaO₆: 377.1437, found: 377.1453 (M+Na)⁺.

4.4.5. 1-Propylinosine (**11c**)

Amorphous solid, mp 185–187 °C; ν_{\max} (neat) 3324, 3302, 1702, 1240 cm⁻¹; ¹H NMR δ_{H} (CD₃OD) 8.43 (br s, 1H, H-2), 8.35 (s, 1H, H-8), 6.01 (d, 1H, *J*=5.5 Hz, H-1'), 4.64–4.60 (m, 1H, H-2'), 4.34–4.31 (m, 1H, H-3'), 4.18–4.11 (m, 1H, H-4'), 4.07 (t, 2H, *J*=7.3 Hz, CH₂N), 3.87 (dd, 1H, *J*=12.5, 2.6 Hz, H-5'_a), 3.75 (dd, 1H, *J*=12.5, 2.6 Hz, H-5'_b), 1.83–1.78 (m, 2H, CH₂CH₃), 0.98 (t, 3H, *J*=7.0 Hz); UV (MeOH) λ_{\max} 252 nm, ϵ =9700; HRESIMS calcd for C₁₃H₁₈N₄NaO₅: 333.1175, found: 333.1207 (M+Na)⁺.

4.4.6. 1-Butylinosine (**11d**)

Amorphous solid, mp 170–172 °C; ν_{\max} (neat) 3334, 3296, 1693, 1384, 1232 cm⁻¹; ¹H NMR δ_{H} (CD₃OD) 8.41 (br s, 1H, H-2), 8.36 (s, 1H, H-8), 6.02 (d, 1H, *J*=5.5 Hz, H-1'), 4.64–4.60 (m, 1H, H-2'), 4.34–4.30 (m, 1H, H-3'), 4.14–4.08 (m, 3H, H-4', CH₂N), 3.87 (dd, 1H, *J*=12.1, 2.6 Hz, H-5'_a), 3.75 (dd, 1H, *J*=12.1, 2.6 Hz, H-5'_b), 1.80–1.71 (m, 2H, CH₂), 1.45–1.35 (m, 2H, CH₂), 0.98 (t, 3H, *J*=7.7 Hz, CH₃); UV (MeOH) λ_{\max} 252 nm, ϵ =9800; HRESIMS calcd for C₁₄H₂₁N₄O₅: 325.1512, found: 325.1490 (M+H)⁺.

4.4.7. 1-Benzylinosine (**11e**)

Amorphous solid, mp 217–220 °C (lit.²⁵ 219–222 °C); ν_{\max} (neat) 3383, 3298, 1698, 1490, 1212 cm⁻¹; ¹H NMR δ_{H} (CD₃OD) 8.44, 8.33 (2s, 2H, H-2, H-8), 7.32–7.26 (m, 5H, Ph), 6.00 (d, 1H, *J*=5.9 Hz, H-1'), 5.29 (s, 2H, CH₂Ph), 4.69–4.63 (m, 1H, H-2'), 4.33–4.30 (m, 1H, H-3'), 4.13–4.09 (m, 1H, H-4'), 3.87 (dd, 1H, *J*=12.5, 2.9 Hz, H-5'_a), 3.75 (dd, 1H, *J*=12.5, 2.9 Hz, H-5'_b); UV (MeOH) λ_{\max} 249 nm, ϵ =10,100; HRESIMS calcd for C₁₇H₁₈N₄NaO₅: 381.1175, found: 381.1173 (M+Na)⁺.

4.4.8. 1-Cyclohexylinosine (**11f**)

Amorphous solid, mp 188–191 °C; ν_{\max} (neat) 3344, 3286, 1706, 1368, 1238 cm⁻¹; ¹H NMR δ_{H} (CD₃OD) 8.37, 8.32 (2s, 2H, H-2, H-8), 6.00 (d, 1H, *J*=5.9 Hz, H-1'), 4.64–4.60 (m, 1H, H-2'), 4.34–4.30 (m, 1H, H-3'), 4.22–4.19 (m, 1H, CHN), 4.11–4.10 (m, 1H, H-4'), 3.85 (dd, 1H, *J*=12.0, 2.9 Hz, H-5'_a), 3.72 (dd, 1H, *J*=12.0, 2.9 Hz, H-5'_b), 2.00–1.30 (m, 10H, 5CH₂); UV (MeOH) λ_{\max} 246 nm, ϵ =9800; HRESIMS calcd for C₁₆H₂₃N₄O₅: 351.1668, found: 351.1699 (M+H)⁺.

4.4.9. 1-[(1*R*,2*S*,3*R*,4*R*)-2,3-(Isopropylidenedioxy)-4-(hydroxymethyl)cyclopentyl]inosine (**11g**)

Amorphous solid, mp over 250 °C (decomp.); ν_{\max} (neat) 3380, 3298, 1685, 1703, 1430, 1210; ¹H NMR δ_{H} (CD₃OD) 8.40 (br s, 1H, H-2), 8.36 (s, 1H, H-8), 6.04 (d, 1H, *J*=5.4 Hz, H-1'), 5.23–5.19 (m, 1H, H-2''), 4.73–4.70 (m, 1H, H-3''), 4.60–4.58 (m, 2H, H-1'', H-2'), 4.33–4.29 (m, 1H, H-3'), 4.10–4.09 (m, 1H, H-4'), 3.75–3.83 (m, 4H, H-5'_{a,b}, H-6''_{a,b}), 2.40–2.12 (m, 3H, H-4'', H-5''_{a,b}), 1.16 (s, 3H, CH₃),

1.30 (s, 3H, CH₃); UV (MeOH) λ_{max} 253 nm, ϵ =9500; HRESIMS calcd for C₁₉H₂₆N₄NaO₈: 461.1648, found: 461.1620 (M+Na)⁺.

4.4.10. 5-Amino-1-(β -D-ribofuranosyl)imidazole-4-[N-(3-hydroxypropyl)]carboxamide (10a**)**

Amorphous solid, mp over 250 °C (decomp.); ν_{max} (neat) 3402, 3322, 1678, 1220 cm⁻¹; ¹H NMR δ_{H} (CD₃OD) 7.31 (s, 1H, H-2), 5.54 (d, 1H, J=6.6 Hz, H-1'), 4.50–4.45 (m, 1H, H-2'), 4.24–4.20 (m, 1H, H-3'), 4.06–4.03 (m, 1H, H-4'), 3.79 (dd, 1H, J=12.1, 2.6 Hz, H-5'_a), 3.74 (dd, 1H, J=12.1, 2.6 Hz, H-5'_b), 3.63 (t, 2H, J=6.2 Hz, CH₂O), 3.31 (2H, CH₂N, partly covered by solvent signal), 1.81–1.74 (m, 2H, CH₂); UV (MeOH) λ_{max} 268 nm, ϵ =10,700; HRESIMS calcd for C₁₂H₂₀N₄NaO₆: 339.1280, found: 339.1302 (M+Na)⁺.

4.4.11. 5-Amino-1-(β -D-ribofuranosyl)imidazole-4-[N-(5-hydroxypentyl)]carboxamide (10b**)**

Amorphous solid, mp over 250 °C (decomp.); ν_{max} (neat) 3409, 3338, 2934, 1623, 1255 cm⁻¹; ¹H NMR δ_{H} (CD₃OD) 7.38 (s, 1H, H-2), 5.56 (d, 1H, J=6.2 Hz, H-1'), 4.50–4.46 (m, 1H, H-2'), 4.23–4.19 (m, 1H, H-3'), 4.08–4.05 (m, 1H, H-4'), 3.77–3.72 (m, 2H, H-5'_{a,b}), 3.55 (t, 2H, J=6.2 Hz, CH₂O), 3.31 (2H, CH₂N, partly covered by solvent signal), 1.62–1.55 (m, 4H, 2CH₂), 1.48–1.42 (m, 2H, CH₂); UV (MeOH) λ_{max} 268 nm, ϵ =10,900; HRESIMS calcd for C₁₄H₂₄N₄NaO₆: 367.1594, found: 367.1586 (M+Na)⁺.

4.4.12. 5-Amino-1-(β -D-ribofuranosyl)imidazole-4-(N-propyl)carboxamide (10c**)**

Amorphous solid, mp 202–205 °C; ν_{max} (neat) 3330, 2980, 1702, 1210, 1166 cm⁻¹; ¹H NMR δ_{H} (CD₃OD) 7.36 (s, 1H, H-2), 5.54 (d, 1H, J=6.6 Hz, H-1'), 4.50–4.45 (m, 1H, H-2'), 4.24–4.20 (m, 1H, H-3'), 4.09–4.06 (m, 1H, H-4'), 3.79 (dd, 1H, J=11.7, 2.6 Hz, H-5'_a), 3.74 (dd, 1H, J=11.7, 2.6 Hz, H-5'_b), 3.31 (2H, CH₂N, partly covered by solvent signal), 1.63–1.57 (m, 2H, CH₂CH₃), 0.98 (t, 3H, J=7.3 Hz, CH₃); UV (MeOH) λ_{max} 267 nm, ϵ =10,400; HRESIMS calcd for C₁₂H₂₀N₄NaO₅: 323.1331, found: 323.1324 (M+Na)⁺.

4.4.13. 5-Amino-1-(β -D-ribofuranosyl)imidazole-4-(N-butyl)carboxamide (10d**)**

Amorphous solid, mp 222–225 °C; ν_{max} (neat) 3398, 3347, 1702, 1239, 1120 cm⁻¹; ¹H NMR δ_{H} (CD₃OD) 7.32 (s, 1H, H-2), 5.52 (d, 1H, J=5.5 Hz, H-1'), 4.50–4.46 (m, 1H, H-2'), 4.20–4.16 (m, 1H, H-3'), 4.13–4.10 (m, 1H, H-4'), 3.79 (dd, 1H, J=12.5, 2.9 Hz, H-5'_a), 3.74 (dd, 1H, J=12.5, 2.9 Hz, H-5'_b), 3.31 (2H, CH₂N, partly covered by solvent signal), 1.60–1.51 (m, 2H, CH₂), 1.45–1.36 (m, 2H, CH₂), 0.96 (t, 3H, J=7.3 Hz, CH₃); UV (MeOH) λ_{max} 267 nm, ϵ =10,300; HRESIMS calcd for C₁₃H₂₂N₄NaO₅: 337.1488, found: 337.1480 (M+Na)⁺.

4.4.14. 5-Amino-1-(β -D-ribofuranosyl)imidazole-4-(N-benzyl)carboxamide (10e**)**

Amorphous solid, mp 170–173 °C (lit.²⁵ 171–172 °C); ν_{max} (neat) 3334, 3256, 1456, 1696, 1198 cm⁻¹; ¹H NMR δ_{H} (CD₃OD) 7.38–7.30 (m, 6H, Ph, H-2), 5.55 (d, 1H, J=6.6 Hz, H-1'), 4.54–4.48 (s, 3H, CH₂Ph, H-2'), 4.19–4.16 (m, 1H, H-3'), 4.08–4.05 (m, 1H, H-4'), 3.79 (dd, 1H, J=12.1, 2.9 Hz, H-5'_a), 3.74 (dd, 1H, J=12.1, 2.9 Hz, H-5'_b); UV (MeOH) λ_{max} 270 nm, ϵ =11,400; HRESIMS calcd for C₁₆H₂₀N₄NaO₅: 371.1331, found: 371.1325 (M+Na)⁺.

4.4.15. 5-Amino-1-(β -D-ribofuranosyl)imidazole-4-(N-cyclohexyl)carboxamide (10f**)**

Amorphous solid, mp 210–212 °C; ν_{max} (neat) 3320, 3295, 1689, 1197, 1172 cm⁻¹; ¹H NMR δ_{H} (CD₃OD) 7.35 (s, 1H, H-2), 5.54 (d, 1H, J=7.0 Hz, H-1'), 4.50–4.45 (m, 1H, H-2'), 4.24–4.19 (m, 1H, H-3'), 4.07–4.04 (m, 1H, H-4'), 3.82–3.72 (m, 3H, H-5'_{a,b}, CHN), 2.00–1.30 (m, 10H, 5CH₂); UV (MeOH) λ_{max} 267 nm, ϵ =10,800; HRESIMS calcd for C₁₅H₂₄N₄NaO₅: 363.1644, found: 363.1635 (M+Na)⁺.

4.4.16. 5-Amino-1-(β -D-ribofuranosyl)imidazole-4-[N-((1R,2S,3R,4R)-2,3-isopropylidenedioxy)-4-(hydroxymethyl)cyclopentyl]carboxamide (10g**)**

Amorphous solid, mp over 250 °C (decomp.); ν_{max} (neat) 3349, 3325, 1706, 1217, 1122 cm⁻¹; ¹H NMR δ_{H} (CD₃OD) 7.37 (br s, 1H, H-2), 5.57 (d, 1H, J=5.5 Hz, H-1'), 5.19–5.15 (m, 1H, H-2'), 4.55–4.40 (m, 3H, H-2', H-1'', H-3''), 4.26–4.22 (m, 1H, H-3'), 4.13–4.09 (m, 1H, H-4'), 3.80–3.68 (m, 4H, H-5'_{a,b}, H-6''_{a,b}), 2.30–2.10 (m, 3H, H-4'', H-5''_{a,b}), 1.18 (s, 3H, CH₃), 1.31 (s, 3H, CH₃); UV (MeOH) λ_{max} 268 nm, ϵ =10,500; HRESIMS calcd for C₁₈H₂₈N₄NaO₈: 451.1805, found: 451.1812 (M+Na)⁺.

4.4.17. 5-Amino-1-[1-(1,3-dihydroxypropan-2-yloxy)-2-hydroxyethyl]imidazole-4-[N-(3-hydroxypropyl)]carboxamide (15a**)**

Amorphous solid, mp over 250 °C (decomp.); ν_{max} (neat) 3378, 3327, 1698, 1220 cm⁻¹; ¹H NMR δ_{H} (CD₃OD) 7.34 (s, 1H, H-2), 5.60 (t, 1H, J=5.7 Hz, H-1'), 3.87–3.83 (m, 2H, CH₂O), 3.75–3.64 (m, 2H, CH₂O), 3.61–3.49 (m, 5H, CH, 2CH₂O), 3.31 (2H, CH₂N, partly covered by solvent signal), 1.80–1.75 (m, 2H, CH₂); UV (MeOH) λ_{max} 268 nm, ϵ =10,200; HRESIMS calcd for C₁₂H₂₂N₄NaO₆: 341.1437, found: 341.1445 (M+Na)⁺.

4.4.18. 5-Amino-1-[1-(1,3-dihydroxypropan-2-yloxy)-2-hydroxyethyl]imidazole-4-[N-(5-hydroxypentyl)]carboxamide (15b**)**

Amorphous solid, mp over 250 °C (decomp.); ν_{max} (neat) 3370, 3323, 1702, 1210 cm⁻¹; ¹H NMR δ_{H} (CD₃OD) 7.35 (s, 1H, H-2), 5.62 (t, 1H, J=5.9 Hz, H-1'), 3.95–3.85 (m, 2H, CH₂O), 3.78–3.64 (m, 2H, CH₂O), 3.60–3.50 (m, 5H, CH, 2CH₂O), 3.32 (2H, CH₂N, partly covered by solvent signal), 1.64–1.54 (m, 4H, 2CH₂), 1.48–1.38 (m, 2H, CH₂); UV (MeOH) λ_{max} 268 nm, ϵ =10,100; HRESIMS calcd for C₁₄H₂₆N₄NaO₆: 369.1750, found: 369.1756 (M+Na)⁺.

4.4.19. 5-Amino-1-[1-(1,3-dihydroxypropan-2-yloxy)-2-hydroxyethyl]imidazole-4-(N-propyl)carboxamide (15c**)**

Amorphous solid, mp 225–229 °C; ν_{max} (neat) 3384, 3332, 1705, 1264, 1176 cm⁻¹; ¹H NMR δ_{H} (CD₃OD) 7.36 (s, 1H, H-2), 5.62 (t, 1H, J=3.3 Hz, H-1'), 3.90–3.83 (m, 2H, CH₂O), 3.78–3.62 (m, 2H, CH₂O), 3.61–3.49 (m, 3H, CH, CH₂O), 3.30 (2H, CH₂N, partly covered by solvent signal), 1.65–1.56 (m, 2H, CH₂), 0.96 (t, 3H, J=7.2 Hz, CH₃); UV (MeOH) λ_{max} 267 nm, ϵ =10,300; HRESIMS calcd for C₁₂H₂₂N₄NaO₅: 325.1488, found: 325.1480 (M+Na)⁺.

4.4.20. 5-Amino-1-[1-(1,3-dihydroxypropan-2-yloxy)-2-hydroxyethyl]imidazole-4-(N-butyl)carboxamide (15d**)**

Amorphous solid, mp 218–222 °C; ν_{max} (neat) 3398, 3340, 1702, 1241, 1160 cm⁻¹; ¹H NMR δ_{H} (CD₃OD) 7.34 (s, 1H, H-2), 5.60 (t, 1H, J=3.3 Hz, H-1'), 3.91–3.84 (m, 2H, CH₂O), 3.79–3.65 (m, 2H, CH₂O), 3.61–3.49 (m, 3H, CH, CH₂O), 3.31 (2H, CH₂N, partly covered by solvent signal), 1.60–1.51 (m, 2H, CH₂), 1.46–1.32 (m, 2H, CH₂), 0.96 (t, 3H, J=7.2 Hz, CH₃); UV (MeOH) λ_{max} 267 nm, ϵ =10,300; HRESIMS calcd for C₁₃H₂₄N₄NaO₅: 339.1644, found: 339.1640 (M+Na)⁺.

4.4.21. 5-Amino-1-[1-(1,3-dihydroxypropan-2-yloxy)-2-hydroxyethyl]imidazole-4-(N-benzyl)carboxamide (15e**)**

Amorphous solid, mp over 250 °C (decomp.); ν_{max} (neat) 3367, 3331, 1705, 1264, 1176 cm⁻¹; ¹H NMR δ_{H} (CD₃OD) 7.36–7.28 (m, 6H, Ph, H-2), 5.60 (t, 1H, J=5.6 Hz, H-1'), 4.51 (s, 2H, CH₂Ph), 3.96–3.84 (m, 2H, CH₂O), 3.78–3.64 (m, 2H, CH₂O), 3.61–3.49 (m, 3H, CH, CH₂O); UV (MeOH) λ_{max} 270 nm, ϵ =11,200; HRESIMS calcd for C₁₆H₂₂N₄NaO₅: 373.1488, found: 373.1476 (M+Na)⁺.

4.4.22. 5-Amino-1-[1-(1,3-dihydroxypropan-2-yloxy)-2-hydroxyethyl]imidazole-4-(N-cyclohexyl)carboxamide (15f**)**

Amorphous solid, mp 210–213 °C; ν_{max} (neat) 3367, 3302, 1708, 1164 cm⁻¹; ¹H NMR δ_{H} (CD₃OD) 7.33 (s, 1H, H-2), 5.59 (t, 1H, J=5.5 Hz, H-1'), 3.94–3.84 (m, 2H, CH₂O), 3.80–3.65 (m, 3H, CH₂O),

CHN), 3.61–3.49 (m, 3H, CH, CH₂O), 2.00–1.30 (m, 10H, 5CH₂); UV (MeOH) λ_{max} 267 nm, $\epsilon=10,800$; HRESIMS calcd for C₁₅H₂₆N₄NaO₅: 365.1801, found: 365.1810 (M+Na)⁺.

4.4.23. 5-Amino-1-[1-(1,3-dihydroxypropan-2-yloxy)-2-hydroxyethyl]imidazole-4-[N-((1R,2S,3R,4R)-2,3-isopropylidenedioxy)-4-(hydroxymethyl)cyclopentyl]carboxamide (15g)

Amorphous solid, mp over 250 °C (decomp.); ν_{max} (neat) 3404, 3387, 1693, 1287, 1193 cm⁻¹; ¹H NMR δ_{H} (CD₃OD) 7.25 (s, 1H, H-2), 5.60 (t, 1H, J=4.7 Hz, H-1'), 5.20–5.17 (m, 1H, H-2''), 4.56–5.50 (m, 2H, H-1'', H-3''), 3.93–3.86 (m, 2H, CH₂O), 3.80–3.67 (m, 2H, CH₂O), 3.61–3.49 (m, 5H, CH, 2CH₂O), 2.36–2.10 (m, 3H, H-4'', H-5''_{ab}), 1.32 (s, 3H, CH₃), 1.20 (s, 3H, CH₃); UV (MeOH) λ_{max} 268 nm, $\epsilon=10,200$; HRESIMS calcd for C₁₈H₃₀N₄NaO₈: 453.1961, found: 453.1969 (M+Na)⁺.

Acknowledgements

This work is supported by Bioindustry Park del Canavese SpA, Torino, Italy in the context of the project iTECHPLAT -M. 3.4 A, DOCUP Piemonte Region 2000/2006. The authors are grateful to the 'Centro di Servizi Interdipartimentale di Analisi Strumentale (CSIAS)' for supplying the NMR facilities.

References and notes

- (a) *Antiviral Nucleosides: Chiral Synthesis and Chemotherapy*; Chu, C. K., Ed.; Elsevier: Amsterdam, The Netherlands, 2003; (b) Simons, C.; Wu, Q.; Htar, T. T. *Curr. Top. Med. Chem.* **2005**, *5*, 1191–1203; (c) De Clercq, E.; Neyts, J. *Rev. Med. Virol.* **2004**, *14*, 289–300.
- (a) Lagoja, I. M. *Chem. Biodivers.* **2005**, *2*, 1–50; (b) Kimura, K.; Bugg, T. D. H. *Nat. Prod. Rep.* **2003**, *20*, 252–273; (c) Rachakonda, S.; Cartee, L. *Curr. Med. Chem.* **2004**, *11*, 775–793; (d) Knapp, S. *Chem. Rev.* **1995**, *95*, 1859–1876.
- (a) Miura, S.; Izuta, S. *Curr. Drug Targets* **2004**, *5*, 191–195; (b) Parker, W. B.; Secrist, J. A.; Waud, W. R. *Curr. Opin. Investig. Drugs* **2004**, *5*, 592–596; (c) Szafraniec, S. I.; Stachnick, K. J.; Skierski, J. S. *Acta Pol. Pharm.* **2004**, *61*, 223–232.
- Gandhi, V.; Keating, M. J.; Bate, G.; Kirkpatrick, P. *Nat. Rev. Drug Discov.* **2006**, *5*, 17–18.
- Matthews, S. J. *Clin. Ther.* **2006**, *28*, 184–203.
- Pui, C. H.; Jeha, S.; Kirkpatrick, P. C. *Nat. Rev. Drug Discov.* **2005**, *4*, 369–370.
- Kaminskas, E.; Farrell, A.; Abraham, S.; Baird, A.; Hsieh, L. S.; Lee, S. L.; Leighton, J. K.; Patel, H.; Rahman, A.; Shidhara, R.; Wang, Y. C.; Pazdur, R. *Clin. Cancer Res.* **2005**, *11*, 3604–3608.
- Rutter, G. A.; Silva Xavier, G.; Lecler, I. *Biochem. J.* **2003**, *375*, 1–16.
- Gaidhu, M. P.; Fediuc, S.; Ceddia, R. B. J. *Biol. Chem.* **2006**, *281*, 25956–25964.
- Frank, R. N. *Am. J. Ophthalmol.* **2002**, *133*, 693–698.
- Lara, D. R.; Dall'Igna, O. P.; Ghisolfi, E. S.; Brunstein, M. G. *Prog. Neuro-psychopharmacol. Biol. Psychiatry* **2006**, *30*, 617–629.
- Kohyama, N.; Katashima, T.; Yamamoto, Y. *Synthesis* **2004**, *17*, 2799–2804.
- Ulrich, S. M.; Sallee, N. A.; Shokat, K. M. *Bioorg. Med. Chem. Lett.* **2002**, *12*, 3223–3227.
- Wall, M.; Shim, J. H.; Benkovic, S. J. *Biochemistry* **2000**, *39*, 11303–11311.
- (a) Minakawa, N.; Kojima, N.; Sasaki, T.; Matsuda, A. *Nucleosides Nucleotides* **1996**, *15*, 251–263; (b) Minakawa, N.; Takeda, T.; Sasaki, T.; Matsuda, A.; Ueda, T. *J. Med. Chem.* **1991**, *34*, 778–786.
- (a) Mizuno, A.; Tsujino, M.; Takada, M.; Hayashi, M.; Atsumi, K. *J. Antibiot. (Tokyo)* **1974**, *27*, 775–782; (b) Kamata, K.; Okubo, M.; Ishigamori, E.; Masaki, Y.; Uchida, H.; Watanabe, K.; Kashiwagi, N. *Transplantation* **1983**, *35*, 144–149.
- (a) Sidwell, R. W.; Huffman, J. H.; Khare, G. P.; Allen, L. B.; Witkowski, J. T.; Robins, R. K. *Science* **1972**, *177*, 705–706; (b) Guezguez, R.; Bougrin, K.; El Akri, K.; Benhida, R. *Tetrahedron Lett.* **2006**, *47*, 4807–4811.
- Kalman, T. I.; Houston, D. M. *Nucleosides Nucleotides* **1989**, *8*, 899–902.
- Oliviero, G.; Amato, J.; Borbone, N.; D'Errico, S.; Piccialli, G.; Mayol, L. *Tetrahedron Lett.* **2007**, *48*, 397–400.
- De Napoli, L.; Messere, A.; Montesarchio, D.; Piccialli, G.; Varra, M. *J. Chem. Soc., Perkin Trans. 1* **1997**, 2079–2082.
- (a) Fujii, T.; Saito, T.; Risata, H.; Shinbo, K. *Chem. Pharm. Bull.* **1990**, *38*, 3326–3330; (b) Casanova, E.; Hernández, A. I.; Priego, E. M.; Liekens, S.; Camarasa, M. J.; Balzarini, J.; Pérez-Pérez, M. J. *J. Med. Chem.* **2006**, *49*, 5562–5570.
- (a) De Napoli, L.; Messere, A.; Montesarchio, D.; Piccialli, G. *J. Org. Chem.* **1995**, *60*, 2251–2253; (b) Fukuoka, M.; Shuto, S.; Minakawa, N.; Ueno, Y.; Matsuda, A. *J. Org. Chem.* **2000**, *65*, 5238–5248.
- For general accounts on lead tetraacetate reactions, see: (a) Criegee, R. *Oxidation in Organic Chemistry*; Wiberg, K. B., Ed.; Academic: New York, NY, 1965; Part A; (b) Sheldon, R. A.; Kochi, J. K. *Org. React.* **1972**, *19*, 279–421; (c) Mihailovic, M. L.; Cekovic, Z.; Lorenc, L. *Organic Synthesis by Oxidation with Metal Compounds*; Mijs, W. J., De Jonge, C. R. H. I., Eds.; Plenum: New York, NY, 1986; pp 741–816.
- Hussain, R. F.; Nouri, A. M.; Oliver, R. T. J. *Immunol. Methods* **1993**, *15*, 86–89.
- Shaw, E. J. *Am. Chem. Soc.* **1958**, *80*, 3899–3902.

Synthesis of *N*-1-alkyl analogues of cyclic inosine diphosphate ribose (cIDPR) by a new solid phase approach

Giorgia Oliviero¹, Stefano D'Errico¹, Nicola Borbone¹, Jussara Amato¹, Vincenzo Piccialli², Michela Varra¹, Gennaro Piccialli^{*1} and Luciano Mayol¹

¹Dipartimento di Chimica delle Sostanze Naturali, Università degli Studi di Napoli "Federico II", Via D. Montesano 49, I-80131 Napoli, Italy and ²Dipartimento di Chimica Organica e Biochimica, Università degli Studi di Napoli "Federico II", Via Cynthia 4, 80126, Napoli, Italy

ABSTRACT

Herein we report an efficient solid-phase synthesis of some *N*-1-alkyl-substituted analogs of cyclic inosine-diphosphate-ribose (cIDPR), a mimic of cyclic ADP-ribose (cADPR) which has been described as an agonist of the cADPR/Ca²⁺ signalling system. The proposed synthetic strategy uses a polystyrene support bearing inosine by a 2',3'-acetal linkage which is converted into several *N*-1-alkylinosine-bis-phosphate derivatives which in turn were cyclized by a solid-phase pyrophosphate bond formation.

INTRODUCTION

Cyclic ADP-ribose (cADPR, **1**) is a metabolite involved in Ca²⁺ signalling in various cells. cADPR is synthesized from NAD⁺ and regulates the calcium mobilization, via ryanodine receptors, from intracellular stores in a wide variety of biological systems.¹ To investigate cADPR mediated Ca²⁺ signalling, new cADPR analogues, exhibiting both biological properties as agonists or antagonists and resistance to the enzymatic and chemical hydrolysis, are required. A number of analogues of cADPR have been synthesized by chemo-enzymatic or chemical approach.² Recently, cIDPR (**2**) analogues have been described as agonist of cADPR/Ca²⁺ signalling system.³ A series of *N*-1-substituted,⁴ *N*-9-substituted⁵ cIDPR have been so far synthesized and some of them retain an interesting biological activity Ca²⁺ related. The chemical synthesis and in particular the total synthetic approach

proposed for the great part of these analogues, make use of multistep and time consuming processes which require the purification of products after each reaction step. In an effort to facilitate the chemical synthesis and to enlarge the number of accessible structurally diverse analogues, we report here a new and general solid-phase approach to prepare *N*-1-alkyl-analogues of cIDPR.

RESULTS AND DISCUSSION

The here proposed solid-phase synthesis uses the nucleoside functionalized support **3** which binds the 5'-O-tert-butyldiphenylsilylinosine to a polystyrenemonomethoxy-trityl resin (MMT) support by an acid labile 2',3'-acetal linkage. In previous papers we have demonstrated that *N*-1-(2,4-dinitrophenyl)-inosine is a good precursor to alkylate the *N*-1-atom of purine ring of inosine by reaction with alkylamines.⁶ Therefore, support **5** was synthesized, in almost quantitative yield, by reaction of **4** with 2,4-dinitrochlorobenzene (DNCB). Reaction of **5** with several ω -hydroxyalkylamines (HO-R₂-NH₂, Table 1) furnished the *N*-1-alkyl-inosine supports **6** in high yields. Treatment of **6** with S,S'-diphenyl dithiophosphate (PSS) in presence of TPSCl furnished the bis-phosphate derivative **7** in 90 % yield. After the complete deprotection of phosphates, the intramolecular cyclization, which lead to the pyrophosphate bond formation, was performed treating **8** with carbonyldiimidazole (CDI). The cyclization yields, calculated by measurements of the diphosphate precursors (**8**) resulted in the range 38-68 % (Table 1).

The cleavage of the nucleoside derivatives from the solid support was achieved by standard acidic treatment. The yield of each reaction and the purity of the compounds were calculated by detachment of the nucleosidic material from a weighted amount of resin. The structures of all HPLC purified products were confirmed by ¹H-, ³¹P-NMR and ESI-MS data. In a typical reaction starting from 50 mg of solid support **3** (1.0 mmol/g) and considering an average molecular weight of 480 g/mol, 4-5 mg of pure **9a-e** could be obtained (20-25% overall yield from **3**).

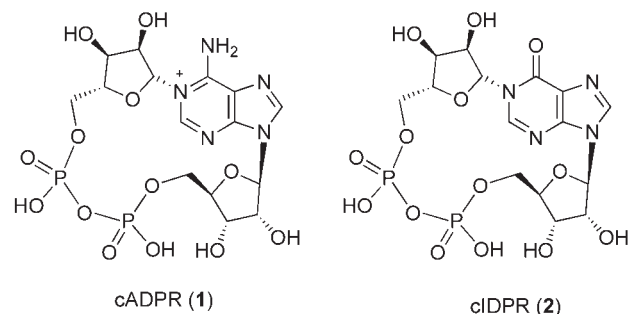
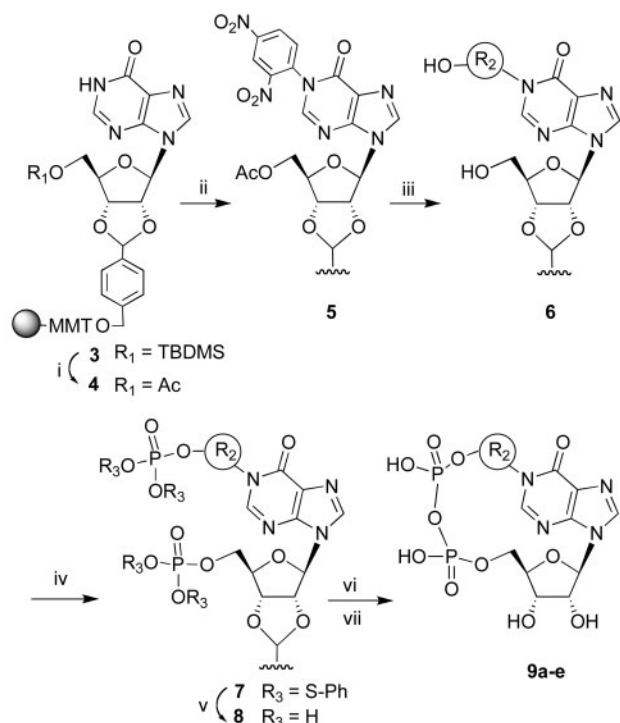


Fig. 1 The structures of cADPR (**1**) and cIDPR (**2**)

CONCLUSION



Scheme 1: Reagents and conditions: (i) a) NH_4F (30 eq.), MeOH at reflux 12 h b) Ac_2O (10 eq.), pyridine 30 min., RT; (ii) DNCB (5 eq.), K_2CO_3 (5 eq.), 2 h, 80 °C.; (iii) $\text{OH-R}_2\text{-NH}_2$ (30 eq.) in DMF, 8h, 50 °C.; (iv) PSS (7.5 eq.), TPSCI (15 eq.), in pyridine, 7 h; RT, (v) AgOAc (20 eq.) in $\text{Py}/\text{H}_2\text{O}$ (2:1, v/v), RT, 15 h; (vi) CDI (1.1 eq.), DMF, 60 °C, 15 h; (vii) TFA 2% in DCM, 8 min. RT followed by H_2O treatment (5 min).

In conclusion, we have successfully utilized the inosine

Table 1 Products **9a-e** and reactions vi yields.

Entry	a	b	c	d	e
R_2	$(\text{CH}_2)_2$	$(\text{CH}_2)_4$	$(\text{CH}_2)_5$	$(\text{CH}_2)_6$	
Cyclization Yields	38%	65%	68%	67%	45%

functionalized solid support **3**, where the nucleoside is anchored to a MMT-polystyrene resin by a 2',3'-acetal linkage to synthesize small libraries of *N*-1-alkyl-substituted analogues of cIDPR. In our opinion this unprecedented solid-phase approach for cIDPR derivatives can be further improved combining in a combinatorial manner a number of derivatization on the purine moiety.

This work is supported by Regione Campania L.5. The authors are grateful to Dr. Luisa Cuorvo for the technical assistance and to Centro di Servizi Interdipartimentale di Analisi Strumentale (CSIAS) for supplying the NMR facilities.

REFERENCES

1. Lee, H. C. (2001) *Annu. Rev. Pharmacol. Toxicol.*, **41**, 317-345.
2. (a) Xu, J., Yang, Z., Dammermann, W., Zhang, L., Guse, A. H., Zhang, L. (2006) *J. Med. Chem.*, **49**, 5501-5512. (b) Potter, B. V. L., Walseth, T. F. (2004) *Curr. Mol. Med.*, **4**, 303-311. (c) Fukuoka, M., Shuto, S., Minakawa, N., Ueno, Y. Matsuda, A. (2000) *J. Org. Chem.*, **65**, 5238-5248.
3. Wagner, G. K., Black, S., Guse, A. H., Potter, B. V. L. (2003) *Chem. Commun.*, **15**, 1944-1945.
4. Gu, X., Yang, Z., Zhang, L., Kunerth, S., Fliegert, R., Weber, K., Guse, A.H., Zhang, L. (2004) *J. Med. Chem.*, **47**, 5674-5682.
5. (a) Guse, A. H., Gu, X., Zhang, L., Weber, K., Kramer, E., Yang, Z., Jin, H., Li, Q., Carrier, L., Zhang, L. (2005) *J. Biol. Chem.*, **280**, 15952-15959. (b) Galeone, A., Mayol, L., Oliviero, G., Piccialli, G., Varra, M. (2002) *Tetrahedron*, **58**, 363-368.
6. Oliviero, G., Amato, J., Borbone, N., D'Errico, S., Piccialli, G., Mayol, L. (2007) *Tetrahedron Lett.*, **48**, 397-400.

*Corresponding Author. E-mail: picciall@unina.it

ACKNOWLEDGEMENTS

Ligand binding to tetra-end-linked (TG₄T)₄ G-quadruplexes: an electrospray mass spectroscopy study

Jussara Amato¹, Giorgia Oliviero¹, Nicola Borbone¹, Stefano D'Errico¹, Gennaro Piccialli¹, Patrick Mailliet², Frédéric Rosu³, Edwin De Pauw³ and Valérie Gabelica^{*3}

¹Dipartimento di Chimica delle Sostanze Naturali, Università degli Studi di Napoli "Federico II", Via D. Montesano 49, I-80131 Napoli, Italy. ²Sanofi-Aventis, Centre de Recherches de Paris, Vitry-sur-Seine, France and ³Laboratoire de Spectrométrie de Masse, Université de Liège, Institut de Chimie Bat. B6c, B-4000 Liège, Belgium

ABSTRACT

The binding properties of a series of known G-quadruplex ligands have been studied by ESI-MS experiments. The tetramolecular (TG₄T)₄ quadruplex and its analogues I and II blocked, respectively, at the 3' or 5'-end by a tetra-end-linker (TEL) unit were chosen as the ligands targets. The stoichiometries of the obtained complexes as well as the ligand affinity and selectivity to the different quadruplexes were determined to deduce the ligand binding site. The TEL derivatives I and II allowed the probing of the grooves contribution to the binding of ligands to G-quadruplexes, demonstrating that the 3' and 5' quartets are not equivalent binding sites for ligand end-stacking.

structures is increasing.⁴ In particular, molecules able to induce G-quadruplex structures are intensively studied for their ability to inhibit telomerase, thus acting as potential antitumoral agents. Several classes of small molecules that induce and/or stabilize G-quadruplex structures and inhibit human telomerase have already been characterized.⁵ The rapid screening of the interaction between ligands and simple G-quadruplex models is surely relevant to assess the binding mode and the structural specificity. Electrospray mass spectrometry (ESI-MS) of non covalent complexes has found important application as a screening tool in drug-nucleic acid interactions.^{6,7}

RESULTS AND DISCUSSION

ESI-MS has been used to study the interactions between some known G-quadruplex ligands and two (TG₄T)₄ analogues in which the 3' or 5' ends, respectively for **I** and **II**, are attached to a tetra-end-linker (TEL) unit⁸ (Fig. 2 and 3). These analogues represent useful models to investigate the ligand interaction sites of (TG₄T)₄ parallel quadruplex, because the presence of the TEL at the top of the 3' or 5' G-quadruplex face is expected to decrease or prevent the end-stacking of the ligands (Fig. 3). We focused on the stoichiometries and on the signal intensities of the complexes formed between the ligands and **I** or **II**, compared to that formed with (TG₄T)₄, to obtain information about ligand affinities and selectivities for the 3' or 5' face. The ligands chosen for this study are the Distamycin A, PIPER and TMPyP4.

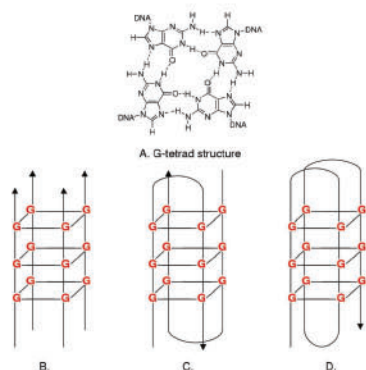


Fig. 1 a) G-tetrads; b) tetramolecular parallel quadruplex; c) bimolecular antiparallel quadruplex; d) monomolecular antiparallel quadruplex.

INTRODUCTION

Guanine-rich oligonucleotides (GROs) tracts of nucleic acids can form four-stranded structures, also known as G-quadruplexes, made up of G-quartet subunits with four coplanar guanines (G) linked together by Hoogsteen hydrogen bonds.^{1,2} G-rich strands can adopt a variety of folds, that can be intra- or intermolecular³ (Fig. 1). Evidence for the *in vivo* formation of G-quadruplex

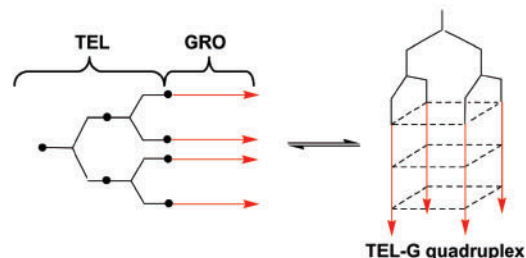


Fig.2 Schematic representation of TEL-oligonucleotides. Unfolded form (left side) and folded TEL-G-Quadruplex (right side).

Distamycin A can associate with G-quadruplex DNA either via stacking interactions with the terminal guanine residues at the ends of G-runs⁹ or by binding to quadruplex grooves.^{10,11} We observed that the binding sites of Distamycin A to $(\text{TG}_4\text{T})_4$ are still present in the linked quadruplexes (**I** and **II**, Fig.2), but the affinities are decrease as $(\text{TG}_4\text{T})_4 > \text{II} > \text{I}$, indicating that some TEL steric hindrance occurs.

In the case of PIPER, for which end-stacking is the main binding mode,¹² we observed that $(\text{TG}_4\text{T})_4$ can accommodate two ligands with high affinity and one with low affinity. **I** and **II** interact with only one PIPER, and with a lower affinity than the two preferred sites of $(\text{TG}_4\text{T})_4$. This result suggests that PIPER could interact with **I** and **II** by the third site of $(\text{TG}_4\text{T})_4$, probably a groove binding site.

Two interacting mode are credited for TMPyP4: external stacking to the end of G-quadruplex and externally binding in the groove.¹⁴ In this case the TEL quadruplexes can still accommodate TMPyP4 in their two binding sites as $(\text{TG}_4\text{T})_4$ and the scale of affinity follows the order $\text{II} > (\text{TG}_4\text{T})_4 > \text{I}$. These results suggest either that TMPyP4 binding sites are in the grooves, or that the insufficient linker rigidity does not prevent end-stacking on the TEL side.

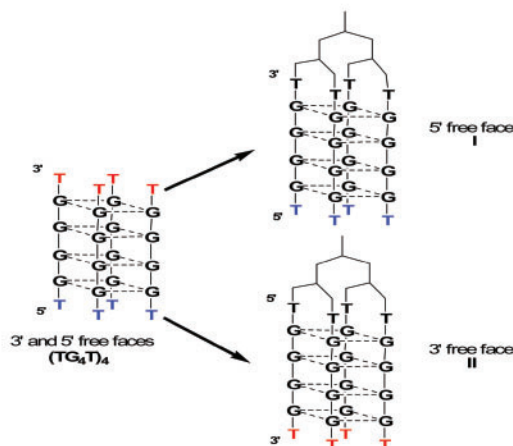


Fig. 3 Comparison between $(\text{TG}_4\text{T})_4$, **I** and **II**.

Table 1 ESI-MS results (150 mM NH_4Cl , pH 7.0).

Ligand	$(\text{TG}_4\text{T})_4$	I	II
Distamycin A	[Q+L]; [Q+2L] [Q+L]; [Q+2L];	[Q+L]; [Q+2L]	[Q+L]; [Q+2L]
PIPER	[Q+3L]	[Q+L]	[Q+L]
TMPyP4	[Q+L]; [Q+2L]	[Q+L]; [Q+2L]	[Q+L]; [Q+2L]

MS experiments using **I** and **II** with shorter and less flexible linkers are under way to better distinguish between different ligand interaction possibilities.

REFERENCES

- Kerwin, S. M. (2000) *Curr. Pharm. Des.*, **6**, 441–478.
- Simonsson, T. (2001) *Biol. Chem.*, **382**, 621–628.
- Parkinson, G. N., Lee, M. P. H., Neidle, S. (2002) *Nature*, **417**, 876–880.
- Chang, C. C., Kuo, I. C., Ling, I. F., Chen, C. T., Chen, H. C., Lou, P. J., Lin, J. J., Chang, T. C. (2004) *Anal. Chem.*, **76**, 4490–4494.
- Riou, J. F. (2004) *Curr. Med. Chem. Anti-Cancer Agents*, **4**, 439–443.
- Rosu, F., De Pauw, E., Gabelica, V. (2008) *Biochimie*, doi: 10.1016/j.biochi.2008.01.005.
- Rosu, F., Gabelica, V., Houssier, C., Colson, P., De Pauw, E. (2002) *Rapid Commun. Mass Spectrom.*, **16**, 1729–1736.
- Oliviero, G., Amato, J., Borbone, N., Galeone, A., Petraccone, L., Varra, M., Piccialli, G., Mayol, L. (2006) *Bioconj. Chem.*, **17**, 889–898.
- Cocco, M. J., Hanakahi, L. A., Huber, M. D., Maizels, N. (2003) *Nucleic Acids Res.*, **31**, 2944–2951.
- Martino, L., Virno, A., Pagano, B., Virgilio, A., Di Micco, S., Galeone, A., Giancola, C., Bifulco, G., Mayol, L., Randazzo, A. (2007) *J. Am. Chem. Soc.*, **129**, 16048–16056.
- David, W. M., Brodbelt, J., Kerwin, S. M., Thomas, P. W. (2002) *Anal. Chem.*, **74**, 2029–2033.
- Neidle, S., Read, M. A. (2001) *Biopolymers*, **56**, 195–208.
- Riou, J. F., Guittat, L., Mailliet, P., Laoui, A., Renou, E., Petitgenet, O., Megnin-Chanet, F., Helene, C., Mergny, J. L. (2002) *PNAS*, **99**, 2672–2677.
- Yamashita, T., Uno, T., Ishikawa, Y. (2005) *Bioorg. Med. Chem.*, **13**, 2423–2430.

*Corresponding Author. E-mail: v.gabelica@ulg.ac.be